Thesis
Reports

Susott,
R.A.

Lang NEX-
Please circ 2/5/91 91-070 4404

FIRE DYNAMICS AND CHEMISTRY OF LARGE FIRES

Ronald A. Susott, Darold E. Ward, Ronald E. Babbitt
Don J. Latham, Lynn G. Weger, and
Patrick M. Boyd

A FINAL REPORT

Date: 6 March 1990

DEFENSE NUCLEAR AGENCY,
IACRO 89-903 (INT-89409-IA)
Title: Fire Dynamics and Chemistry of Large Fires
DNA Work Unit Manager: Major Richard S. Hartley

Submitted by:
USDA Forest Service
Intermountain Research Station
Fire Chemistry Research Work Unit
P.O. Box 8089
Missoula, Montana 59807

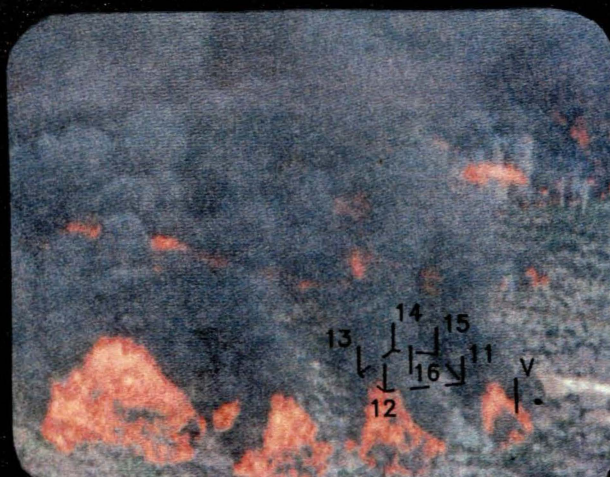

Log NEX-
Clearance 2/5/91 91-070 4404

FIRE DYNAMICS AND CHEMISTRY OF LARGE FIRES

Ronald A. Susott, Darold E. Ward, Ronald E. Babbitt
Don J. Latham, Lynn G. Weger, and
Patrick M. Boyd

RRK

A FINAL REPORT

Date: 6 March 1990

DEFENSE NUCLEAR AGENCY,
IACRO 89-903 (INT-89409-IA)
Title: Fire Dynamics and Chemistry of Large Fires
DNA Work Unit Manager: Major Richard S. Hartley

Submitted by:
USDA Forest Service
Intermountain Research Station
Fire Chemistry Research Work
Unit
P.O. Box 8089
Missoula, Montana 59807

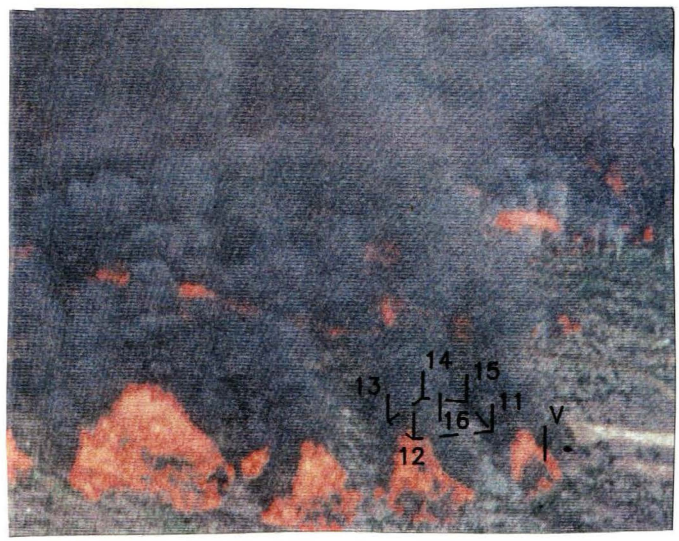

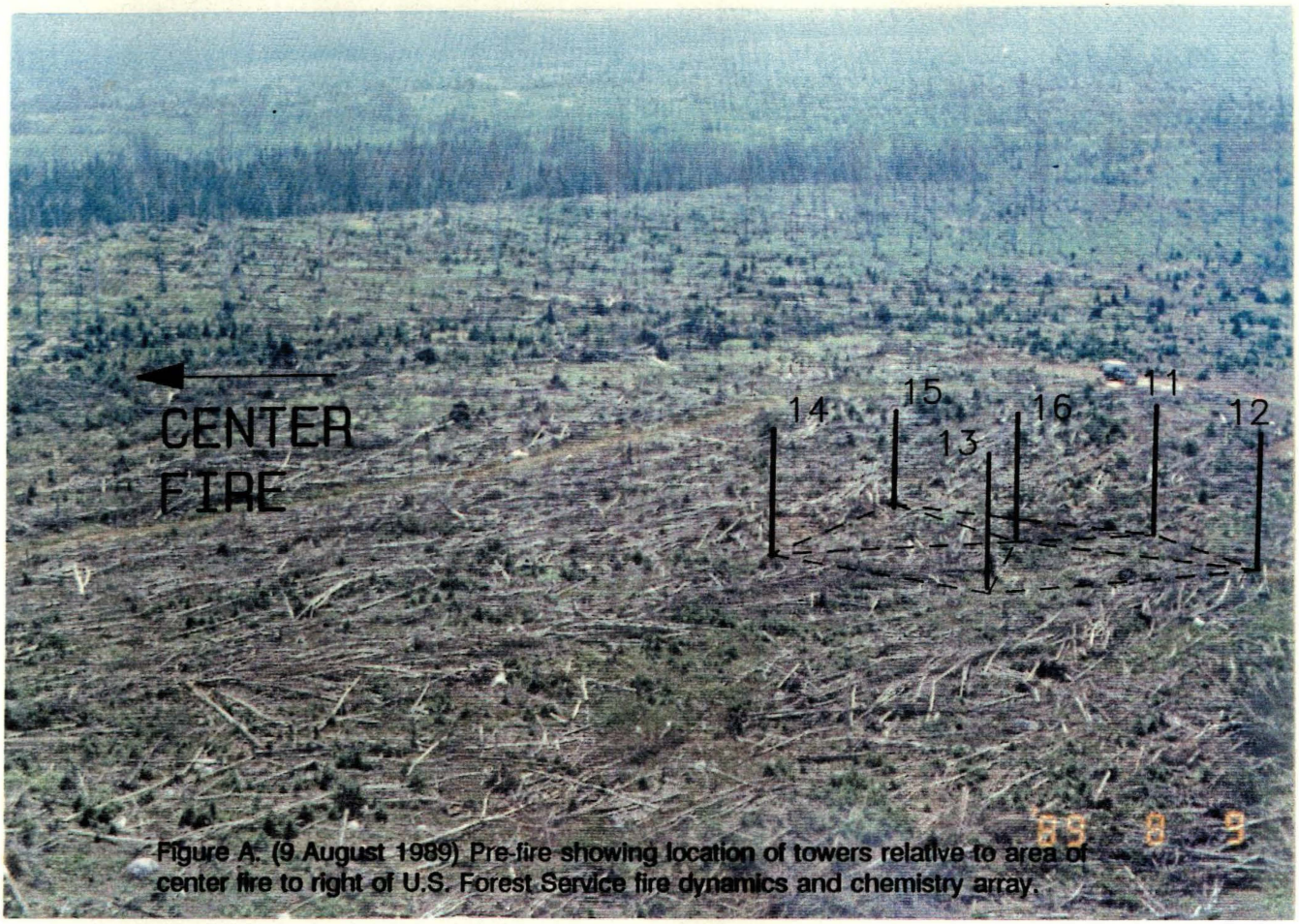

Figure A. (9 August 1989) Pre-fire showing location of towers relative to area of center fire to right of U.S. Forest Service fire dynamics and chemistry array.

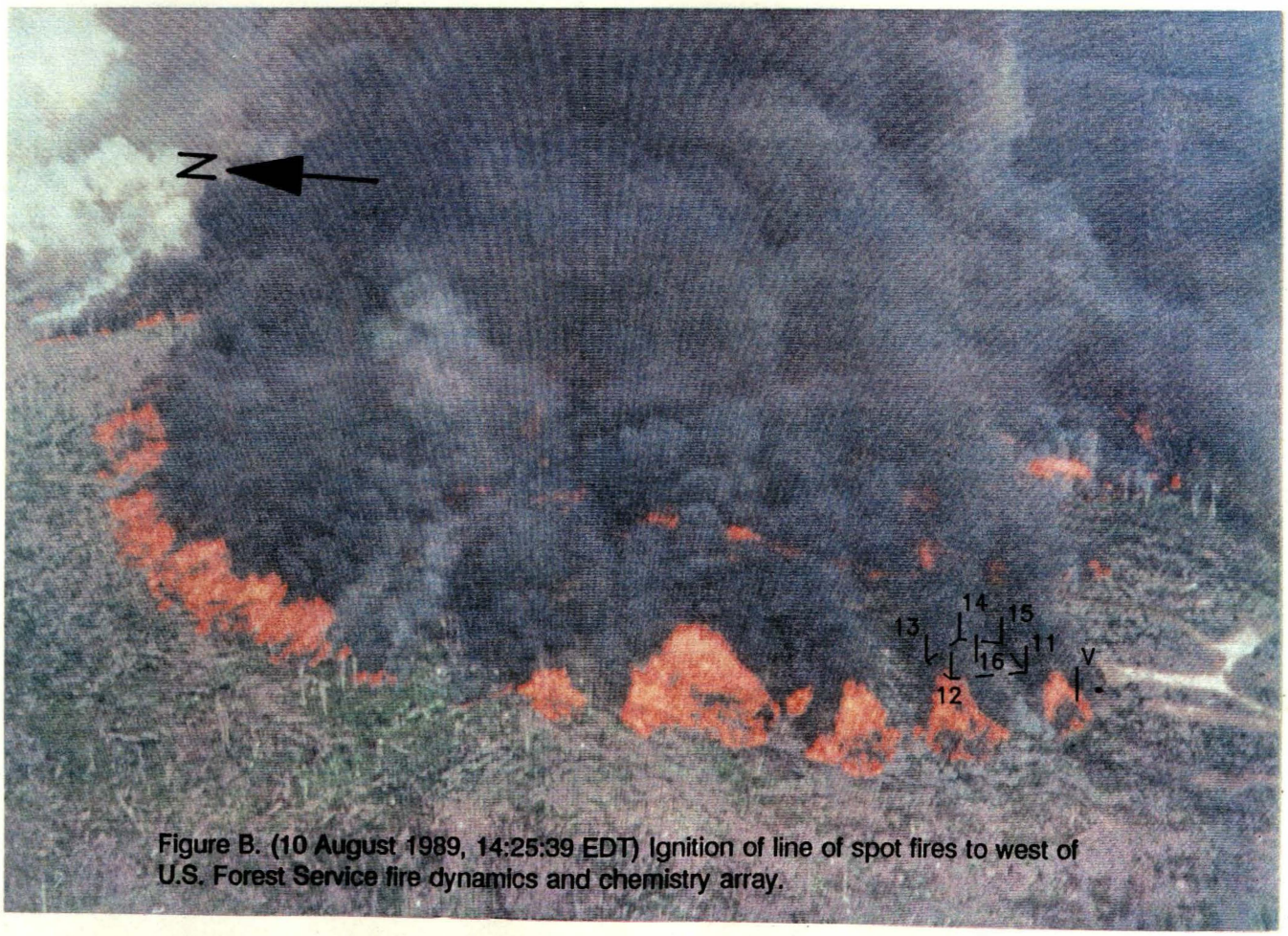

Figure B. (10 August 1989, 14:25:39 EDT) Ignition of line of spot fires to west of U.S. Forest Service fire dynamics and chemistry array.

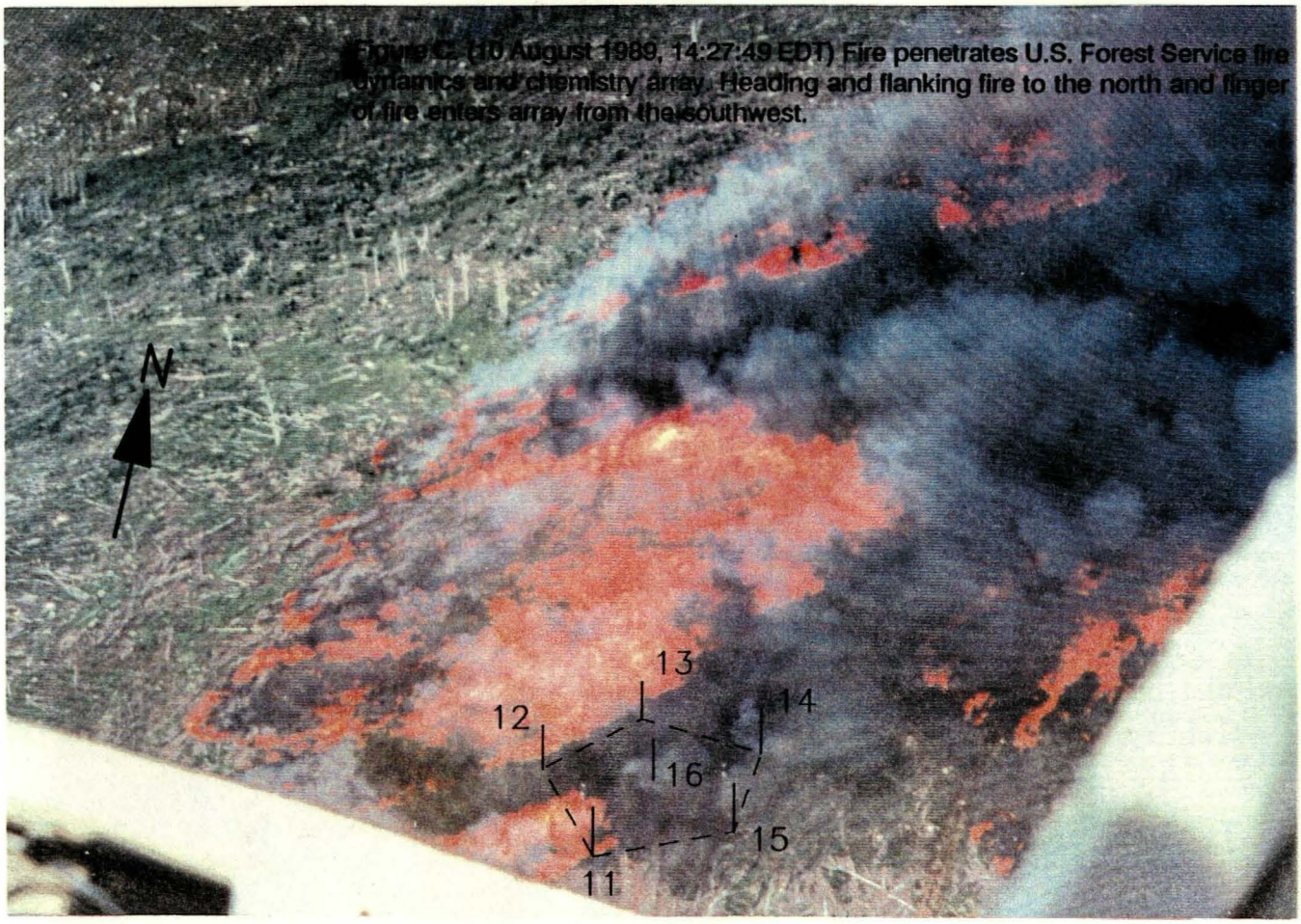

Figure C. (10 August 1989, 14:27:49 EDT) Fire penetrates U.S. Forest Service fire dynamics and chemistry array. Heading and flanking fire to the north and finger of fire enters array from the southwest.

Figure D. (10 August 1989, 14:29:03 EDT) Fires from the north and southwest converge in vicinity of array location 16.

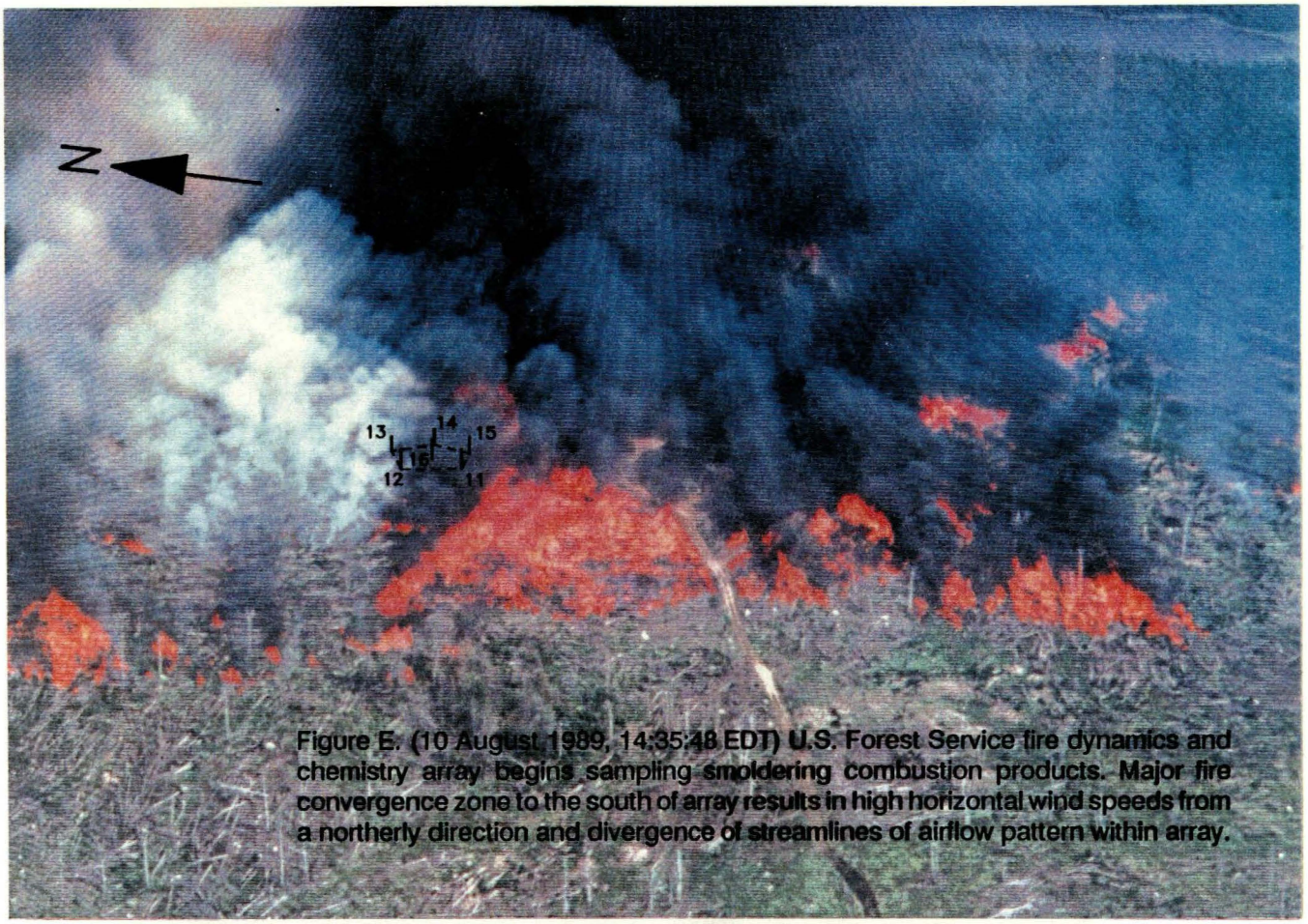

Figure E. (10 August 1989, 14:35:48 EDT) U.S. Forest Service fire dynamics and chemistry array begins sampling smoldering combustion products. Major fire convergence zone to the south of array results in high horizontal wind speeds from a northerly direction and divergence of streamlines of airflow pattern within array.

Figure F. (9 August 1989) U.S. Forest Service fire dynamics and chemistry array sample package during pre-fire installation.

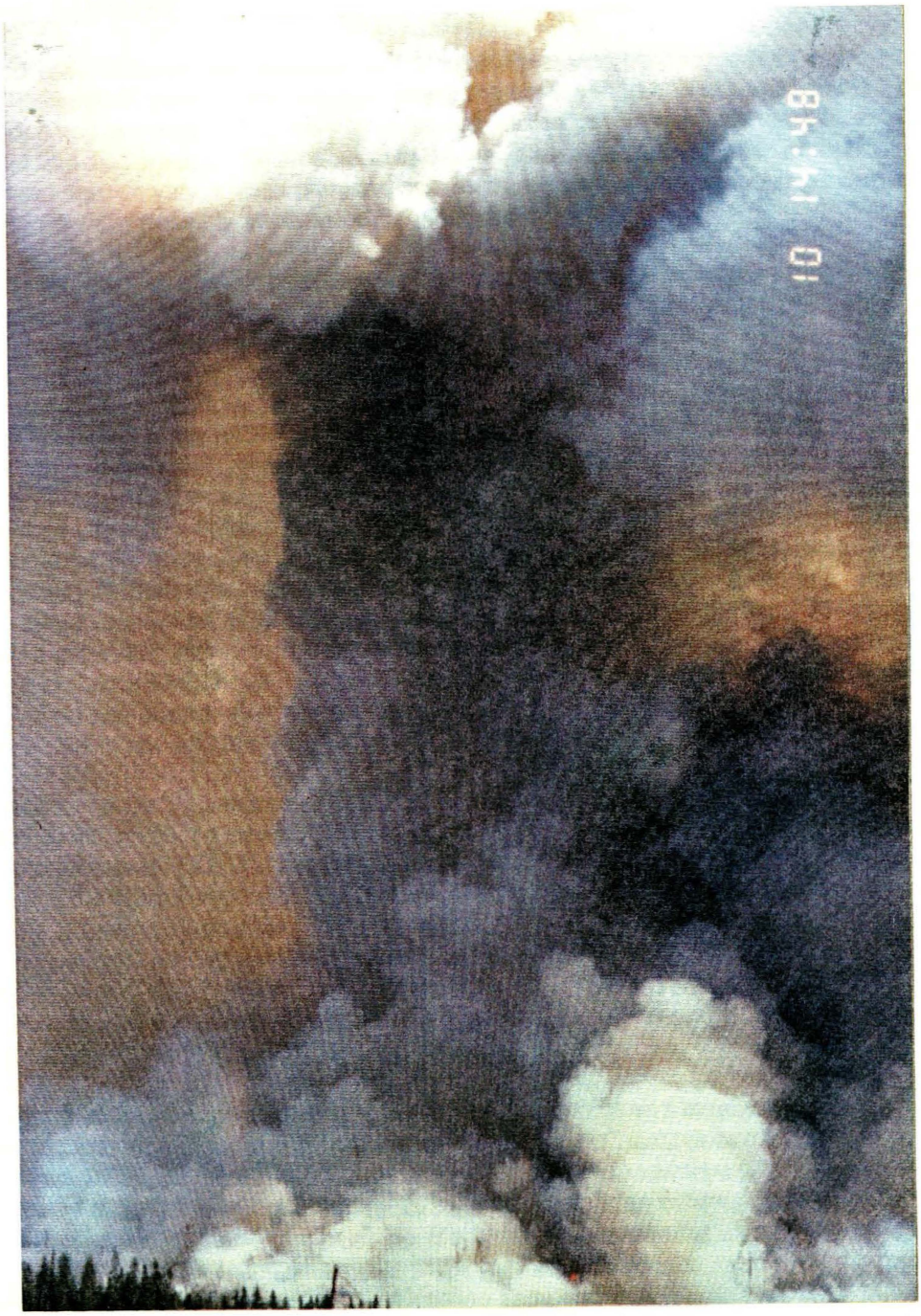

Figure H. (10 August 1989, 14:48 EDT) Major convection Activity observed from observation Hill to the north of Block A. Increase in surface wind speeds measured at location of U.S. Forest Service fire dynamics and chemistry array.

EXECUTIVE SUMMARY

Erratic and unpredictable fire behavior and smoke emissions from large fires are major problems globally. The ignition source and to some extent the fuels consumed are incidental to the problem since major fires have occurred on very large-scales, historically, in many different fuel situations from the tropical forested areas to the arctic and in biomass fuels as well as urban complexes. The study of large fires requires very special planning and instrumentation of such major proportions that one organization cannot possibly accommodate all of the complexity.

Because of the need to understand the fundamental dynamics of large fires for a variety of reasons, the U.S. Defense Nuclear Agency, U.S. Forest Service, and Forestry Canada jointly studied the physical, chemical, and atmospheric aspects of large prescribed fires in the Canadian Province of Ontario. Some of these fires have been as large as 900 hectares. The Hill Township Prescribed Burn (Hill PB) was 486 hectares in size and burned on the 10 August 1989. Airborne sampling of the emissions was performed by the University of Washington, Aerosol and Cloud Physics Research Group; fire dynamics measurements were made by Pacific Sierra Research Corporation; wind field and fire dynamics measurements were made by the University of Iowa; surface temperature measurements by the National Institute of Standards and Technology; fuel characterization, weather, and fire temperatures by Forestry Canada; and the chemical and fire dynamics interactions study by the Intermountain Fire Sciences Laboratory (IFSL). The result was a highly integrated research study. The IFSL served as overall coordinator for the United States effort and fielded a Fire Chemistry and Dynamics experiment within a portion of the large mass-fire. This report is a compilation of the equipment development, measurements, and interpretation of the results for the IFSL research. It does not cover the coordinated study which is being reported on separately through a document being prepared jointly with the National Institute of Standards and Technology.

The objectives for the IFSL included the development of several specially designed sampling packages for collecting detailed measurements. The variables measured included temperature at several heights and locations; CO, CO_2, and O_2 concentrations; wind speed and direction at 3-, 6-, 9-, and 14-m heights. Discrete samples of particulate matter and gases were collected as grab samples from each of the 6 towers sequentially for a 10-minute flaming, 10-minute intermediate, and 20-minute smoldering period. The samples were analyzed for trace gas composition, and graphitic, organic, and inorganic content of the particles. The measurements were needed to define the combustion parameters associated with the production of various emissions including graphitic carbon and trace gases as a function of oxygen deficiency and combustion efficiency.

Perturbations of fires on the wind field are poorly understood and measurements near the surface were needed to correlate the wind phenomena with the rate of heat release both locally and in nearby areas removed from the sampling location. An array of 13-meter towers was positioned in a pentagon shape around a central tower on about a 25 m spacing. A video camera was aimed at the fire area and used to document some of the visible fire phenomena associated with the spread of the fire through the array. The sampling was triggered by thermocouples located around the perimeter of the array which started a 40 minute period of intense sampling that netted nearly 12 Mbytes of data.

The 100 hectare Block A was ignited with a center fire to the east of the sampling array prior to ignition of a line of fire to the west of the sampling array. A westerly wind of about 3 to 4 m/s pushed the line of fire through the sampling array in one head fire-flanking action on the north, while a finger of fire penetrated the array to the south. The net effect was a time lag between the major fire features at the various tower locations. The fires from the north and south burned together near the centerline of the array. Horizontal wind speeds increased by a factor of two during the period of convergence of the fires. Vertical air movement measurements were made that showed pulses of vertical motion away from the fire. The correlation of these pulses with the fire is visually associated with windrows

of heavy concentrations of fuel across the array and potentially secondarily associated with other fire phenomena.

The streamlines of air motion through the array of towers showed periods of convergence and divergence periodically during the time that the fire was spreading through the array. The divergence of the streamlines of airflow through the array was particularly pronounced for one 5 minute period of time. The general distribution of wind direction across the array showed a 20 degree differential wind direction from over the 50 m separation from north to south.

The vertical measurements of air flow are coupled with the concentration of CO_2 and CO to calculate the mass flux of carbon released by the fire. The rate of carbon release is coupled to the mass loss rate of fuel. The rate of consumption of the fuel is modeled with a rapidly increasing linearly fit function and an exponential decay function. The total consumption measured through a pre- and post-fire fuel inventory indicated that 10.63 kg/m^2 of fuel was consumed. The measured fuel consumption based on the carbon mass-flux indicated 11.46 kg/m^2 or about 8% greater than the ground inventory.

Peak rates of heat release of 500 kW/m^2 were measured during the time that the flame front was passing through the FASS array. Combustion efficiency ranged from near 100% to a low of 88% as calculated from the real time sensor information. The combustion efficiency calculations from the grab samples were lower than the real time measurements.

The modeled rate of fuel consumption was adjusted to the inventory value and used to distribute the fuel over the duration of the fire for any given square meter from the time of ignition to extinction. In this way, by knowing the rate of ignition, an evaluation of the rate of fuel consumption for the entire unit, by flaming and smoldering combustion processes, was made. Measurements of the combustion efficiency were used to adjust the heat of combustion to a mean value of 19.22 MJ/kg. The rate of release of heat, particulate matter, CO, and CO_2 for Block A are estimated based on an assumed rate of ignition for Block A. The maximum rates of release for heat, particulate matter, CO, and CO_2 were 75,000 MW and 0.047, 0.326, and 6.34 tonnes/s, respectively.

Emission factors were calculated using the carbon mass-balance method for the flaming, intermediate, and smoldering combustion phases. The emission factors were weighted dependent on the fuel consumed by combustion phase and yielded emission factors for PM5.0, CO, and CO_2 of 12.4, 86, and 1673 g/kg for the Hill PB. Graphitic carbon content of the PM5.0 averaged 8.1% during the 10-minute flaming period and dropped to 1.5% during the 20-minute smoldering period. This is consistent with other measurements and with the positive correlation of graphitic carbon with the rate of heat release.

Cross covariance techniques were used to evaluate the lag of fire induced phenomena between FASS packages as the fuel consumption wave moved through the array. The technique verified a time differential of from 20 seconds to 3 minutes dependent on the pairs of FASS packages used in the analysis. Other phenomena associated with the waves of combustion gases moving through the array showed correlations between towers of less than 10 seconds--consistent with the horizontal wind speed measurements.

The Hill PB plume cloud produced several cloud-to-ground and intracloud lightning discharges. Electric field measurements taken near the base of the plume combined with lightning location network data indicate that the majority, if not all, discharges to ground were positive. The electric field measurements, taken together with photogrammetry of the plume, suggest that the electric dipole within the cloud was reversed in sign from that generated by a normal thunderstorm. The results of our investigation are presented in Appendix C.

The results from this experiment demonstrate the practicality of using reasonably sophisticated measurement systems inside the perimeter of very large fires. It makes possible a new range of experiments heretofore impossible to perform because of instrumentation limitations. Characterization of air flow in conjunction with scaling criteria based on the relative size of fires is now practical. The response of chemical phenomena in conjunction with large area fires is extremely important relative to the emissions source strength for these chemical species leaving the turbulent boundary layer and becoming entrained in convection from the fire. The equipment described in this report is highly modular and can be configured for a variety of research studies both within fires and for ambient air sampling.

The chemical structure associated with flame lengths in the lower 30 m of the atmosphere are poorly understood. This hampers further research on rates of fuel consumption, rate of heat release, and the overall entrainment of oxygen into the combustion system near the surface. The features of the test unit discussed in this report were but one cell within the large Hill PB. The interrelations with the other fire activity have only partially been explained. The size of the fire hampered investigations of entrainment, airflow, observations of fire behavior associated with airflow events, and a number of other considerations. We strongly recommend a series of smaller scale fires that could be structured to yield various rates of heat release, burned under different prescription conditions to meet objectives for surface winds, atmospheric lapse rates, interactions between area fires, fuel loading by size classes, potential incorporation of rubble or other hydrocarbon fuels, and a host of other objectives that could illuminate the interactions between major sources of heat and lower atmospheric boundary layer conditions. The potential to investigate the chemical phenomena occurring in areas of intense rates of heat release would be much greater if performed on a smaller scale. A carefully designed set of treatments with some replication seems essential.

Scaling of the size of the area fires involved in producing different combustion phenomena is important in planning future studies. The atmospheric processes acting to remove or to change the character of the emissions released from the combustion of the biomass fuels under different combustion conditions are nearly completely decoupled. Hence, work to improve our understanding of the production of smoke particles by size classes, gases of importance in the atmosphere from a chemical reaction standpoint, and the heat release rates can be studied on much smaller fires than the Hill PB. Fires of a hectare in size would be plenty large enough to fully explore the concepts of modeling these phenomena before graduating once again to the very large mass-fire. The important concepts of induced buoyancy, inflow near the perimeter, heat release rates, vertical velocity and horizontally induced wind flow, the enhancement of flow velocities by rotation, and other phenomena are tractable on a much reduced scale.

FIRE DYNAMICS AND CHEMISTRY OF LARGE FIRES

Ronald A. Susott
Darold E. Ward
Ronald E. Babbitt
Don J. Latham
Lynn G. Weger
Patrick M. Boyd

A FINAL REPORT

Date: 6 March 1990

DEFENSE NUCLEAR AGENCY, IACRO 89-903 (INT-89409-IA)
Title: Fire Dynamics and Chemistry of Large Fires
DNA Work Unit Manager: Major Richard S. Hartley

Submitted by:

USDA Forest Service
Intermountain Research Station
Fire Chemistry Research Work Unit
P.O. Box 8089
Missoula, Montana 59807

TABLE OF CONTENTS

	LIST OF FIGURES		ii
	LIST OF TABLES		v
1.0	**INTRODUCTION**		1
2.0	**BACKGROUND**		2
	2.1	Past Research	2
	2.2	Results for 1988 Canadian Fires	3
3.0	**SCOPE AND STUDY OBJECTIVES**		4
4.0	**METHODS**		5
	4.1	Selection of the Site and Fire Information	5
	4.2	Equipment Development	6
		4.2.1 Design	6
		4.2.2 Video Camera Controller	6
		4.2.3 Field Mill Data Logger	7
		4.2.4 Ground O_2 Depletion Monitor	7
		4.2.5 Fire Atmosphere Sampling System	7
	4.3	Analytical Methods for Real Time Measurements and Basic Calibrations	7 9
		4.3.1 CO_2, CO, and O_2 Sensors	9
		4.3.2 Wind Sensors	10
		4.3.3 Thermocouples	10
	4.4	Sampling Protocol	11
		4.4.1 Real Time Sensors	11
		4.4.2 Integrated Filter, Gas Bag, and Canister Samples	12
	4.5	Analytical Methods for Post-Fire Sample Analysis	13
		4.5.1 CO_2, CO, and Trace Gases	13
	4.6	Calculated Parameters and Methods of Adjusting Data	13
		4.6.1 Emission Factors	13
		4.6.2 Rate of Fuel Consumption	15
		4.6.3 Source Strength	15
		4.6.4 Rate of Heat Release	15
5.0	**PRESENTATION OF DATA**		17
	5.1	Fire Behavior	17
	5.2	Gas Concentration	18
	5.3	Particulate Matter Concentrations	19
	5.4	Temperature Measurements	20
	5.5	Wind Speed and Direction	20
	5.6	GODM O_2 Depletion and Temperature Measurements	21
	5.7	Z-Values	23
6.0	**RESULTS**		24
	6.1	Rate of Fuel Consumption	24
		6.1.1 Measured Rates of Fuel Consumption	24
		6.1.2 Total Fuel Consumption	25
		6.1.3 Mathematical Fit of Rate of Fuel Consumption	25

6.2 Emission Factors and Emissions Released Per Unit Area 26
6.3 Source Strength Calculations 27
6.4 Rate of Heat Release 28
6.5 Fire Induced Winds 29
6.5.1 Horizontal Wind Speed and Direction 29
6.5.2 Vertical Component of the Wind Field 29
6.5.3 Local Areas Affected by High-intensity Combustion 30
6.6 Periodicity, Data Dynamics 31

7.0 SUMMARY AND CONCLUSIONS 33

8.0 RECOMMENDED CONTINUATION STUDIES 35
8.1 Need for Continuation Fires 35
8.2 Measurement System Improvements 36
8.3 Software Improvements 36
8.4 Laboratory Studies 36

9.0 ACKNOWLEDGMENTS 37

10.0 REFERENCES 38

11.0 CONVERSION FACTORS FOR METRIC TO ENGLISH 40

FIGURES

TABLES

APPENDICES

APPENDIX A DEVELOPMENT OF EQUIPMENT A-1
APPENDIX B COMPUTER PROGRAMS FOR CONTROLLING DATA GATHERING FOR THE HILL FIRE B-1

LIST OF FIGURES

Figure 4.1-1	Location of the Hill PB relative to Chapleau and Sault Ste. Marie, Ontario, Canada.	F-1
Figure 4.1-2	General location of FASS packages, GODM packages and video camera relative to the fire break study area.	F-2
Figure 4.2.4-1	Functional block diagram of the GODM system.	F-3
Figure 4.2.5-1	Position of the FASS sensors on the tower.	F-4
Figure 4.3.1-1	Diagram of the flow of the gases through the analyzers in the FASS packages.	F-5
Figure 5.1-1	Pattern of fire spread through the matrix of towers from 14:25 to 14:30 on August 10, 1989.	F-6
Figure 5.2-1	Example of real time gas concentration measurements on FASS 11; A) CO_2, B) CO.	F-7
Figure 5.2-2	Comparison of the average real time gas concentrations with measurements based on sample bags; A) CO_2, B) CO.	F-8
Figure 5.2-3	Example of real time gas concentration measurements of oxygen depletion on FASS 11.	F-9
Figure 5.2-4	Theoretical oxygen levels calculated as a function of measured CO_2 fractions. Fuel composition is assumed to be $C_6H_9O_4$.	F-10
Figure 5.2-5	Comparison of measured oxygen levels to theoretical calculations based on CO_2 fractions; A) based on average values, B) based on maximum values.	F-11
Figure 5.3-1	Inorganic composition of particulate matter compared to Pacific Northwest literature values on logging slash.	F-12
Figure 5.3-2	Inorganic composition of particulate matter compared to literature values for Pacific Northwest and Lodi Canyon, California burns.	F-13
Figure 5.4-1	Comparison of the FASS 11 internal gas flow temperature to the external air temperature of the fire environment.	F-14

Figure 5.5-1	Fire induced wind field variations before ignition and during the first few minutes of the fire; A) 3-m wind speed, B) 3-m wind direction, C) 6-m wind speed, D) 6-m wind direction, E) 9-m wind speed, and F) 9-m wind direction.	F-15
Figure 5.5-2	Vertical wind velocity measured at the 14-m height for FASS packages during the 40 minutes of sampling.	F-16
Figure 5.5-3	Horizontal wind direction measured at the 14-m height for FASS packages during the 40 minutes of sampling.	F-17
Figure 5.5-4	Horizontal wind speed measured at the 14-m height for FASS packages during the 40 minutes of sampling.	F-18
Figure 5.6-1	Real time measurements for GODM #1; A) oxygen depletion relative to ambient air, B) air temperature.	F-19
Figure 5.6-2	Real time measurements for GODM #3; A) oxygen depletion relative to ambient air, B) air temperature.	F-20
Figure 5.6-3	Real time measurements for GODM #4; A) oxygen depletion relative to ambient air, B) air temperature.	F-21
Figure 5.6-4	Real time measurements for GODM #6; A) oxygen depletion relative to ambient air, B) air temperature.	F-22
Figure 5.7-1	Z-value data before time-adjustment and following adjustment.	F-23
Figure 6.1.1-1	Calculated rate of fuel consumption based on carbon flux measurements for packages 11, 12, 14, and 16 for the Hill PB.	F-24
Figure 6.1.2-1	Cumulative fuel consumption for each of the four sets of data (packages 11, 12, 14, and 16) for Hill PB.	F-25
Figure 6.1.3-1	Average rate of fuel consumption in the area measured by the FASS array in the Hill PB (curves for 11, 12, 14, and 16 were averaged).	F-26
Figure 6.1.3-2	Fit of a simple model to the average rate of fuel consumption.	F-27

Figure 6.2-1	Comparison of emission factors measured for the Hill PB (CAN) with data from Pacific Northwest Douglas-fir (PND) and Pacific-Northwest hardwood (PNH); A) CO, B) PM5.0. Flaming, intermediate and smoldering phases are indicated by f, i, s.	F-28
Figure 6.3-1	Hypothetical rate of ignition of Block A of Hill PB.	F-29
Figure 6.3-2	Source strength over time for particles less than 5.0 micrometers.	F-30
Figure 6.4-1	Average combustion efficiency for all FASS data from the Hill PB.	F-31
Figure 6.4-2	Calculated heat evolution for the FASS array area; A) rate of heat release, B) total heat from integration of the rate.	F-32
Figure 6.4-3	Total heat release estimate for Block A of the Hill PB.	F-33
Figure 6.5.1-1	Difference in wind direction between pairs of FASS towers as indicated on right margin of figure. The wind direction of the southerly towers was subtracted from the wind direction of the northerly towers.	F-34
Figure 6.5.2-1	Distribution of vertical velocities across FASS array for each 30 seconds during the flaming phase.	F-35
Figure 6.6-1A and 6.6-1B	Power spectra of real time measurements for FASS 14; a) flaming, B) smoldering.	F-36
Figure 6.6-2A and 6.6-2B	Auto correlation plots for FASS 14; A) flaming, B) smoldering.	F-37
Figure 6.6-3	Auto Correlation of the heat release rate for FASS 16 flaming and smoldering phases.	F-38
Figure 6.6-4A and 6.6-4B	Heat release cross-covariances between FASS towers.	F-39

LIST OF TABLES

Table 2.2-1	Elemental analysis of Canadian fuels from 1988 mass fire. Compositions are on a dry weight and an ash free basis.	T-1
Table 5.2-1	FASS sample bag gas concentrations.	T-2
Table 5.2-2	FASS real time combustion gas sensor summary.	T-3
Table 5.2-3	FASS canister primary gas concentrations.	T-4
Table 5.3-1	FASS filter particulate matter (PM5.0) concentrations.	T-5
Table 5.3-2	FASS glass fiber filter carbon analysis.	T-6
Table 5.3-3	Teflon filter inorganic trace elements, precent of PM5.0	T-7
Table 5.4-1	FASS air temperatures at the sample level.	T-8
Table 5.6-1	Ground oxygen depletion monitor (GODM) data sensor.	T-9
Table 6.1.2-1	Fuel consumption by phase of combustion and the total, for each of the four FASS packages.	T-10
Table 6.1.3-1	Fuel consumption for 5-minute intervals based on the linear growth/exponential decay model. Total consumption was adjusted to the Forestry Canada inventoried fuel consumption of 10.64 kg/m^2.	T-11
Table 6.2-1	Emission factors and combustion efficiency by fire phase for the six FASS packages.	T-12
Table 6.2-2	Total emissions released on a per m^2 basis for Block A of the Hill PB.	T-13
Table 6.4-1	Effective heat of combustion of fuels typical of the Hill PB area, after correction for CO emissions.	T-14

FIRE DYNAMICS AND CHEMISTRY OF LARGE FIRES

1.0 INTRODUCTION

Fires resulting from the detonation of nuclear weapons or from other mechanisms that create large area fires are not well characterized. Full-scale tests are not practical and simulations of the destructive forces of these weapons are only possible on a reduced scale. Several possibilities exist for developing analog methods for testing mechanisms associated with large fires that would be similar to that of a nuclear weapon ignited fire. Probably the closest simulation is possible and practical by studying the large, rapidly ignited fires of natural biomass fuels. Large area fires are routinely burned by the Ontario Ministry of Natural Resources in Canada. Large naturally occurring wildfires, at times, offer excellent opportunities for studying atmospheric interactions between the smoke emitted and dynamics of the atmosphere; however, the inability to instrument and to measure phenomena within the fire makes the study of fire dynamics near the surface nearly intractable. Up until this time, little work has been accomplished even for planned large-scale fires.

This study, performed in cooperation with several other research groups, was an effort to increase the level of knowledge concerning emissions, heat release, and turbulence near the surface (0 to 15 m) during a major fire event. Indeed, information concerning the spread of a fire through natural fuels and the chemistry associated with the fire environment are important considerations to both the survivability and the overall impact of mass-ignited fires whether ignited using nuclear weapons or from other causes--natural or man-induced.

The USDA Forest Service and Forestry Canada have for many years had mutual aid compacts for assisting in the control of wildfires during major fire episodes. In addition, the countries have frequently participated in joint research ventures. Hence, the opportunity provided by the Defense Nuclear Agency to facilitate the joint study of mass-ignited large fires was of great value to both countries and to further the cooperative activities between our countries.

The control of large fires remains a problem of major concern to both the United States and Canadian governments. 1988 was one of the worst fire seasons in recent times in the United States with over 2 million hectares of wildland burned. Large fires such as the Canyon Fire in Montana burned over 100,000 hectares in less than 24 hours--an incredible rate of growth. Even though fire behavior associated with surface fires is reasonably well understood and predictable (Rothermel 1972, 1983), models for predicting the behavior of blow-up fires, mass fires, and crown fires are not available (Albini 1984, 1986). A better understanding of fire behavior, spatial distribution of gaseous fuels, temperature profiles, and fluid motions within and adjacent to large fires is needed. The new information will assist in developing models for predicting the transition from surface fires to 3-dimensional fires, the growth of large fires, and other fire behavior. Feedback mechanisms resulting in rapid increases in the rate of heat release, and rate of spread, are poorly understood as are mechanisms associated with the formation of emissions--especially emissions important from an atmospheric radiation transfer standpoint. The results discussed in this report demonstrate the rate of heat release for a portion of one large mass-ignited fire and correlate the rate of heat release with the production of emissions.

In addition, the lack of knowledge about the interactions between fire chemistry dynamics and fire fluid dynamics hampers the modeling study of fire-generated plumes. At present, there is not sufficient data from large fires to know how to generate proper boundary conditions for this kind of model. In particular, there is evidence from past fires that simply inserting an integrated source term for buoyancy and water vapor may not be adequate. The time-dependent features on a scale of one to hundreds of meters should be taken into account to obtain a proper parameterization for boundary conditions to a larger scale. The fluid dynamics resulting from the ignition and burning patterns associated with large fires is complex. This study maps the advance of fingers of fire through an array

of sampling devices that give new information concerning the interactions of fire fronts converging during the spread of a large fire.

Results are presented of a continuing study of research that was started in 1988. Oxygen deficiency coupled with the release of volatile hydrocarbons from the decomposition and vaporization of solid fuels is extremely important in the rate of release of heat and other emissions. These same parameters affect the flame length and the fluid mechanics in the vicinity of the flame structure. It is extremely important that the wind field be measured in conjunction with CO, CO_2, and O_2 concentrations. These measurements are reported for a 40 minute period of time from ignition through the critical period of maximum release of heat to the near extinction of the smoldering combustion phase.

2.0 BACKGROUND

2.1 Past Research

Past studies of large "mass fires" within Forest Service Research were done in the Flambeau series in 1964-1967 as part of the Office of Civil Defense, Office of the Secretary of the Army task "Interaction of Mass Fire and its Environment" (Countryman 1964). The test fires were configured to represent surrogates for urban fires. Observations were made of airflow both inside and outside of the fuel bed, and attempts made, through use of Doppler radar, to measure airflow in the convection column. Measurements were made of the concentration of CO, CO_2, and O_2 at or near street level between the piles of brush which simulated houses along streets.

At the time of the Flambeau experiments, there were no computer airflow models available for application to the data, and as far as we know, no relationships between wind and fire behavior were generated from the data. However, several very valuable sets of information were developed from these experiments. For example, Countryman (1964) published guidelines for mass fires from the Flambeau data and information from wildfires. These criteria are still the best available and establish rate of heat release criteria for the onset of blow-up fires ($> 10^3$ kW/m^2 over an area of at least 1 hectare). Undoubtedly, the criterion integrates fire dynamics, i.e., fire intensity, turbulence, and fuel interactions into a "blowup fire" threshold.

Recent prescribed burns, conducted by Forestry Canada, together with more recent modeling efforts provide better possibilities for understanding burning and fire behavior in large fires. In particular, the models developed by Albini (1979, 1980, 1981, 1985a, 1985b) need further testing, especially for large values of flame length and wind speed.

Work completed by Hegg et al. (1989), Einfeldt et al. (1989), and Ward and Hardy (1989) for the Lodi tests in California suggest emissions of graphitic carbon to be correlated positively with the rate of heat release. Emissions of chlorofluorocarbons, oxides of nitrogen, and lead are related to the deposition of anthropogenically produced air pollutants. The fire resuspends these materials. Ward and Hardy (1984) found that emission factors for total particulate matter without regard to size increase with an increase in fire intensity, but emission factors for particles less than 2.5 um[1] mean mass cut point diameter tend to decrease as the rate of heat release increases. Emission factors for particles less than 2.5 um diameter, particles without regard to size, CH_4, CO, and CO_2 are all correlated with combustion efficiency (Ward and Hardy 1990). Generally, emission sampling has been done outside of the direct influence of the fire to minimize effects due to elevated temperature. Among other parameters, this study will test for non-standard O_2 conditions on emissions production.

[1]In this document um refers to micons or micrometers.

2.2 Results for 1988 Canadian Fires

In 1988, Pacific Sierra Research Corporation and the Intermountain Fire Sciences Laboratory (IFSL) performed detailed fire dynamics and emissions characterization tests for two large-scale prescribed fires near Timmins, Ontario, Canada. The experiments performed by the IFSL included:

1. Measurement of the range of emission concentrations of CO_2, CO, O_2, and combustible gas.

2. Collection of grab samples of primary combustion gases and trace gases.

3. Measurements of the temperature profile in the sampling zones for points at 1 and 12 m above the ground.

A combination of real time and grab sampling methods were employed to fulfill an expanded set of objectives. The sampling system was controlled and the data logging functions performed using a Hewlett Packard data acquisition/computer. Each of the sample packages contained about $9,000.00 of equipment. One of the packages was destroyed during the Battersby Experiment.

In spite of the loss, valuable data were generated for the first 2 to 4 minutes of the Thomas and Battersby Fires during the flaming combustion phase which is the period of most active fuel consumption and heat release. Results from the tests include:

1. A maximum temperature measurement of 960 C with profiles of temperature from the 1 m and 12 m heights for both prescribed fires during the first two minutes.

2. Oxygen concentration decreased at 12 m height to 19% and at the 1 m height to 14.5% for Thomas PB. The 1 m height instrument did not respond for the Battersby PB but the 12 m height reading reached a low of 18% before the tower collapsed.

Representative samples of the fuels typical of those burned during the Thomas and Battersby PB's were collected by Forestry Canada and shipped to the IFSL. These fuel samples were analyzed for chemical composition and thermal behavior. Table 2.2-1 provides a list of the species and size ranges analyzed, along with the approximate analysis or elemental composition of the fuel (C,H,N). The moisture and ash component available from thermogravimetric analysis were used to reduce composition values to an ash-free, moisture-free basis. This basis allows easier comparison of just the organic component of the forest fuels. The woody component comprises the largest fraction of the fuel and the carbon fraction of the woody material approaches 50%.

Generally ash is low (0.5% to 1%) in the woody material but is up to 7% of black spruce twigs. The duff and litter samples have 10% to 20% ash. This ash component should be investigated in more detail as a source of potential hazardous emissions, or useful tracers for smoke from forest burning. Since oxygen is the only other major component it can be estimated by difference. The propensity for soot or particulate matter emissions to form may be indicated by the oxygen content which covers a range of 35.6% to 46.2% for the Canadian samples. Soot formation is expected to increase with lower oxygen content, making the white birch bark an important source of soot.

of sampling devices that give new information concerning the interactions of fire fronts converging during the spread of a large fire.

Results are presented of a continuing study of research that was started in 1988. Oxygen deficiency coupled with the release of volatile hydrocarbons from the decomposition and vaporization of solid fuels is extremely important in the rate of release of heat and other emissions. These same parameters affect the flame length and the fluid mechanics in the vicinity of the flame structure. It is extremely important that the wind field be measured in conjunction with CO, CO_2, and O_2 concentrations. These measurements are reported for a 40 minute period of time from ignition through the critical period of maximum release of heat to the near extinction of the smoldering combustion phase.

2.0 BACKGROUND

2.1 Past Research

Past studies of large "mass fires" within Forest Service Research were done in the Flambeau series in 1964-1967 as part of the Office of Civil Defense, Office of the Secretary of the Army task "Interaction of Mass Fire and its Environment" (Countryman 1964). The test fires were configured to represent surrogates for urban fires. Observations were made of airflow both inside and outside of the fuel bed, and attempts made, through use of Doppler radar, to measure airflow in the convection column. Measurements were made of the concentration of CO, CO_2, and O_2 at or near street level between the piles of brush which simulated houses along streets.

At the time of the Flambeau experiments, there were no computer airflow models available for application to the data, and as far as we know, no relationships between wind and fire behavior were generated from the data. However, several very valuable sets of information were developed from these experiments. For example, Countryman (1964) published guidelines for mass fires from the Flambeau data and information from wildfires. These criteria are still the best available and establish rate of heat release criteria for the onset of blow-up fires ($> 10^3$ kW/m^2 over an area of at least 1 hectare). Undoubtedly, the criterion integrates fire dynamics, i.e., fire intensity, turbulence, and fuel interactions into a "blowup fire" threshold.

Recent prescribed burns, conducted by Forestry Canada, together with more recent modeling efforts provide better possibilities for understanding burning and fire behavior in large fires. In particular, the models developed by Albini (1979, 1980, 1981, 1985a, 1985b) need further testing, especially for large values of flame length and wind speed.

Work completed by Hegg et al. (1989), Einfeldt et al. (1989), and Ward and Hardy (1989) for the Lodi tests in California suggest emissions of graphitic carbon to be correlated positively with the rate of heat release. Emissions of chlorofluorocarbons, oxides of nitrogen, and lead are related to the deposition of anthropogenically produced air pollutants. The fire resuspends these materials. Ward and Hardy (1984) found that emission factors for total particulate matter without regard to size increase with an increase in fire intensity, but emission factors for particles less than 2.5 um[1] mean mass cut point diameter tend to decrease as the rate of heat release increases. Emission factors for particles less than 2.5 um diameter, particles without regard to size, CH_4, CO, and CO_2 are all correlated with combustion efficiency (Ward and Hardy 1990). Generally, emission sampling has been done outside of the direct influence of the fire to minimize effects due to elevated temperature. Among other parameters, this study will test for non-standard O_2 conditions on emissions production.

[1]In this document um refers to micons or micrometers.

2.2 Results for 1988 Canadian Fires

In 1988, Pacific Sierra Research Corporation and the Intermountain Fire Sciences Laboratory (IFSL) performed detailed fire dynamics and emissions characterization tests for two large-scale prescribed fires near Timmins, Ontario, Canada. The experiments performed by the IFSL included:

1. Measurement of the range of emission concentrations of CO_2, CO, O_2, and combustible gas.

2. Collection of grab samples of primary combustion gases and trace gases.

3. Measurements of the temperature profile in the sampling zones for points at 1 and 12 m above the ground.

A combination of real time and grab sampling methods were employed to fulfill an expanded set of objectives. The sampling system was controlled and the data logging functions performed using a Hewlett Packard data acquisition/computer. Each of the sample packages contained about $9,000.00 of equipment. One of the packages was destroyed during the Battersby Experiment.

In spite of the loss, valuable data were generated for the first 2 to 4 minutes of the Thomas and Battersby Fires during the flaming combustion phase which is the period of most active fuel consumption and heat release. Results from the tests include:

1. A maximum temperature measurement of 960 C with profiles of temperature from the 1 m and 12 m heights for both prescribed fires during the first two minutes.

2. Oxygen concentration decreased at 12 m height to 19% and at the 1 m height to 14.5% for Thomas PB. The 1 m height instrument did not respond for the Battersby PB but the 12 m height reading reached a low of 18% before the tower collapsed.

Representative samples of the fuels typical of those burned during the Thomas and Battersby PB's were collected by Forestry Canada and shipped to the IFSL. These fuel samples were analyzed for chemical composition and thermal behavior. Table 2.2-1 provides a list of the species and size ranges analyzed, along with the approximate analysis or elemental composition of the fuel (C,H,N). The moisture and ash component available from thermogravimetric analysis were used to reduce composition values to an ash-free, moisture-free basis. This basis allows easier comparison of just the organic component of the forest fuels. The woody component comprises the largest fraction of the fuel and the carbon fraction of the woody material approaches 50%.

Generally ash is low (0.5% to 1%) in the woody material but is up to 7% of black spruce twigs. The duff and litter samples have 10% to 20% ash. This ash component should be investigated in more detail as a source of potential hazardous emissions, or useful tracers for smoke from forest burning. Since oxygen is the only other major component it can be estimated by difference. The propensity for soot or particulate matter emissions to form may be indicated by the oxygen content which covers a range of 35.6% to 46.2% for the Canadian samples. Soot formation is expected to increase with lower oxygen content, making the white birch bark an important source of soot.

3.0 SCOPE AND STUDY OBJECTIVES

The Intermountain Research Station served as overall coordinator for the United States effort and fielded a Fire Chemistry and Dynamics experiment within a portion of the large mass-fire. This report is a compilation of the equipment development, measurements, and interpretation of the results for the IFSL effort. It does not cover the coordinated study which is being reported on separately through a document being prepared jointly with the National Institute of Standards and Technology.

This report covers work performed for the 390 hectare Hill Township Prescribed Burn (Hill PB) conducted on August 10, 1989. The Hill PB was located near Chapleau, Ontario, Canada and was typical of management fires performed by the Ontario Ministry of Natural Resources in the Chapleau Region. The data collected for the fire dynamics experiment are for one fire and one section of the Hill PB, and although the quality of the data is good, the overall representativeness of the data can only be judged subjectively. Regardless, the objectives listed below were partially satisfied through the study of the Hill PB using a sophisticated system of sensors on towers and located in conjunction with ground packages for monitoring critical parameters for the prescribed burn.

Measurements were made of gas and particulate emissions, temperature, and airflow at a series of locations on an area of about 1 hectare. The objectives were:

1. To develop a Fire Air Sampling System (FASS) that can survive the harsh fire environment. (Appendix A)

2. To make multiple real time measurements of the concentration of major combustion gases including CO_2, CO, and O_2 as the fire spread through the array of towers.

3. To collect particles less than 5.0 um on filters for three phases of the fire; i.e. flaming, intermediate, and smoldering phases. The filter samples were used for graphitic, organic, and inorganic analysis of the content of the particulate matter.

4. To collect integrated samples of the gases for each fire phase for subsequent analysis and profiling of the trace organic compounds.

5. To obtain data for airflow parameters to improve fire behavior models.

6. To measure the rate of release of carbon from the fire on a unit area basis and develop a model for both the rate of consumption of the fuel and the rate of heat release on a unit area basis.

4.0 METHODS

This chapter provides details on the experimental methods used for the Canadian Mass Fire Experiments. The combustion chemistry and fire dynamics measurement protocols required the development of specialized sampling equipment to be used in the extremely hostile sampling environment. This section describes details of:

1. Selection of the site and location of the sampling packages (Section 4.1).

2. Development of the equipment that both operates in the hostile environment and that provides reliable sampling in an unattended sampling mode (Section 4.2 and Appendix A):

   A. Tower instruments for gases, particles, wind, and temperature.

   B. Ground instruments for O_2 and temperature.

   C. Controllers for video camera and field mill.

3. Sampling protocols used for real time and grab sampling of emissions (Section 4.3).

4. Analytical protocols to use on-board for real time measurements of gas concentration, vector winds, and temperature (Section 4.4).

5. Analytical protocols used for post-fire sample analysis Section 4.5).

6. Methods for calculating and analyzing results (Section 4.6).

4.1 Selection of the Site and Fire Information

Hill Township near Chapleau, Ontario, Canada was selected as the site for the initial PB. The area is located about 30 km northwest of Chapleau and about 200 km north of Sault Ste. Marie, Ontario, Canada. The site was selected because of the uniformity of fuels and the relatively flat terrain. The site consisted of tramped fuels of white birch (*Betula papyrifera* Marsh.) and poplar (*Populus tremuloides* Michx.) with some jack pine (*Pinus banksiana* Lamb.) and black spruce (*Picea mariana* (Mill.) B.S.P.). The area had been twice treated with herbicides prior to the prescribed burn on August 10, 1989.

The Hill Township PB was divided into four blocks with a total combined area of 486 hectares (Figure 4.1-1). Block A was about 100 hectares in size and located on a slightly elevated knoll. The IFSL Fire Chemistry and Dynamics array of towers and sampling devices was located on the west side of Block A.

Fuel loading as determined by Forestry Canada (McRae 1989) for the unit was about 19.4 kg/m^2. The fuel consumption for the 10 fuel triangles, excluding the area of wetlands, averaged 10.63 kg/m^2 with about 25%, 50%, and 25% consisting of fuels less than 7 cm, greater than 7 cm, and duff, respectively. The fuel moisture content for the fine fuels less than 0.5 cm in diameter averaged 23.3% with the duff fuel top two cm averaging 43.6% and lower layer 85.9%.

Weather associated with the Hill PB was influenced by a large area of high pressure loosely centered in Illinois eastward through Ohio (Rangno and Radke 1989). Generally, winds of less than 5.14 m/s carried moist, warm air from the central region of high pressure to the north across Ontario. The

dewpoint temperature was about 14 to 15 C during the time of the Hill PB with surface temperature of 26.0 to 26.9 C and relative humidity declining from 58% at 13:30 to 49% by 16:00. Surface winds were generally from the southwest at 3 to 4 m/s.

The Ontario Ministry of Natural Resources was responsible for all aspects of preparation for the prescribed burn, ignition of the unit, and fire suppression. Each block was burned in sequence starting with the block furthest to the east.

The Fire Chemistry and Dynamics array of sensors and towers was located on the northwest side of unit A. A 25 m spacing was selected for the six towers with five of the towers placed in a pentagon around a central tower. The tower placement and scale (Figure 4.1-2) were selected to optimize the measurement of fire parameters during the time that the lines of fire were burning together. Details concerning the fabrication and testing of the instrumentation are discussed in the following sections and in Appendix A. The fire behavior observations are presented in section 5.1.

4.2 Equipment Development

4.2.1 Design

Four types of instruments were developed to meet joint U.S. Forest Service-U.S. Defense Nuclear Agency 1989 Canadian Mass Fire Experiments project objectives. A Video Camera Controller (VCC), a Field Mill Data Logger (FMDL), a Ground O_2 Depletion Monitor (GODM), and a Fire Atmosphere Sampling System (FASS) were designed and fabricated by IFSL personnel. The operation of all systems is controlled by a microprocessor-based computer which has been designed primarily for instrument applications. Special considerations in the design of all of the systems were portability, power consumption, and exposure to the harsh fire environment. One each of the camera controller and field mill instruments, and six each of the ground O_2 monitor and atmosphere sampling systems were deployed to the field.

4.2.2 Video Camera Controller

A high resolution Panasonic Model AG-450 Super-Video Home System (S-VHS)[2] camera was purchased to provide a visual record of the fire as it passed through the FASS tower array. The camera was placed in a tower-mounted protective shroud which was approximately 30 m from the FASS

[2] The use of trade names and names of manufacturers of products does not constitute an endorsement for that product by the U.S. Department of Agriculture.

array. One disadvantage of this high resolution camera is that it has only a two hour recording capacity. This constraint forced the development of a camera controller to start recording only when the fire was approaching. It would have been far too dangerous for a person to be in the experimental unit to manually start the camera as the fire approached the array. Consequently the camera and VCC were turned on several hours before ignition of the unit and the VCC was programed to toggle the camera between the pause and record modes (240 seconds pause, 4 seconds record) until the fire was detected by the VCC. Upon detection of the fire, the VCC placed the camera in the full record mode. This combination produced a time lapse record of more distant events while still providing a continuous record of the fire as it passed through the array. Details of the VCC electronics design are given in Appendix A.

4.2.3 Field Mill Data Logger

A field mill was used to record electrical charge buildup in the plume. This field mill produced an output signal proportional to the charge in the plume. A computer-based data logger was developed to capture and store the data. The field mill and data logger were placed on the observation hill and data collection was started just prior to the ignition of the first unit. Refer to Appendix A for details on the field mill and data logger.

4.2.4 Ground O_2 Depletion Monitor

A limited amount of O_2 data was collected during 1988 which indicated the need for a higher sampling frequency to better characterize O_2 depletion in large fires. Because of the problems encountered with the previous year's system, development of an improved system to measure O_2 depletion was undertaken. Six such systems were fabricated and deployed for the 1989 mass fire experiments.

This new system (Figure 4.2.4-1) was designed to measure and record O_2 and temperature levels at 0.5 and 1.5 m above the ground surface. To protect the instruments from the intense heat, they were buried approximately 30 cm below the surface. Sample lines constructed of stainless steel tubing were used to transport combustion gases from the 0.5 and 1.5 m heights to the instrument. A buried cooling coil, also made of stainless steel tubing, and a glass wool filter were incorporated into each sample line to prevent damage to the pump and O_2 sensor. Electrolytic type O_2 sensors were used to measure the O_2 levels. Temperature was measured at the inlet of each sample line by a type K thermocouple. A more detailed discussion of the GODM hardware is given in Appendix A.

The instrument, which requires very little power to operate, can be buried several days before the burn takes place. For the 1989 experiments, the GODM was programed to start collecting pre-fire (background) information at 11:30 the morning of the burn. Data was collected at a low rate until the fire was detected, at which time the GODM went into a much higher frequency sampling mode (refer to Section 4.4.1, for a detailed discussion of sampling protocol).

4.2.5 Fire Atmosphere Sampling System

The FASS was the most sophisticated instrument developed by IFSL personnel for the 1989 Canadian Mass Fire Experiments. This system was designed to collect information needed to characterize the atmosphere just above the flaming zone. Information collected includes real time combustion gas concentrations, particulate matter production, combustion gas samples, and several fire dynamics parameters. The instruments were suspended, using standard television antenna towers, at a height of 12 m above the ground. The systems were designed to operate either independently, or, they could be electronically linked to each other for synchronization of data collection. To meet 1989 mass fire project objectives, the systems were configured to operate in the linked mode. The FASS network consisted of six systems for the 1989 mass fire experiments. A detailed description of the FASS design is given in Appendix A.

As with the other instruments developed for the 1989 Canadian Mass Fire Experiments, the FASS had an ONSET Corp. Model 5 computer controlling the acquisition of data. Test, calibration and data acquisition programs are written in TTBASIC (a special version of BASIC that runs on this computer) and loaded into the instrument using a ZENITH lap top computer. The lap top computer was used to display FASS data during calibration and testing, and can also be used to retrieve data from the FASS at the end of a field experiment.

Probably the most unique feature of the FASS is it's capability to measure important combustion gases in real time. Electrolytic type sensors were used to measure O_2 (0-21%) and CO (0-2000 ppmv) levels. The outputs of both the CO and O_2 sensor were linear over their specified ranges. An infrared type sensor was used to measure CO_2 (0-20,000 ppmv) concentration. The output of this sensor was non-linear and corrections, based on the manufacturer's information, were applied to the raw CO_2 data. During normal FASS operation, sample gases were pumped through the sensors at a rate of 250 ml/min. The FASS had an on-board supply of known concentration of CO and CO_2 gases, permitting calibration of the sensors prior to and/or during the experiment.

Both glass fiber and Teflon filter mats are used to collect particulate during each of the flaming, intermediate, and smoldering phases of the fire (for a total of 6 filters per FASS). For each of these fire phases, there are always two filters (one glass fiber and one Teflon) collecting particulate. Accompanying each filter there is a companion cyclone, which functions to exclude particles greater than 5.0 um in size. A pump, regulated to produce a flow of about 1.7 liters per minute, samples the fire atmosphere through the cyclone and filter. The FASS computer, through the use of electrically actuated valves, controls the exposure sequence and combination of filters by phase of combustion.

Two methods to collect and store samples of combustion gases are employed by the FASS. First, a sample of the gases is continuously pumped into special 5-layer, 2 liter mylar sample bags. There are three such sample bags for this purpose; one being used during each of the flaming, intermediate, and smoldering phases of the fire. Second, 0.8 liter stainless steel canisters are used to collect a high integrity, short duration (a canister takes about 15 seconds to fill) sample of the combustion gases. Again there were three canisters, one filled during each of the three phases of the fire. The timing of the filling of each canister is also controlled by the FASS computer. Details of the canister sampling protocol are given in section 4.4.2.

Fire dynamics sensors consisted of wind and temperature measuring devices located on the tower (Figure 4.2.5-1). A three dimensional wind measuring array was located at the top of each tower, at a height of 14 m above the ground. This array was constructed of three separate turbine type anemometers placed in an x-y-z configuration. Standard cup and vane type anemometers, as well as shielded thermocouple probes, were placed along the tower at the 3-, 6-, and 9-m heights.

The system was designed to be deployed in the field several days before the burn. Prior to being taken to the field each instrument was equipped with filters, gas sample bags, canisters, and sensor calibration gases. The data acquisition program was then down-loaded into the FASS from the lap-top PC. Before leaving the preparation site, each instrument was wrapped in a heavy duty aluminum foil shield. For the 1989 mass fire experiments, the systems were prepared and taken to the field the day prior to the burn. At this time the systems were placed on the towers and fire dynamics sensors connected to the instruments. To help prevent false triggering of the systems, the systems were not activated (armed) until noon of the day of the burn.

4.3 Analytical Methods for Real Time Measurements and Basic Calibrations

4.3.1 CO_2, CO and O_2 Sensors

Combustion gases passing through the FASS particulate filter pumps were available at the sampling manifold (Figure 4.3.1-1). In the normal (de-energized) state, a three-way solenoid valve selected these gases for the sensor pump. A 1.5 m coil of 3.2 mm stainless steel tube placed before the valve cooled the gas stream to the internal temperature of the package. This protected the valve and sensors from potentially high gas temperatures, and condensed excess water in the stream. A thermocouple in the gas stream recorded temperatures for post-burn evaluation. Voltage to the sensor pump was set to maintain a flow of 250 ml/min through the O_2, CO, and CO_2 sensors, plumbed in series. By minimizing volumes in the connecting tubing, the gas transit time between the external sample port and the sensors was kept to a few seconds. The sensor gas flow was finally vented outside the package.

The alternate selection (energized) for the three-way valve connected the sensor pump to a sample bag filled with calibration gas. A mixture of CO_2 (7310 ppmv) and CO (500 ppmv) in air provided a check of the sensor span during the fire. One liter of span gas in the bag allowed up to four minutes of span measurements.

The O_2 sensors were electrolytic cells manufactured by G. C. Industries Inc. The model 33-270 cells used are designed to measure O_2 in gas mixtures with CO_2 concentrations up to 20%. Both the sample packages mounted on the towers, and those buried in the ground used these O_2 sensors. The cells develop a voltage (nominally 45 mV in air) that is directly proportional to partial pressure of O_2 in the sample gas. All O_2 measurement channels were trimmed to read 422 +/- 1 at the A/D converter with 45.00 mV connected. Cells were sealed in a small cavity in an aluminum block, with gas ports to direct the gas sample past the sensing surface. This configuration gave a response time of about 15 seconds to 90% of a step change in O_2 concentration. Sensor accuracy was specified to be 2% of full scale (or 0.5% O_2) at constant temperature, and 5% of full scale over the range of 0 to 50 C. Several cells were tested to verify linearity, and zero mV response to pure N_2. A number of the cells proved to be defective (low response to air) and were replaced prior to the Hill PB.

The CO sensors were also electrolytic cells manufactured by G. C. Industries Inc. (model 44-300). These cells develop a nominal 200 microamp current for 1000 ppmv CO, and the current output is linear with concentration. A signal conditioning circuit converts this current to a voltage readable by the system A/D converter. Cells were sealed in flow-through aluminum blocks, similar to those used for the O_2 sensors. Response time was expected to be about 15 seconds, as for O_2 sensors. Linearity was specified to be 1%, and accuracy depended on the CO concentration accuracy of a calibration gas mixture.

The CO_2 sensors were non-dispersive infrared gas monitors manufactured by Valtronics (Model 2015 BMC). This sensor is supplied on a single printed circuit board that contains the signal conditioning. The board develops 0 volts at 0 ppmv, and 1 volt at 20000 ppmv. Sensor response is not linear but a calibration curve is supplied by the manufacturer. This curve was assumed to apply to all of the sensors after zero and gain adjustments of the system A-D converter were accounted for. A two point calibration, using ambient air (assumed to be 375 ppmv CO_2) and a standard gas mixture (7310 ppmv CO_2), allowed calculation of the zero and gain adjustments. Tests with zero air either dry or humidified (about 100% relative humidity at 25 C) showed negligible (less then 0.25% full scale) interference due to water vapor. Accuracy was specified to be within 3% of full scale.

A final calibration check was performed on all real time gas sensors within two weeks before the Hill PB. The sample packages were set to either draw span gas or dry air in the calibration mode. Air pulled through an anhydrous calcium sulfate scrubber (to remove water) was used to check the O_2

sensor span, and the zero level of the other sensors (assuming a 21% v/v O_2, 1 ppmv CO, and 375 ppmv CO_2). A calibration mixture of 7310 ppmv CO_2 and 500 ppmv CO was supplied from a small tank to calibrate the span of CO_2 and CO sensors.

An unexpected leak in the gas bag valves was discovered that caused uncertainty in calibrating the real time CO and CO_2 sensors. The valves only seal in the closed position, but have a small leak when connected to the package plumbing with the valve open. This leak causes a slow loss of gas, and a more serious composition change. Apparently, there is a significant exchange of the bag contents with outside air. Thus, the bag concentration of CO and CO_2 approaches that of air. Tests on bags of calibration mixture (7310 ppmv CO_2 and 500 ppmv CO) showed a decrease of about 1% of the initial value per hour. The largest errors occur in the real time sensor calibration bags that were in the package for about 28 hours. This probably allowed a decrease in the concentration of 25 to 30%. The calibration measurements based on these bags were rejected, and instead the final calibration checks made with direct flow from the span tank (see previous paragraph) were used to calculate real time CO_2 and CO. These data do not allow for instrument span drift but, are the best data available. This source of errors will be eliminated in future experiments.

4.3.2 Wind Sensors

Wind anemometers for horizontal measurements were manufactured by Digitar (model AN-2). These are inexpensive plastic cup and vane anemometers giving wind direction and speed. The direction vane was connected to a one turn resistance potentiometer, of nominally 20 kohms. The actual resistance was measured for each anemometer with an accurate ohm meter and used to correct the direction measuring circuit to read 0 to 360 degrees. The vanes were attached to the anemometers such that winds from the north would read 0 degrees. Cup rotation causes a switch closure that can be sensed and counted to relate to wind speed. The calibrated wind tunnel facility at the Intermountain Fire Sciences Laboratory was used to check the calibration of each anemometer at 4.5 m/s. Calibration of six anemometers at wind speeds up to 18 m/s showed that cup rotation frequency was a non linear function of wind speed, and that all six had essentially the same sensitivity. The threshold where cup rotation started was 1.3 m/s, so no data are available below this. The average rotation frequency at 4.5 m/s for the 18 anemometers used in the Hill PB was 6.9 Hz with a standard deviation of 0.4 Hz. Lack of time prevented more accurate calibration so the average at 4.5 m/s was used for all and the response was assumed for simplicity to be linear from 1.3 to 4.5 m/s. Wind speeds measured the day of the Hill PB were mostly below 5 m/s. Counting accuracy in the 0.5 second measurement period was potentially a source for considerably larger errors (+/- 1 count out of 3 or 4).

Tri-axial wind speed was measured by three turbine anemometers manufactured by Qualimetrics (model 24201). Construction of the device is described in Appendix A. These anemometers were much more sensitive to low wind speeds than the Digitar devices described above. Calibration of one of these anemometers in the IFSL wind tunnel was used for all 18 anemometers placed in the Hill PB. A two segment linear equation was used to convert the sensor reading to wind speed. One segment was in the range of 0 to 1 m/s (20 counts on the A-D converter) with a zero intercept, and the other for 1 m/s and above with a non zero intercept. Wind speed accuracy is expected to be within about 0.25 m/s. The analog measurement method did not have the measurement errors associated with digital counting of small numbers (the optical sensors also failed during the measurement rendering the digital wind speed measurements unreliable).

4.3.3 Thermocouples

All thermocouples exposed to the fire environment were constructed of 24 gage type K (chromel/alumel) wire protected by a braided stainless steel sheath. Thermocouples within the sample packages were 30 gage with a glass fiber sheath. The temperature measuring circuit included electronic

cold junction compensation. All external temperature measuring channels were trimmed to read 512 +/- 1 counts at the A/D converter with 41.574 mV (corresponding to 1024 C, assuming .0406 mV per degree C) applied to the amplifier input. Temperatures inside the sample package were measured with circuits trimmed to read 512 +/- 1 counts at the converter with 20.787 mV applied to the amplifier input (about 1 C per A/D count). This simplified linear approximation gives temperature accuracy within 4 C from 0 to 400 C, with a larger error of 19 C high at 900 C. Considering other expected errors in temperature measurements within fires, no other corrections were made to the data.

4.4 Sampling Protocol

The system computer was programed to time and control data acquisition events during the experiment. Separate programs controlled the tower mounted fire atmosphere sampling systems (FASS), buried ground O_2 depletion monitoring (GODM) systems, and the field mill experiment. These programs are listed in Appendix B. In general, the objective was to maximize the data collected during the most intense 10 to 40 minutes of the fire. It was also necessary to record baseline data (at a lower sampling rate) prior to the fire as well as smoldering data for several hours after the fire front had passed. Frequency of data collection was limited by the computer speed in digitizing and saving a set of readings, and the size of storage memory. All computer clocks were set to real time (EDT) based on the Hill PB experimental clock. This section gives details on the timing and sampling used.

4.4.1 Real Time Sensors

The FASS was programed to wait until 1200 hours before any data was taken. At 12:00, the sampling pumps were activated to sample the calibration gas bag for a span check on the real time gas sensors. After a one minute stabilization delay, all sensors were read for 5 seconds at 2 reading per second. These 10 readings were saved as a pre-fire calibration check. From this time on the FASS was armed and could accept a trigger from a temperature activated fire sensor. Every 2 minutes the program activated the pumps and other electronics for 30 seconds and then made one reading of background (no fire) data. These data provide an ambient air measurement for the gas sensors, pre-fire wind speed and direction, air temperatures, and internal system parameters. A circular buffer in computer memory saved only the last 2 hours (60 points) of background data prior to fire detection.

The tower packages had 2 ways to enter the main fire monitoring mode: either a temperature sensor on the ground exceeded 67 C; or a wire link indicated that one of the other tower packages had sensed the trigger temperature (all tower packages were linked). Thus, the first package to detect a fire signaled all packages that a fire was approaching. The temperature sensors used for triggers were placed in piles of fuel up to 30 m west of the tower array, in the direction anticipated for ignition.

The next 40 minutes after fire detection were viewed as 3 fire phases: a 10 minute flaming phase; a 10 minute intermediate phase; and, a 20 minute smoldering phase. There is little difference in the sampling protocol for real time sensors during these phases. All parameters were sampled every 0.5 second, and all data were saved to EPROM (4800 points). The only difference was at the start of the smoldering phase when the calibration bag gas was pumped through the gas sensors for 1 minute (120 readings) to provide a check for CO_2 and CO sensor span drift. After the 40 minutes of high frequency sampling, the package returned to taking 1 reading every 2 minutes, as in the pre-fire sampling phase. This extended smoldering phase continued until the tower package was turned off, or filled storage memory (all readings were saved).

The buried GODM primarily measured O_2 depletion and air temperature. The sampling protocol was somewhat simpler than the tower packages, but similar. The buried packages started testing for a fire every 2 seconds at 11:30. Every 2 minutes the program activated the pumps and other electronics for 30 seconds and then saved one reading of background (no fire) data. These data provide an

ambient air measurement for the O_2 sensors, air temperatures, and internal system values. Only 60 of these readings were saved, as for the tower packages.

A reading of 33 counts (about 66 C air above the buried package) on either of the 2 external temperature channels triggered the GODM program to advance to the flaming phase. There was no link between buried packages so all 6 triggered independently. During the next 10 minutes the sensors were read every 0.2 seconds to provide nearly continuous data (3000 points). After 10 minutes, the package switched to taking 1 reading every 2 minutes, as in the initial background phase. This final smoldering phase lasted until the program was stopped or memory filled. All data were transferred to a more powerful computer after the package was retrieved.

4.4.2 Integrated Filter, Gas Bag, and Canister Samples

The tower packages collected physical samples during 3 of the sampling phases, for later analysis. The program selected a different pre-weighed membrane (Gelman Teflo R2PL037) and glass fiber (Millipore AP40 037 05) filter for each phase. One of 3 solenoid valves selected the correct filter for each filter type. These phases were described in section 4.4.1, above. Thus, particulate matter was collected for a 10-minute flaming phase, a 10-minute intermediate phase, and a 20-minute smoldering phase. Filter flow rate was controlled at about 1.7 l/min to provide a 5 um particle diameter cut point. Initial and final filter weights were made in the IFSL balance room. Filters were conditioned at 50% relative humidity and 22 C for 24 hours prior to weighing. Filters were weighed to 0.001 mg on a Cahn model C-32 microbalance. Filter blanks were within 0.010 mg before and after the experiment. Filters were stored in sealed plastic filter cassetts (Millipore M000037A0) between weighings. The cassettes attached directly to the sample package during the experiment.

A portion of the filtered gases from the filter pump was routed to gas sampling bags. Three bags were filled in each tower package over the same time intervals as the three filter particulate samples discussed above. A filling rate of 150 ml/min provided a 1500 ml sample for the 10 minute flaming and intermediate phases, and a 50 ml/min provided a 1000 ml sample for the 20 minute intermediate phases. New, unused bags were opened and connected to the sample pump the day before the Hill burn, and sealed and removed about 5 hours after the burn. Bags were returned to IFSL for CO_2 and CO analysis, 28 days after the burn.

Other samples of combustion gases were collected in 800 ml canisters. The canisters were specially cleaned and evacuated by the Oregon Graduate Center. Three of these canisters were connected through a three way Teflon manifold to a 25 cm, stainless steel sample probe. The goal was to collect an uncontaminated sample of the gases for analysis of trace components. Each canister was filled by opening the electrically activated filling valve for 30 seconds. Tests showed that the canisters filled at a nearly linear rate to about 95% of atmospheric pressure in 15 seconds. The flaming phase canister was filled either six minutes after the fire was detected or if the 3 m air temperature exceeded 500 C, indicating intense burning. The intermediate and smoldering phase canisters were filled three minutes into the phase. The main canister valve was closed about 5 hours after the burn when the packages were removed from the burn area.

4.5 Analytical Methods for Post-fire Sample Analysis

4.5.1 CO_2, CO, and Trace Gases

The gas sample bags filled during the Hill PB (see section 4.4.2, above) were analyzed for CO_2 and CO composition using infrared gas analyzers (Horiba model PIR-2000). A specialized method that required a minimum of gas was used since most bags contained only 500 to 900 ml of gas. Both analyzers were plumbed in series and connected through a valve to a vacuum pump. A second valve was connected to a hypodermic needle that was inserted through the septum on the gas bag. The analyzers were evacuated to < 0.002 kg/cm^2, then quickly filled to atmospheric pressure (about 0.92 kg/cm^2) with the contents of the gas bag. This method requires about 200 ml of gas. Bags of zero air and a span gas mixture (7310 ppmv CO_2 with 500 ppmv CO) were analyzed along with the sample bags in order to adjust the instrument zero, and to calculate bag composition. The analyzers have a linear output such that an unknown composition can be calculated by multiplying the instrument output (Volts) by the sensitivity to span gas (ppmv/Volt). The accuracy of this method is about +/- 1% composition for both CO_2 and CO. The problem with the leaky valve on the bag (discussed in section 4.3.1) could have caused some dilution of sampled gases with ambient air. This would result in CO_2 and CO levels about 5% low, assuming a 1%/hour change for the 5 hour period before the valve was closed. This problem will be eliminated in future experiments.

The gas canisters were analyzed for CO, CO_2, and CH_4 by the Oregon Graduate Center in Portland, Oregon. Standard gas chromatography techniques were used.

The membrane and glass fiber filters were weighed at IFSL to determine smoke particle loading. Particles smaller than a mean mass cutpoint diameter of 5.0 um were collected with the combination of cyclone and flow rate used. The membrane filters were also analyzed for trace metals using an x-ray fluorescence method at NEA Inc. of Beaverton, Oregon. The glass fiber filters were analyzed for graphitic and organic carbon fractions by Sunset Laboratories, using a ramped temperature protocol for carefully volatilizing the organic carbon fraction while retaining the graphitic carbon fraction.

4.6 Calculated Parameters and Methods of Adjusting Data

4.6.1 Emission Factors

The carbon-mass balance (CMB) method was used to estimate the amount of fuel consumed that produced emissions and all the emission factors reported here. The technique was first used successfully under field condition by Ward and colleagues (1979). The method is based on the stoichiometric partial oxidation of a typical fuel ($C_6H_9O_4$) to CO_2 mixed with products of incomplete combustion. The carbon contained in the fuel is assumed to be 50% of the fuel mass. Further refinement of this percent carbon composition is not warranted given the complexity of the fuel array that typically burns. The total carbon contained with the combustion products is measured and divided by 0.5 to calculate the mass of fuel involved in the combustion. Emission factors are calculated by dividing the mass of the emission by the total fuel consumed and expressed in units of g/kg.

Basically, the CMB method accounts for carbon released due to fuel combustion by measuring the concentration of important carbon-containing combustion products. The total fuel consumed was computed based on the sum of the mass of carbon of the combustion products as follows:

$$W_v = \frac{\sum C_n}{R} \tag{1}$$

where,

W_v = fuel consumed, g/m^3,
C_n = the carbon mass of emission n, g/m^3,
n = CO_2 , CO, PM, and
R = the carbon fraction of the fuel elemental analysis.

It immediately follows that an emission factor (EF) for a specific emission can be computed by dividing the mass of the emission contained in a unit volume by the total fuel consumed in producing the emission in that volume as follows:

$$EF_{n[p]} = \frac{E_{n[p]}}{W_v} \tag{2}$$

where,

$EF_{n[p]}$ = emission factor for emission n, g/kg,
$E_{n[p]}$ = concentration of emission n, mg/m^3, *and*
$[p]$ = phase of combustion–flaming, intermediate, or smoldering.

The instrument deployed in the fire collected bags of combustion gas and smoke particles on several types of filters. These samples were integrated for the length of time assigned to flaming, intermediate and smoldering phases. The mass concentrations of carbon in CO_2 and CO needed for equation (1) follow directly from the gas analysis on the bags:

$$C_n = \frac{(CV_{n[p]} - CV_{n[Air]})12}{MV} \tag{3}$$

where,

CV = volume concentration ratio for emission n, ppmv,
MV = molar volume of gas at experiment temperature and pressure, $l/mole$, and
$CV_{n[Air]}$ = the ambient concentration of emission n.

The weight of a mole of carbon is 12 and the molar volume of the gases was assumed to be 24.5 l/mole. The background concentrations of CO_2 and CO in air were assumed to be 375 and 1 ppmv, respectively. A similar calculation using the weight of a mole of emission gives the concentration of emissions, needed in equation (2).

Smoke particle concentrations for equation (2) were calculated from the average of the mass collected on the two filter media (membrane and glass fiber) divided by the volume of air sampled. These volumes were calculated by integrating the real time filter flow rates over the time the filter was selected. Multiplying the mass concentration by 0.55 (the assumed carbon fraction of the particles), gives the particle carbon mass needed in equation (1). Other emissions not measured were assumed to make a negligible contribution to the calculation of fuel consumed.

The real time CO_2 and CO sensors give concentrations that can be used in equation (3) as a check on the gas bag concentrations. The sample flow rate to the bag can be assumed to be constant during the bag filling time for each phase. Then, the average of the real-time sensor over that filling time should equal the concentration measured for the bag. These alternate values are compared in a following section.

4.6.2 Rate of Fuel Consumption

The rate of fuel consumption during the fire was measured by the carbon flux technique. By measuring the concentration of carbon, converting this carbon to fuel according to equation (1), and multiplying the fuel per unit volume by the vertical velocity of the emissions, the resulting flux represents the rate of fuel consumption (with units of mass per unit area per unit time), as follows:

$$\dot{w} = (W_v)(v_2) \qquad (4$$

where,

$\dot{w}$ = rate of full consumption, $g/m^2/s$, *and*
v_2 = vertical velocity of plume, m/s.

The real time CO_2 and CO sensors are used for individual emission concentrations, and all other emissions are assumed negligible. A cumulative fuel consumption is calculated by integrating the rate of fuel consumption curve from time i to j as follows:

$$W = \int_{i=1}^{j} \dot{w} dt \approx \sum_{i}^{j} \dot{w} \Delta t$$

where,

W = total full consumed, g/m^2, and
Δt = time interval between measurements of $\dot{w}$, s.

A constant value of 5.0 s for the time interval between measurements gives a reasonably accurate sum.

4.6.3 Source Strength

The rate of emission production is calculated by multiplying the emission concentrations by the vertical velocity of the emission, similar to equation (4). The resulting emission flux (source strength) has units of mass per unit area per unit time.

4.6.4 Rate of Heat Release.

The rate of heat release (reaction intensity) can be computed by multiplying the rate of fuel consumption by the fuel heat of combustion corrected for the heat remaining in the products of incomplete combustion (such as CO). This total heat release rate is calculated as follows:

$$I_r = \dot{w}(H_f - \sum((H_n)(EF_n/1000))) \quad (6$$

where,

I_r = rate of energy release, kW/m^2,
H_f = heat of combustion of fuel, kJ/g, and
H_n = heat of combustion of emission$n$, kJ/g.

The real time CO concentrations are used as the only significant emission in the calculation. A heat of combustion of 20 kJ/g is estimated for the fuel (McRae's slash value) and 10.1 kJ/g for CO (Perry's Chemical Engineers' Handbook, 4th edition). The resulting reaction intensities were not corrected for heat losses due to radiation and soil heating.

5.0 PRESENTATION OF DATA

In this chapter, the general fire behavior and deviations from ambient conditions for each of the measured parameters are discussed. Concentration of combustion products and the "normalcy" of the data are presented. Comparisons are made of the concentrations of various combustion gases and the multiple measurements of these gases through grab sampling and real time techniques. Oxygen deficiency for the various locations relative to the concentrations of biomass and height above the fire are discussed. The general measurements of the wind field parameters are presented.

5.1 Fire Behavior

Block A of the Hill PB had a total area of 96.98 hectares. Ignition of Block A commenced at 14:19 hours with approximately 8 hectares involved by 14:23 hours. At 14:22 hours, a line of fire was ignited 50 m to the east of the array of towers (Figure 5.1-1). Approximately 2 minutes later, three segments of fire were ignited 60 m to the west of the tower array and this line of fire terminated at the fire break test site just to the south. By 14:25:44, the fire had advanced from the central segment of fire to within 25 m of the base of FASS package tower 12. The triggering mechanism was activated in this location and the six FASS packages were awakened simultaneously and began sampling the environmental parameters.

Fuels were distributed across the tower array non-uniformly. This contributed ultimately to the spread of the fire through the FASS array. Windrows of concentrated heavy fuels, resulting from the cable clearing of the area, extended toward the NNE and FASS tower 12 was on the easterly edge of one of these windrows. FASS towers 16 and 13 were in a second windrow with a third windrow passing just to the east of FASS towers 14 and 15. The centerline of each of the 3 windrows of heavy slash are shown by the lines of x's in Figure 5.1.1. The fire spread along these windrows more rapidly than between the windrows so that the spread pattern actually tended to follow the windrows and seemed to move forward from windrow to windrow in pulsing actions. Potentially, some of the pulsing periodicity of the fire could have been associated, on a micro scale, with the spread of the fire between windrows of fuel.

The rate of spread of the fire from the line of ignition to the trigger location was calculated to be about 0.5 m/s. Flame lengths were on the order of 8 to 15 m based on video coverage of the burn area and from photographs taken from a helicopter observation point. The main fire front flanked along a line extending from FASS tower 12 to 13 toward FASS tower 16 in the middle of the sample array while a finger of fire was running through the array from FASS tower 11 toward FASS tower 15. The north flank of the finger along a line from FASS 11 to FASS 15 and the southerly flank spreading southward from FASS 12 and FASS 13 converged in the vicinity of FASS packages 16 at approximately 14:29:00 or about 4.25 minutes after the FASS packages were activated.

The burnout time for the fire was on the order of 1 to 3 minutes depending on the location in or between windrows. This affected the duration of the flaming phase emissions production at all of the FASS package locations as well as the GODMS measurements at ground level.

There were three major convergence zones associated with the fire ignition pattern for Block A of the Hill PB that could have affected the measured patterns of airflow in the vicinity of the FASS packages.

1. The first of these occurred during the time that the center fire was converging to the east of the FASS array. This was believed to occur during the time period from 14:26 to 14:30.

2. The second occurred soon after ignition of the area to the west of the fire break test area during the time that the lines of fire were converging at approximately 14:34.

3. The third occurred during the time that major segments of the fire on the southwestern flank of Block A were converging to the south and slightly to the east of the FASS array.

The ignition of Block A was completed by 14:38.

5.2 Gas Concentrations

The concentrations of the primary gases needed for carbon balance calculations and emission factors are available from the analyses on gas sampling bags and the real time sensors. Table 5.2-1 contains the results of the sample bag analysis for CO_2 and CO, by sampling phase. CO_2 is highest for the flaming phase, with the highest level measured for package number 14, at 4490 ppmv. Intermediate phase values drop to about 50% of the flaming value, and the lowest levels (1224 ppmv) occur during the smoldering phase on package 13. CO_2 levels were quite uniform across the sample array with deviations from the average of about 11% during flaming, and only 3% during smoldering. Trends in CO concentrations with fire phase are less obvious, and these values tend to be uniformly between 120 and 200 ppmv. Both the highest and lowest CO concentrations were measured during the intermediate phase. Flaming phase CO averaged about 12% lower than the later phases but the data are not very consistent.

Primary gas concentrations were measured by the real time CO_2 and CO sensors. Continuous measurements were made during the three fire phases. The average of the concentration curve over the time assigned to a phase should be equal to the sample bag concentration (assuming the flow to the bag is constant). Figure 5.2-1 shows the real time sensor concentrations for FASS package 11. The CO_2 levels in curve A show the high variability of these levels; from near ambient levels to 9000 ppmv during the 10 minutes of the flaming phase. The rapid response of the CO sensor, in curve B, emphasizes the variability even more. Comparison of curves A and B in the first 200 to 300 seconds of flaming show the high efficiency of the initial flaming pulse, with little CO produced. The CO concentrations increase relative to CO_2 as the fire goes to the smoldering phase. The nearly constant region at about 14:46:40 is due to switching a flow of calibration gas to the sensors. The composition of the gas bag decreased due to a leaky valve, so these calibrations were not used in the data analysis. However, these calibration regions show that the sensors are stable when the composition is constant, and that the system response to a step change is fairly fast.

Table 5.2-2 provides a summary of real time sensor results for all tower packages, by phase of combustion. The second smoldering phase data were taken from the two hours of sampling following the initial forty minutes of the fire. Figure 5.2-2 (A and B) shows a comparison of average CO_2 and CO as a scatter plot of the real time results versus the sample bag measurements. Clearly, there is good agreement between the two methods. A linear regression of the CO_2 data gave a slope of 1.17 with $r^2=0.93$ (the intercept is forced to zero). The high slope is attributed to remaining difficulties in calibrating the sensor and a slight decrease in bag CO_2 due to leaky valves. The valve leak is not expected to account for more than a 5% drop in the CO_2 concentration, so the sample bag measurements are considered to be the most accurate. A plot of the CO data (in figure 5.2-2 B) gave a linear regression line slope of 0.966 with $r^2=0.28$. The relatively small range of concentrations measured leads to the poor fit, but the two methods give comparable concentrations. The agreement should improve as we improve the real time sensor calibration methods. Relative differences of 3 to 5% should be possible in future experiments.

Oxygen levels were measured in real time by the tower mounted systems. An example of the O_2 measurements is shown in figure 5.2-3 with the O_2 level calculated as a percent of the average pre-fire air level (presumably close to 0.21 volume fraction). The curve shows early minima of about 90 to 92% of air level, or a decrease of about 0.02 volume fraction. Some broad decreases in O_2 level can be seen in the remaining curve, but most of the detail is lost in noise and drift of the sensor. Table 5.2-2 includes O_2 averages by phase for all the tower systems. The averages in all phases were 98 to 100%,

except for the final smoldering phase where sensor drift dominates. The O_2 sensors should be improved in resolution or accuracy for this application on relatively dilute combustion gases.

Theoretical O_2 levels can be calculated for a $C_6H_9O_4$ fuel, using the CO_2 and CO concentrations also listed in Table 5.2-2. Figure 5.2-4 shows a theoretical plot of O_2 level versus measured CO_2 volume fractions, for several levels of CO production. More CO in the products (smaller $[CO_2]/[CO]$ ratio) tends to slightly decrease the O_2 level for the same CO_2 concentration. Since most of the CO_2 measurements during the Hill PB were below 10000 ppmv (0.01 volume fraction), the O_2 levels are predicted to be more than 93% of background air levels. More typical CO_2 levels of 3000 to 5000 ppmv result in O_2 levels more than 97% of background air levels. Figure 5.2-5 A shows a scatter plot of the measured O_2 averages against the theoretical values. Curve 5.2-5 B shows corresponding data for the maximum CO_2 and CO (minimum O_2). The O_2 values are in the correct range but sensor noise limits the value of the measurements. Measured O_2 levels were generally lower than theory values at the maximum rate of combustion during the flaming phase. The O_2 system needs to be improved for future experiments.

Gas canisters were filled during each phase of the fire. A summary of the canister composition analysis for CO_2, CO, and CH_4 is given in Table 5.2-3. Attempts to validate the real time sensor calibrations with canister data failed due to the short filling time for the canisters (<15 seconds) and rapid composition changes at the sample point. Also, the canisters sampled gases from a different location on the tower package, where the composition could be quite different at any given time. In general, the canister CO_2 values are lower than the real time sensors at the sample time, while the canister CO analyzed higher. Future experiments should collect canister samples over longer time periods to obtain a better average composition for the phase. The CH_4 concentrations are a factor of 10 or more lower than those for CO. Calculations of fuel consumption rate and combustion efficiency can ignore the contribution of CH_4, considering other measurement uncertainties.

5.3 Particulate Matter Concentrations

The tower packages collected particulate matter by fire phase on two filter media (glass fiber and Teflon). The measured particulate matter weight divided by the average real time flow rate during a sampling phase gives the particulate matter concentration. Table 5.3-1 gives these results by fire phase. Particulate concentrations ranged from 15.1 mg/m^3 to 39.9 mg/m^3. These concentrations are about 5 to 10 times lower than those of CO, and therefore make a smaller contribution to the carbon balance and combustion efficiency calculations. Concentrations calculated for the glass fiber substrate are generally highest. All packages were within about 25% of the average value for a phase. The smoldering phase has slightly higher concentrations and produces more total particulate matter in the 20 minutes sampling time. The average for the two filter media was used to calculate emission factors for PM 5.0.

The glass fiber filters were analyzed for carbon content, proportioned between graphitic and organic carbon. Table 5.3-2 lists the filter carbon analysis, with mass percents separated into percentages of organic particles and graphitic carbon particles. The organic carbon percent averaged lowest for the flaming phase (45.5%) and increased at later times into the smoldering phase (53.6%). There is considerable variation during the flaming phase, reflecting the highly turbulent fire and entrainment of ash and soil particles. Graphitic carbon averaged 8.1% during the 10 minutes of flaming, and decreased dramatically in the smoldering phase (1.5%). The intermediate phase results are in close agreement with those for the smoldering phase. Low graphitic carbon during the intermediate 10 minutes indicates a substantial decrease in flaming combustion. The total percent carbon in the fine particles is approximately equal for all three fire phases.

The Teflon filters were analyzed for trace inorganic elements. Table 5.3-3 (A,B,C,D) lists the trace element composition as a percent of the total particulate mass, by combustion phase. The calcium

levels were very high compared to other reports and are probably due to the soil chemistry at the burn site. Considerable levels of elements from aluminum to calcium were measured, along with manganese, iron and zinc. Although there is considerable variation between tower boxes, the S, Cl, and K are highest during flaming, while Al, Si, Ca, and Fe tend to increase in the smoldering phases. These results are consistent with other studies. The weighted profile in the table is a function of the fuel type, and can be useful to trace the dispersion of smoke from these prescribed burns. Figures 5.3-1 and 5.3-2 show a comparison of the Hill PB elemental profile to those from experimental burns in California and the Pacific Northwest. The two figures have different scales to emphasize the range of element concentrations. The high calcium and manganese from the Hill PB are quite distinctive.

5.4 Temperature Measurements

Air temperatures were measured with thermocouples placed at 3-, 6-, and 9-m heights on the FASS towers. A fourth thermocouple just outside the FASS (at about 12 m) measured gas temperatures at the inlet of the smoke sampling system. The GODM system also had thermocouples near the sampling probe orifice at 0.5 and 1.5 m above mineral soil. Both types of sampling packages had thermocouples near the gas sensors inside the packages, for monitoring internal temperature changes during the fire.

Survival of the sensitive instruments in a harsh fire environment requires the internal temperatures to remain close to ambient. The buried GODM's had the large heat sink of moist soil, and were expected to remain cool. Internal GODM temperatures remained within 2 degrees C of their pre-fire values through the most intense flaming phase. GODM number 4, however, increased about 10 degrees in four hours due to the burnout of a large pile of logs on the surface. This increase was well within the operating parameters of the GODM. Additional data on the GODM air temperatures are given in Section 5.6, below.

Thermal protection of the FASS depended on a low density ceramic insulation and a highly reflective aluminum outer wrap. Figure 5.4-1 compares the internal gas flow temperature to the external fire environment temperature of the inlet, for FASS 11. While the outside temperatures reached over 150 C, the internal box temperatures increased only about 10 C. Table 5.4-1 lists the average and maximum exposure temperature by fire phase for all six FASS packages. Although FASS 12 was exposed to air temperatures as high as 450 C, average temperatures for the flaming phase ranged from 80 C to 137 C. There was no damage to any of the FASS packages. The modest internal temperature changes suggest that both ground and tower system designs can withstand much more severe fires.

The 3, 6, and 9 m air temperatures measured by the FASS units were subject to high noise and drift caused by electronic noise generated within the systems. Some of this problem was apparently caused by ground loops, which will be corrected in future modifications. Generally the FASS packages show only a 1 to 2 minute time period during the flaming combustion phase when temperatures are above 100 C. Maximum temperatures during this most intense time were 250 C to 350 C, although FASS 15 had a thermal pulse to 470 C. Air temperatures quickly dropped below 100 C with only brief pulses above 100 C during the first 10 minutes of flaming. Noise and drift problems in the present systems limit more detailed analysis of the dynamic behavior of the temperature field in this fire. The computer control and high sampling rates possible with the FASS should provide data from future fires for such analysis, after current problems are corrected.

5.5 Wind Speed and Direction

Wind speed and direction in the horizontal plane were measured prior to and into the initial moments of flaming, at 3-, 6-, and 9-m heights on the FASS towers. We also measured the vector components of the wind field at the 14 m height using a more robust triaxial system (discussed in section 6.5.1

and 6.5.2). The anemometers at the 3-, 6-, and 9-m heights were quickly destroyed by the fire, but provided information on the effect of the fire's approach on the local wind field. Figure 5.5-1 (A and B) shows how the wind speed and direction changed up to the time of sensor failure for the 3-m height. In general, there was good agreement for all six tower anemometers at all heights and the average can be used. Exceptions to this are discussed in the results section and are thought to show minor perturbations due to fire induced winds. Low sensor resolution limits the accuracy of the wind velocity measurements to about +/- 25%. Wind speed is seen to increase from around 3.5 m/s at the time of ignition (14:20) to as high as 6.5 m/s when the fire crossed the array. There is considerable uncertainty in anemometer accuracy just before the end of the data when they were destroyed. The ambient wind direction was about 270 degrees (west) at ignition and tends to increase slightly during the fire (but becomes quite variable).

Wind speeds were also measured in three dimensions by the set of turbine anemometers positioned above the FASS, at the top of the tower. The positive or negative direction sensors on these anemometers failed but the absolute values of the vector wind speed are considered reliable. Other data indicate that the wind was always from the west, and predominately slightly south of west. Of special interest was an azimuth deviation built into the alignment of the triaxial system which allowed the north-south quadrants of the wind field to be identified. In other words, during placement of the anemometer heads on the towers, the alignment proved to be about 20 degrees different between FASS 11 and FASS 14. It can be deduced by examining the absolute values that when FASS 11 was larger than FASS 14, the wind was from the southwest quadrant. When FASS 14 was greater than FASS 11, the wind direction was from the northwest quadrant. These results are consistent with the 2-dimensional horizontal wind direction measuring system located at the same tower locations.

Vertical wind directions should be mostly up, due to buoyancy of the hot combustion gases. Generally, we expected the temperature and CO_2 concentrations to be correlated with the vertical velocity of the combustion gases. In fact this was found to be a valid correlation and for the FASS tower location, we found no evidence during the flaming and intermediate sampling periods for significant down drafts. On occasion, the concentration of excess CO_2 dropped to near zero and for these same times, the vertical velocity was noted to be near zero. We concluded that the errors in calculating the rate of fuel consumption and the rate of heat release from the carbon mass balance considerations to be minimal. Future system modifications will provide more accurate direction data. The vertical velocity was used in conjunction with the real time gas sensors to calculate the mass flux of carbon from the fire site (discussed in section 6.1). Figure 5.5-2 shows the vertical velocity, Figure 5.5-3 shows the horizontal direction, and Figure 5.5-4 shows the vector velocity, for the forty minutes of most active fire for the FASS packages that were operational during the fire. FASS 13 never responded and may not have been connected during deployment and FASS 15 developed sensor failure in the vertical dimension at 14:28 due to the plastic direction indicator slipping into the turbine.

5.6 GODM O_2 Depletion and Temperature Measurements

The ground O_2 depletion monitoring systems provided O_2 levels and temperatures at 0.5 m and 1.5 m heights above the mineral soil. O_2 readings before the fire ignition were used to scale all readings to percent of the background air level (0.21 volume fraction). Figures 5.6-1 through 5.6-4 show sets of GODM curves for the four packages that triggered correctly on the fire. Table 5.6-1 summarizes the data obtained from these systems.

The trigger times in Table 5.6-1 indicate the rapid rate of fire spread when it entered our sensor array. Each GODM was programed to trigger and change to a rapid reading rate when a thermocouple temperature of 66 C or more was sensed. (The two systems that triggered prematurely probably received a noise spike or had bad thermocouple connections). GODM 1 sensed the fire first at 14:27:40, and GODM 4 triggered last, 28 seconds later at 14:28:08 (Figure 5.1-1). Since these

locations were about 38 m apart, the fire could have been spreading at about 1.5 m/s (if the fire front moved along a line between these two sensors).

The O_2 level reached a minimum of 41.9% of the background air level, at the 0.5 m height at GODM 4. The O_2 depletion was greatest at the 0.5 m level. GODM 4 was located within a large pile of logs that contributed to the resulting low O_2 levels. GODM 1 was in an area of relatively low fuel loading, on the southwest side of the array. This system showed the least O_2 depletion and highest average O_2 level during the fire. GODM 6 was in the center of the tower array and had only slightly less depletion at the 1.5 m height compared to the 0.5 m height, for the first 3 minutes of the fire. There was also a large pile of small diameter fuel within a meter upwind of the probes from GODM 6. The large flame structure from this pile probably caused both sample probes to be in the flame envelope for much of the flaming time. Based on these data, it seems clear that the fuels within a few meters of the air sampling probes are very important to the magnitude and duration of O_2 depletion. The local fuels must be thoroughly characterized for interpretation of results from future experiments with these systems.

The O_2 depletion at ground level lasts for only a short time. The pulse for GODM 1 was only about 1 minute long, with a rapid return to levels of 90 to 95 % of background air. The other systems had somewhat longer depletion times (up to 3 minutes) and were slower to reach a constant level after the main pulse had passed. The duration of the pulse should be a good measure of the flaming time, and could be used to separate flaming and smoldering periods of the fire. All systems showed repeated minor pulses of 15 to 20 seconds duration, in both the O_2 level and temperature curves. None of the curves showed a return to ambient temperature or O_2 levels, indicating that large volumes of fresh air do not move through the fire area. Mixing between combustion gases and fresh air is fairly complete, as indicated by the relatively smooth decay of the O_2 depletion and thermal pulses.

The fine fuels (< 1 cm) that burn out in the first few minutes of a fire are expected to experience the most pronounced effects of O_2 depletion on emission factors (for the products of incomplete combustion). Larger fuels with burning times more than about 3 minutes are likely to burn with O_2 levels 80 to 90% of normal ambient levels, even in large area fires such as the Hill PB. The much longer duration smoldering phase has close to normal O_2 concentrations available. Thus, it is likely that only small fractions of the total emissions of smoke particles, CO, and hydrocarbons were produced under highly O_2 starved conditions in the Hill PB. Fires in areas with predominately fine fuels may exhibit a much stronger dependence of emission factors on fire size due to significant O_2 depletion.

At the 1.5 m height there seems to be considerable mixing with fresh air to bring O_2 levels closer to near normal (even though the flame heights were much higher at times). The O_2 levels at the FASS height (12 m) are within a few percent of those at the 1.5 m height. This indicates that most of the mixing and cooling due to fresh air occurs within the first 1 or 2 m above the ground. This is consistent with Albini's model (1981) where 10 times the stoichiometric air volume can be entrained within the flame structure.

The air temperatures generally follow the O_2 depletion sensors, except that there is little difference between temperatures at the two sensor heights. Maximum temperatures were generally close to 1100 C, although GODM 1 only reached about 800 C. Problems with the temperature sensing circuit limit the accuracy of these estimates. The close agreement between temperatures at the two heights was seen for all systems, so it does not seem to be an artifact of the data. It is unclear if the sensors were within a flame envelope, or outside the flame where mixing with fresh air could occur. Mixing that increased the O_2 level should also lower the air temperature. However, changes in O_2 level from the 0.5 m to 1.5 m height were not reflected in lower temperatures. This result should be investigated in more detail in future experiments.

5.7 Z-Values

Because of the response time for the different sensors, it was necessary to adjust the data sets for each sensor to a common time base. This was done through converting the data to Z-values which is a way of normalizing the deviations from their respective means. The four sets of data (vertical wind speed, CO concentration, CO_2 concentration, and temperature) were transformed into their respective z-values by the formula:

$$Z_i = \frac{(X_i - X)}{\sigma}$$

where,

X = Average of the data set,

σ = Standard deviation of the data set.

The resulting transformed data sets were then each centered about zero, with positive values representing original data that is above average and negative values representing original data that is below average.

The use of z-values removes the effects of differences in averages and variances between data sets. Furthermore, the magnitudes of variation about the common average of zero are comparable. Consequently the transformed data sets can be compared for common patterns or different behaviors over their common time frame.

Once the z-values were plotted, it was evident that a small time lag of a few seconds existed for the response of the CO and CO_2 analyzers relative to wind speed and temperature. Upon adjusting for this lag, the patterns for all four transformed data sets match extremely well (Figure 5.7-1). The temperature and wind speed lag values were set to zero, the CO times lagged 5 seconds, and the CO_2 times lagged 10 seconds.

6.0 RESULTS

In this chapter, we discuss some of the interactions between fuels, weather, and fire behavior on rate of release of emissions and heat. Unusual patterns are identified in conjunction with wind direction, pulsations of the wind field, and fire spread in the vicinity of the FASS array. The rate of fuel consumption is used in evaluating the rate of emissions production for Block A over time as well as the total rate of heat release corrected for combustion efficiency. The emission factors are presented by combustion phase and weighted for the entire fire.

6.1 Introduction to Rate of Fuel Consumption

The rate of fuel consumption was measured by the carbon flux technique using equation 4.6.2-(4). The rate of fuel consumption is important for calculating source strength and the rate of heat release over the life history of the fire. Here we use the data from the vertical wind velocity, CO concentration, and CO_2 concentration to calculate the rate of release of carbon from the biomass fuel. In an effort to develop a generalized rate of fuel consumption expression for the Hill PB, the general shape of the rate of fuel consumption from ignition to extinction is fit with a linear expression for the flaming phase and an exponential decay function for the diedown phase. Four of the six FASS packages yielded satisfactory data for calculating rate of fuel consumption (FASS packages 11, 12, 14, and 16). The integrated fuel consumption is compared with the fuel inventory measurements of total fuel consumption by Forestry Canada (McRae 1989).

6.1.1 Measured Rate of Fuel Consumption

The measured rates of fuel consumption for individual packages are presented in Figure 6.1.1-1. The peak rate of fuel consumption occurred in each case during the time when the fine fuels were consumed by the advancing fire. Peak rates of fuel consumption were measured of 40.8, 64.5, 61.4, and 36.1 g/m²/s for packages 11, 12, 14, and 16, respectively. Figure 5.1-1 shows the time of ignition for the fuel immediately surrounding each tower location. The maximum rate of fuel consumption occurred at an elapsed time from triggering of the FASS sample packages of 2.83, 1.00, 4.33, 2.5, and 4.33 for packages 11, 12, 14, 16A, and 16B, respectively. (For FASS package 16, two peaks of fuel consumption were measured and are identified as 16A and 16B.) The spread of the fire through the FASS array and the peak rates of fuel consumption coincide with the distribution of windrows of high concentration fuel and the streets between the windrows. From Figure 5.1-1 and section 5.1, the windrows adjacent to and upwind from FASS towers 12 and 14 contributed to the high rates of fuel consumption. In addition to a windrow being immediately upwind of FASS tower 16, the fire converged immediately under FASS tower 16 and probably contributed to both the sustained high rate of fuel consumption and the double peak phenomena observed for the rate of fuel consumption curve shown in Figure 6.1.1-1 for FASS 16.

The ambient winds were substantial averaging 3.1 m/s at 1400 (McRae 1989) immediately prior to ignition of block A of the Hill PB. Undoubtedly smoke drifted into the region of flux measurements, since the fire was ignited in steps starting with the center-fire and extending out past the FASS array in an ever increasing circle. This could have influenced the measurements more during the diedown phase than during the initial ignition phase. It is likely that some of the emissions created in the vicinity of the FASS packages exited the area without being accounted for through the carbon mass-balance and flux measurements. The overall significance is not known, but is thought to be no greater than the level of error associated with the fuel consumption measurements.

The region of low rate of fuel consumption for the 4 sample packages demonstrated in Figure 6.1.1-1 from time 14:31 to 14:38 lasted about 5 to 6 minutes. This apparent lull in the fire is believed to have resulted from the convergence of the flame fronts outside of the FASS array. A very high horizontal air flow component and an apparent zero carbon flux could have resulted from the large inflow of air

across the FASS array. In fact, by viewing Figures 5.5-2 to 5.5-4, this is well-illustrated showing the higher than normal horizontal airflow component and a near-zero vertical air flow.

6.1.2 Total Fuel Consumption

Total fuel consumption for each of the 4 sets of measurements was calculated by integrating the area under the rate of consumption curves shown in Figure 6.1.1-1 as a function of time according to equation 4.6.2-(5). The cumulative fuel consumption over time is shown in Figure 6.1.2-1. Total fuel consumption averaged 11.46 kg/m^2 with a standard deviation of 1.65 kg/m^2. The range of fuel consumption of 9.76 to 13.61 kg/m^2 coincides with the areas of total fuel loading (Figure 5.1-1). The rate of fuel consumption was still decreasing at the end of the sample period and averaged 1.06 g/m^2/s after 40 minutes of sampling. The slope of the integral of fuel consumption continues to have a significant positive component through the end of the smoldering sample period. Figure 6.1.2-1 shows a very steep rate of fuel consumption component over the first 4 to 6 minutes following ignition during the time when the fine fuel component is consumed. The time of occurrence of the periods with high rates of fuel consumption coincide with the arrival of the fire at the respective tower locations.

The fuel consumption was calculated for the flaming, intermediate, and smoldering combustion periods by integrating the rate of fuel consumption curves over the limits of integration for those periods of time (Table 6.1.2-1).

The average total fuel consumption for the area of the six FASS towers was computed to be 11.46 kg/m^2. This compares with the inventory value from data collected by Forestry Canada of 10.63 kg/m^2 or about 8% greater than the ground inventory. The fuel consumption for the flaming phase may have been overestimated based on temperature, CO/CO_2 ratios, and typical burnout times for loadings of fine fuels such as were inventoried on the Hill PB. In other words, we used a sampling time of 10 minutes which could have been longer than necessary for the flaming phase. Examining the fuel consumed for the first 6 minutes for each FASS package yields measured fuel consumption averaging 4.22 kg/m^2. This is about twice the fine fuel loading on the unit. However, an additional component of fuel including a portion of the duff and larger diameter fuel fractions was consumed during the flaming phase.

6.1.3 Mathematical Fit of Rate of Fuel Consumption

In this section, mathematical expressions are fit to the rate of fuel consumption data so that other source strength and heat release calculations can be made for the entire area of the Hill PB. Modeling the fuel consumption process is beyond the scope of this report. Ward and Hardy (1984, 1986) and Ward et al. (1989) modeled the rate of fuel consumption using a similar set of carbon flux data for broadcast burns of logging slash on clearcut units in Oregon and Washington. They used an equation that provides for an exponential growth and decay of the combustion process. We use a linear growth function to describe the buildup phase and an exponential decay function for the diedown phase.

The four sets of data for the rate of fuel consumption illustrated in Figure 6.1.1-1 were averaged (Figure 6.1.3-1). The maximum rate of fuel consumption was approximately 20 g/m²/s which occurred 4.5 minutes after the sensors were first challenged by the approaching fire. A linear fit with a slope of 0.074 g/m²/s was used for the buildup phase. The diedown phase uses an exponential decay function stretched over 2 hours of time with a time-decay constant of 10 minutes. The two equations are of the form:

$$w_f = \frac{0.0714 t_f^2}{2}, \quad \frac{g}{m^2}$$

and

$$w_s = 20 t_s \left(1 - \text{EXP}\left(\frac{-t_s}{\text{T}}\right)\right), \quad \frac{g}{m^2}$$

where,

w_f = fuel consumed during the flaming phase,

t_f = duration of flaming phase,

w_s = fuel consumed during the smoldering phase,

t_s = duration of smoldering phase, and

T = time decay constant.

The fit of the curves to the averaged rate of fuel consumption curve, yielded a fit with about a 28% larger total fuel consumption than the measured inventory value (Figure 6.1.3-2). Several factors were involved in developing the fit. First of all, the shape of the rate of fuel consumption curve was assumed to be similar to that measured for other prescribed burns of logging slash (Ward and Hardy 1986, Ward et al. 1989). Secondly, the period of time from about 10 minutes to 12 minutes after the sampling started was assumed to be a result of the large convergence zone for the fires burning together to the south of the FASS array. This convergence outside of the area of the towers, is believed to have influenced the wind field in the vicinity of the towers but probably did not affect the rate of fuel consumption, but did affect the measurement of the rate of carbon release. Therefore, some of the carbon was blown horizontally away from the region of the towers. Evidence for this is supported by the low vertical wind speed during this period, and the high horizontal wind speed vectored toward the fire convergence zone. By using the exponential decay function, a good fit was achieved for the period from 12 minutes to the end of the sampling period. In addition, because of the indicated high rate of fuel consumption sustained at the end of the sampling period, the model was extended for another 80 minutes.

The general shape of the rate of fuel consumption was scaled to the average total fuel consumption for the Hill PB as measured by Forestry Canada. This was done by ratioing the 5-minute interval fuel consumption increments by the ratio of the Forestry Canada fuel consumption of 10.64 kg/m² divided by the measured/modeled fuel consumption of 14.70 kg/m² (Table 6.1.3-1).

The Fuel consumption values by 5 minute intervals will be used in computing the source strength for particulate matter, CO, CO_2, and other compounds as a function of the rate of ignition for the unit.

6.2 Emission Factors and Emissions Released Per Unit Area Burned

Emission factors were calculated from equation 4.6.1-(3) as discussed in section 4.6.1. The CO_2 and CO concentrations from Table 5.2-1, and the averaged filter particulate PM5.0 concentrations from Table 5.3-1 were used in these calculations. Table 6.2-1 shows the resulting emission factors for each of the FASS packages, by phase of combustion. Combustion efficiencies are also listed in Table 6.2-1. Both the CO and PM5.0 emission factors increase with time during the fire, from initial flaming

to final smoldering. Results from the six sample packages showed good agreement. The average PM5.0 increased from 7.17 g/kg during flaming to 25.6 g/kg during smoldering. Emission factors for CO increased from 46 g/kg during flaming to 174 g/kg during smoldering. Combustion efficiency decreased from 95% for flaming to 82% for smoldering as a result of the increased emissions of incompletely oxidized combustion products.

Figure 6.2-1A shows the average CO emission factors compared to results from fires in Douglas-fir and hardwood slash in the pacific northwest. There is excellent agreement with the hardwood slash, but the Hill PB has somewhat lower CO emission factors than for Douglas-fir slash. Figure 6.2-1B shows the average fine particle emission factors from the Canada fuels compared to the northwest US fuels. There is good agreement during the flaming phase, but emission factors for the Canada fuels are about twice those for the US northwest fuels. For PM5.0 during the smoldering combustion phase.

Emission factors are weighted based on the fuel consumed during each of the sampling periods for the flaming, intermediate, and smoldering combustion phases of 5.679, 3.154, and 1.831 kg/m^2, respectively (Table 6.1.3-1). The emission factor data from Table 6.2-1 for each sampling period is multiplied by the fuel consumed during the sampling period and summed. This sum represents the total emissions produced by the fire on a square meter basis (Table 6.2-2).

The total emissions released per square meter of area burned was 132.6, 917.4, and 17843 g/m^2 for PM5.0, CO, and CO_2, respectively, based on the adjusted total fuel consumption measured by Forestry Canada. By dividing the total emissions by the total fuel consumed, a fire-weighted emission factor is calculated for the Hill PB of 12.4, 86.0, and 1673 g/kg for PM5.0, CO, and CO_2, respectively.

6.3 Source Strength Calculations

The total emissions released from the Hill PB can be calculated based on the Forestry Canada fuel consumption and the fire weighted emission factors developed through this research. The total area burned of 390 hectares multiplied by the emissions released per square meter (section 6.2) yields a total emissions production of 581, 4012, and 66425 tonnes of PM5.0, CO, and CO_2 for the Hill PB. Block A, the area of most intense interest of about 100 hectares in size, released about 25% of the emissions of the total Hill PB.

To compute a source strength requires information pertaining to the rate of ignition of the fuels and the rate of consumption during the burnout time for the fuels. We have fit mathematical expressions to the rate of consumption of the fuel on a square meter basis. The fuel consumption lags behind the ignition as shown in Figures 6.1.3-2. The exponential decay function shows that 99.6% of the fuel is consumed within one hour following ignition.

The next step, which both Forestry Canada and NIST are developing, is to estimate the rate of ignition of the area. We are suggesting that this be done by 5 minute intervals and have gone through an example demonstrating how the data would be used for estimating source strength of the various emissions and the total heat release for Block A as a function of time. Figure 6.3-1 shows the hypothetical rate of ignition of Block A. The ignition may have progressed much differently than that illustrated, however, the same analysis can easily be extended to the real data when it becomes available.

Assuming that the ignition reached a steady state 20 minutes after starting the center fire and that the remaining fires burned together within 10 minutes following the end of the helitorch ignition, the ignition would have reached a steady state of about 350 m^2/s. This would have resulted in maximum rates of production of PM5.0, CO, and CO_2 of nearly 0.047, 0.326, and 6.341 tonnes/s. Of special interest is the time from ignition of the center fire over the following 15 minutes when the bulk of the

emissions are from the flaming combustion phase (Figure 6.3-2). After the first 25 minutes, the PM5.0 emissions are produced at a higher rate by the smoldering combustion process. Other emissions can be computed accordingly.

6.4 Rate of Heat Release

The rate of fuel consumption, discussed in section 6.1, can be combined with the heat of combustion of the burned fuels to calculate a rate of heat release. Equation 4.6.4-(6) shows that the rate of heat release calculation should consider the heat of combustion of all the unburned products of combustion. In practice only the major unburned product, CO, needs to be considered to make a significant, contribution. The other products of incomplete combustion, such as particulate matter, CH_4, and other hydrocarbons, make up a relatively minor fraction of the carbon flux. This mixture may have a heat of combustion close to the original fuel. Essentially, these other products can be left out of the carbon flux as well as the heat balance calculations. The loss in accuracy due to this assumption is relatively minor compared to other experimental uncertainties.

The real time CO_2 and CO analyzers provide all the data needed to estimate combustion efficiency and the rate of heat release for the area of the FASS array. Figure 6.4-1 shows how the combustion efficiency averaged over the six towers changes over the 40 minutes we sampled the gases. Combustion efficiency was calculated simply from concentrations, $[CO_2]/([CO_2]+[CO])$, after corrections for ambient levels of these gases. Combustion efficiency is initially high (near 100%) since no CO was measured. The combustion efficiency steadily decreased to around 94% over the first 6 or 7 minutes, and remained fairly constant for the next 10 minutes. At 14:45 the efficiency dropped again over about 10 minutes to about 88%, where it remained for the rest of the sampling period. The heat released by combustion of the fuels would be equal to the theoretical fuel heat of combustion (assumed to be 20 kJ/g) early in the flaming, and decrease as more CO is produced and the heat of combustion of that CO is not converted by the fire. For example, if 10% of the original fuel carbon is converted to CO, the heat of combustion of that CO can be subtracted from the heat expected from the total fuel burned.

Figure 6.4-2A shows the calculated rate of heat release, averaged for 4 of the FASS packages. Note that this curve follows the rate of fuel consumption curve very closely since the effective heat of combustion is fairly constant (due to the relatively small amount of CO produced). Peak heat release rates of about 500 kW/m² were calculated about 5 minutes after the fire was detected near the array. The heat release quickly decreased to levels of from 100 to 200 kW/m² for the remainder of the burn. The total heat released is found by integrating the heat release rate curve over time. This total heat release is shown in Figure 6.4-2B for packages 11, 12, 14 and 16. The total heat release expressed in MJ is approximately 20 times the total fuel consumption expressed in kg. Values for the effective heat of combustion during the first 10 minutes of flaming, 10 minutes of intermediate burning, and final 20 minutes of smoldering are calculated in Table 6.4-1. The overall average heat of combustion for the area was calculated as 19.22 MJ/kg, or about 96% of the theoretical total (20 MJ/kg). Effective heat of combustion decreases with time from ignition, as expected from the decrease in combustion efficiency. The decreases are small and could be ignored in a first order approximation, given the expected uncertainty in measuring the heat of complete combustion for these mixed fuel arrays.

The average effective heats of combustion can be applied to the calculation of the total heat release rate over the entire area burned in block A of the Hill PB. These calculations parallel those for source strength, developed in section 6.3. The rate of fuel consumption shown in Figure 6.1.2-1 is combined with effective heats of combustion by fire phase from Table 6.4-1, and with the hypothetical function for the area ignited over time (Figure 6.3-1). The entire block rate of heat release is shown in Figure 6.4-3. The contributions from the 10 minutes of flaming and subsequent 30 minutes of smoldering are also indicated in the figure. An estimated 75,000 MW heat release rate is predicted about 45 minutes after the helitorch ignition started. These estimates can be improved with better models for

the area ignition rate being developed by Forestry Canada and NIST. Some of this heat is lost to soil heating or is radiated away, but a majority heats the surrounding air and smoke to provide the driving force to build the strong convection column.

6.5 Fire Induced Winds

In this section, we discuss in more detail the pattern of air flow through the FASS array during four periods: 1) the arrival of the fire fronts, 2) the 10 minute period of intense flaming combustion in the vicinity of the FASS array, 3) the period of intense flaming combustion immediately to the south of the FASS array, and 4) the period of intense flaming combustion further to the south of the FASS array. The limitations of the air flow measuring systems are discussed in detail in sections 4 and 5.

6.5.1 Horizontal Wind Speed and Direction

The horizontal wind speed and direction at the 6- and 9-meter levels on the FASS tower along with the triaxial wind measurements at the 14-meter level are analyzed here. Figure 5.1-1 shows the position of the fire front for various times following ignition on both the eastern and western sides of the FASS array. Such factors as slope and the distribution of fuels along with the wind influence were important to the spread of the fire through the FASS array. These factors tended to confound the effect of buoyancy on wind flow patterns through the array. However, for the period from 14:24 to 14:34, the action and interactions of the areas of intense release of heat and rapid combustion of fuels had a major impact on both the horizontal and vertical air flow.

Detailed wind speed and direction data for the 3-, 6-, 9-, and 14-meter levels for each of the FASS packages is presented in Figures 5.5-1 to 5.5-4. The sharp spikes noted in Figures 5.5.1A to 5.5-1F occurred during the time of maximum heat load on the anemometers and, in general, directly preceded failure of the plastic anemometers (as planned). As a result of the ambient wind field speed of about 3.5 m/s, any fire induced effect would most likely occur as the main fire front approached the wind sensors. In effect, the change in direction noted for FASS packages 14 and 15 at the 6-meter level from time 14:27:45 to 14:28:45, resulted from the two fire fronts burning together between these two towers (Figure 5.1-1D). The same general trend is noted at the 9-meter level for FASS 14 but not for FASS 15 (Figure 5.1-1F). An examination of the 14-meter level data for the same time period for FASS 15 and FASS 16 towers shows a reversal in the delta direction during the time period. The direction indicator was not operable for the 14-meter height for FASS 14. The anemometer failure coincides with the arrival of the fire front at the FASS packages as documented from photography and other means, e.g., anemometer failure (Figure 5.1-1).

Other periods of convergence and divergence of the wind field are noted by examining Figure 6.5.1-1. A positive difference indicates that there is a convergence of the streamlines between FASS packages. For example, a positive deviation for (16-11) at the bottom of Figure 6.5.1-1 indicates that the wind direction at FASS 16 is further toward the north than at FASS 11. If the difference is negative, this would suggest that the general circulation relatively between the towers is diverging. It is apparent from Figure 6.5.1-1 that long periods of convergence and divergence were sustained during various periods of the fire. For example, divergence existed between FASS packages 12 and 15 preceding the intense burnout period between the towers which occurred at 14:29 to 14:32. This latter period resulted in a convergence between 12 and 15.

6.5.2 Vertical Component of the Wind Field

The vertical component of the wind field changed as the fire moved through the FASS array. The disposable plastic anemometers were lost and the fluid motion was only describable from the triaxial vector measuring system. Several prominent features were exhibited including an acceleration of the horizontal and vertical motion, an apparent pulsing of the vertical component of the windfield, and

minor shifts in wind direction during the fire convergence and diedown stages. Generally, the horizontal convergence and divergence should be coupled to the vertical motion of the wind field in the vicinity of the activity. The perturbations resulting from the line fire and the finger of fire moving into the FASS array makes the analysis and interpretation very complex. Our original study plan called for two lines of fire to join along a centerline bisecting the FASS array. This would have occurred if the line of fire resulting from the southerly finger of fire had advanced toward the east further to the south by about 20 m. Then, the two flanks of fire from the north and the south would have converged inside the FASS array. Alternatively, some useful information is available from the chance spread of the fire through the array. We examine in detail the distribution of vertical velocities within the FASS array and attempt to interpolate between FASS packages.

Generally, three major pulses were noted as the fires moved through the FASS array (Figure 5.4-2). The periodicity of the vertical motion could have resulted from influences from the larger fire on the FASS array or the distribution of fuels in the windrows and streets in the vicinity of the FASS array (Figure 5.1-1). We have mapped the apparent distribution of vertical motion across the FASS array onto the fire spread map by 30-second time intervals (Figures 6.5.2-1a to 6.5.2-1o). The maximum vertical wind speed over a 15-second averaging period ranged from 4.5 to 5.3 m/s for 5 of the 6 FASS towers (Figure 5.4-2 and 6.5.2-1). No measurements were made with FASS package 13. In general, the vertical wind velocity tracked the areas of maximum rates of heat release. The association of the maximum vertical speeds with convergence is not evident from a preliminary visual examination of the data set. There is a general shift in the relative differences in direction that takes place at 14:29 as the fire converges and moves on out of the FASS array.

6.5.3 Local Areas Affected by High-Intensity Combustion

Local areas of high-intensity combustion affected the airflow through the FASS array. Immediately to the south of the FASS array, the ignition was delayed because of the intersection of the lighting path with the fire break test matrix. As a consequence, there was little heat from the southerly flank during the time discussed in 6.5.2 above. However, once this area was lit, the fire ran slightly upslope across the fire breaks and created an extremely intense area of flaming combustion that lasted for about 4 minutes. The result was a strong shift in wind direction and speed at the FASS array location. All of the vector anemometers responded to this change in wind motion.

It is of particular interest to examine the convergence that preceded the change in wind direction and then the long period of divergence from 14:34 to 14:36 followed by a period of general convergence (Figure 6.5.1-1). Just to the south and slightly to the east of the FASS array, the flank fire increased in intensity and became a heading fire during this 2 to 3 minute period. It is clear that the wind direction shifted to a greater extent closest to this area of high intensity fire activity. Our data shows that the streamlines of air flow into the area of intense burning shifted further to the north for the southerly FASS packages during this period. The surface wind speed increased from about 4 to 6 m/s. The photography tends to corroborate this change in direction at the surface as seen from the smoke tracers from smoldering combustion sources in the vicinity of the FASS array and elsewhere to the north of the fire break test area.

It is not as clear from the preliminary analysis what caused the second shift in wind direction noted from time 14:45 to 14:50. Generally, it is accepted that a major convergence of lines of ignition took place to the south of the fire spread matrix during this time period which tended to pull the wind around from the southwest to a northwesterly direction. The same decrease in vertical velocity accompanying the shift in direction from the converging fires close to the FASS array were not noted during this second time period.

6.6 Periodicity, Data Dynamics

An investigation of the periodicity of the data was undertaken to determine if there was a cyclic nature to the fire (i.e., if the fire was pulsing at a consistent frequency) and to characterize the power distribution of the fluctuations.

To determine how the FASS measured parameters changed dynamically, Z-values (Section 5.7) were calculated for the gas, temperature, and vertical wind data sets. The Z-values fix the fluctuations of the data around a zero mean. Graphs of the power spectra (periodograms) were generated using Fourier series techniques. Auto correlations were calculated within a data set (e.g., auto correlation of CO_2 for the flaming phase of FASS 14), and cross covariances were calculated between two data sets (usually between two FASS packages). The latter two statistical techniques basically give a measure of how well events can be predicted at some time in the future, given information about the present.

Analysis of the power spectral densities, determined that only data collected from FASS 11 during the flaming phase displayed a significant periodic character. More typical data are shown in Figures 6.6-1A and 6.6-1B, which are periodograms of the CO_2, CO, temperature, and vertical wind speed as measured by FASS 14 during the respective flaming and smoldering phases of the fire. Neither diagram displays any strong periodicity in the data, although there are a couple of interesting peaks on both graphs in the frequency range of .0158 to .0398. Both graphs, however, indicate that most of the energy lies in the lower frequencies (less than .1 Hz or 1 cycle per 10 seconds). It is clear that the vertical wind speed has a more prominent low frequency energy component during the flaming phase as compared to the smoldering phase. Differences between CO_2, CO and temperature are more difficult to assess, however it appears that CO_2 and temperature have a greater composition of higher frequencies during the flaming phase, while the inverse is true for CO.

Figures 6.6-2A and 6.6-2B are correlograms of FASS 14 data collected during the flaming and smoldering phases of the fire. Note how closely the CO_2 and temperature correlation coefficients track during the flaming phase of the fire. This is not surprising, since the majority of CO_2 production occurs during the hottest portion of the fire. Probably of greater interest is the differences between the phases. The slope of the temperature and CO_2 graphs decrease and probably this indicates the relatively greater importance of the longer time lags (lower frequencies). Changes in the CO_2 coefficient more closely follow the fluctuations of the CO during the smoldering phase. The two CO correlations, show the least amount of change, although the coefficients drop off more quickly during the smoldering phase, which tends to support the power spectrum analysis that there is a shift towards greater energy at the higher frequencies. The vertical wind speed, which has a significant correlation coefficient out to almost one minute during the flaming phase, goes to zero almost immediately, indicating a random process, during the smoldering phase.

Figure 6.6-3 is a correlogram of the heat release rates for flaming and smoldering phases of the fire as calculated from FASS 16 data. The correlation coefficient continues to drop for the duration of the flaming phase. During the smoldering phase of the fire, the coefficients drop off rapidly for the first 30 seconds of lag. For lag times greater than 30 seconds, the correlation coefficient remains about 0.3. Although the coefficient is low during the smoldering phase, it is relatively consistent, and this indicates that the heat release rate is more constant during this phase.

Figure 6.6-4A and 6.6-4B are heat release cross covariances of FASS systems 12, 11, 14, and 16. Systems 11, 14, 16 were correlated with 12, which was used as the reference since it was the first to measure fire parameters. Figure 6.6-4A shows the correlations for flaming phase. Significant rises in the 12-11 coefficient at a lag of 20 to 30 seconds, in the 12-16 coefficient at a lag of 1 minute, and in the 12-14 coefficient of approximately 3 minutes, are related to the spread of the fire through the array (see Figure 5.1-1).

Figure 6.6-4B shows the corresponding cross covariances for the smoldering phase. Note the slight rise in FASS 14 and 16 coefficients at approximately 5 to 10 seconds of lag. These phenomena are probably due to wind transported CO_2 and CO, which are used in heat release rate calculations. In comparison to the flaming phase, the fluctuations are much less extreme and have the same general form, indicating that heat is being released more uniformly across the array in the smoldering phase.

7.0 SUMMARY AND CONCLUSIONS

Erratic and unpredictable fire behavior and smoke emissions from large fires are major problems globally. The ignition source and to some extent the fuels consumed are incidental to the problem since major fires have occurred on very large-scales, historically, in many different fuel situations from the tropical forested areas to the arctic and in biomass fuels as well as urban complexes. The study of large fires requires very special planning and instrumentation of such major proportions that one organization cannot possibly accommodate all of the complexity.

Because of the need to understand the fundamental dynamics of large fires for a variety of reasons, the U.S. Defense Nuclear Agency, U.S. Forest Service, and Forestry Canada have jointly studied the physical, chemical, and atmospheric aspects of large prescribed fires in the Canadian Province of Ontario. Some of these fires have been as large as 900 hectares. The Hill Township Prescribed Burn (Hill PB) was 390 hectares in size and burned on the 10 August 1989. Airborne sampling of the emissions was performed by the University of Washington, Aerosol and Cloud Physics Research Group; fire dynamics measurements were made by Pacific Sierra Research Corporation; wind field and fire dynamics measurements were made by the University of Iowa; surface temperature measurements by the National Institute of Standards and Technology; fuel characterization, weather, and fire temperatures by Forestry Canada; and the chemical and fire dynamics interactions study by the Intermountain Fire Sciences Laboratory (IFSL). The result was a highly integrated research study. The IFSL served as overall coordinator for the United States effort and fielded a Fire Chemistry and Dynamics experiment within a portion of the large mass-fire. This report is a compilation of the equipment development, measurements, and interpretation of the results for the IFSL research. It does not cover the coordinated study which is being reported on separately through a document being prepared jointly with the National Institute of Standards and Technology.

The objectives for the IFSL included the development of several specially designed sampling packages for collecting detailed measurements. The variables measured included temperature at several heights and locations; CO, CO_2, and O_2 concentrations; wind speed and direction at 3-, 6-, 9-, and 14-m heights. Discrete samples of particulate matter and gases were collected as grab samples from each of the 6 towers sequentially for a 10-minute flaming, 10-minute intermediate, and 20-minute smoldering period. The samples were analyzed for trace gas composition, and graphitic, organic, and inorganic content of the particles. The measurements were needed to define the combustion parameters associated with the production of various emissions including graphitic carbon and trace gases as a function of oxygen deficiency and combustion efficiency.

Perturbations of fires on the wind field are poorly understood and measurements near the surface were needed to correlate the wind phenomena with the rate of heat release both locally and in nearby areas removed from the sampling location. An array of 13-meter towers were positioned in a pentagon shape around a central tower on about a 25 m spacing. A video camera was aimed at the fire area and used to document some of the visible fire phenomena associated with the spread of the fire through the array. The sampling was triggered by thermocouples located around the perimeter of the array which started a 40 minute period of intense sampling that netted nearly 12 Mbytes of data.

The 100 hectare Block A was ignited with a center fire to the east of the sampling array prior to ignition of a line of fire to the west of the sampling array. A westerly wind of about 3 to 4 m/s pushed the line of fire through the sampling array in one head fire-flanking action on the north, while a finger of fire penetrated the array to the south. The net effect was a time lag between the major fire features at the various tower locations. The fires from the north and south burned together near the centerline of the array. Horizontal wind speeds increased by a factor of two during the period of convergence of the fires. Vertical air movement measurements were made that showed pulses of vertical motion away from the fire. The correlation of these pulses with the fire is visually associated with windrows

of heavy concentrations of fuel across the array and potentially secondarily associated with other fire phenomena.

The streamlines of air motion through the array of towers showed periods of convergence and divergence periodically during the time that the fire was spreading through the array. The divergence of the streamlines of airflow through the array was particularly pronounced for one 5 minute period of time. The general distribution of wind direction across the array showed a 20 degree differential wind direction from over the 50 m separation from north to south.

The vertical measurements of air flow are coupled with the concentration of CO_2 and CO to calculate the mass flux of carbon released by the fire. The rate of carbon release is coupled to the mass loss rate of fuel. The rate of consumption of the fuel is modeled with a rapidly increasing linearly fit function and an exponential decay function. The total consumption measured through a pre- and post-fire fuel inventory indicated that 10.63 kg/m^2 of fuel was consumed. The measured fuel consumption based on the carbon mass-flux indicated 11.46 kg/m^2 or about 8% greater than the ground inventory.

Peak rates of heat release of 500 kW/m^2 were measured during the time that the flame front was passing through the FASS array. Combustion efficiency ranged from near 100% to a low of 88% as calculated from the real time sensor information. The combustion efficiency calculations from the grab samples were lower than the real time measurements.

The modeled rate of fuel consumption was adjusted to the inventory value and used to distribute the fuel over the duration of the fire for any given square meter from the time of ignition to extinction. In this way, by knowing the rate of ignition, an evaluation of the rate of fuel consumption for the entire unit, by flaming and smoldering combustion processes, was made. Measurements of the combustion efficiency were used to adjust the heat of combustion to a mean value of 19.22 MJ/kg. The rate of release of heat, particulate matter, CO, and CO_2 for Block A are estimated based on an assumed rate of ignition for Block A. The maximum rates of release for heat, particulate matter, CO, and CO_2 were 75,000 MW and 0.047, 0.326, and 6.34 tonnes/s, respectively.

Emission factors were calculated using the carbon mass-balance method for the flaming, intermediate, and smoldering combustion phases. The emission factors were weighted dependent on the fuel consumed by combustion phase and yielded emission factors for PM5.0, CO, and CO_2 of 12.4, 86, and 1673 g/kg for the Hill PB. Graphitic carbon content of the PM5.0 averaged 8.1% during the 10-minute flaming period and dropped to 1.5% during the 20-minute smoldering period. This is consistent with other measurements and with the positive correlation of graphitic carbon with the rate of heat release.

Cross covariance techniques were used to evaluate the lag of fire induced phenomena between FASS packages as the fuel consumption wave moved through the array. The technique verified a time differential of from 20 seconds to 3 minutes dependent on the pairs of FASS packages used in the analysis. Other phenomena associated with the waves of combustion gases moving through the array showed correlations between towers of less than 10 seconds--consistent with the horizontal wind speed measurements.

8.0 RECOMMENDED CONTINUATION STUDIES

The results from this experiment demonstrate the practicality of using reasonably sophisticated measurement systems inside the perimeter of very large fires. It makes possible a new range of experiments heretofore impossible to perform because of instrumentation limitations. Characterization of air flow in conjunction with scaling criteria based on the relative size of fires is now practical. The response of chemical phenomena in conjunction with large area fires is extremely important relative to the emissions source strength for these chemical species leaving the turbulent boundary layer and becoming entrained in convection from the fire. The equipment described in this report is highly modular and can be configured for a variety of research studies both within fires and for ambient air sampling. This section focuses on priority areas for future studies and improvements to the systems that can be accomplished that would be natural follow-on studies based on the results discussed in sections 6.0 and 7.0 of this report.

8.1 Need for Continuation Fire Tests

The chemical structure associated with flame lengths in the lower 30 m of the atmosphere are poorly understood. This hampers further research on rates of fuel consumption, rate of heat release, and the overall entrainment of oxygen into the combustion system near the surface. The features of the test unit discussed in this report were but one cell within the large Hill PB. The interrelations with the other fire activity have only partially been explained. The size of the fire hampered investigations of entrainment, airflow, observations of fire behavior associated with airflow events, and a number of other considerations. We strongly recommend a series of smaller scale fires that could be structured to yield various rates of heat release, burned under different prescription conditions to meet objectives for surface winds, atmospheric lapse rates, interactions between area fires, fuel loading by size classes, potential incorporation of rubble or other hydrocarbon fuels, and a host of other objectives that could illuminate the interactions between major sources of heat and lower atmospheric boundary layer conditions. The potential to investigate the chemical phenomena occurring in areas of intense rates of heat release would be much greater if performed on a smaller scale. A carefully designed set of treatments with some replication seems essential.

Scaling of the size of the area fires involved in producing different combustion phenomena is important in planning future studies. The atmospheric processes acting to remove or to change the character of the emissions released from the combustion of the biomass fuels under different combustion conditions are nearly completely decoupled. Hence, work to improve our understanding of the production of smoke particles by size classes, gases of importance in the atmosphere from a chemical reaction standpoint, and the heat release rates can be studied on much smaller fires than the Hill PB. Fires of a hectare in size would be plenty large enough to fully explore the concepts of modeling these phenomena before graduating once again to the very large mass-fire. The important concepts of induced buoyancy, inflow near the perimeter, heat release rates, vertical velocity and horizontally induced wind flow, the enhancement of flow velocities by rotation, and other phenomena are tractable on a much reduced scale.

A much wider array of fuel types, loadings, moistures, and fire intensities should be sampled to improve the scope of results. Ignition patterns should be varied and carefully documented by video or photographic methods. This is needed to completely investigate single combustion waves moving past the sampling array. The present study pointed out the need for estimating the fire movement relative to the systems used for measuring the phenomena. Fires in a variety of wind fields should provide a better picture of the accuracy of these systems under all potential conditions. Fuels near the sampling array should be documented better by type, load and location of piles or windrows. Performance of the systems in a more uniform fuel array, such as grass, or needle litter would be especially informative. The effects of these variables might then be separated from wind variations.

Backing, heading and flanking fires should all be analyzed for effects on emissions and smoke plume development.

8.2 Measurement System Improvements

The overall implementation of the FASS and GODM packages was sound and does not need to be changed. All systems worked as designed and provided valuable data. Minor problems appeared as expected given the short development time. Improvements could easily be made in the temperature monitoring electronics, vertical wind direction sensors, and gas sample bag composition integrity. There will always be a need to incorporate the latest improvements in sensor technology and calibration protocol, to provide the best possible measurement of key parameters. Implementation of electronics on printed circuit boards, rather than wire wrap, should eliminate many minor ground loop problems and improve signal to noise ratios. Selected amplifier gains should be optimized for the expected signal ranges identified by the Hill fire experiment. The canister sample flow rate should be restricted to lengthen sample time and provide better average composition of trace components. The post fire canister analysis can then be extended to include a more complete survey of compounds in the smoke.

Improvements in the deployment strategy of the FASS and GODM packages can be made that will greatly enhance the collection of data from different areas removed from the laboratory. This proven technology can be deployed days before the experiment and onboard calibration, solar panels for maintaining full electrical power, and other improvements in the way canisters are handled for collecting grab samples will tremendously expedite this process of setting up for experiments.

The modular capabilities of the FASS and GODM packages makes for tailoring of experiments to the emerging needs as more is learned about the conditions encountered in various fire environments. Being able to assure the integrity of the basic packages has been paramount in the design of the packages. Certain losses could be tolerated as far as external sensors are concerned if the main package remains functional. This was demonstrated with the deployment of the low-cost plastic anemometers.

8.3 Software Improvements

Experience with the Hill PB provided valuable data on optimal sampling rates for all the parameters. The software programs should be modified to decrease sampling rates in some cases, and perhaps provide more data for other selected parameters. Part of the attraction of our system was the ease with which substantial changes in experimental design could be made in software. Calibration and system warm-up protocols should be optimized to reduce calibration uncertainties and starting transients. A comprehensive set of data analysis software can now be developed to routinely reduce the large data set generated for each experiment. This would facilitate data reduction and allow many more experimental burns to be conducted. Such software should produce informative reports and plots for each burn and greatly reduce analysis time.

8.4 Laboratory Studies

A considerable amount of peripheral data can be supplied by carefully designed studies in the IFSL combustion laboratories. Many of the independent variables can be selectively controlled to aid development of physical models for combustion phenomena. Numerous fuel types can be investigated quickly -- a task that is difficult in field studies. Indications are that the Hill PB experiment was exceptional in meeting project objectives, and we would be very fortunate to repeat this success in a large percent of our future field experiments. Laboratory studies would eliminate many of the problems due to adverse weather and logistics.

9.0 ACKNOWLEDGEMENTS

The efforts of many groups and individuals aided the development, construction, and deployment of our experiment--we gratefully acknowledge their contributions. We particularly acknowledge the donation of time, expertise, and facilities by other Research Units at IFSL. INT Research Support is to be commended for purchasing the hundreds of components needed, in the short time available. The research personnel of Forestry Canada provided needed support in site selection, fuels characterization, and tower assembly, and were gracious hosts during our visit to Canada. Of special recognition is the space, accommodations, telephone, facsimile, and aircraft support provided by the Ontario Ministry of Natural Resources. We are particularly indebted to DNA for encouraging our participation in this highly worthwhile endeavor.

10.0 REFERENCES

Albini, Frank A.; Stocks, Brian J. 1986. Predicted and observed rates of spread of crown fires in immature Jack Pine. Combustion Science and Technology, *48*:65-76.

Albini, Frank A. 1985a. A model for fire spread in wildland fuels by radiation. Combustion Science and Technology, *42*:229-258.

Albini, Frank A. 1985b. Wildland fire spread by radiation--a model including fuel cooling by natural convection. Combustion Science and Technology, *45*:101-113.

Albini, Frank A. 1984. Wildland fires. American Scientist, *72*:590-597.

Albini, Frank A. 1981. A model for the wind-blown flame from a line fire. Combustion and Flame, *43*:155-174.

Albini, Frank A. 1980. Thermochemical properties of flame gases from fine wildland fuels. Res. Pap. INT-243. Ogden, UT: U.S. Department of Agriculture, Forest Service, Intermountain Forest and Range Experiment Station.

Albini, Frank A. 1979. Spot fire distance from burning trees-a predictive model. Gen. Tech. Rep. INT-56. Ogden, UT: U.S. Department of Agriculture, Forest Service, Intermountain Research Station. 73 p.

Countryman, Clive M. 1964. Mass fires and fire behavior. Res. Paper PSW-19 Berkeley, CA: U.S. Department of Agriculture, Forest Service, Pacific Southwest Forest & Range Experiment Station. 53 p.

Einfeldt, W. 1989. Particle and trace element production from fires in the chaparral fuel type, Paper No. 89-025.002, IN: Proceedings of the 1989 National Air and Waste Management Association Meeting; 1989 June 25-30; Anaheim, CA, Air and Waste Management Association: Pittsburgh, PA.

Grinberg, I. M.; Putnam, A. A. 1964. A model study of the interaction effects of mass fires. Sum. Rep. No. 3. Office of Civil Defense, OCD-OS-62-89; U.S. Department of Commerce, National Bureau of Standards, Washington, DC; Battelle Memorial Inst., Columbus, Ohio. 28 p.

Hegg, D. A.; Radke, Lawrence F.; Hobbs, Peter V.; Rasmussen, Rei A.; Riggan, Phillip J. 1989. Emissions of some trace gases from biomass fires. Distributed at 82nd APCA Annual Meeting, Anaheim, CA, June 25-30. 13 p.

Heikes, K. E.; Ransohoff, L. M.; Small, R. D. 1987. Early smoke plume and cloud formation by large area fires. Tech. Rep. DNA-TR-87-176, Contr. No. DNA 001-85-C-0089. Washington, DC: Defense Nuclear Agency. 74 p.

McRae, D. 1989. Data presented at joint review meeting in Missoula, MT October 1989. On file Forestry Canada, Saulte Ste. Marie, Ontario, Canada. National Research Council, (1985). The effects on the atmosphere of a major nuclear exchange. National Academy Press. Washington, DC. 193 p.

Perry, 1963. Chemical Engineer's Handbook, 4th edition. 3-142 p.

Radke, Lawrence; Lyons, Jamie H.; Hegg, Dean A; Sandberg, David V.; and Ward, Darold E. [In press]. Airborne monitoring and smoke characterization of prescribed fires on forest lands in western Washington and Oregon, U.S. Department of Agriculture, Forest Service, Pacific Northwest Research Station, Portland, OR.

Rangno, A. L.; Radke, L. F. 1989. Rawinsonde data and synoptic analysis for Hill and Hornepayne prescribed fires, Ontario, Canada, August 1989. Report on file USDA Forest Service, Intermountain Fire Sciences Laboratory, Missoula, MT.

Reid, D. G. and Vines, R. G. 1972. A radar study of the smoke plume from a forest fire. Div. of Applied Chemistry Technical Paper No. 2. Commonwealth Scientific and Industrial Research Organization, Australia. 12 p.

Reinhardt, T. E. and Ward, D. E. [unpub manus]. Factors affecting methyl chloride emissions from burning forest biomass, unpublished manuscript at U.S. Department of Agriculture, Forest Service, Pacific Northwest Research Station, Seattle, WA.

Rothermel, Richard C. 1972. A mathematical model for predicting fire spread in wildland fuels. Res. Pap. INT-115, Ogden, UT: U.S. Department of Agriculture, Forest Service, Intermountain Forest and Range Experiment Station. 40 p.

Rothermel, Richard C. 1983. How to predict the spread and intensity of forest and range fires. Gen. Tech. Rep. INT-143. Ogden, UT: U.S. Department of Agriculture, Forest Service, Intermountain Forest and Range Experiment Station. 161 p.

Storey, T. G.; Bush, A. F.; Leonard, J. J.; Yundt, W. H. 1969. Project Flambeau...an investigation of mass fire (1964-1967). Final Report-Volume III: Appendixes. Berkeley, CA: U.S. Department of Agriculture, Forest Service, Pacific Southwest Forest & Range Experiment Station. 90 p. illust.

Taylor, R. J.; Corke, D. G.; King, N. K.; MacArthur, D. A.; Packham, D. R.; and Vines, R. G. (1971). Some meteorological aspects of three intense forest fires. Div. of Meteorological Physics Technical Paper No. 21. Commonwealth Scientific and Industrial Research Organization, Australia. 20 p.

Ward, D. E. and Hardy, C. C. 1984. Advances in the characterization and control of emissions from prescribed fires, Paper No. 84-36.3, presented at the 78th annual meeting of the Air Pollution Control Association; 1984 June 24-29; San Francisco, CA, Air Pollution Control Association, Pittsburgh, PA, 1984.

Ward, D. E. and Hardy, C. C. 1989. Emissions from prescribed burning of chaparral. For presentation at 1989 Annual Meeting of the Air and Waste Management Association, Anaheim, CA. in June '89. 22 p.

Ward, D. E. and Hardy, C. C. 1990. Smoke Emissions from Wildland Fires. Manuscript on file USDA Forest Service, Intermountain Fire Sciences Laboratory, Submitted to Environment International.

Ward, D. E.; Nelson, R. N.; and Adams, D. F. 1979. Forest Fire Smoke Plume Documentation. In: Proceedings of the 72nd Annual Meeting of the Air Pollution Control Association, Cincinnati, OH. June 24-29, 1979. 24p.

11.0 CONVERSION FACTORS FOR METRIC TO ENGLISH

To convert		multiply by	to obtain
Tg	Teragram	10^{12}	g
g	grams	0.002205	pounds
ha	hectare	2.471	acres
^{o}C	Celcius	(^{o}C x 9/5) + 32	Fahrenheit
mm	millimeters	0.03937	inches
m	meters	3.281	feet
m/s	meters/second	2.237	miles/hour
um	micrometers	10^{-6}	meters
g/kg	grams per kilogram	2	pounds/ton
km	kilometers	0.6214	miles
kg/m^2	kilograms/sq.meter	0.2048	lbs/sq.ft.
kW	kiloWatts	56.92	B.t.u./min.
kJ/g	kiloJoules per gram	429.95	B.t.u./lb.

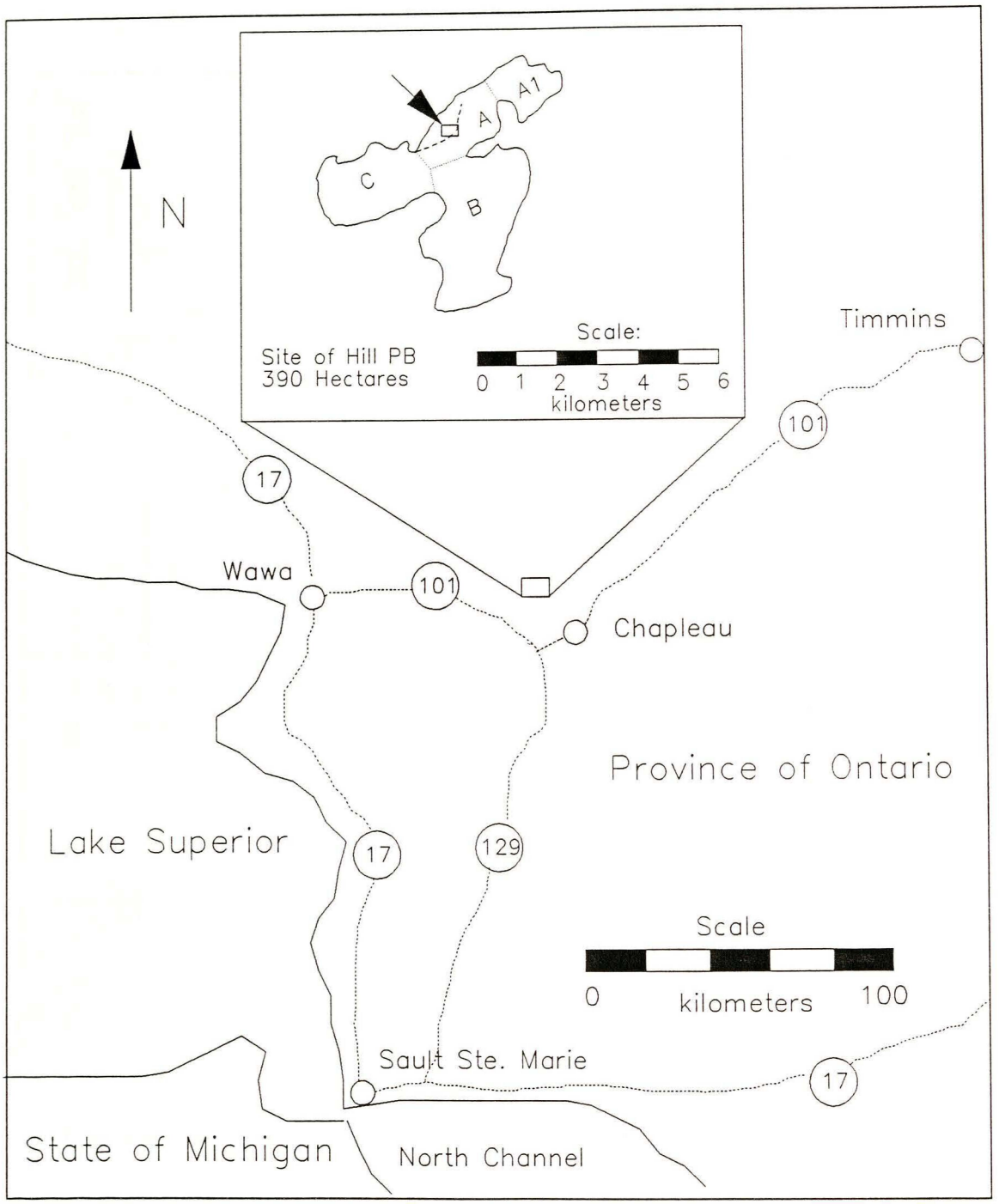

Figure 4.1-1 Location of the Hill PB relative to Chapleau and Sault Ste. Marie, Ontario, Canada.

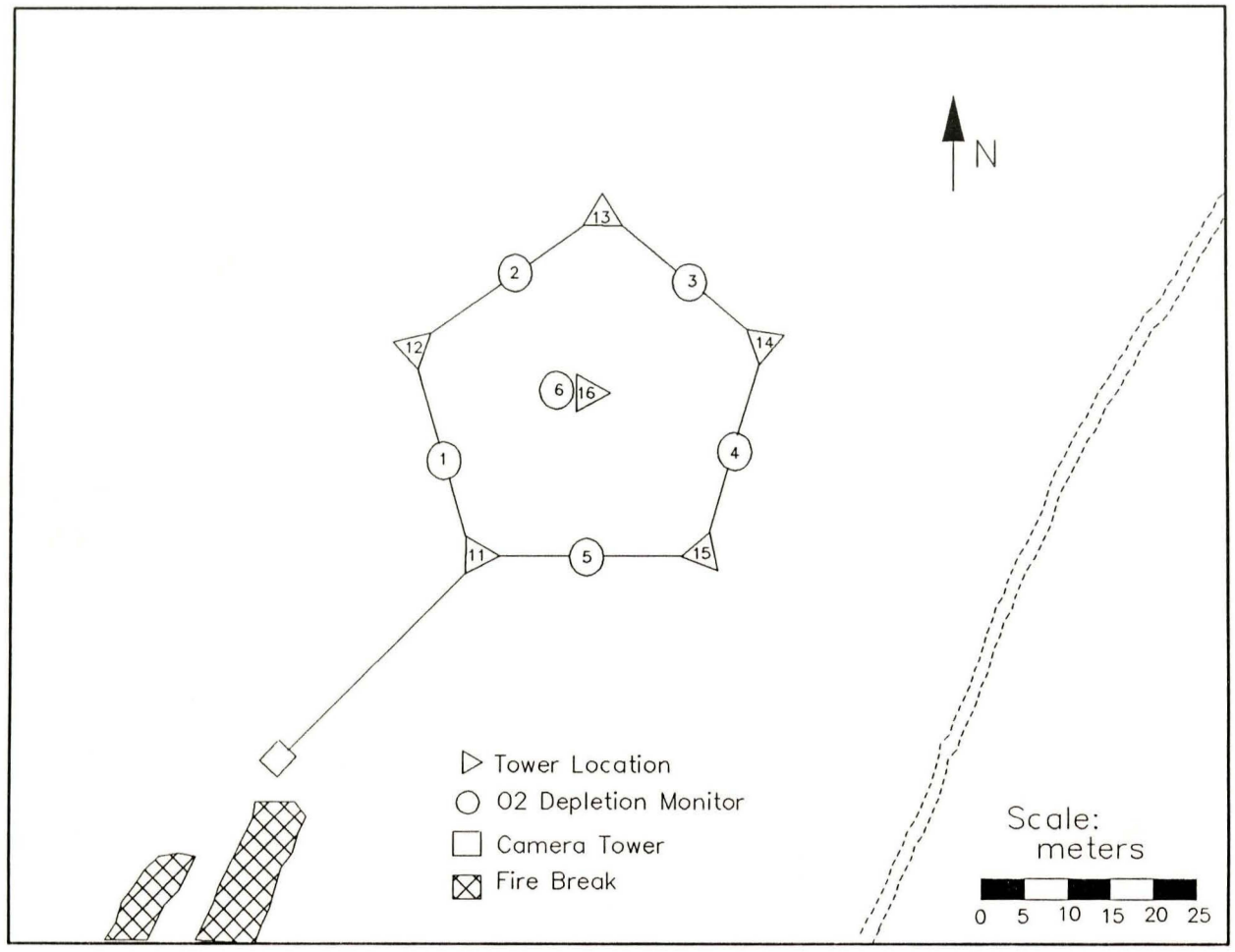

Figure 4.1-2 General location of FASS packages, GODM packages and video camera relative to the fire break study area.

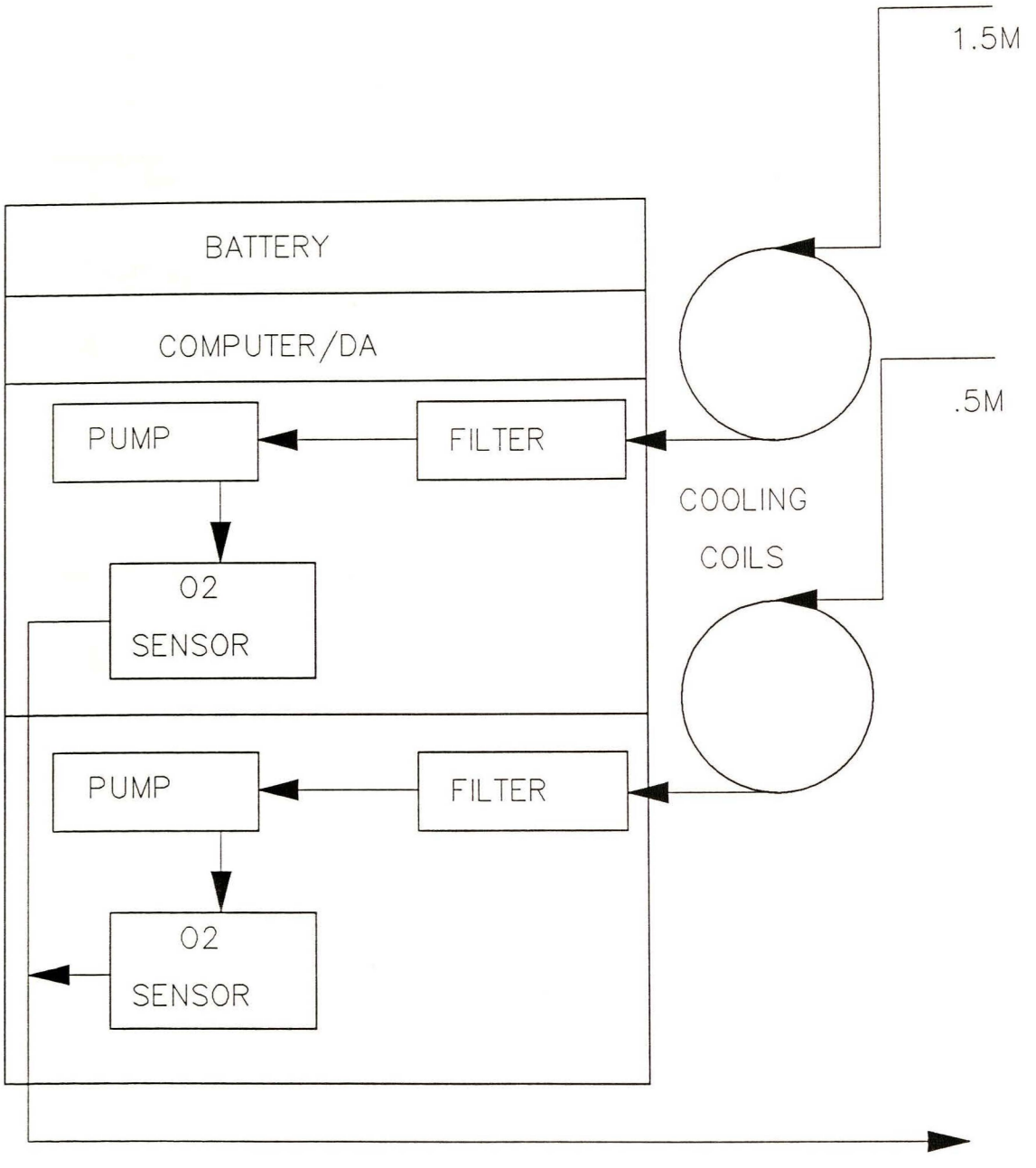

Figure 4.2.4-1 Functional block diagram of the GODM system.

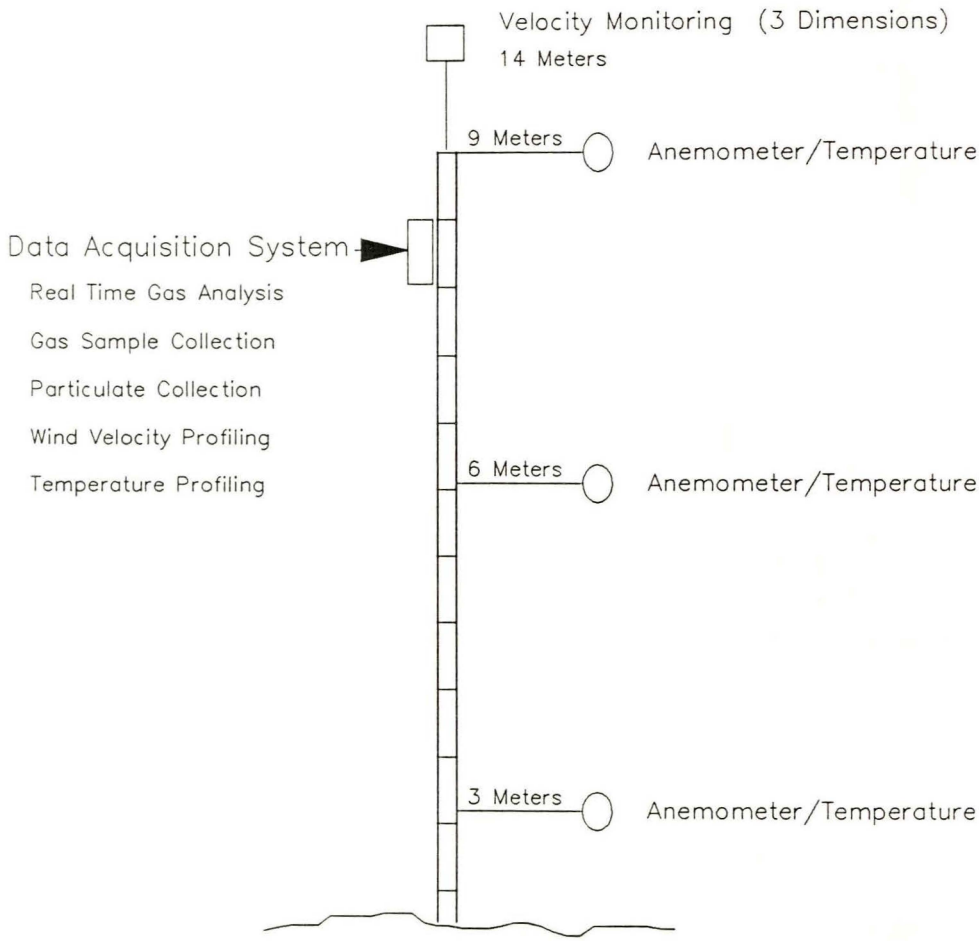

Figure 4.2.5-1 Position of the FASS sensors on the tower.

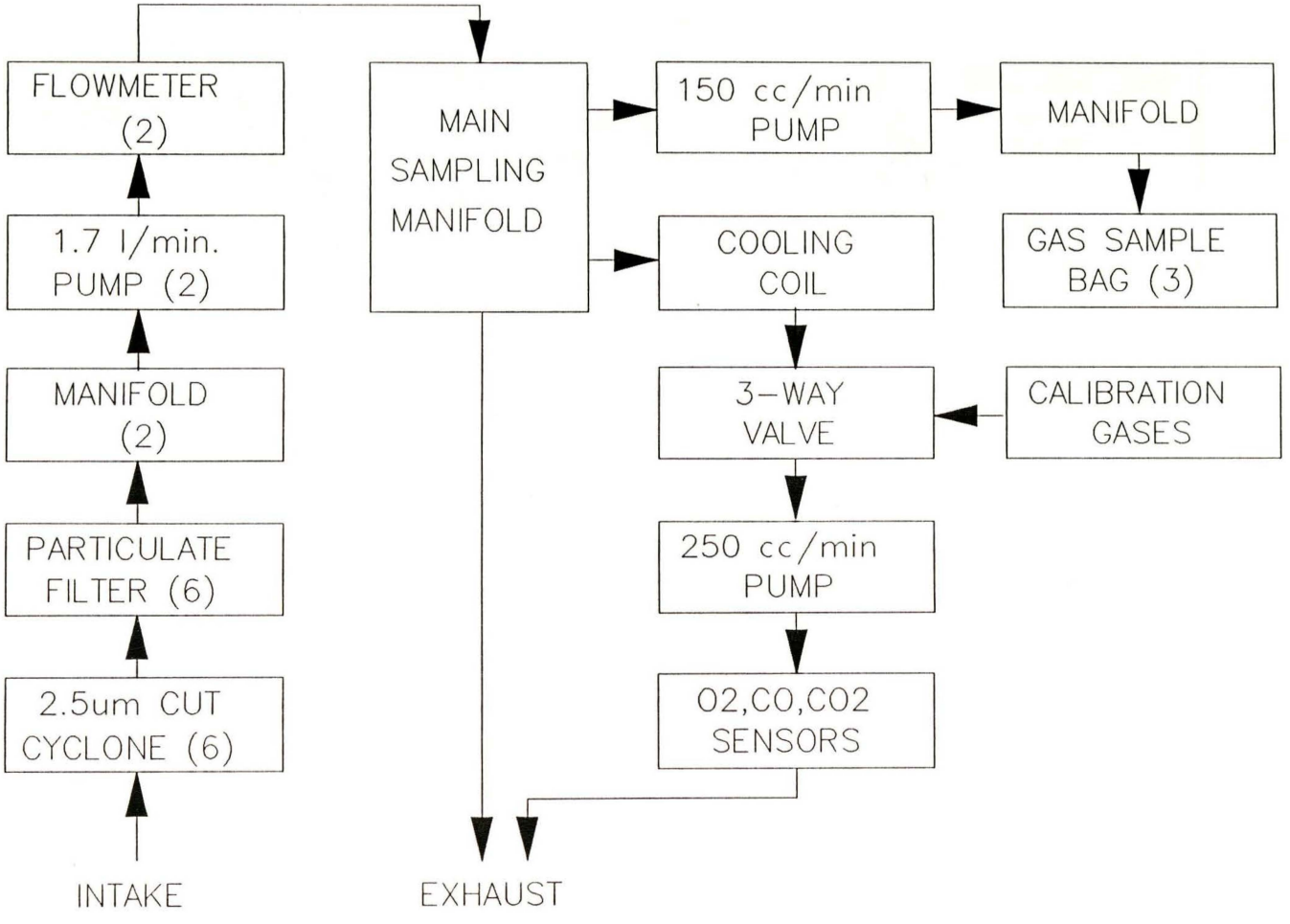

Figure 4.3.1-1 Diagram of the flow of the gases through the analyzers in the FASS packages.

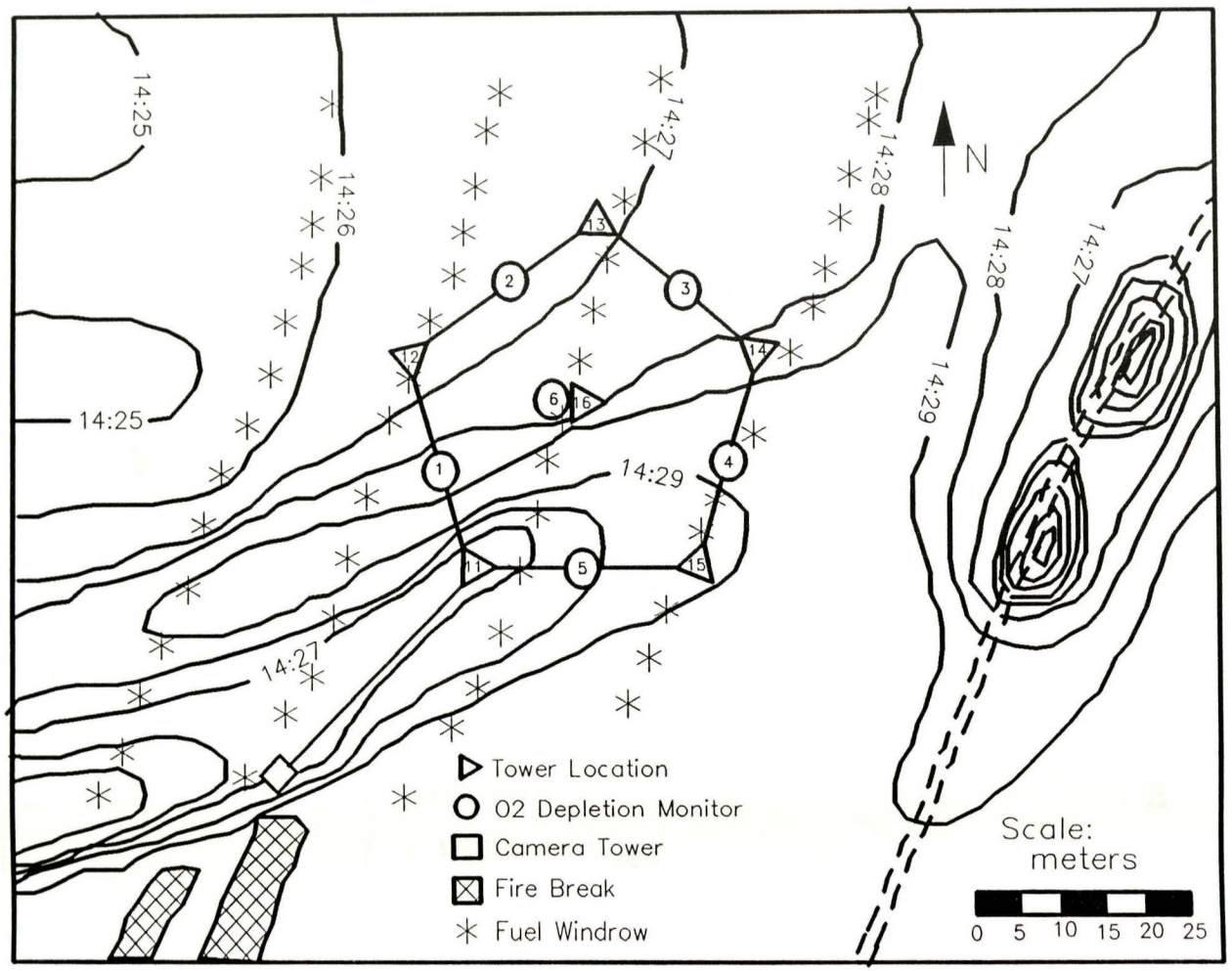

Figure 5.1-1 Pattern of fire spread through the matrix of towers from 14:25 to 14:30 hours on August 10, 1989.

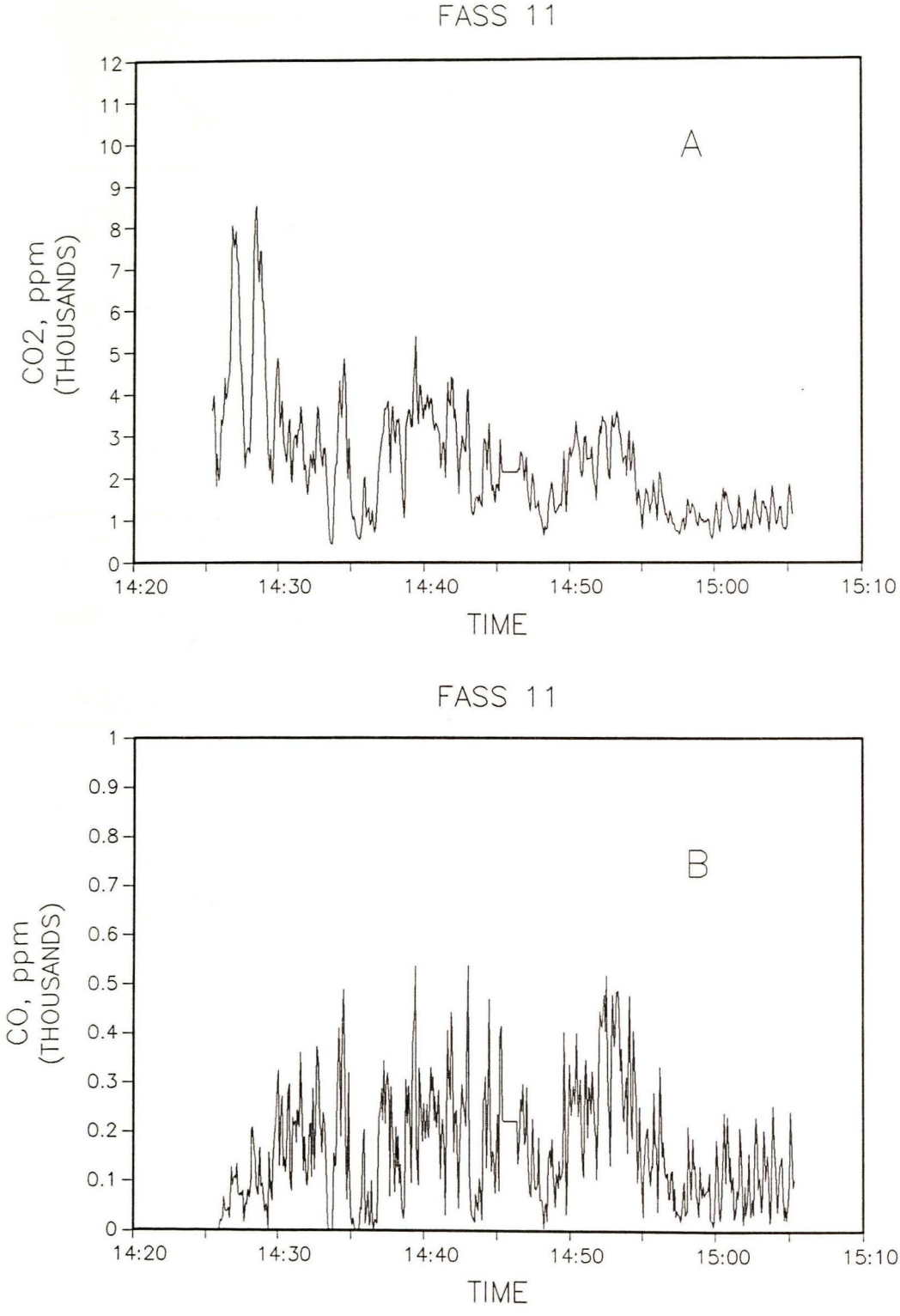

Figure 5.2-1 Example of real time gas concentration measurements on FASS 11; A) CO_2, B) CO.

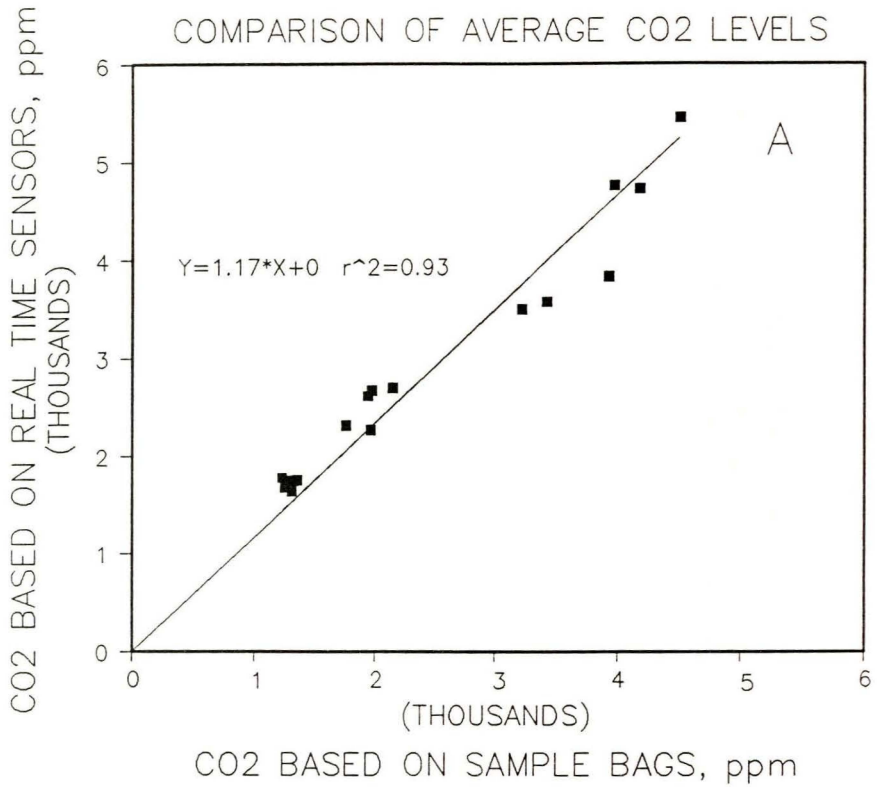

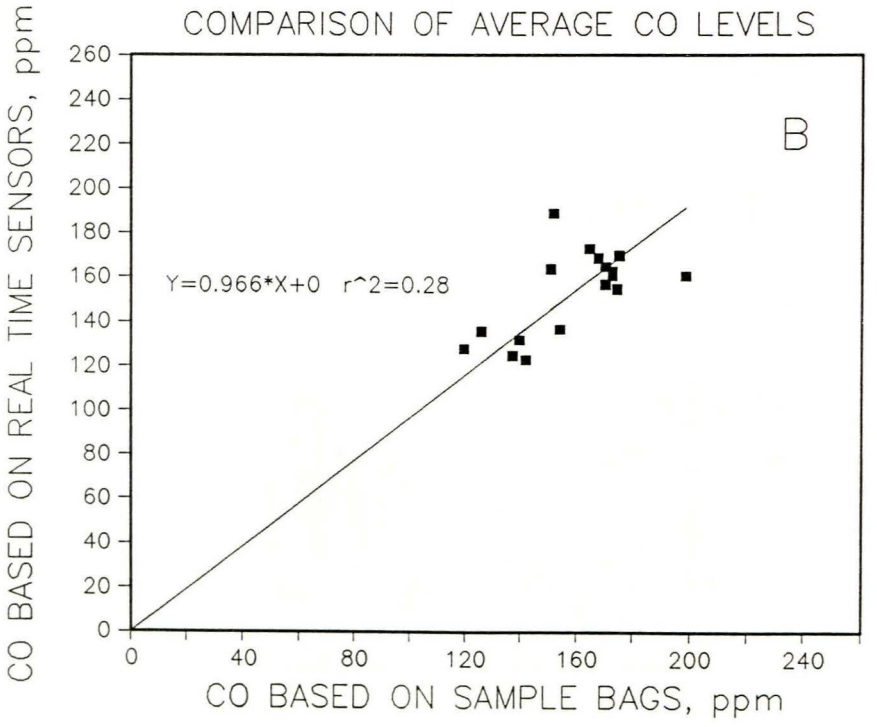

Figure 5.2-2 Comparison of the average real time gas concentrations with measurements based on sample bags; A) CO_2, B) CO.

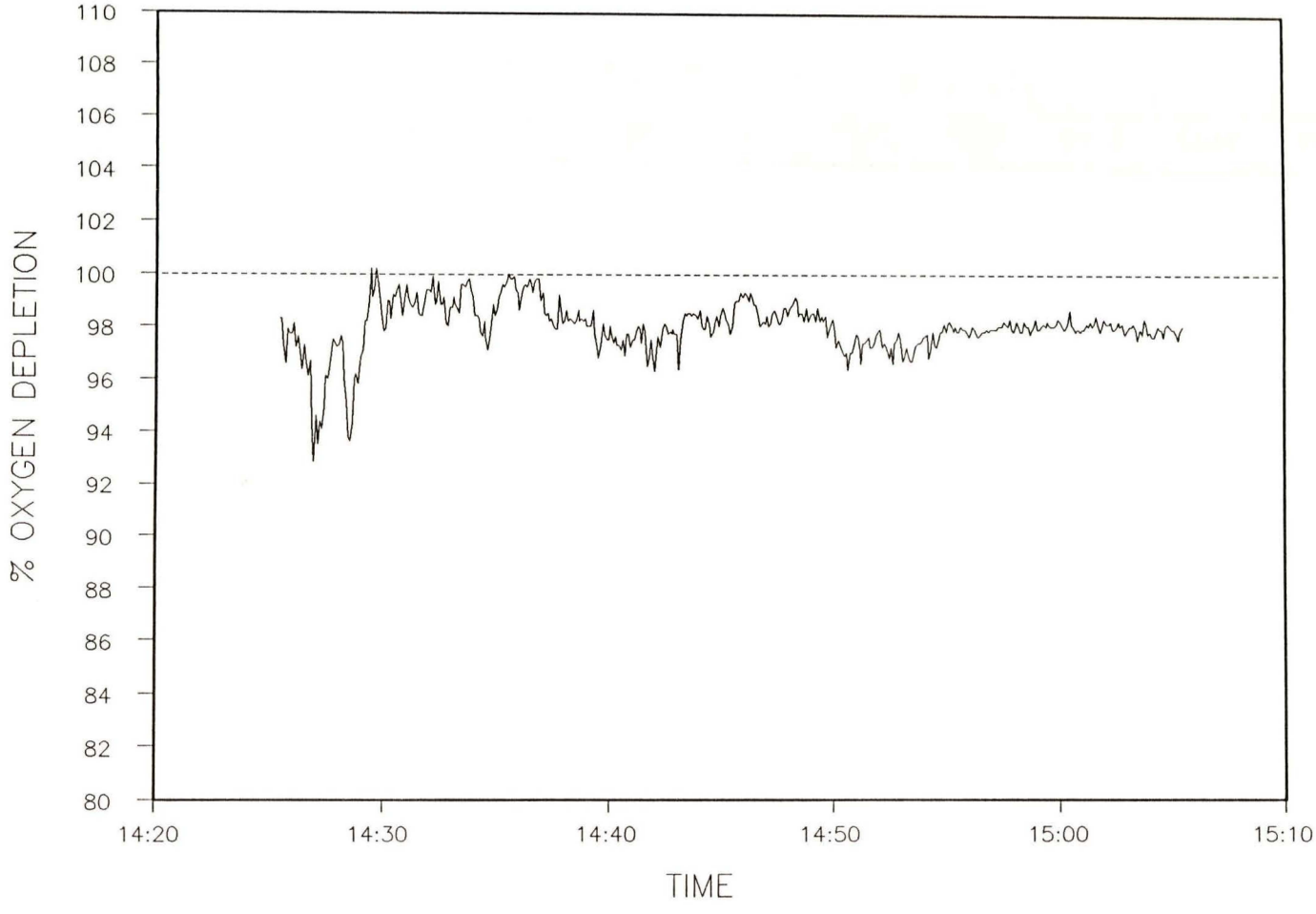

Figure 5.2-3 Example of real time gas concentration measurements of oxygen depletion on FASS 11.

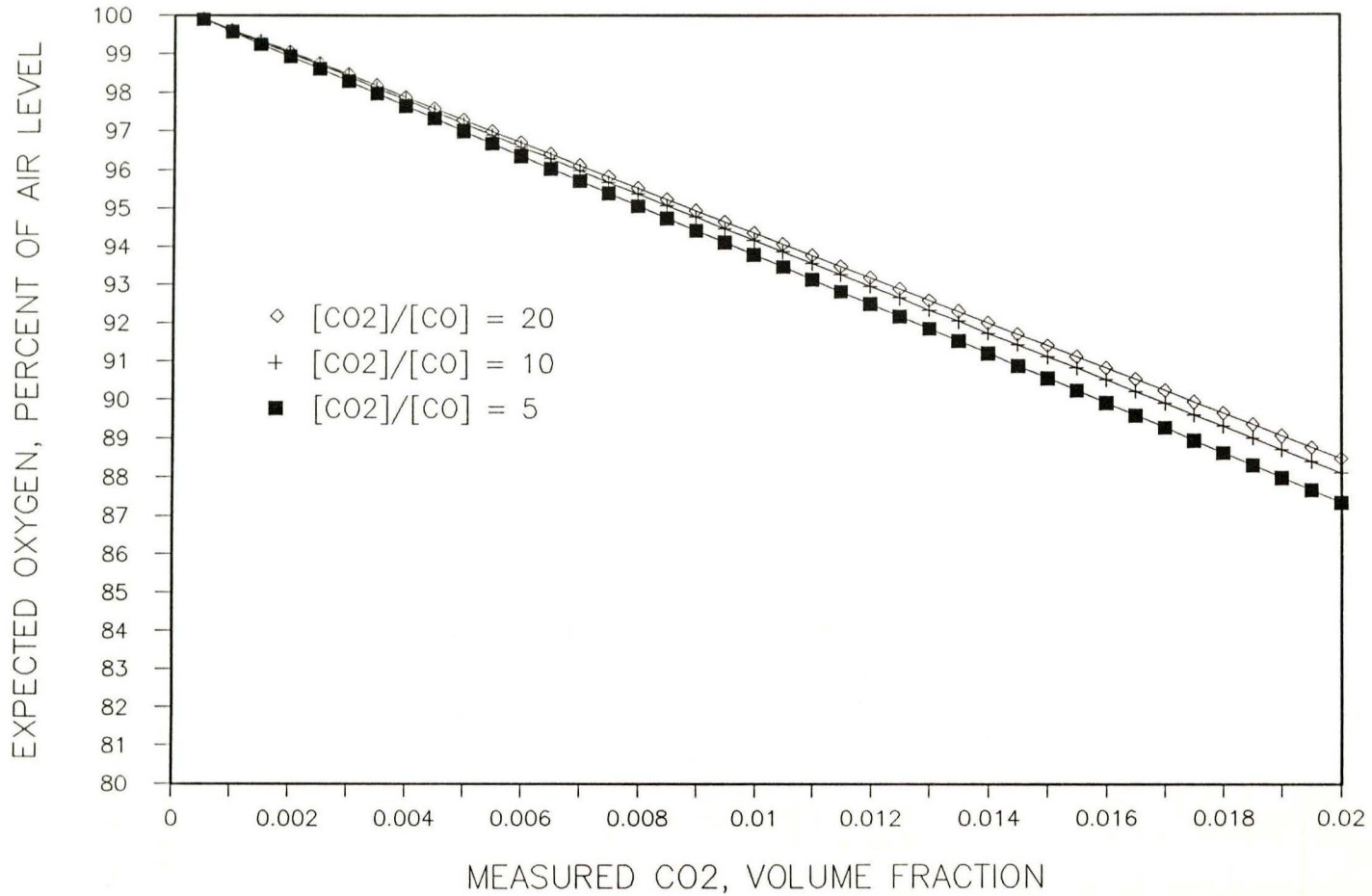

Figure 5.2-4 Theoretical oxygen levels calculated as a function of measured CO_2 fractions. Fuel composition is assumed to be $C_6H_9O_4$.

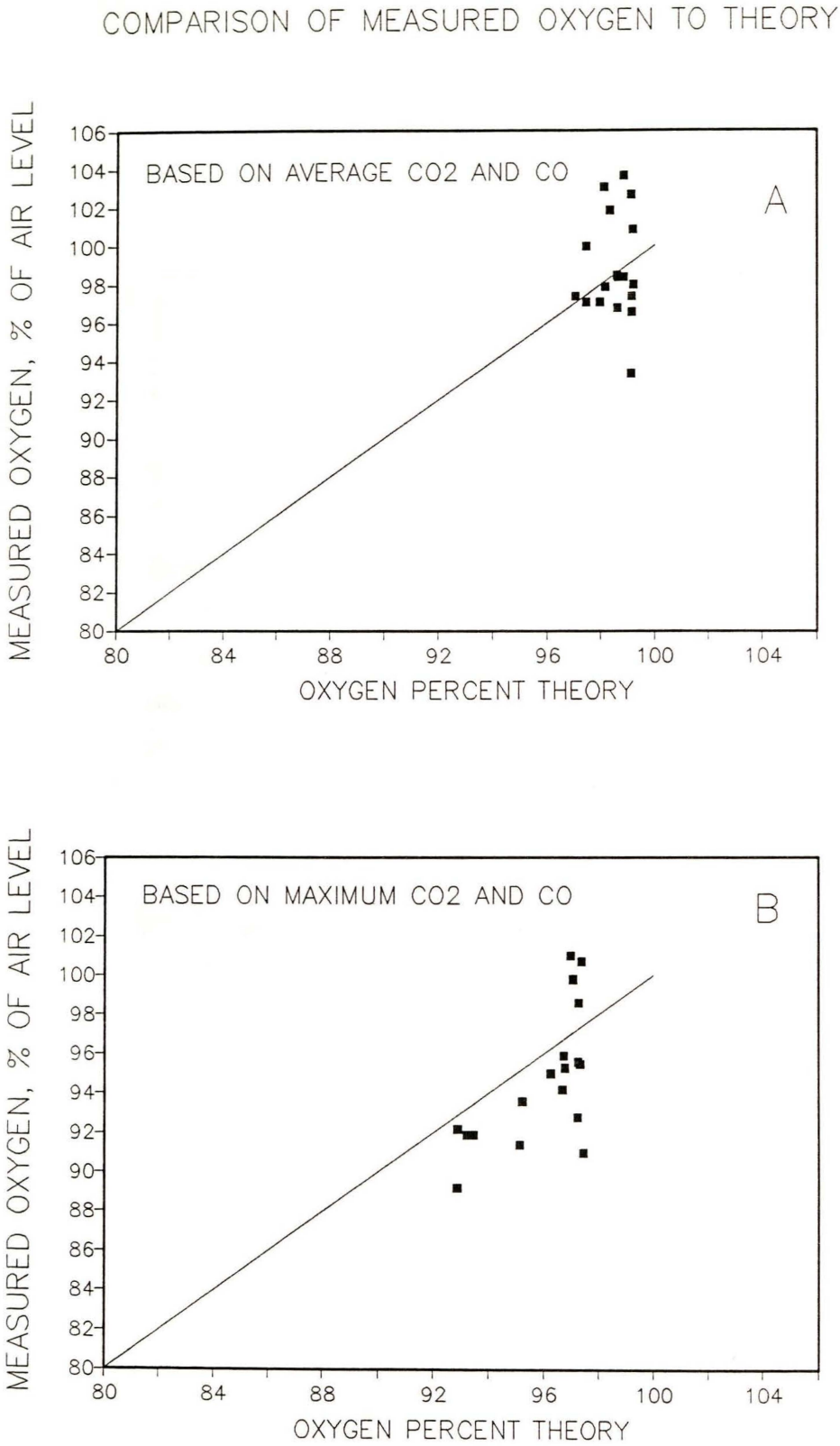

Figure 5.2-5 Comparison of measured oxygen levels to theoretical calculations based on CO_2 fractions; A) based on average values, B) based on maximum values.

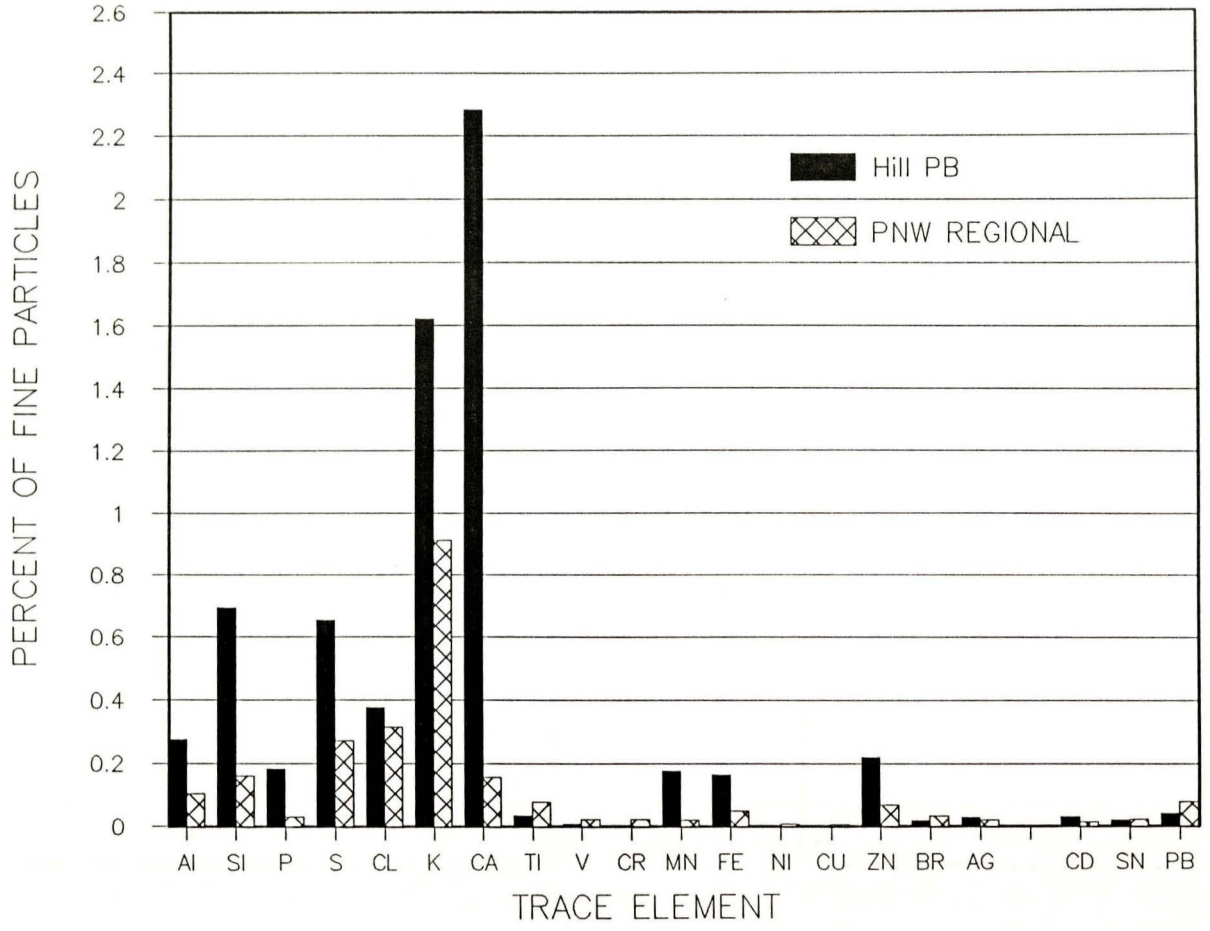

Figure 5.3-1 Inorganic composition of particulate matter compared to Pacific Northwest literature values on logging slash.

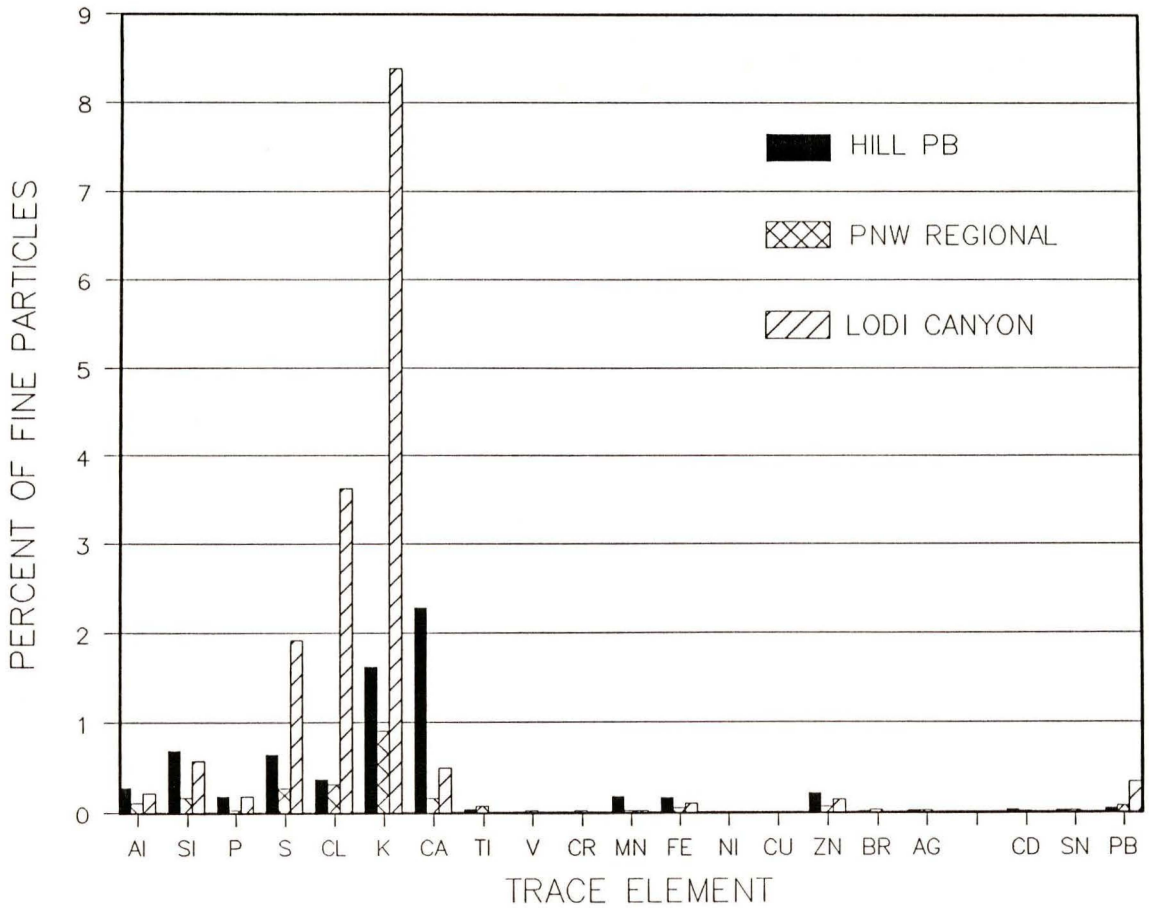

Figure 5.3-2 Inorganic composition of particulate matter compared to literature values for Pacific Northwest and Lodi Canyon, California burns.

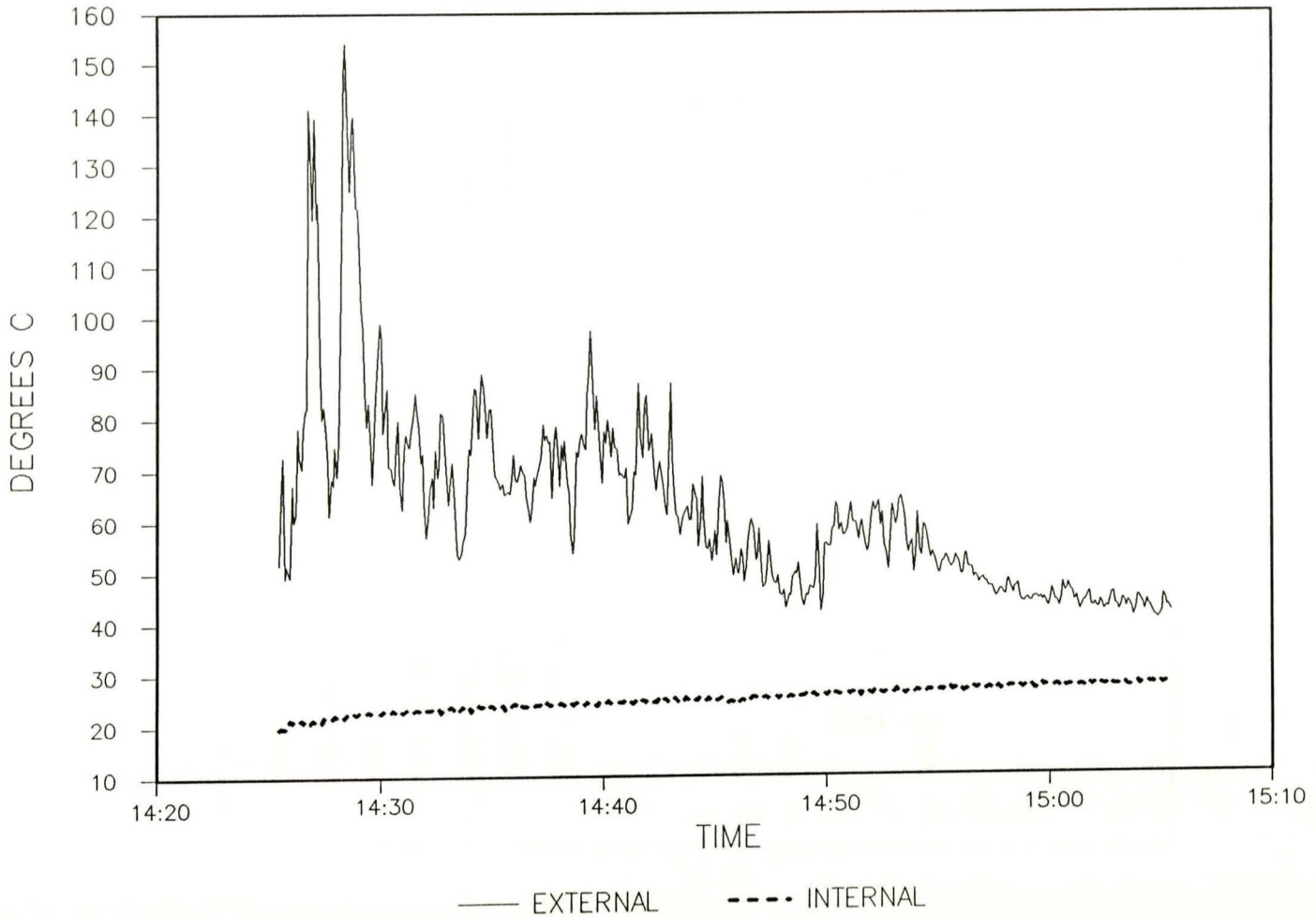

Figure 5.4-1 Comparison of the FASS 11 internal gas flow temperature to the external air temperature of the fire environment.

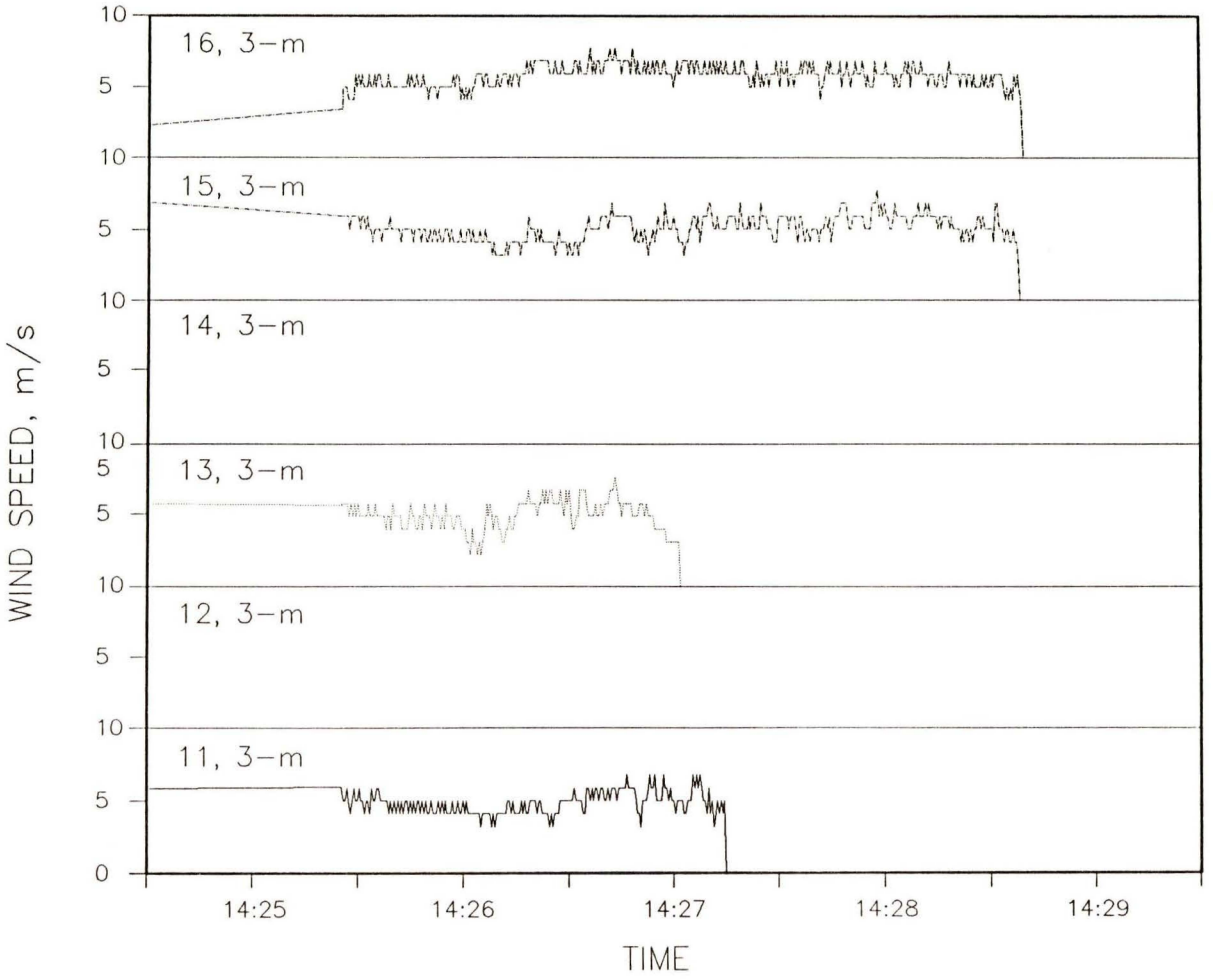

Figure 5.5-1A Fire induced wind field variations before ignition and during the first few minutes of the fire: A) 3-m wind speed.

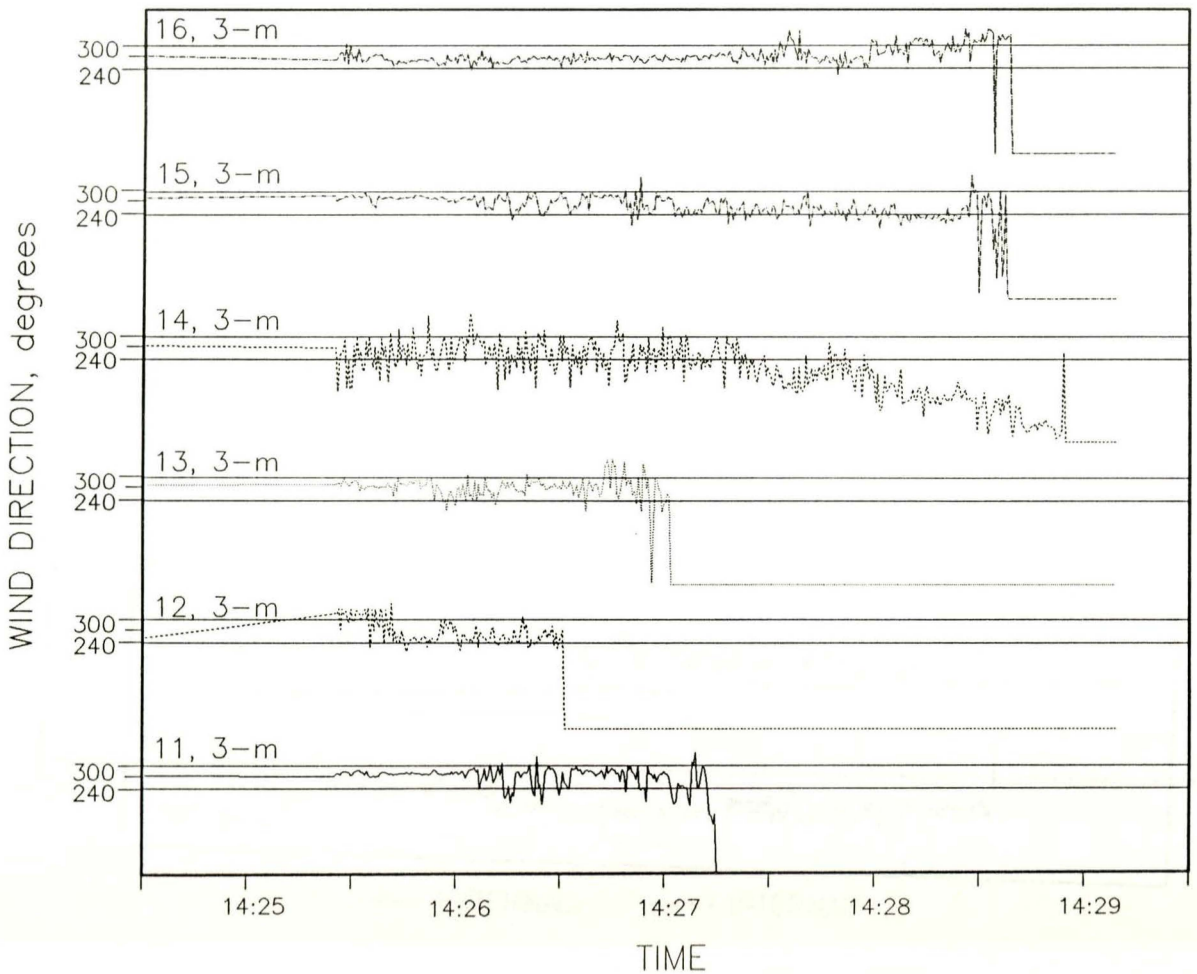

Figure 5.5-1B Fire induced wind field variations before ignition and during the first few minutes of the fire: B) 3-m wind direction.

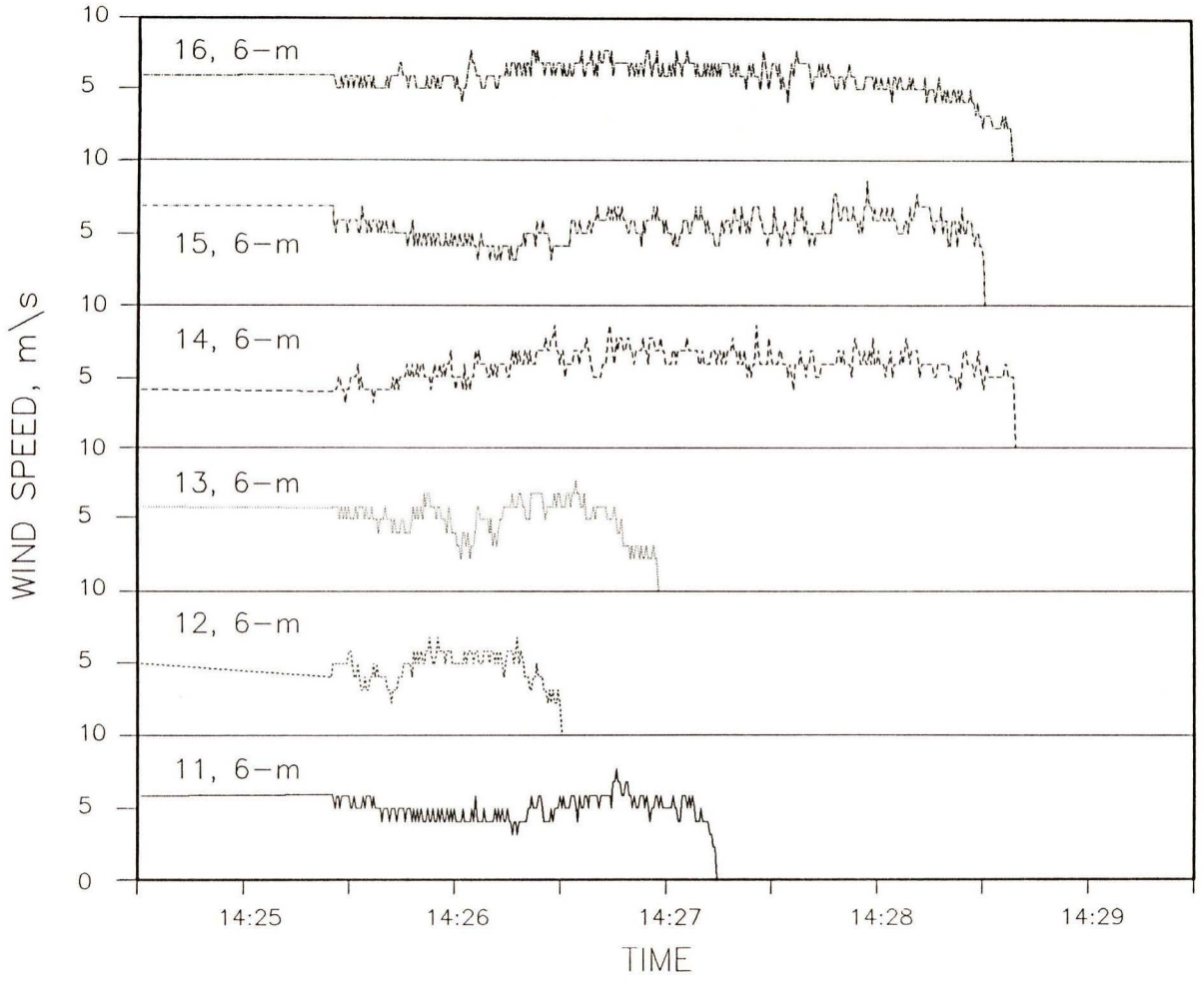

Figure 5.5-1C Fire induced wind field variations before ignition and during the first few minutes of the fire: C) 6-m wind speed.

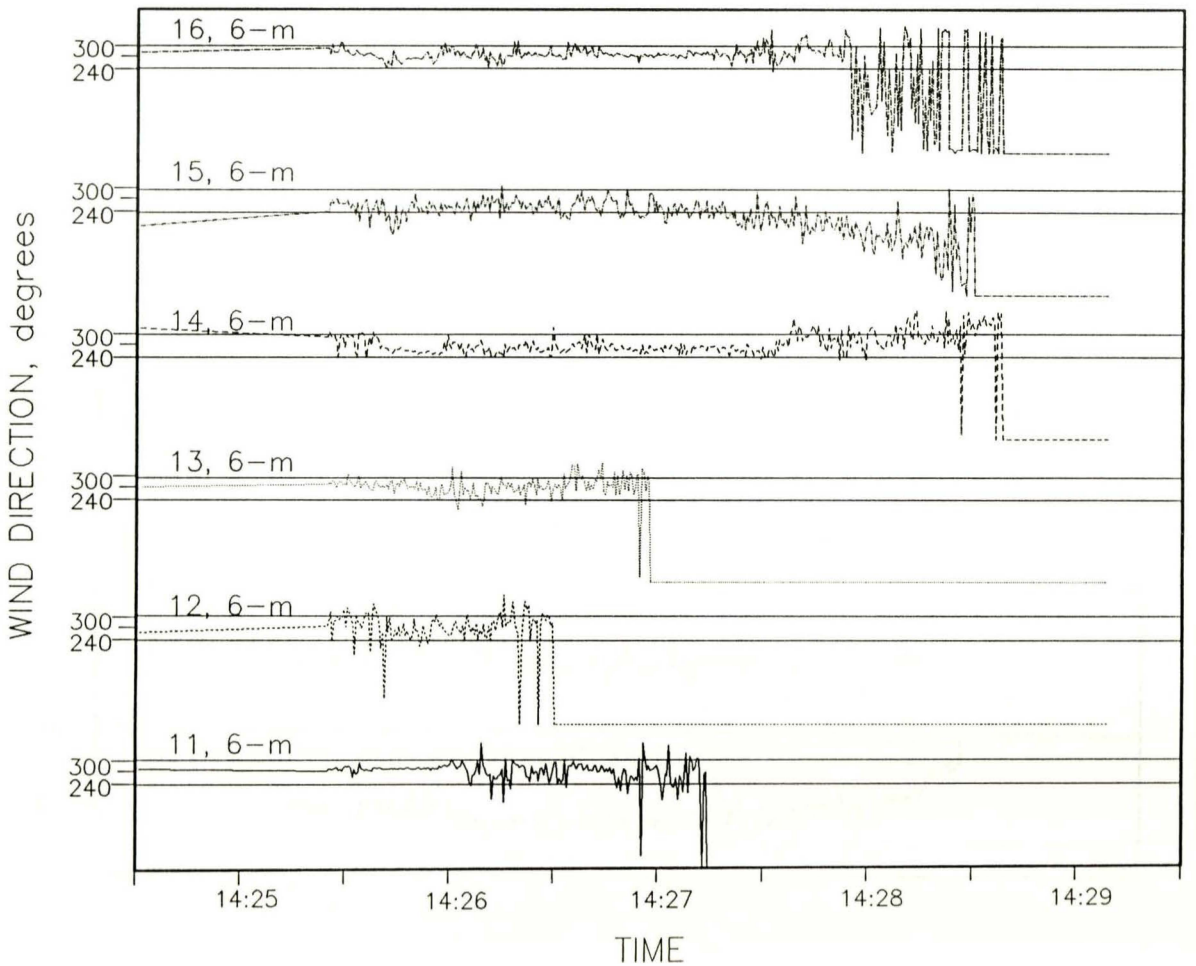

Figure 5.5-1D Fire induced wind field variations before ignition and during the first few minutes of the fire: D) 6-m wind direction.

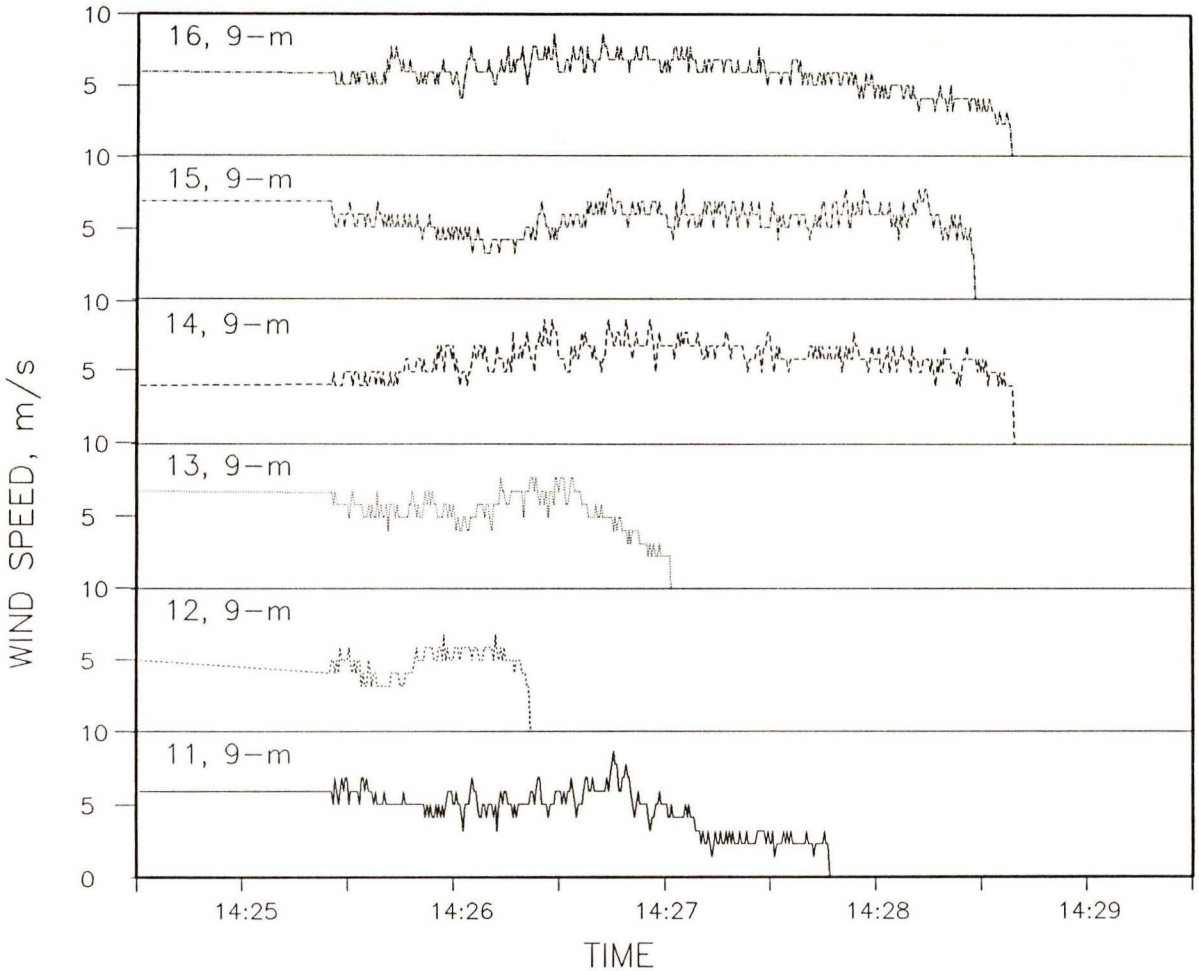

Figure 5.5-1E Fire induced wind field variations before ignition and during the first few minutes of the fire: E) 9-m wind speed.

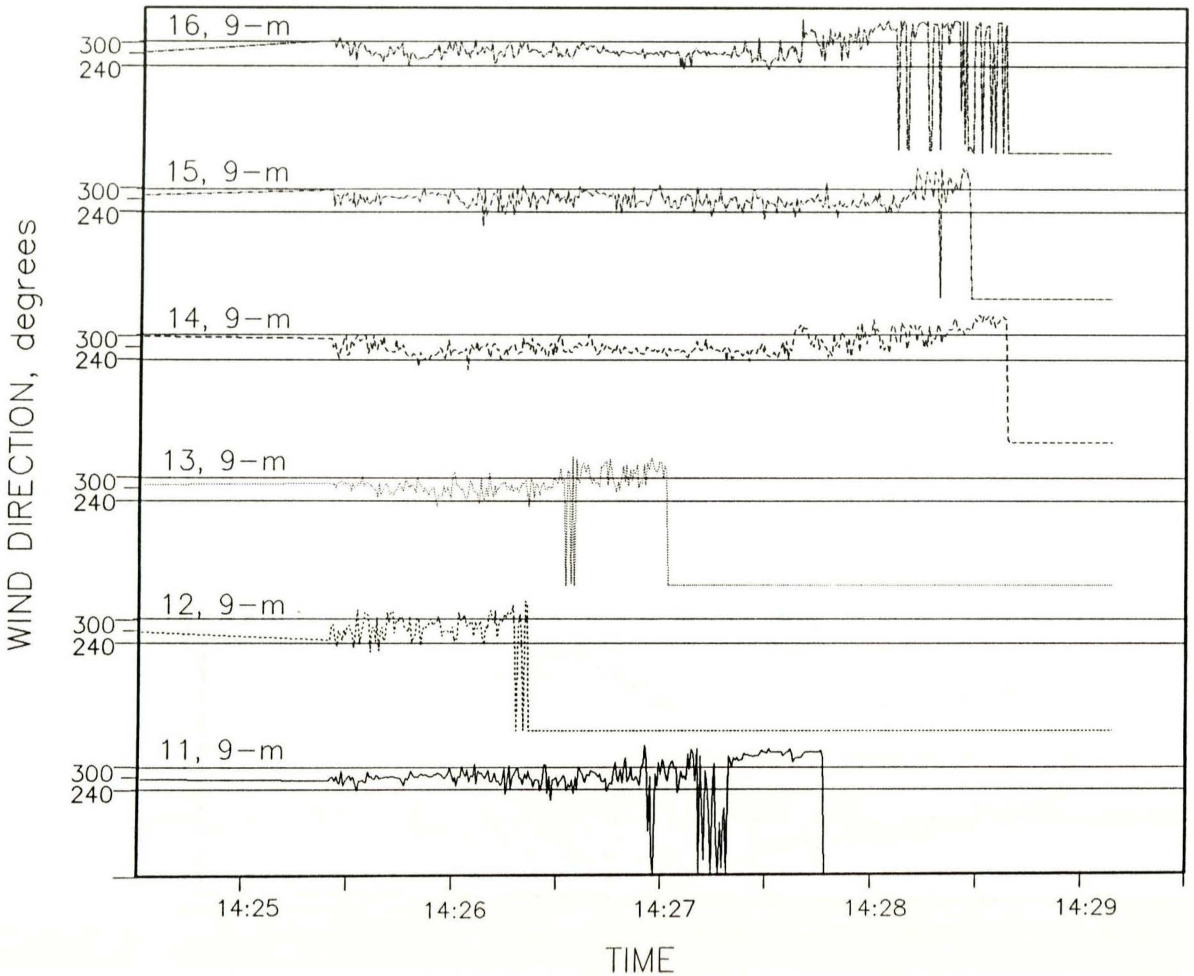

Figure 5.5-1F Fire induced wind field variations before ignition and during the first few minutes of the fire: F) 9-m wind direction.

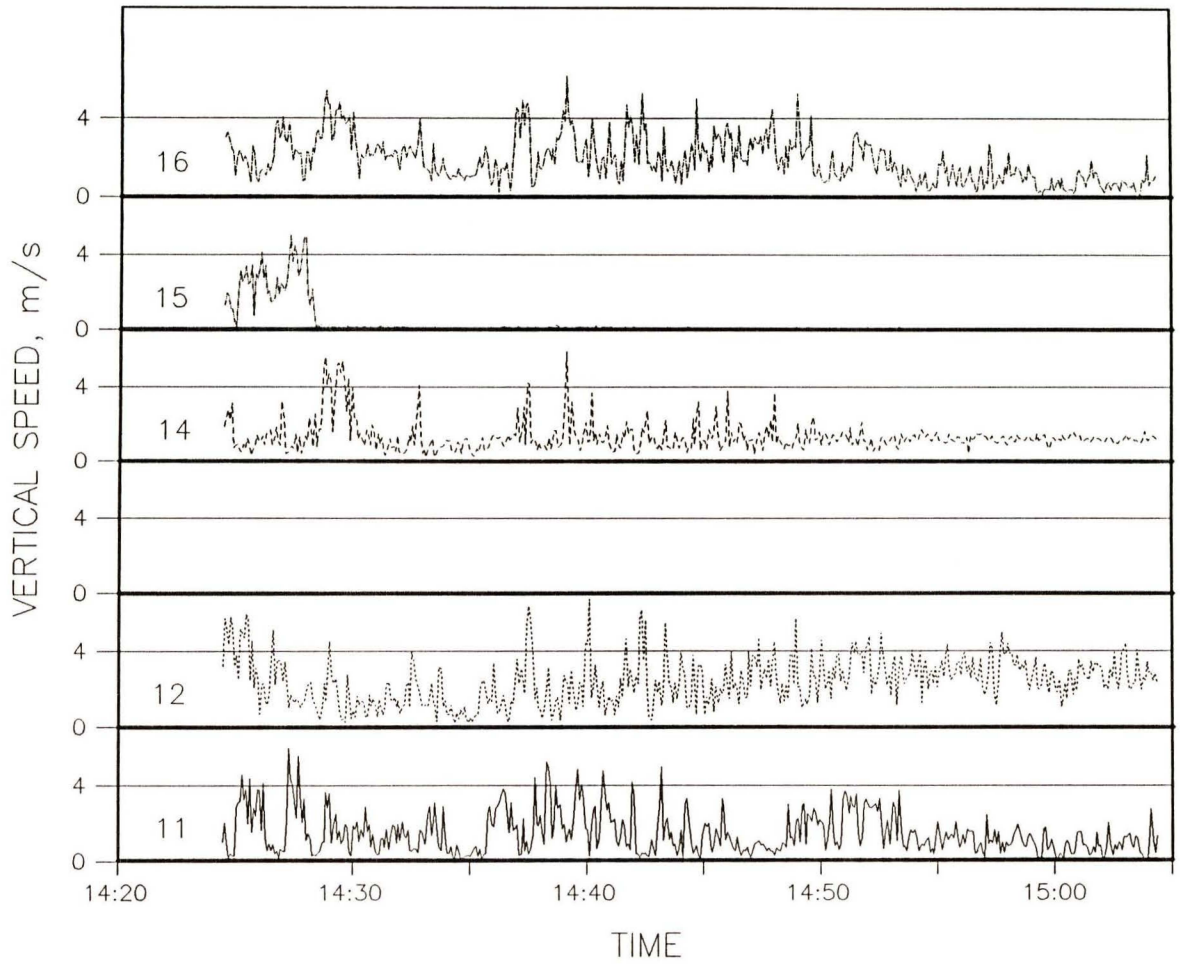

Figure 5.5-2 Vertical wind velocity measured at the 14-m height for FASS packages during the 40 minutes of sampling.

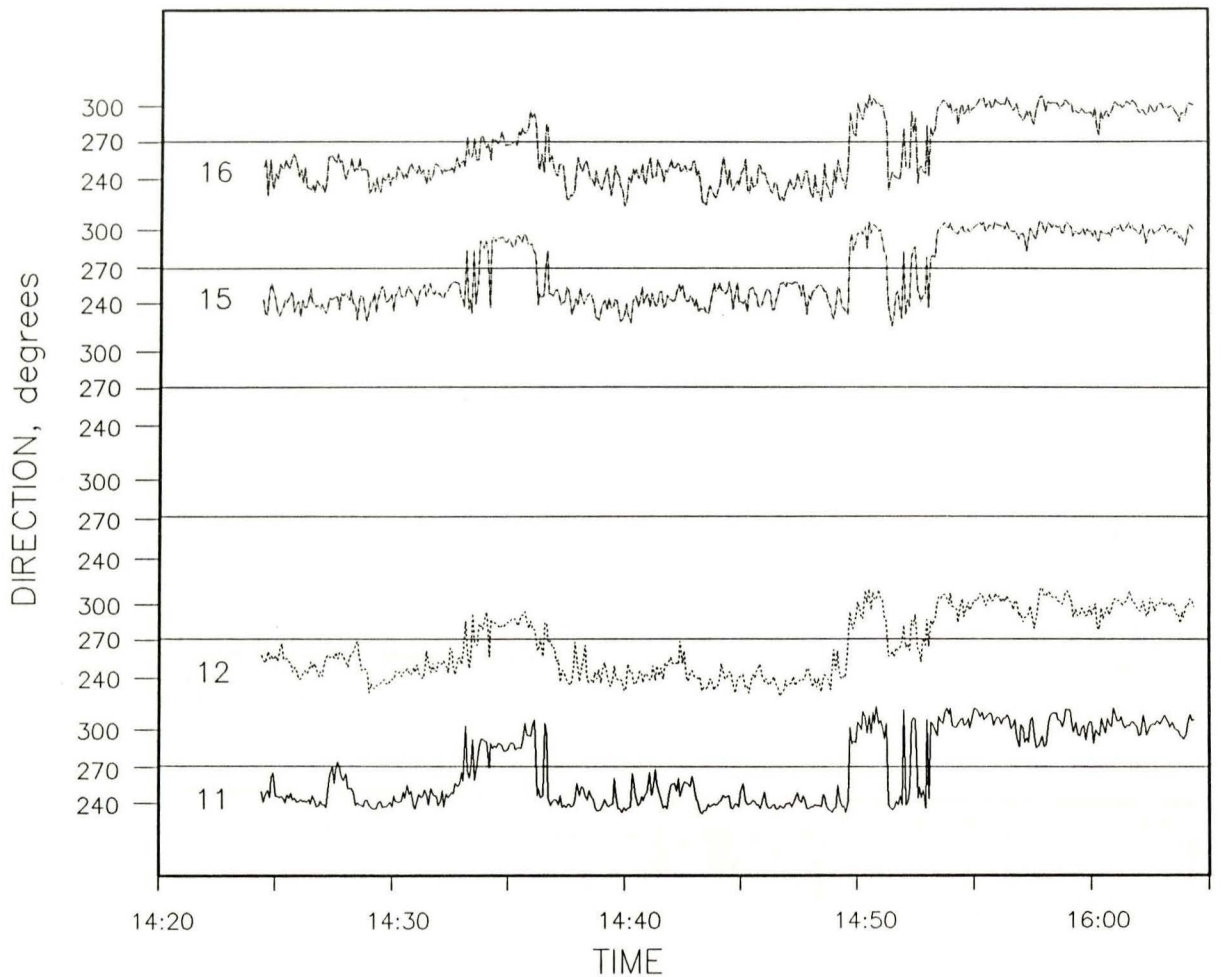

Figure 5.5-3 Horizontal wind direction measured at the 14-m height for FASS packages during the 40 minutes of sampling.

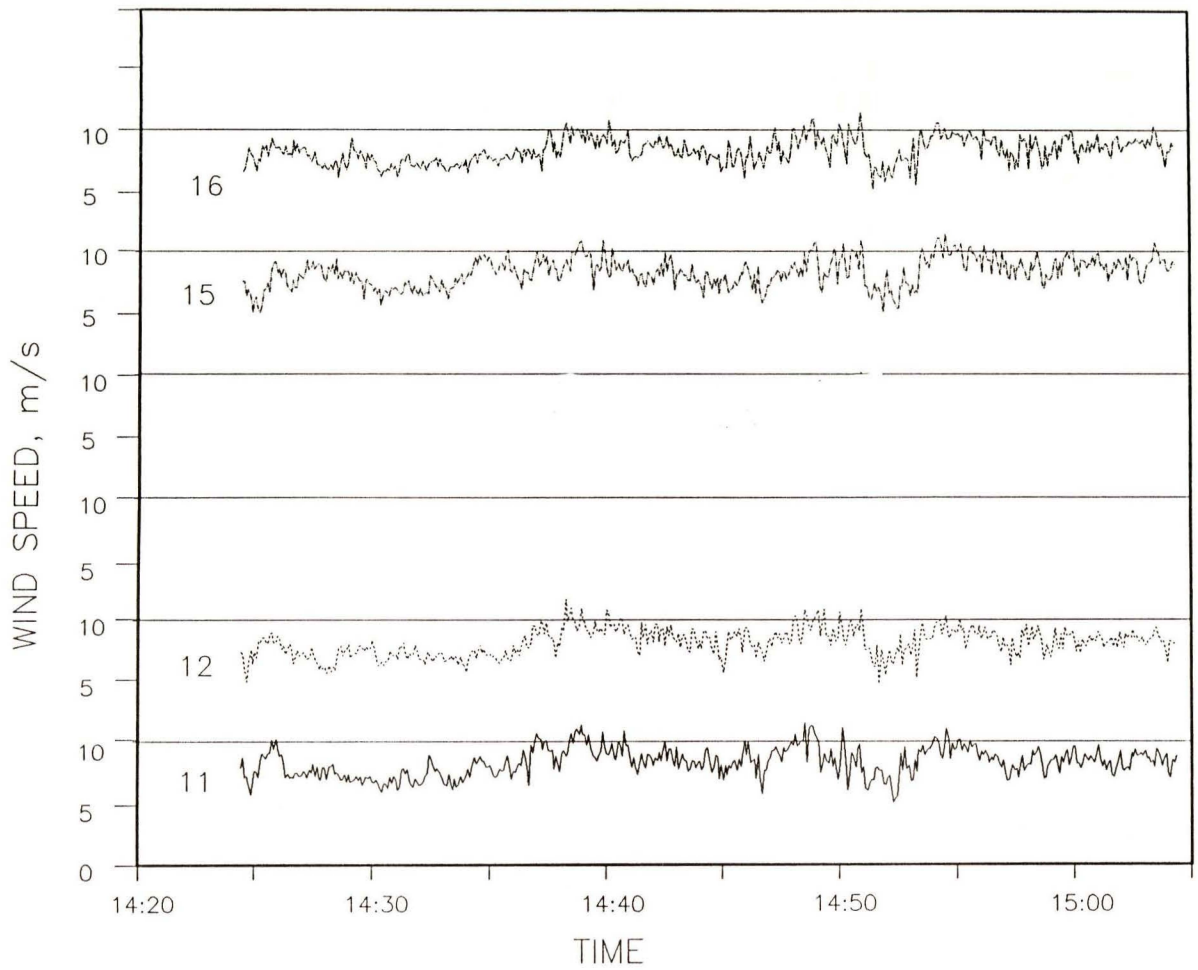

Figure 5.5-4 Horizontal wind speed measured at the 14-m height for FASS packages during the 40 minutes of sampling.

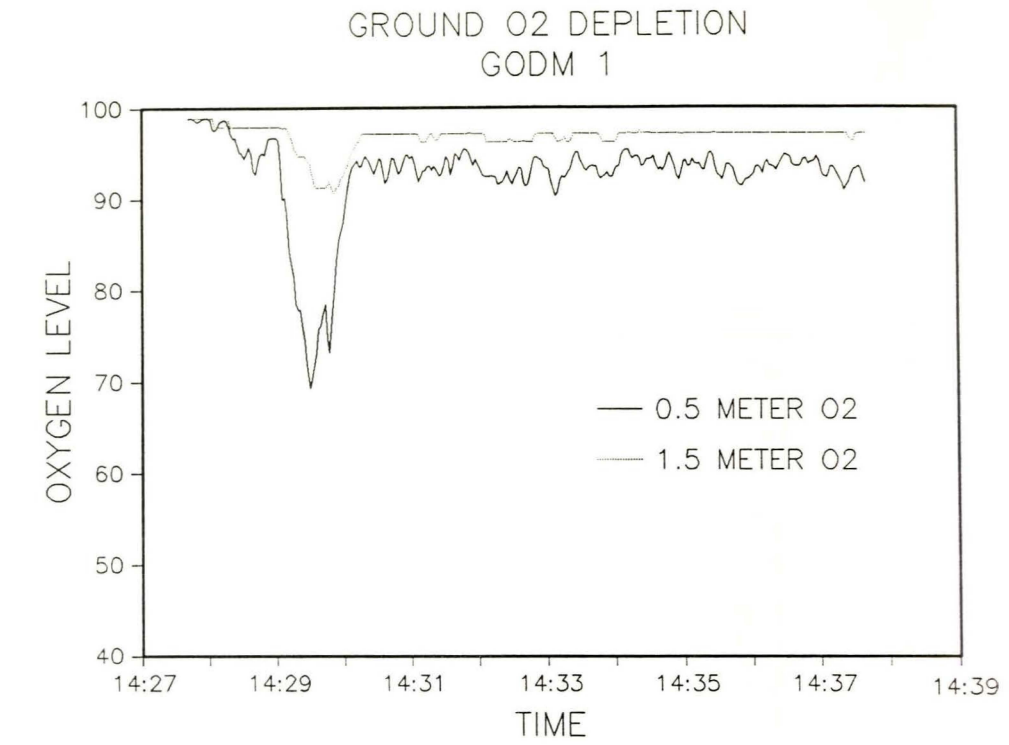

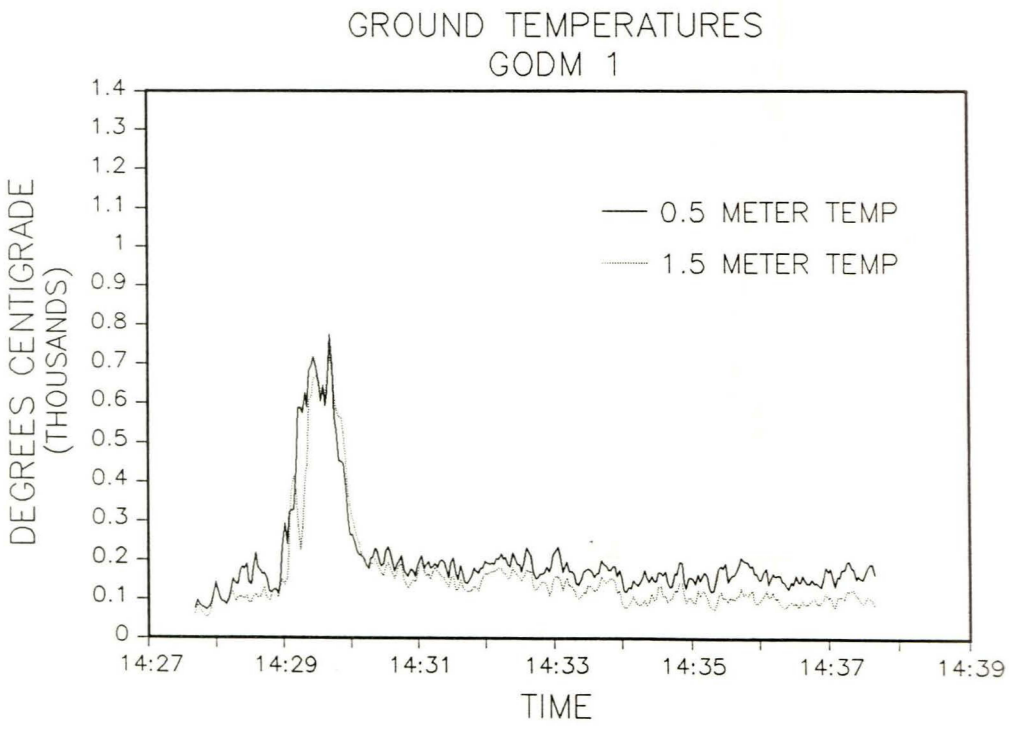

Figure 5.6-1 Real time measurements for GODM #1; A) oxygen deple
relative to ambient air, B) air temperature.

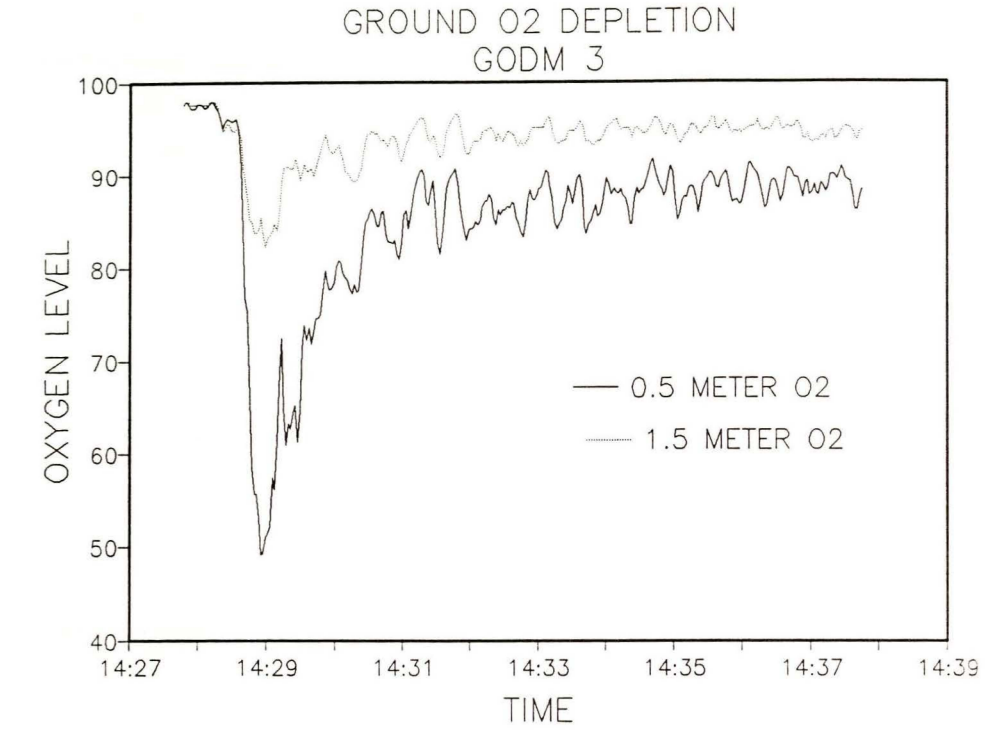

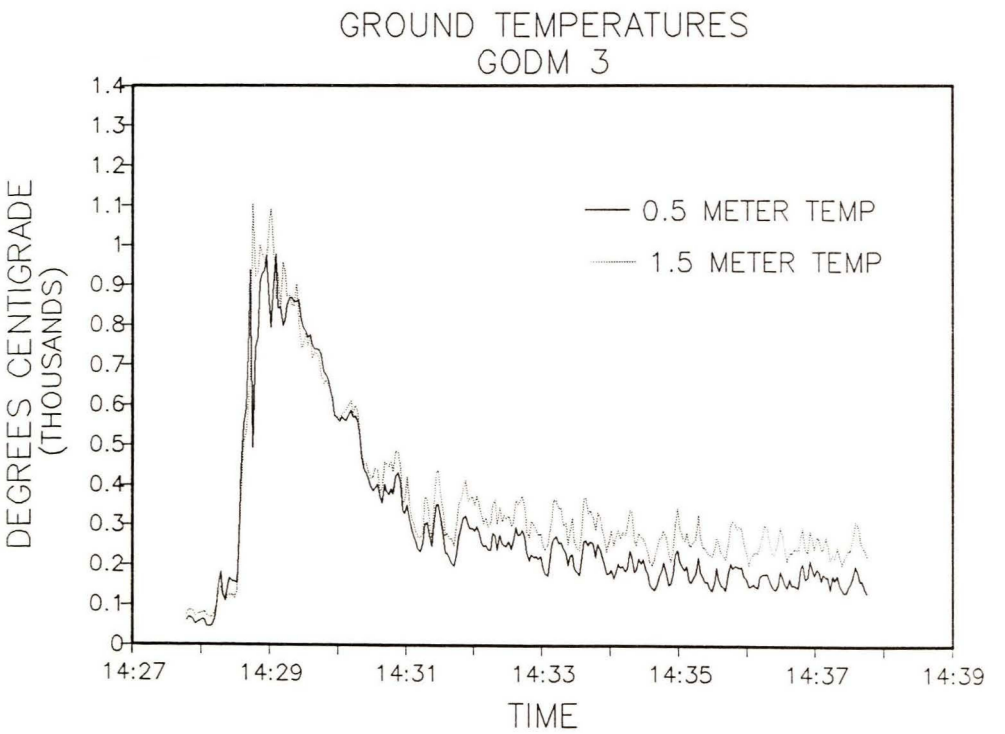

Figure 5.6-2 Real time measurements for GODM #3; A) oxygen depletion relative to ambient air, B) air temperature.

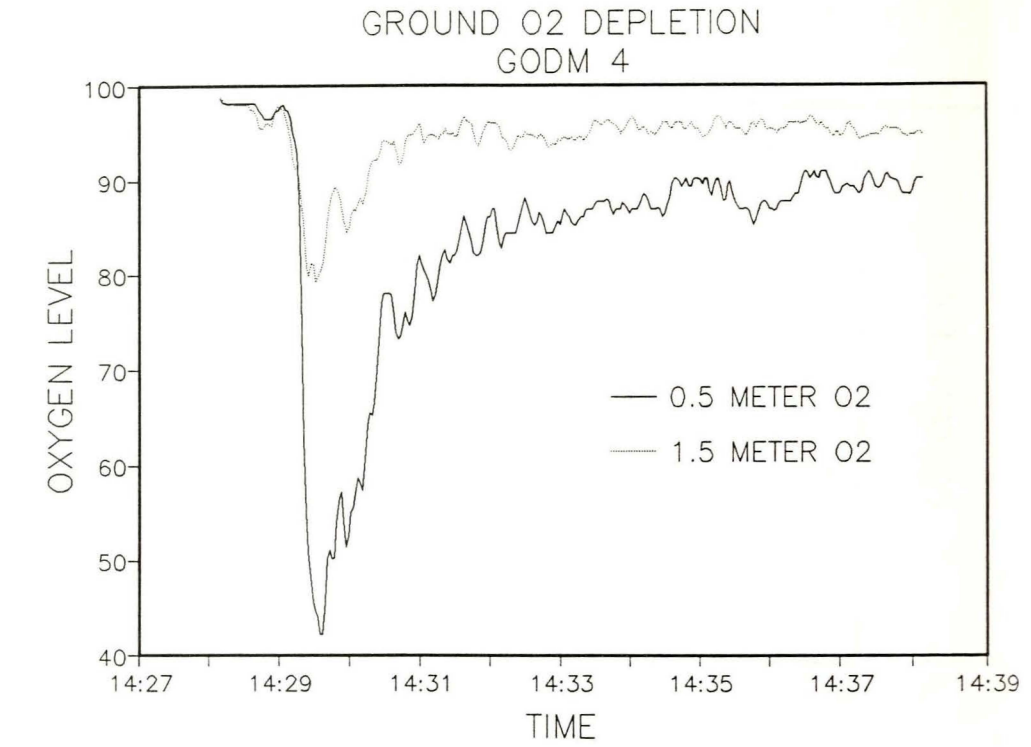

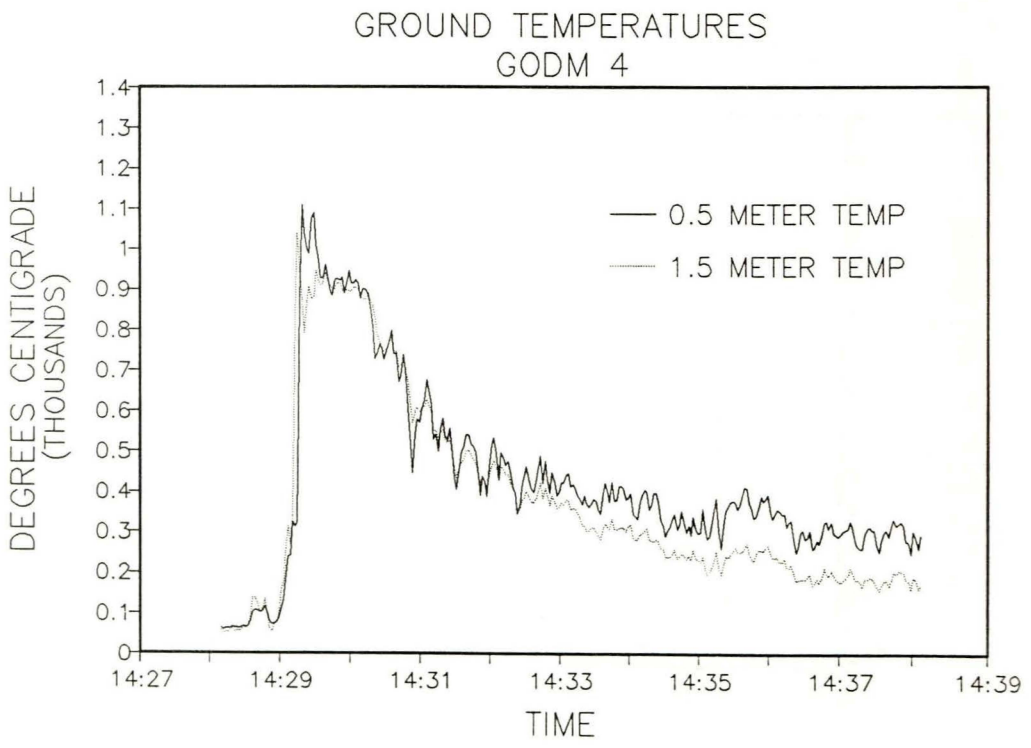

Figure 5.6-3 Real time measurements for GODM #4; A) oxygen depletion relative to ambient air, B) air temperature.

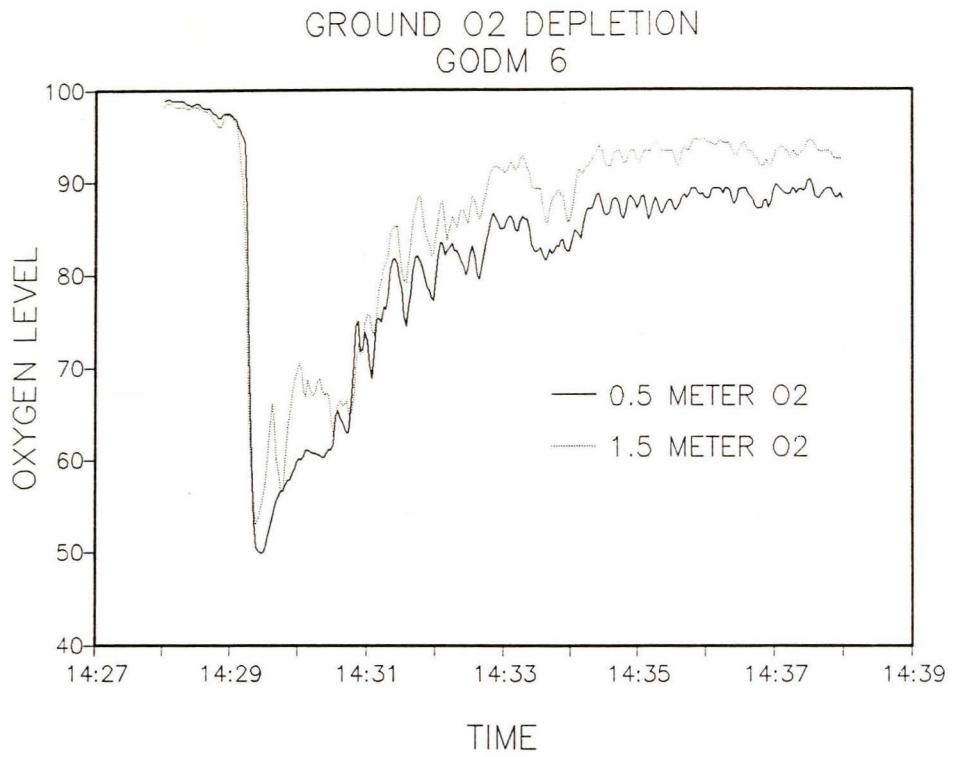

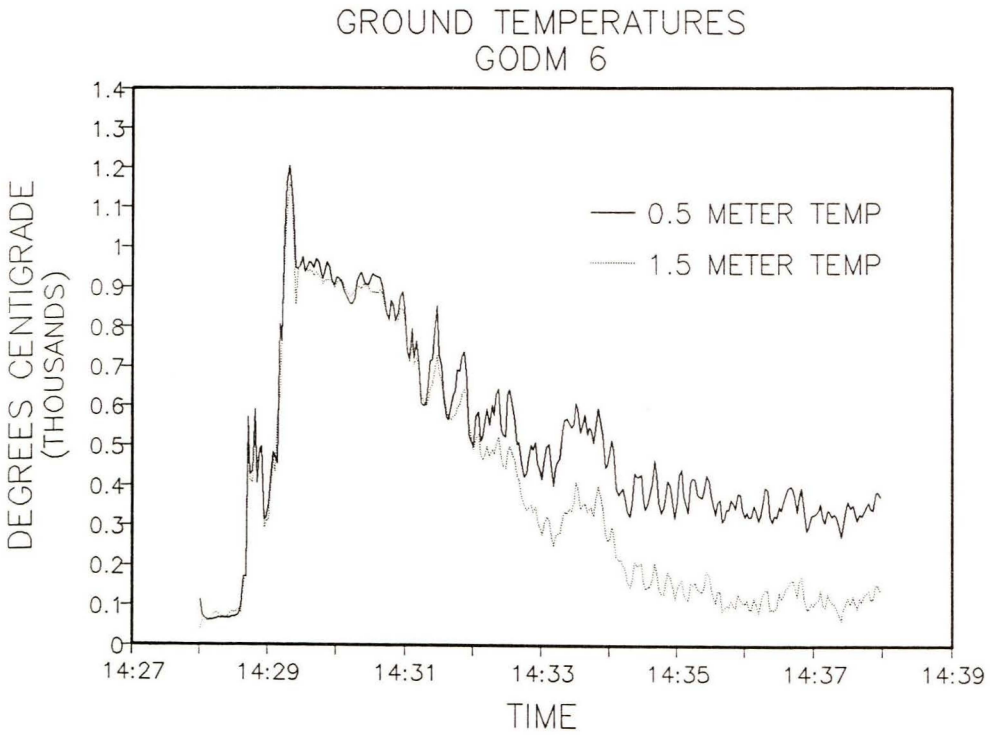

Figure 5.6-4 Real time measurements for GODM #6; A) oxygen depletion relative to ambient air, B) air temperature.

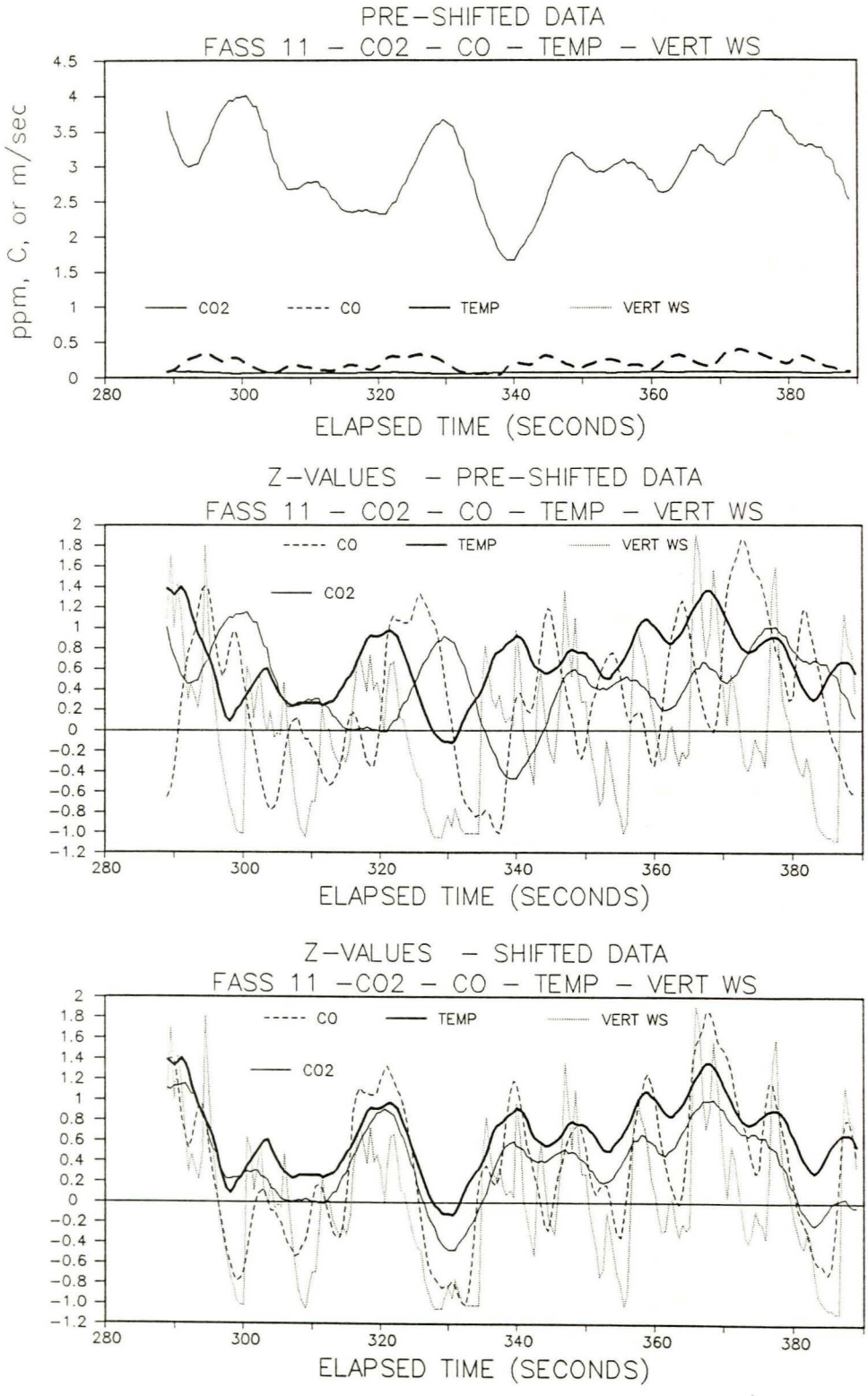
PRE-SHIFTED DATA
FASS 11 - CO2 - CO - TEMP - VERT WS
ppm, C, or m/sec
CO2
CO
TEMP
VERT WS
ELAPSED TIME (SECONDS)
Z-VALUES - PRE-SHIFTED DATA
FASS 11 - CO2 - CO - TEMP - VERT WS
ELAPSED TIME (SECONDS)
Z-VALUES - SHIFTED DATA
FASS 11 -CO2 - CO - TEMP - VERT WS
ELAPSED TIME (SECONDS)

Figure 5.7-1 Z-value data before time-adjustment and following adjustment.

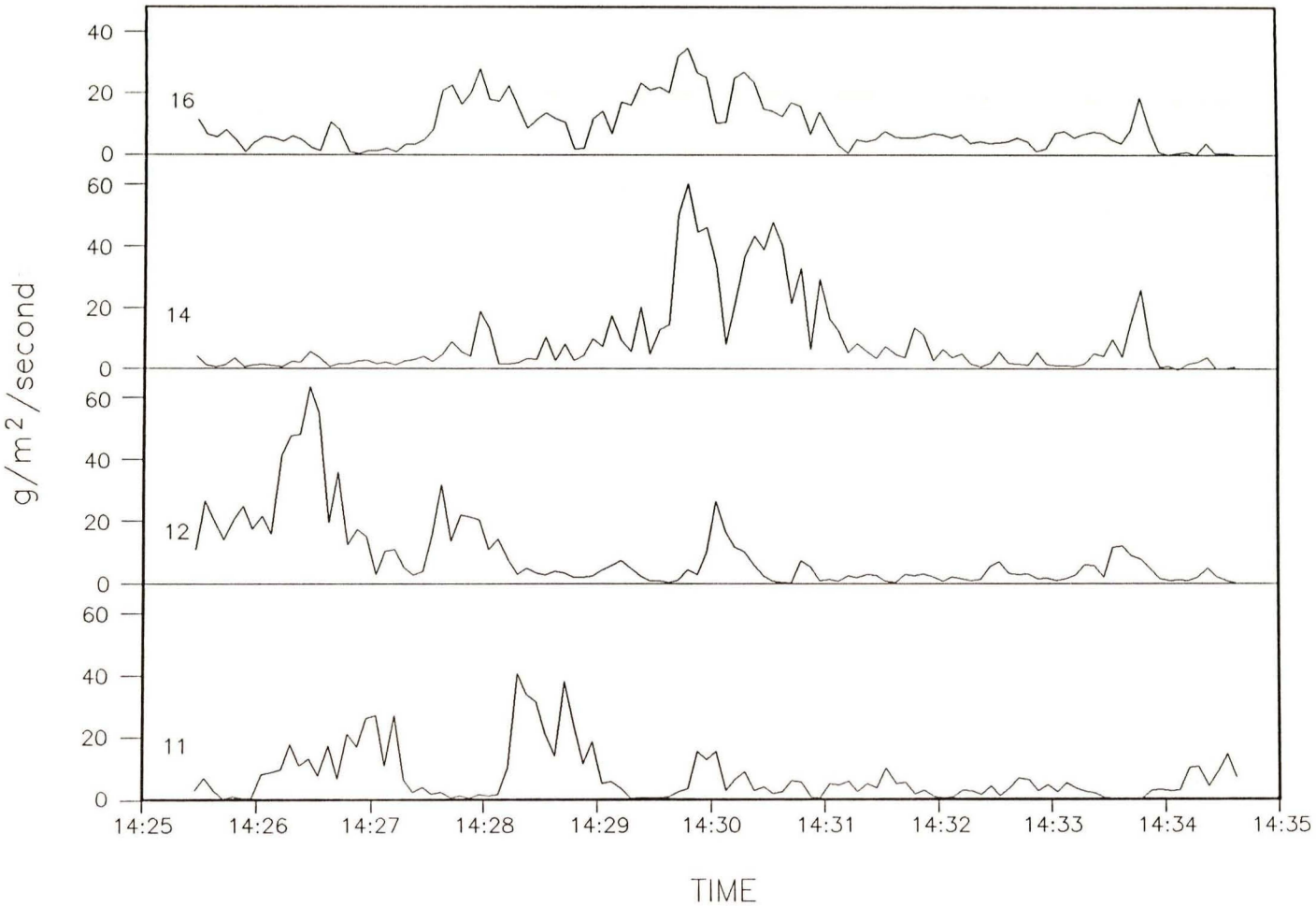

Figure 6.1.1-1 Calculated rate of fuel consumption based on carbon flux measurements for packages 11, 12, 14, and 16 for the Hill PB.

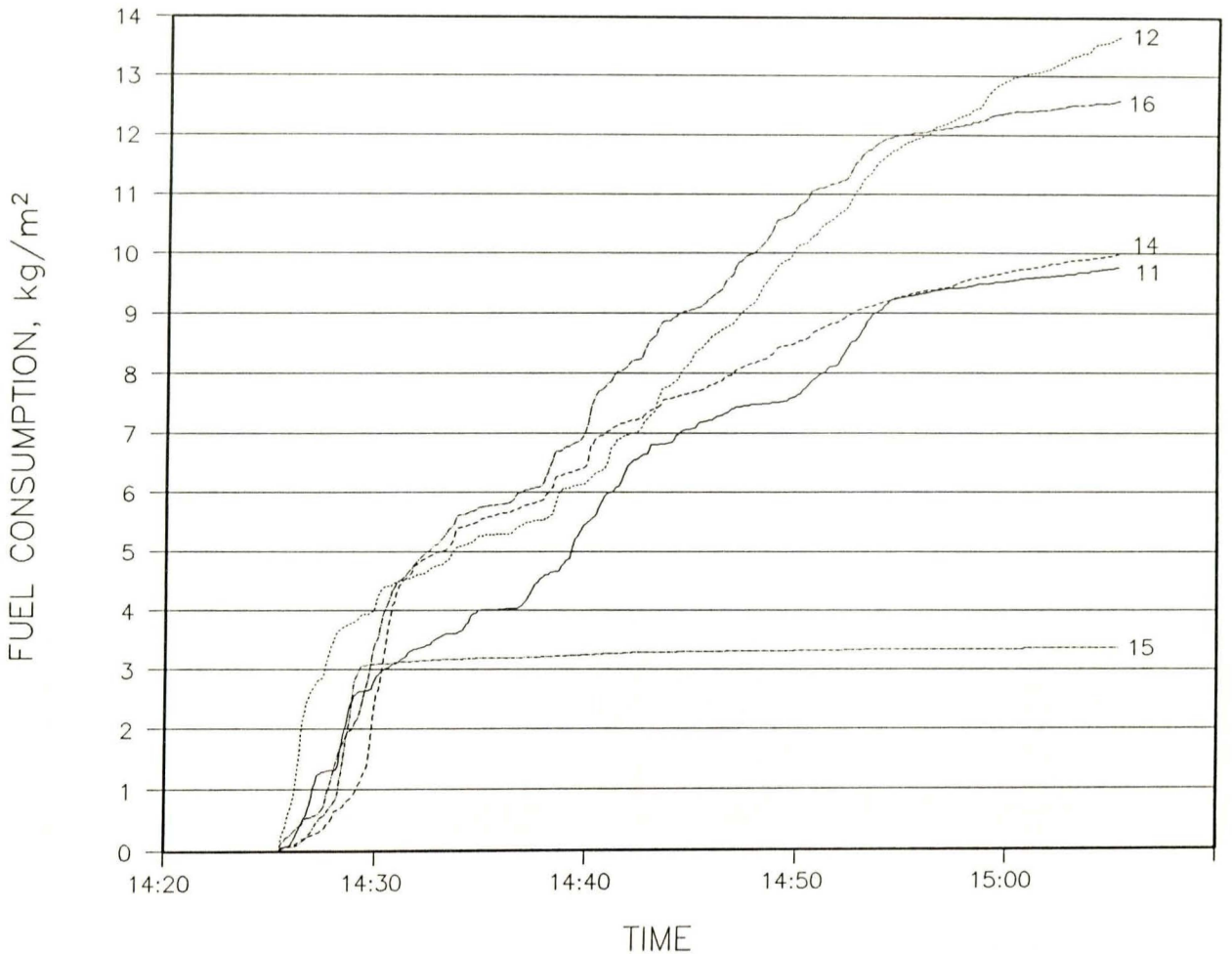

Figure 6.1.2-1 Cumulative fuel consumption for each of the four sets of data (packages 11, 12, 14, and 16) for Hill PB.

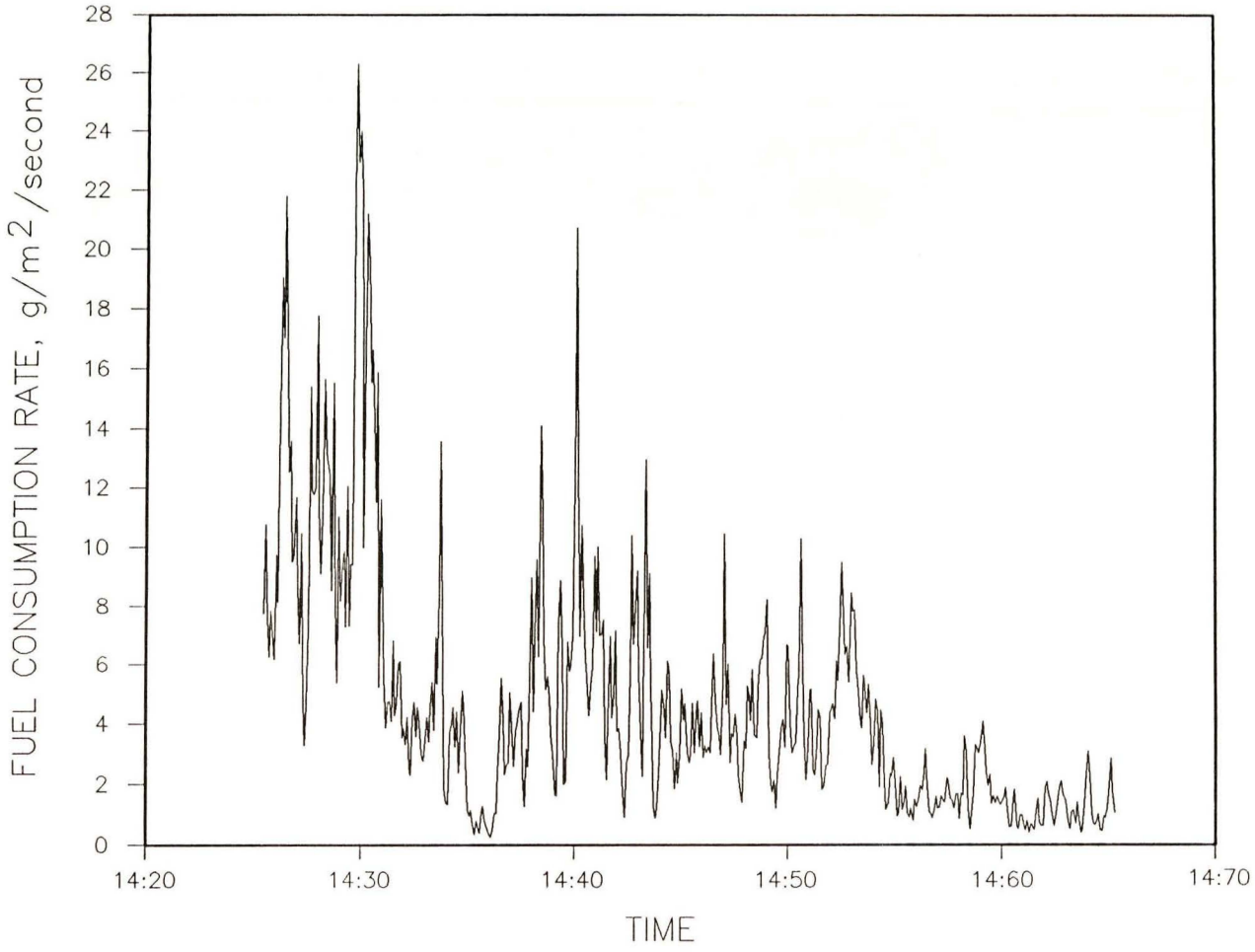

Figure 6.1.3-1 Average rate of fuel consumption in the area measured by the FASS array in the Hill PB (curves for 11, 12, 14, and 16 were averaged).

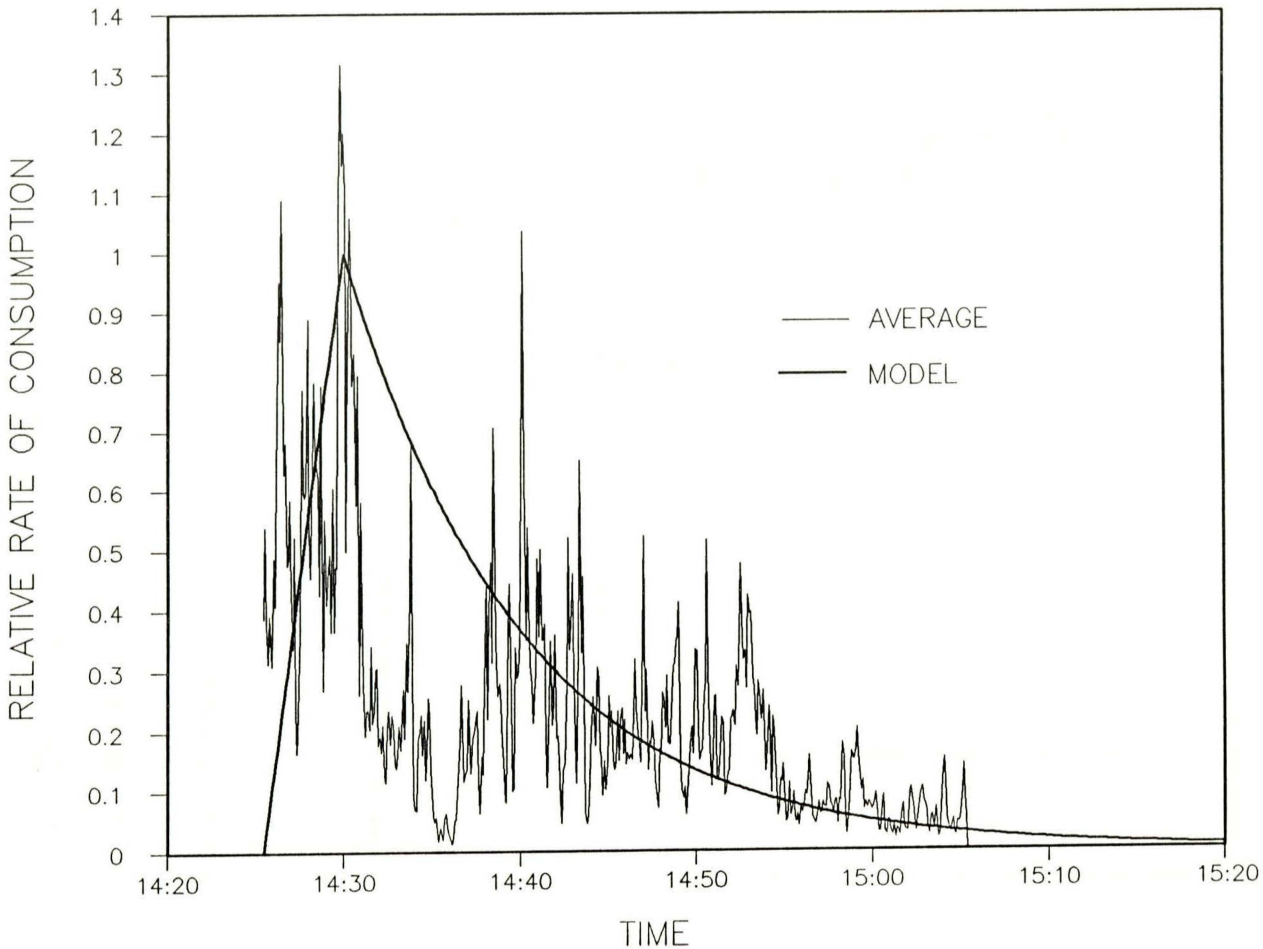

Figure 6.1.3-2 Fit of a simple model to the average rate of fuel consumption.

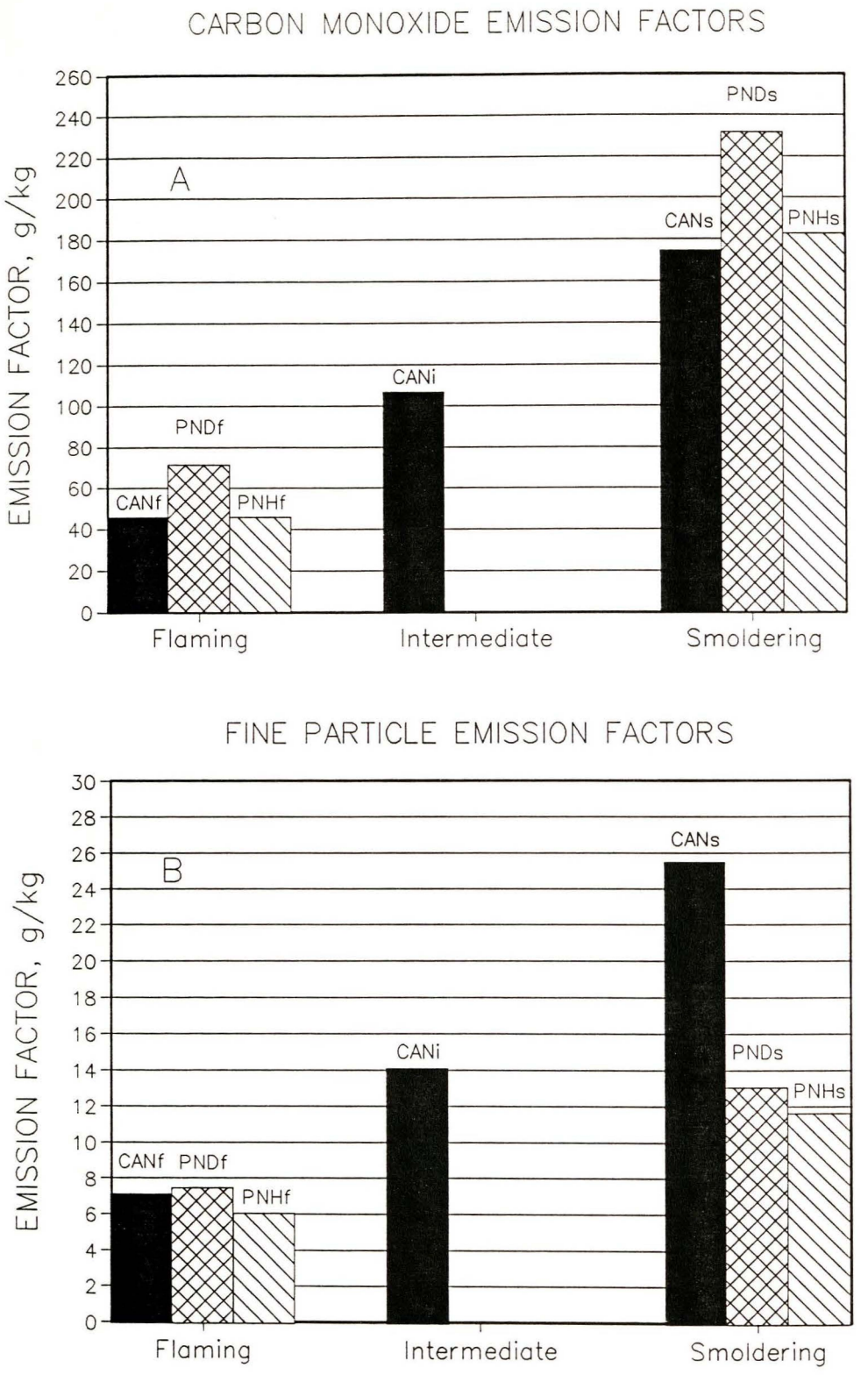

Figure 6.2-1 Comparison of emission factors measured for the Hill PB (CAN) with data from Pacific Northwest Douglas-fir (PND) and Pacific-Northwest hardwood (PNH); A) CO, B) PM 5.0. Flaming, intermediate and smoldering phases are indicated by f, i, s.

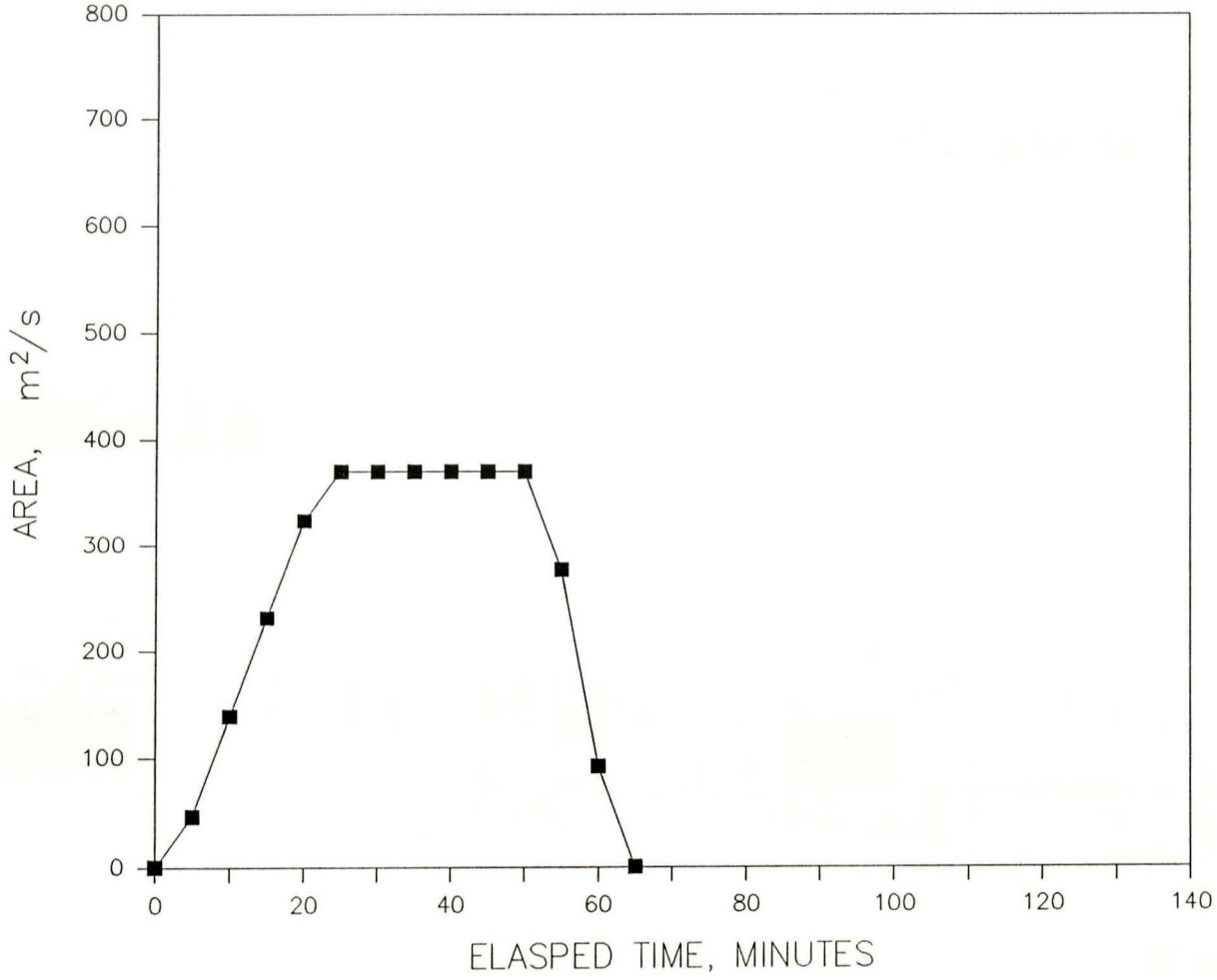

Figure 6.3-1 Hypothetical rate of ignition of Block A of Hill PB.

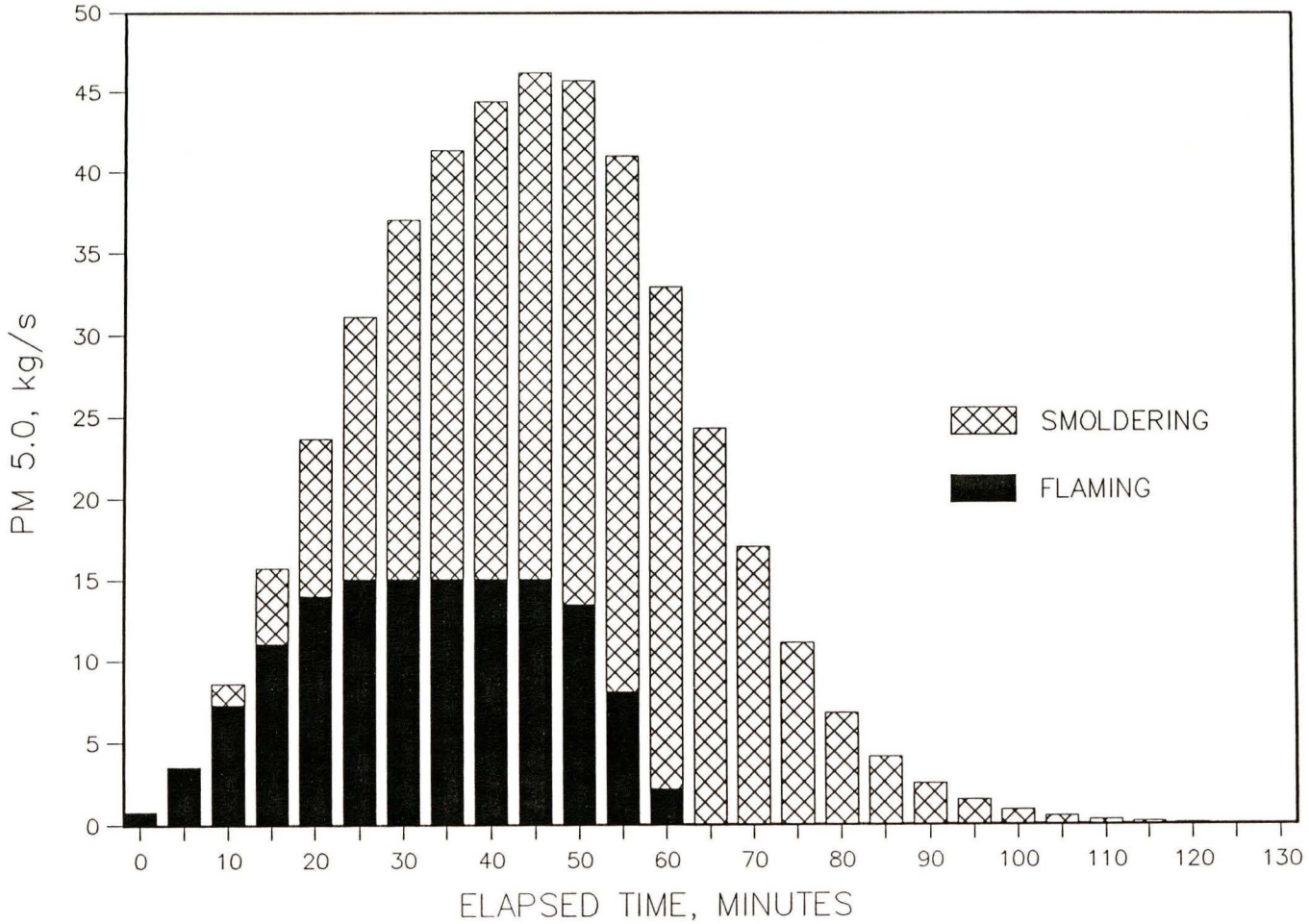

Figure 6.3-2 Source strength over time for particles less than 5.0 micrometers.

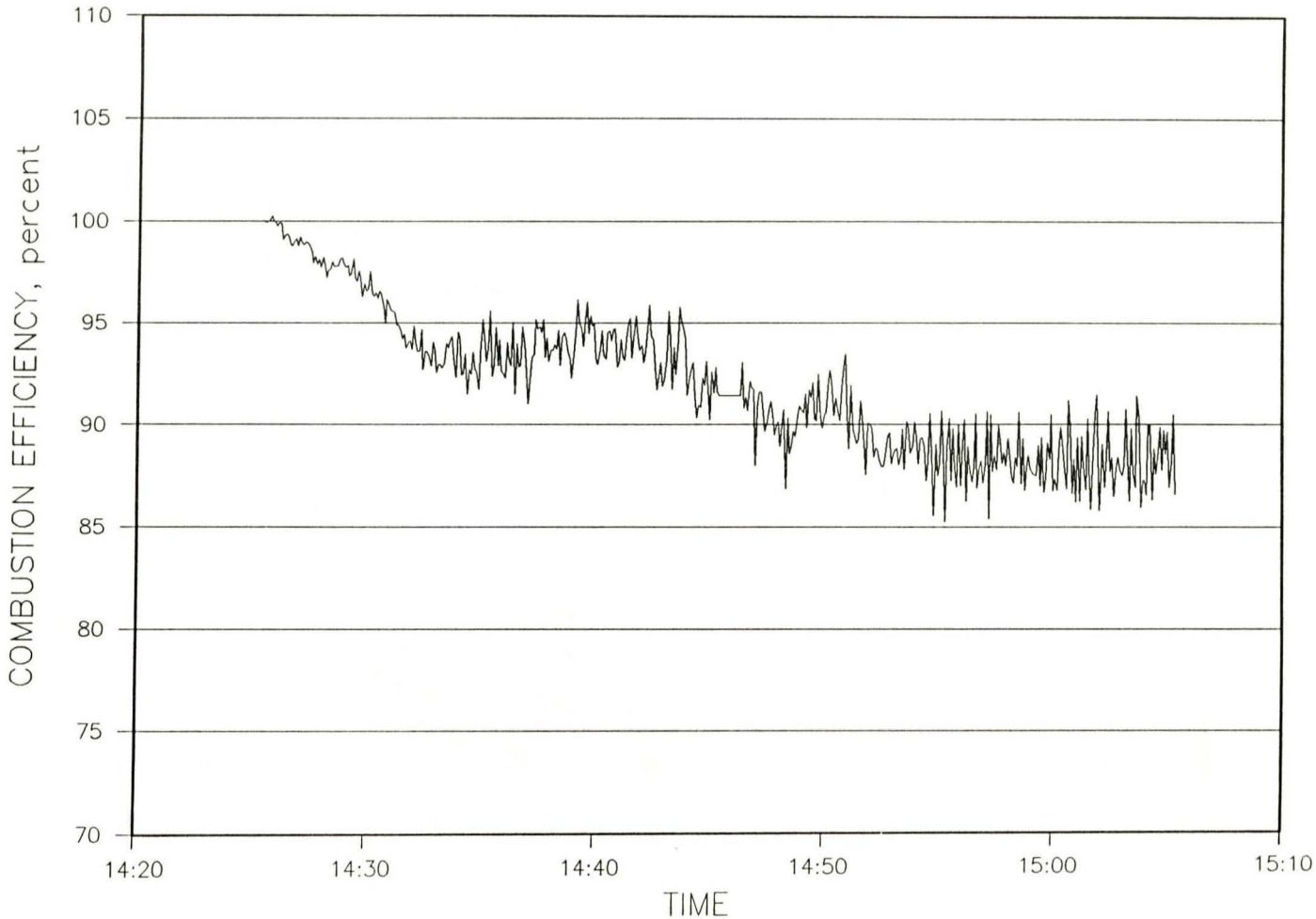

Figure 6.4-1 Average combustion efficiency for all FASS data from the Hill PB.

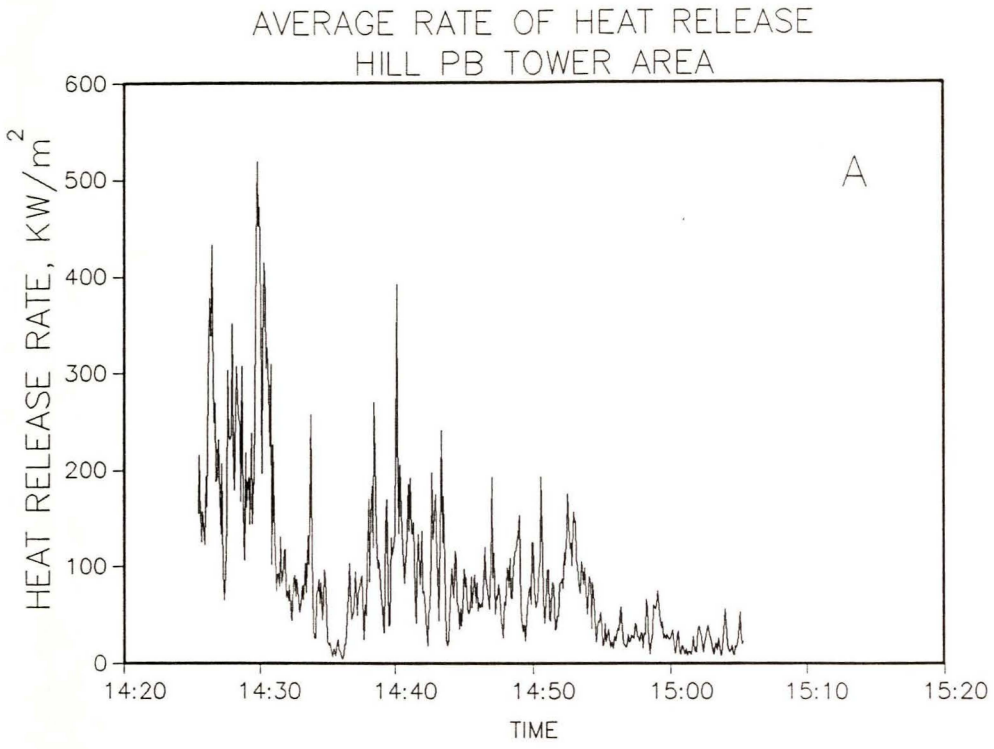

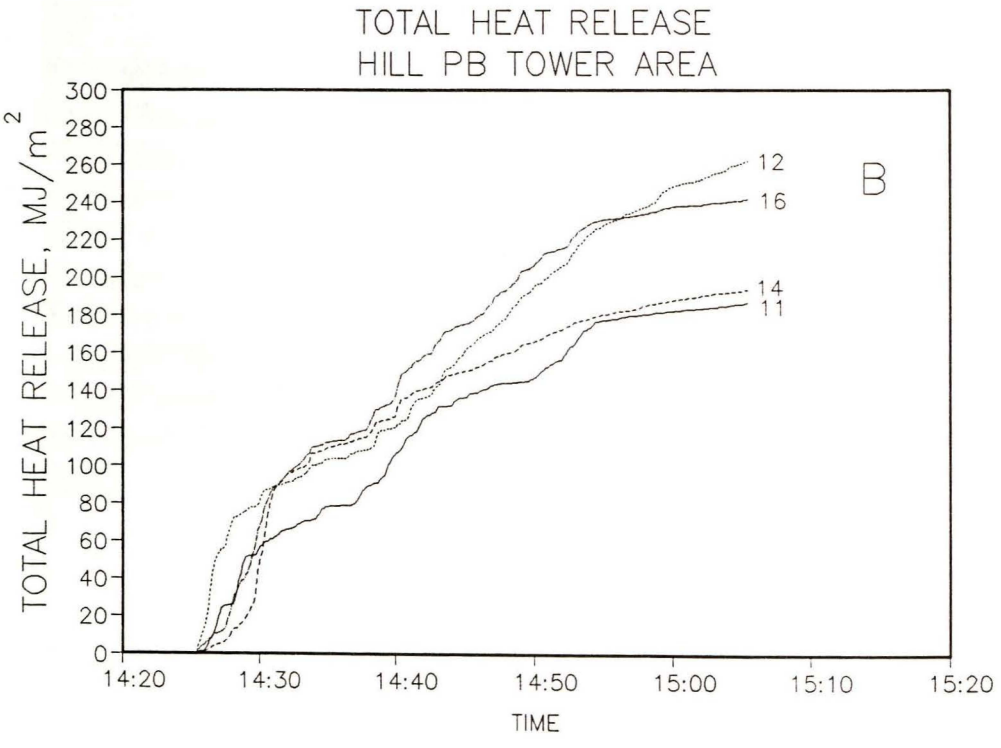

Figure 6.4-2 Calculated heat evolution for the FASS matrix area; A) rate of heat release, B) total heat from integration of the rate.

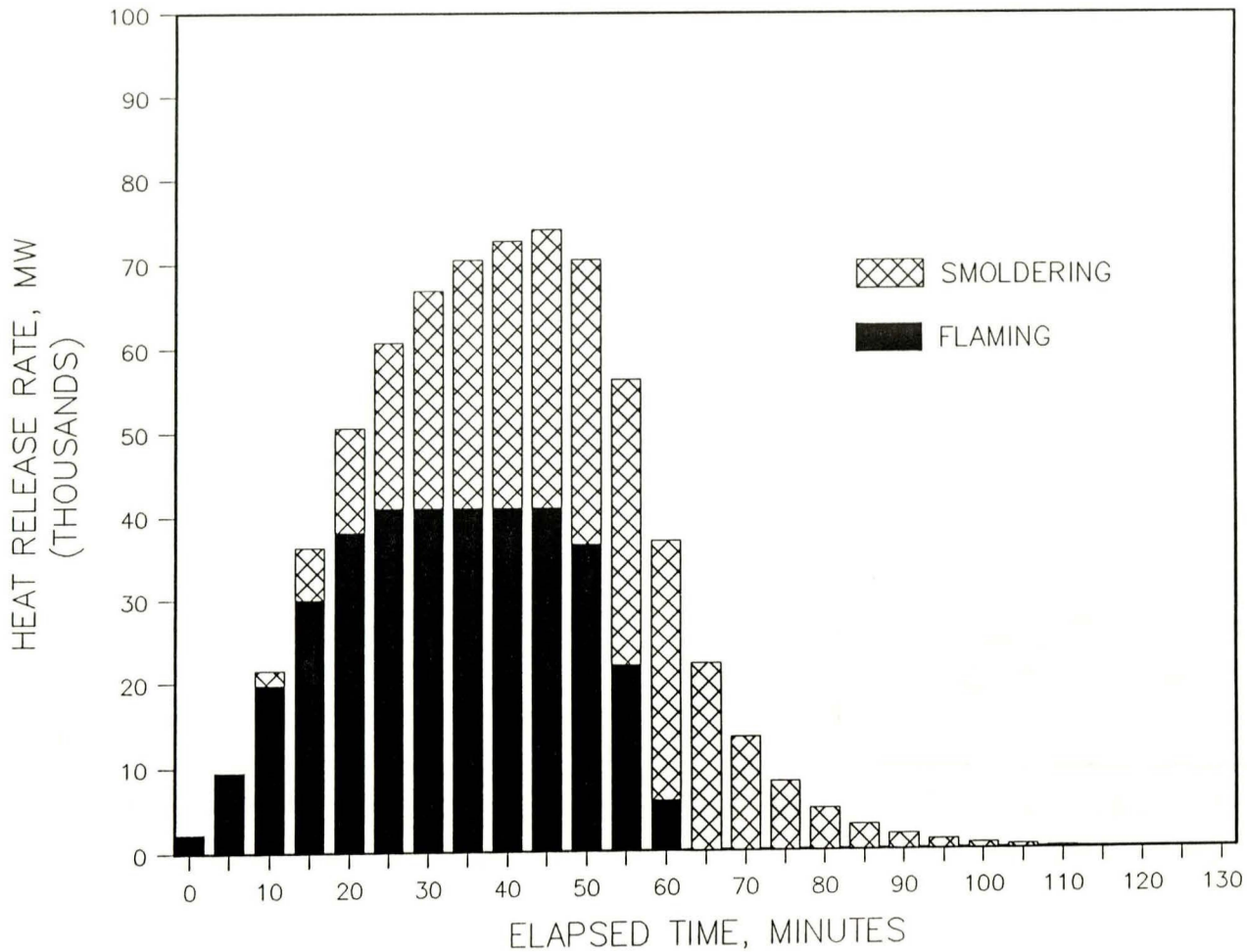

Figure 6.4-3 Total heat release estimate for Block A of the Hill PB.

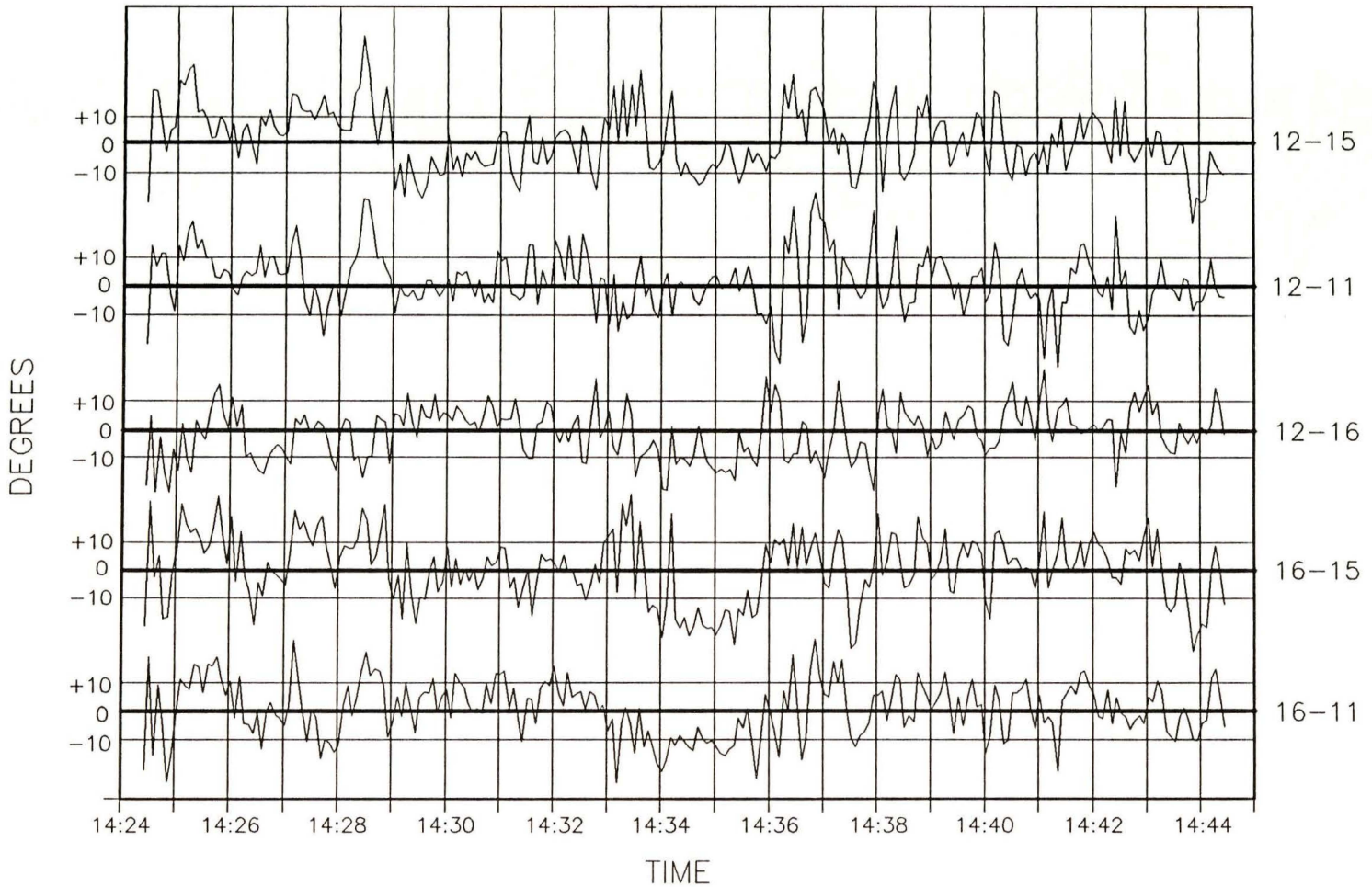

Figure 6.5.1-1 Difference in wind direction between pairs of FASS towers as indicated on right margin of figure. The wind direction of the southerly towers was subtracted from the wind direction of the northerly towers.

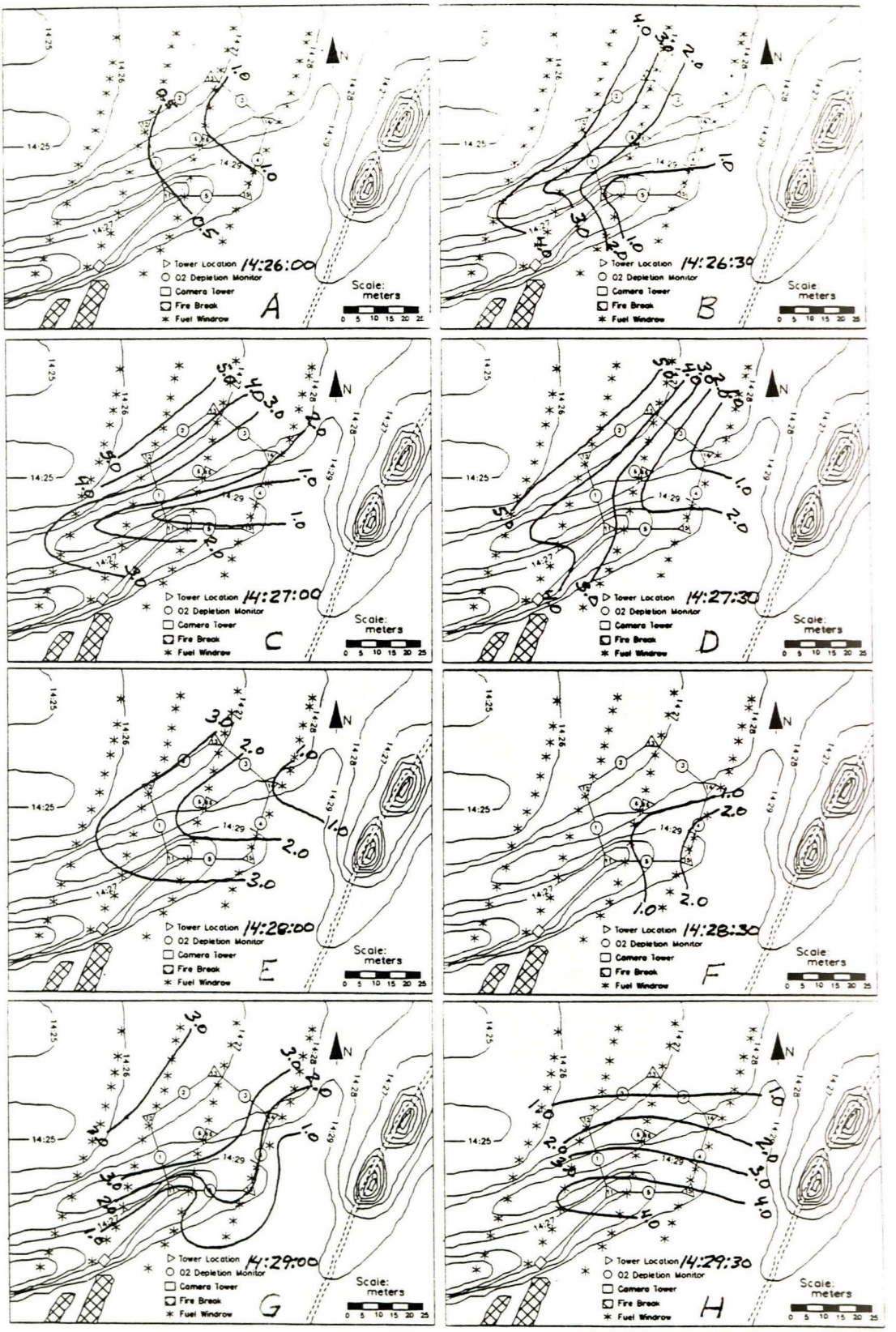

Figure 6.5.2-1A to 6.5.2-1H Distribution of vertical velocities across FASS array for each 30 seconds during the flaming phase.

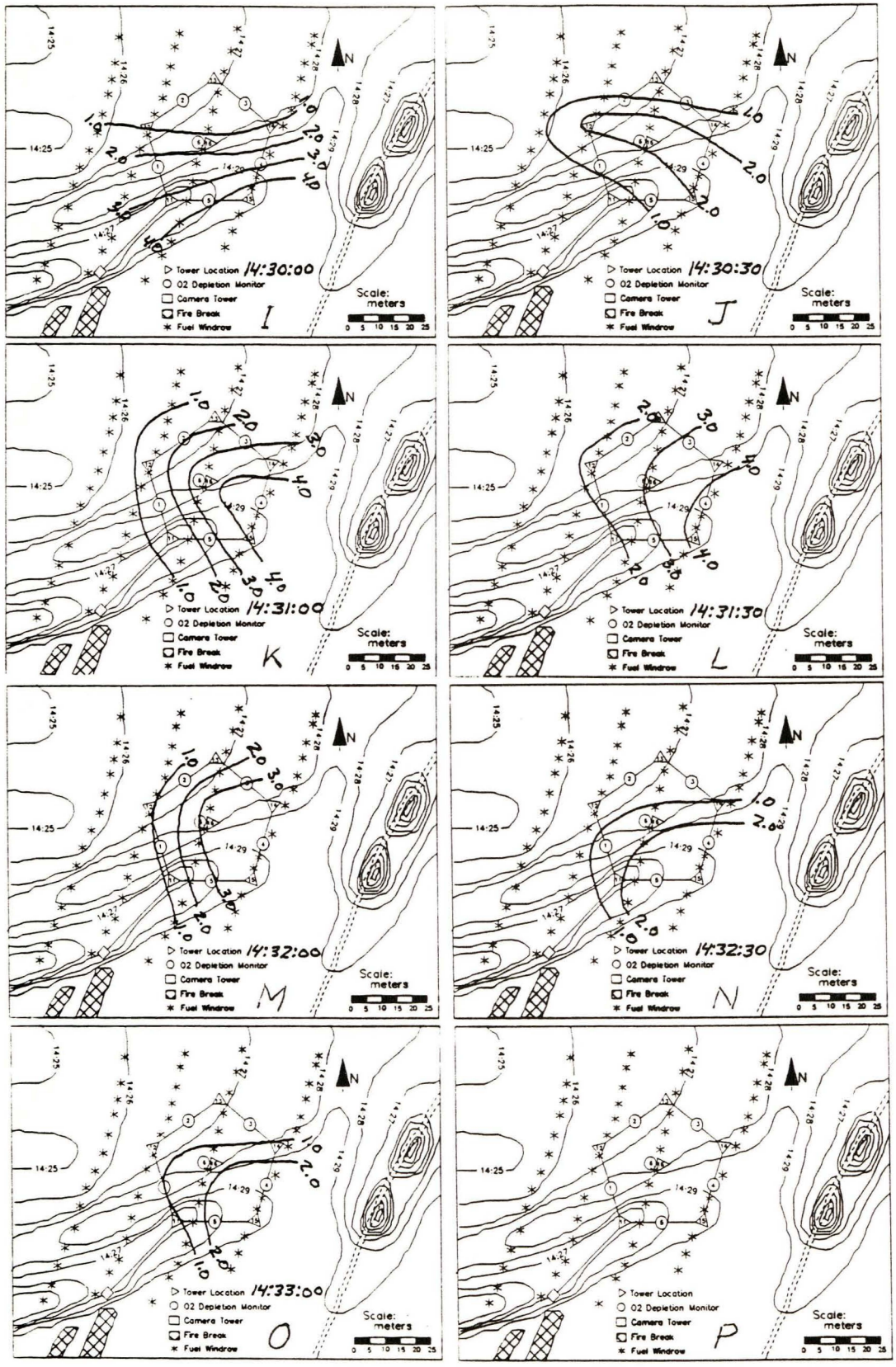

Figure 6.5.2-1I to 6.5.2-1P Distribution of vertical velocities across FASS array for each 30 seconds during the flaming phase.

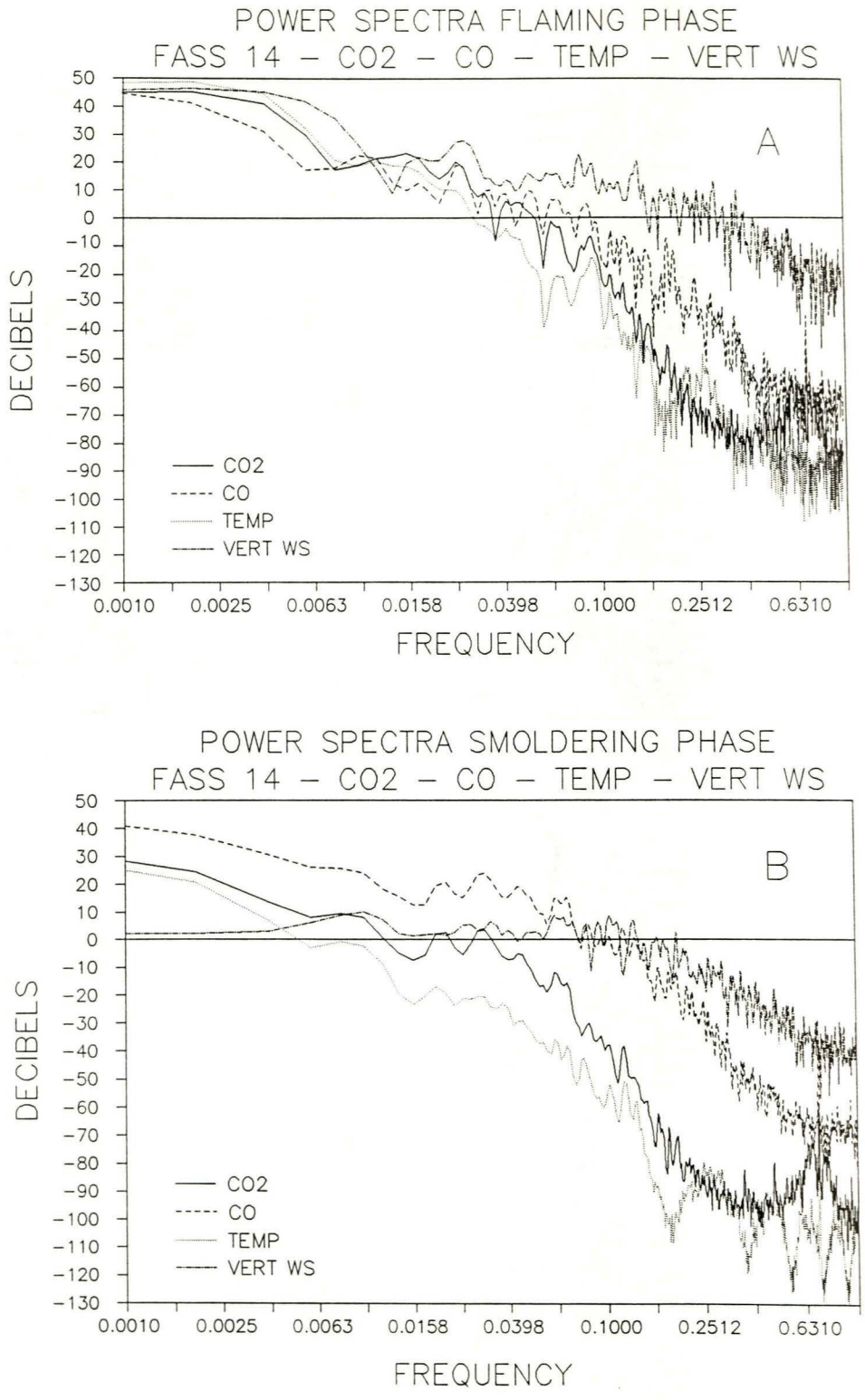

Figure 6.6-1 Power spectra of real time measurements for FASS 14; a) flami
B) smoldering.

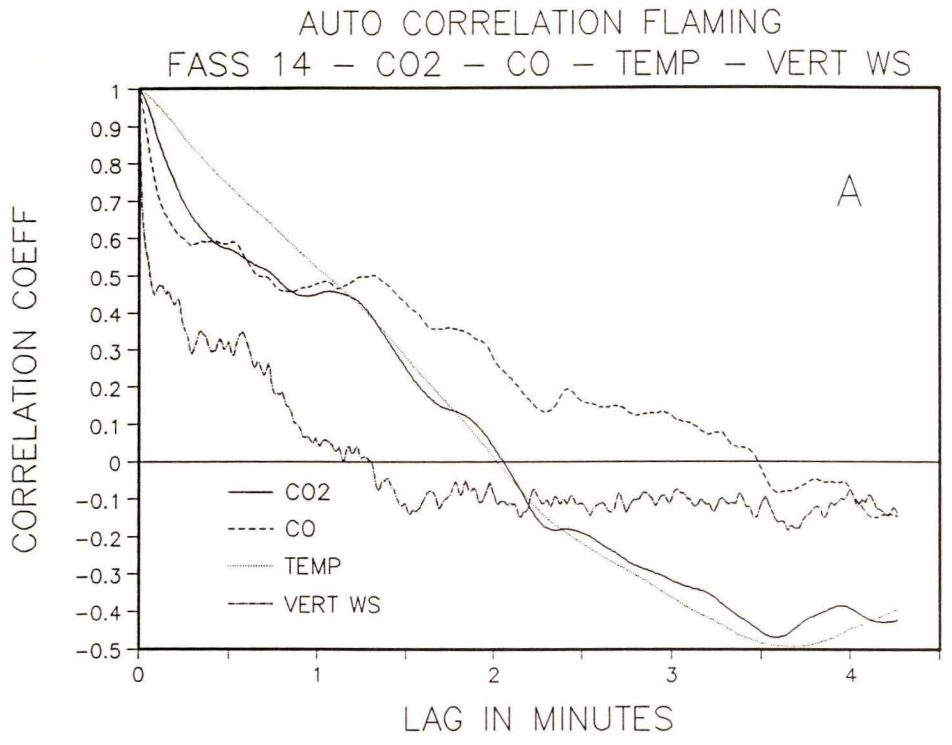

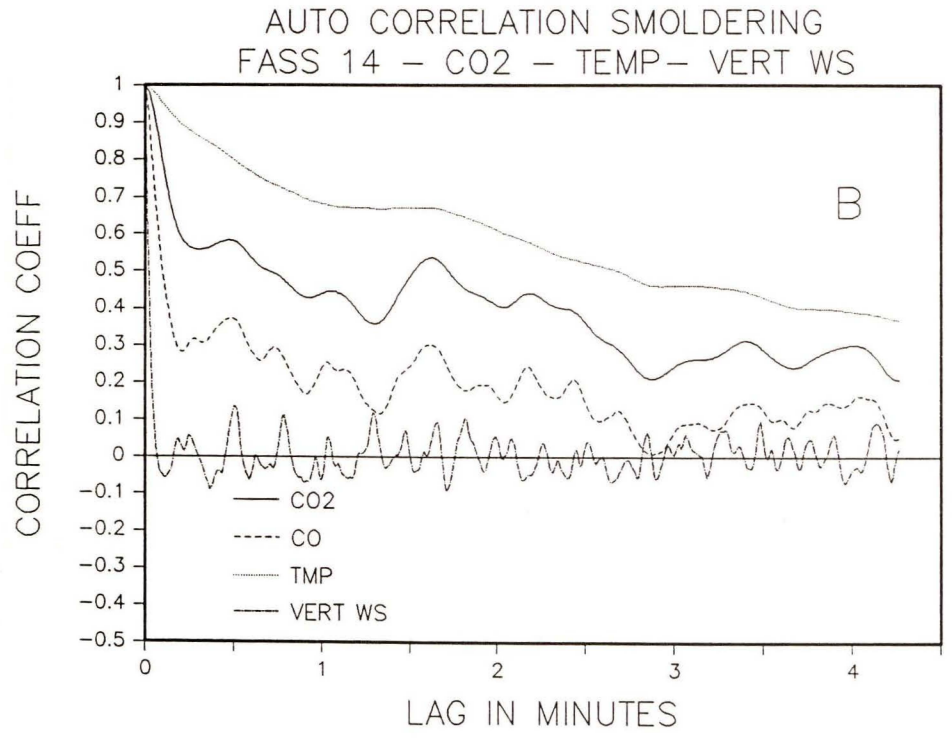

Figure 6.6-2 Auto correlation plots for FASS 14; A) flaming, B) smoldering.

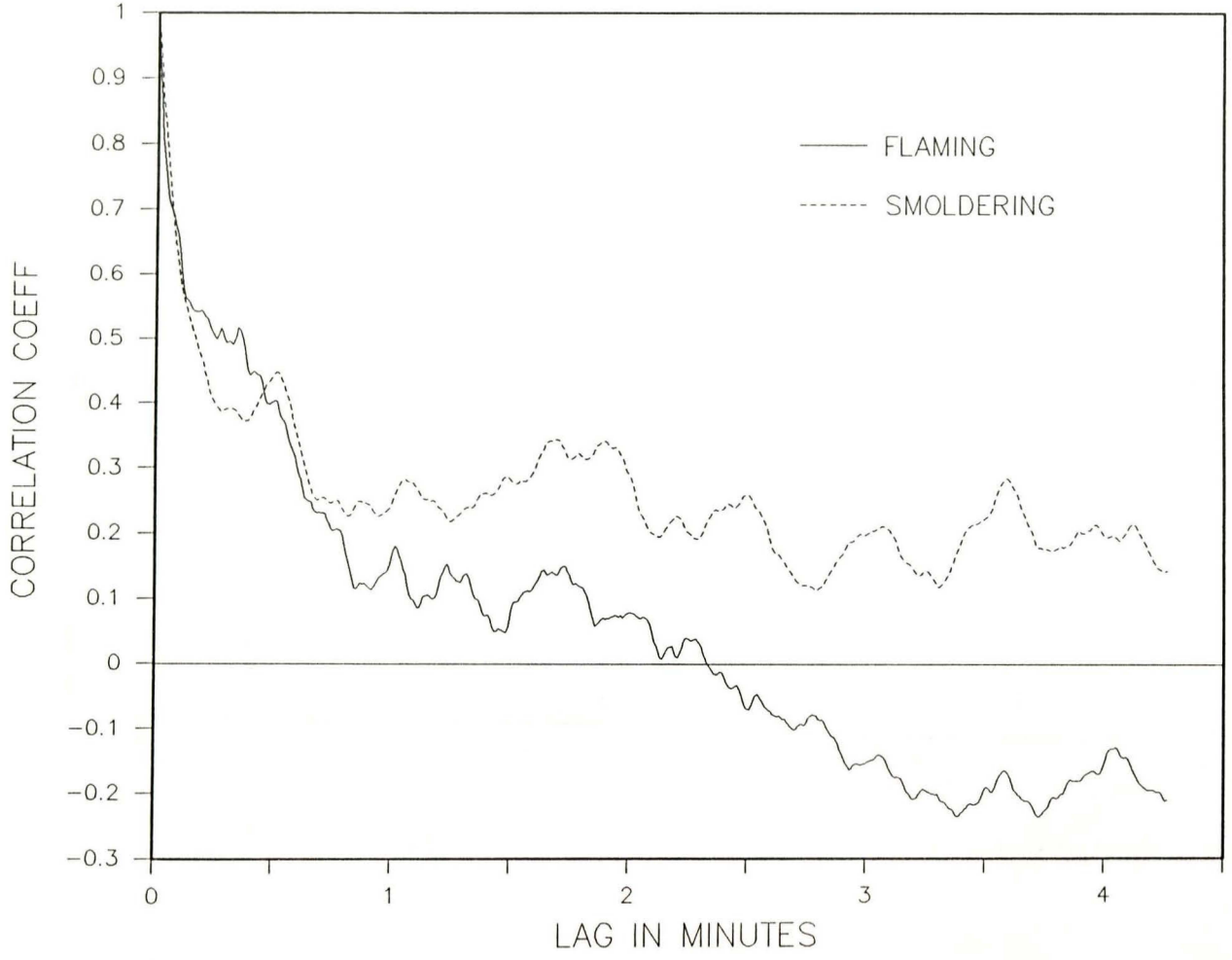

Figure 6.6-3 Auto Correlation of the heat release rate for FASS 16 flaming and smoldering phases.

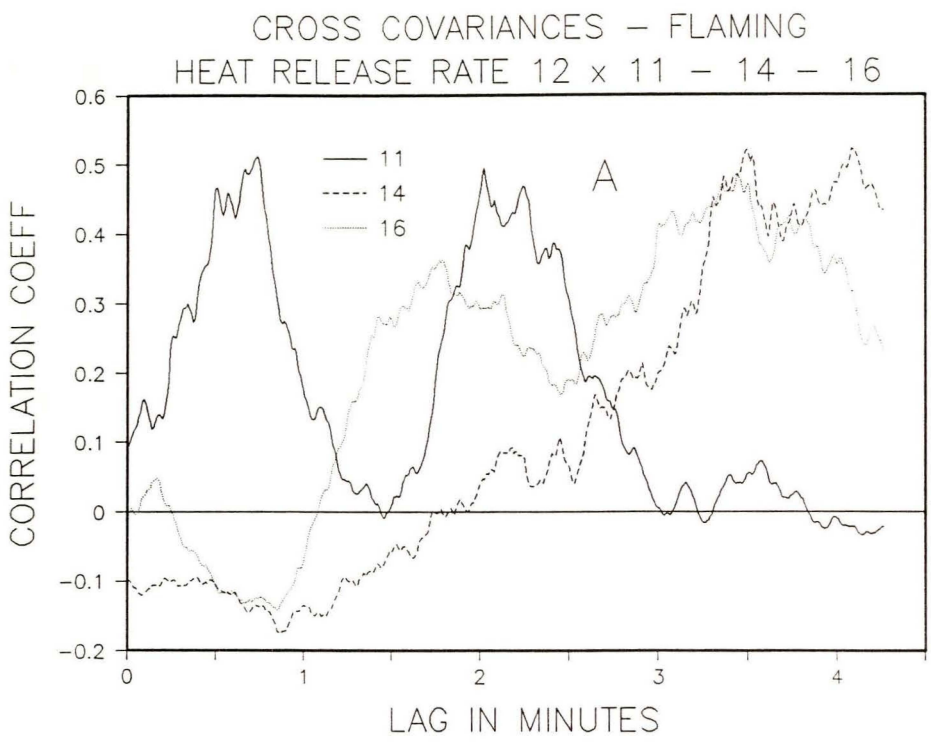

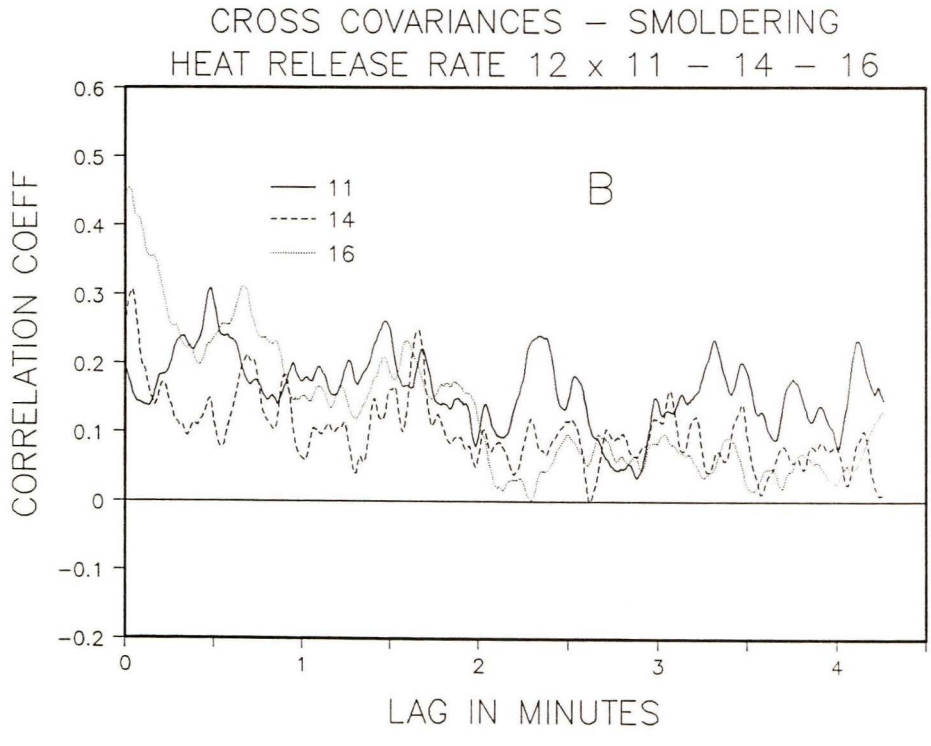

Figure 6.6-4 Heat release cross-covariances between FASS towers.

Table 2.2-1 Elemental analysis of Canadian fuels from 1988 mass burn. Compositions are on a dry weight and an ash free basis.

Sample Identification	%C	%H	%N	%O
Timmons Duff	58.19	5.29	1.82	43.59
Timmons litter	57.54	6.33	1.26	39.47
White Birch Twig (0.0-0.49 cm)	54.39	6.30	0.85	40.25
White Birch Wood (3.0-4.99 cm)	49.86	6.01	0.10	45.61
White Birch Wood (7.0+ cm)	49.50	6.07	0.09	46.06
White Birch Bark (3.0-4.99 cm)	57.82	6.82	0.47	36.64
White Birch Bark (7.0+ cm)	58.74	7.08	0.49	35.59
Black Spruce Twig (0.0-0.49 cm)	56.45	6.37	0.61	38.63
Black Spruce Wood (3.0-4.99 cm)	52.02	6.10	0.18	43.67
Black Spruce Wood (7.0+ cm)	50.59	6.05	0.05	45.18
Black Spruce Bark (3.0-4.99 cm)	57.92	6.06	0.48	37.99
Black Spruce Bark (7.0+ cm)	53.34	5.77	0.29	42.82
Jack Pine Twig (0.0-0.49 cm)	55.03	6.26	0.57	40.15
Jack Pine Wood (3.0-4.99 cm)	51.38	5.97	0.05	44.82
Jack Pine Wood (7.0+ cm)	51.37	6.15	0.04	44.25
Jack Pine Bark (3.0-4.99 cm)	52.31	5.91	0.48	43.73
Jack Pine Bark (7.0+ cm)	54.34	5.92	0.24	41.84
Poplar Twig (0.0-0.49 cm)	56.52	6.60	1.06	37.68
Poplar Wood (3.0-4.99 cm)	50.71	6.09	0.15	44.44
Poplar Wood (7.0+ cm)	49.25	6.07	0.05	46.25
Poplar Bark (3.0-4.99 cm)	54.80	6.54	0.82	39.52
Poplar Bark (7.0+ cm)	52.75	6.33	0.40	42.15

Table 5.2-1 FASS sample bag gas concentrations.

FASS #	CO_2 ppm	CO ppm
a. Flaming phase 10 minutes		
11	3217	126
12	3420	142
13	4166	168
14	4490	154
15	3963	137
16	3922	140
Ave.	3863	144
b. Intermediate phase 10 minutes		
11	1937	152
12	1751	120
13	1969	175
14	2140	198
15 \1	-	-
16	1961	174
Ave.	1951	164
c. Smoldering phase 20 minutes		
11	1305	172
12	1353	164
13	1224	151
14	1264	170
15	1248	170
16	1321	172
Ave.	1286	167

1. Valve did not open.

Table 5.2-2 FASS real time combustion gas sensor summary.

FASS #	CO_2 ppm. Ave.	CO_2 ppm. Max.	CO ppm. Ave.	CO ppm. Max.	O_2 % of air Ave.	O_2 % of air Min.
a. Flaming phase (10 minutes)						
11	3518	8616	136	515	97.9	91.4
12	3595	11551	123	500	103.1	91.9
13	4737	12536	169	523	97.1	92.2
14	5467	11995	137	442	97.4	91.9
15	4772	12660	125	394	100.0	89.2
16	3848	8370	132	637	97.1	93.6
Ave.	4323	10955	137	502	98.8	91.7
b. Intermediate phase (10 minutes)						
11	2623	5604	189	767	98.4	95.9
12	2322	5233	128	664	103.7	101.0
13	2683	5798	170	648	96.8	94.2
14	2709	6602	161	545	98.5	95.0
15	3162	5219	197	468	101.9	99.8
16	2272	5514	155	808	98.4	95.3
Ave.	2629	5662	167	650	99.6	96.9
c. Smoldering phase 1 (20 minutes)						
11	1648	4666	163	595	98.0	95.5
12	1763	4659	173	493	102.7	100.7
13	1786	4501	164	555	93.4	91.0
14	1757	4889	157	524	96.6	92.8
15	1688	4772	165	577	100.9	98.6
16	1759	4628	161	839	97.4	95.6
Ave.	1734	4686	164	597	98.2	95.7
d. Smoldering phase 2 (2 hours)						
11	722	1830	40	222	95.5	93.9
12	641	1201	61	169	99.7	98.7
13	729	1313	52	159	89.1	88.2
14	717	1259	47	130	91.2	90.0
15	613	1409	64	115	98.3	97.3
16	830	1252	37	134	94.8	93.9
Ave.	709	1377	50	155	94.8	93.7

Table 5.2-3 FASS canister primary gas concentrations.

FASS #		CO_2 ppm	CO ppm	CH_4 ppm
a. Flaming phase				
11	\1.	396	2	2.9
12		1148	94	9.0
13		4236	461	34.8
14	\2.	-	-	-
15		7892	168	8.8
16		2370	28	2.5
b. Intermediate phase				
11		1136	144	15.1
12		1200	261	22.1
13		1940	175	15.0
14	\2.	-	-	-
15		2376	213	16.6
16		3000	293	24.3
c. Smoldering phase				
11	\2.	-	-	-
12		2112	300	26.1
13		844	88	8.9
14	\2.	-	-	-
15		1188	149	15.3
16		2127	361	32.2

1. Canister opened prematurely.
2. Canister valve did not open.

Table 5.3-1 FASS filter particulate (PM 5.0) concentrations.

FASS #	Glass mg/m^3	Teflon mg/m^3
a. Flaming phase 10 minutes		
11	24.5	28.9
12	21.2	15.1
13	29.1	26.2
14	28.8	24.9
15	28.7	28.5
16	32.1	18.3
Ave.	27.4	23.6
b. Intermediate phase 10 minutes		
11	39.9	24.8
12	19.5	15.8
13	26.7	23.3
14	26.5	24.0
15	\1 -	-
16	23.7	21.1
Ave.	27.3	21.8
c. Smoldering phase 20 minutes		
11	36.1	24.6
12	28.7	25.6
13	27.4	24.5
14	27.0	25.2
15	30.4	28.2
16	28.9	25.8
Ave.	29.8	25.7

1. Valve did not open.

Table 5.3-2 FASS glass fiber filter carbon analysis.

FASS #	Organic	Graphitic	Total
	-- Percent of PM 5.0 --		
a. Flaming phase 10 minutes			
11	63.5%	11.4%	74.9%
12	39.7%	6.2%	45.9%
13	45.0%	5.9%	50.9%
14	43.9%	6.6%	50.4%
15	38.9%	12.3%	51.2%
16	41.8%	6.0%	47.9%
Ave	45.5%	8.1%	53.5%
b. Intermediate phase 10 minutes			
11	50.9%	2.4%	53.3%
12	47.9%	3.8%	51.7%
13	53.0%	3.4%	56.4%
14	53.8%	2.8%	56.6%
15 \1	-	-	-
16	54.8%	2.2%	57.0%
Ave	52.1%	2.9%	55.0%
c. Smoldering phase 20 minutes			
11	54.0%	1.5%	55.5%
12	53.0%	1.7%	54.7%
13	54.5%	2.1%	56.7%
14	53.6%	1.3%	54.9%
15	54.3%	1.2%	55.5%
16	51.9%	1.2%	53.1%
Ave	53.6%	1.5%	55.1%

1. Valve did not open.

Table 5.3-3A Teflon filter inorganic trace elements, percent of PM 5.0

FASS #	Al	SI	P	S	CL	K	CA	TI	V
a. Flaming phase									
11	0.0240	0.1363	0.0729	0.5720	0.2984	1.6005	0.5177	0.0106	0.0023
12	0.1095	0.2635	0.1023	0.9182	0.5386	2.6664	1.0734	0.0150	0.0070
13	0.1480	0.2754	0.1447	0.7708	0.6471	2.2020	1.3146	0.0197	0.0041
14	0.4211	1.1677	0.2723	0.9581	0.7779	2.7561	3.3780	0.0509	0.0109
15	0.3273	0.6364	0.3214	0.8946	0.6471	2.2483	3.1547	0.0456	0.0129
16	0.2463	0.5952	0.1849	1.0785	0.6355	2.8489	1.9512	0.0310	0.0097
Ave	0.2130	0.5120	0.1830	0.8650	0.5910	2.3870	1.8980	0.0290	0.0080
S.D.	0.1470	0.3770	0.0970	0.1750	0.1620	0.4690	1.1570	0.0170	0.0040
% R.S.D	69.1%	73.6%	53.1%	20.2%	27.5%	19.6%	61.0%	57.7%	52.4%
b. Intermediate phase									
11	0.2475	0.6178	0.1602	0.5129	0.2211	1.1107	1.8792	0.0326	0.0066
12	0.3416	0.8901	0.2398	0.7982	0.3338	1.7336	3.0999	0.0456	0.0121
13	0.3071	0.7745	0.1993	0.6339	0.3539	1.4366	2.5328	0.0414	0.0094
14	0.5117	1.3185	0.2135	0.6271	0.2506	1.2732	3.1775	0.0592	0.0131
15	\1								
16	0.3365	0.8722	0.2194	0.5570	0.2744	1.3713	2.7455	0.0469	0.0088
Ave	0.3490	0.8950	0.2060	0.6260	0.2870	1.3850	2.6870	0.0450	0.0100
S.D.	0.0980	0.2600	0.0300	0.1090	0.0560	0.2300	0.5220	0.0100	0.0030
% R.S.D	28.2%	29.1%	14.4%	17.4%	19.5%	16.6%	19.4%	21.4%	26.2%
c. Smoldering phase									
11	0.2150	0.5301	0.1164	0.3452	0.1796	0.7809	1.6022	0.0220	0.0036
12	0.2639	0.6145	0.1739	0.4304	0.1956	0.8557	2.6764	0.0313	0.0060
13	0.3405	0.8735	0.2066	0.4846	0.2236	1.0035	3.0698	0.0390	0.0079
14	0.3518	0.9260	0.1385	0.3776	0.1780	0.8050	2.2513	0.0363	0.0076
15	0.3942	0.9174	0.2137	0.4872	0.1909	0.8499	2.8924	0.0416	0.0077
16	0.2318	0.5996	0.1341	0.3367	0.1774	0.7753	1.9238	0.0277	0.0053
Ave	0.3000	0.7440	0.1640	0.4100	0.1910	0.8450	2.4030	0.0330	0.0060
S.D.	0.0730	0.1810	0.0400	0.0670	0.0180	0.0850	0.5750	0.0070	0.0020
% R.S.D	24.2%	24.3%	24.7%	16.4%	9.3%	10.0%	23.9%	22.4%	26.9%
Weighted profile \2									
	0.28	0.70	0.18	0.66	0.38	1.62	2.29	0.03	0.01

1. Valve did not open.
2. Weighting assumes 40% flaming, 30% intermediate, 30% smoldering.

Table 5.3-3B Teflon filter inorganic trace elements, percent of PM 5.0 (cont)

FASS #	CR	MN	FE	NI	CU	ZN	GA	AS
a. Flaming phase								
11	0.0014	0.0538	0.0382	0.0028	0.0017	0.243	0	0.0059
12	0	0.0815	0.0667	0.0012	0.0034	0.4117	0	0.0044
13	0.0026	0.0906	0.0665	0.0034	0.0057	0.3352	0	0
14	0.0047	0.2903	0.2480	0.0042	0.0083	0.5018	0	0.0136
15	0.0025	0.3983	0.2134	0.0027	0.0102	0.3874	0	0
16	0.0028	0.1720	0.1248	0.0048	0.0072	0.4417	0.0012	0.0024
Ave	0.0020	0.1810	0.1260	0.0030	0.0060	0.3870	0.0000	0.0040
S.D.	0.0020	0.1370	0.0860	0.0010	0.0030	0.0900	0.0000	0.0050
% R.S.D	67.0%	75.5%	68.4%	39.8%	51.8%	23.2%	244.9%	116.2%
b. Intermediate phase								
11	0	0.1561	0.1474	0.0032	0.0019	0.1601	0	0.0088
12	0.0043	0.2217	0.2177	0.0043	0	0.2099	0.0007	0.0055
13	0.0019	0.1743	0.1916	0.0038	0	0.1559	0	0.0034
14	0.0036	0.2558	0.2887	0.0026	0.0039	0.1402	0.0003	0
15	\1							
16	0.0033	0.2208	0.2062	0.0026	0.0033	0.1583	0	0.0042
Ave	0.0030	0.2060	0.2100	0.0030	0.0020	0.1650	0.0000	0.0040
S.D.	0.0020	0.0400	0.0510	0.0010	0.0020	0.0260	0.0000	0.0030
% R.S.D	65.1%	19.5%	24.4%	22.7%	99.6%	16.0%	154.1%	73.1%
c. Smoldering phase								
11	0.0017	0.1010	0.1281	0.0025	0.0024	0.0521	0	0.0038
12	0.0006	0.1208	0.1501	0.0010	0.0015	0.0564	0.0002	0.0020
13	0.0023	0.1720	0.2128	0.0011	0.0019	0.0648	0	0.0016
14	0.0007	0.1423	0.1844	0.0019	0.0039	0.0546	0.0007	0.0054
15	0.0007	0.2339	0.2379	0.0016	0.0038	0.0641	0	0.0025
16	0.0001	0.1157	0.1461	0.0010	0.0014	0.0508	0.0006	0.0020
Ave	0.0010	0.1480	0.1770	0.0020	0.0020	0.0570	0.0000	0.0030
S.D.	0.0010	0.0490	0.0430	0.0010	0.0010	0.0060	0.0000	0.0010
% R.S.D	80.3%	33.2%	24.2%	39.9%	44.9%	10.5%	128.4%	50.3%
Weighted profile \2								
	0.0000	0.1800	0.1700	0.0000	0.0000	0.2200	0.0000	0.0000

1. Valve did not open.
2. Weighting assumes 40% flaming, 30% intermediate, 30% smoldering.

Table 5.3-3C Teflon filter inorganic trace elements, percent of PM 5.0 (cont)

FASS #	SE	BR	RB	SR	Y	ZR	MO	PD	AG
a. Flaming phase									
11	0.0015	0.0167	0.0069	0.0014	0	0	0.0058	0.0063	0
12	0	0.0264	0.0123	0.0106	0.0075	0.0012	0	0.0210	0.0162
13	0.0037	0.0269	0.0108	0.0104	0.0003	0.0085	0.0308	0.0254	0.0041
14	0.0006	0.0272	0.0061	0.0180	0	0	0	0.0068	0.0014
15	0.0033	0.0239	0.0085	0.0253	0.0047	0.0112	0.0175	0.0208	0
16	0.0018	0.0358	0.0117	0.0091	0	0.0388	0	0.0115	0.2960
Ave	0.0020	0.0260	0.0090	0.0120	0.0020	0.0100	0.0090	0.0150	0.0530
S.D.	0.0010	0.0060	0.0030	0.0080	0.0030	0.0150	0.0130	0.0080	0.1190
% R.S.D	80.3%	23.5%	27.6%	65.8%	155.4%	149.8%	140.3%	53.3%	225.2%
b. Intermediate phase									
11	0	0.0131	0.0047	0.0038	0	0.0159	0	0	0.0091
12	0.0069	0.0176	0.0017	0.0228	0	0.0038	0.0178	0.0491	0.0299
13	0.0017	0.0220	0.0070	0.0175	0.0034	0.0019	0.0145	0.0085	0.0216
14	0.0031	0.0144	0.0027	0.0240	0.0016	0.0271	0	0.0249	0.0216
15	\1								
16	0.0009	0.0172	0.0040	0.0146	0.0012	0.0388	0	0.0277	0.0067
Ave	0.0030	0.0170	0.0040	0.0170	0.0010	0.0180	0.0060	0.0220	0.0180
S.D.	0.0030	0.0030	0.0020	0.0080	0.0010	0.0160	0.0090	0.0190	0.0100
% R.S.D	107.2%	20.4%	50.5%	48.9%	113.1%	89.4%	138.1%	86.1%	54.4%
c. Smoldering phase									
11	0.0011	0.0054	0.0003	0.0052	0	0	0.0079	0.0065	0.0039
12	0.0003	0.0058	0.0035	0.0116	0	0.0087	0	0.0036	0
13	0.0008	0.0065	0.0033	0.0149	0	0.0046	0.0134	0.0069	0
14	0.0003	0.0070	0.0024	0.0111	0	0.0109	0	0.0044	0.0109
15	0.0010	0.0049	0.0037	0.0143	0	0.0082	0	0.0069	0
16	0.0014	0.0071	0.0034	0.0087	0	0.0189	0	0	0.0172
Ave	0.0010	0.0060	0.0030	0.0110	0.000	0.0090	0.0040	0.0050	0.0050
S.D.	0.0000	0.0010	0.0010	0.0040	0.000	0.0060	0.0060	0.0030	0.0070
% R.S.D	54.4%	14.6%	46.6%	33.0%	-	74.2%	162.5%	57.1%	135.0%
Weighted profile \2									
	0.0000	0.0200	0.0100	0.0100	0.0000	0.0100	0.0100	0.0100	0.0300

1. Valve did not open.
2. Weighting assumes 40% flaming, 30% intermediate, 30% smoldering.

Table 5.3-3D Teflon filter inorganic trace elements, percent of PM 5.0 (cont)

FASS #	CD	IN	SN	SB	BA	LA	HG	PB
	a. Flaming							
11	0.0175	0	0.0393	0	0.0096	0.0338	0.0022	0.0324
12	0.0609	0	0.0762	0	0.3493	0.1784	0.0041	0.0728
13	0.0183	0.0090	0.0324	0	0.1784	0.1478	0.0042	0.0741
14	0.0141	0	0.0179	0	0	0	0.0017	0.0963
15	0.0066	0.0263	0.0019	0.0348	0.1499	0.1383	0.0009	0.0645
16	0.1690	0	0	0.0292	0.0082	0	0.0052	0.0761
Ave	0.0480	0.0060	0.0280	0.0110	0.1160	0.0830	0.0030	0.0690
S.D.	0.0620	0.0110	0.0280	0.0170	0.1380	0.0810	0.0020	0.0210
% R.S.D	130.8%	180.7%	101.7%	155.8%	119.5%	97.2%	55.3%	30.2%
	b. Intermediate							
11	0.0159	0	0	0	0.0387	0	0.0007	0.0231
12	0.0335	0.0283	0	0.0335	0.2464	0.1947	0.0007	0.0499
13	0.0453	0.0267	0.0827	0	0.0835	0.3178	0	0.0367
14	0.0210	0.0268	0.0500	0.0573	0	0.0163	0	0.0350
15	\1							
16	0.0414	0	0	0.0397	0.0109	0.1332	0.0011	0.0304
Ave	0.0310	0.0160	0.0270	0.0260	0.0760	0.1320	0.0010	0.0350
S.D.	0.0130	0.0150	0.0380	0.0250	0.1010	0.1320	0.0000	0.0100
% R.S.D	40.4%	91.4%	143.7%	97.2%	132.6%	99.4%	97.0%	28.1%
	c. Smoldering							
11	0	0.0025	0.0104	0.0027	0.1404	0	0.0038	0.0114
12	0.0084	0	0	0	0.1443	0	0.0023	0.0112
13	0.0103	0	0	0.0140	0.1333	0	0	0.0186
14	0.0121	0.0153	0.0150	0	0	0	0	0.0108
15	0	0.0031	0	0.0001	0.08	0	0	0.0118
16	0.0119	0.0070	0.0014	0.0058	0.0896	0.0212	0	0.0119
Ave	0.0070	0.0050	0.0040	0.0040	0.0980	0.0040	0.0010	0.0130
S.D.	0.0060	0.0060	0.0070	0.0060	0.0550	0.0090	0.0020	0.0030
% R.S.D	79.7%	125.1%	146.9%	146.3%	56.3%	244.9%	161.8%	23.5%
	Weighted profile \2							
	0.0300	0.0100	0.0200	0.0100	0.1000	0.0700	0.0000	0.0400

1. Valve did not open.
2. Weighting assumes 40% flaming, 30% intermediate, 30% smoldering.

Table 5.4-1 FASS air temperatures at the sample level.

FASS #	Flaming		Intermediate		Smoldering	
	Ave	Max	Ave	Max	Ave	Max
11	81	174	69	110	50	72
12	137	452	125	170	109	160
13	83	302	65	88	52	82
14	111	238	75	104	48	72
15	100	200	83	108	51	74
16	80	290	64	98	48	78

Table 5.6-1 Ground oxygen depletion monitor (GODM) data summary.

GODM #	Trigger Time	Oxygen, % of Air Level				Temperature, Degrees C			
		0.5 Meter		1.5 Meter		0.5 Meter		1.5 Meter	
		Ave	Min	Ave	Min	Ave	Max	Ave	Max
1	14:27:40	92.5	69.2	96.8	90.5	192	788	182	763
2	11:30:02 /1	-	-	-	-	-	-	-	-
3	14:27:46	85.1	48.5	93.8	82.1	324	1181	353	1200
4	14:28:08	84.2	41.9	94.4	79.3	427	1140	384	1141
5	11:52:58 /1	-	-	-	-	-	-	-	-
6	14:28:00	82.5	50.0	86.6	52.9	510	1448	357	1015

1. System triggered prematurely and fire data was lost.

Table 6.1.2-1 Fuel consumption by phase of combustion and the total, for each of the four FASS packages.

FASS #	Flaming	Intermediate	Smoldering	Total
	(kg/m^2)			
11	4.00	3.17	2.57	9.76
12	5.24	3.13	5.24	13.61
14	5.58	2.12	2.26	9.96
16	5.73	3.35	3.45	12.53
Average	5.14+/-0.68	2.94+/-0.48	3.38+/-1.16	11.46+/1.65

Table 6.1.3-1 Fuel consumption for 5-minute intervals based on the linear growth/exponential decay model. Total consumption was adjusted to the Forestry Canada inventoried fuel consumption of 10.64 kg/m^2.

Time (minutes)	Fuel consumption (kg/m^2)	Percent of total (%)	Cumulative (%)	
0	0.0	0	0.0	Ignition
5	2.442	22.6	22.6	
10	3.237	30.4	53.0	End of flaming
15	1.963	18.4	71.4	
20	1.191	11.2	82.6	End of intermediate
25	0.722	6.8	89.4	
30	0.438	4.1	93.5	
35	0.266	2.5	96.0	
40	0.161	1.5	97.5	End of smoldering
45	0.098	0.9	98.4	
50	0.059	0.6	99.0	
55	0.036	0.4	99.4	
60	0.022	0.2	99.6	
65	0.013	0.1	99.7	
70	0.008	0.1	99.8	
75	0.005	0.1	99.9	
80	0.003	0.05	99.95	

Table 6.2-1 Emission factors and combustion efficiency by fire phase for the six FASS packages.

FASS #	PM5.0 g/kg	CO g/kg	CO_2 g/kg	Combustion Efficiency
a. Flaming phase 10 minutes				
11	9.09	48.6	1739	94.7%
12	5.78	51.3	1741	94.9%
13	7.08	48.7	1742	95.0%
14	6.38	41.5	1755	95.7%
15	7.77	42.3	1751	95.4%
16	6.92	43.5	1751	95.4%
Ave.	7.17	46.0	1747	95.2%
b. Intermediate phase 10 minutes				
11	18.88	100.5	1637	89.2%
12	11.92	91.3	1666	90.8%
13	14.21	112.9	1627	88.7%
14	12.97	115.6	1626	88.6%
15 \1	-	-	-	-
16	12.84	113.1	1630	88.8%
Ave.	14.16	106.7	1637	89.2%
c. Smoldering phase 20 minutes				
11	27.29	176.2	1501	81.8%
12	23.65	162.6	1530	83.4%
13	25.77	170.1	1514	82.5%
14	24.51	181.3	1499	81.7%
15	27.86	183.5	1489	81.1%
16	24.32	174.2	1511	82.3%
Ave.	25.57	174.7	1507	82.1%

1. Valve did not open.

Table 6.2-2 Total emissions released on a per m^2 basis for Block A of the Hill PB.

Emission	Flaming	Intermediate Smoldering	Smoldering	Total
	(g/m^2)			
PM5.0	40.9	44.8	46.9	132.6
CO	261.2	336.3	319.9	917.4
CO_2	9921	5163	2759	17843

Table 6.4-1 Effective heat of combustion of fuels typical of the Hill PB area, after correction for CO emissions.

FASS #	Flaming	Intermediate	Smoldering
	(MJ/kg)		
11	19.55	19.01	18.59
12	19.65	19.21	18.65
14	19.72	19.20	18.80
16	19.56	19.02	18.73
Average	19.62+/-0.07	19.11+/-0.10	18.70+/-0.08

--- APPENDIX A ---

Development of Equipment

APPENDICES

APPENDIX A DEVELOPMENT OF EQUIPMENT

A.1 FIRE ATMOSPHERE SAMPLING SYSTEM A-1
A.1.0 Introduction A-1
A.1.1 Computer/Support Electronics A-1
A.1.1.1 System Board A-1
A.1.1.2 Digital Board A-3
A.1.1.3 Analog Board A-3
A.1.1.4 Data Storage Board A-4
A.1.2 Particulate Collection Sub-Systems A-4
A.1.3 Phase Integrated Gas Collection Sub-System A-5
A.1.4 Real Time Gas Analysis Sub-System A-6
A.1.5 Canister Sampling Sub-System A-6
A.1.6 Fire Dynamics Sub-System A-6
A.1.7 System Tests A-7
A.1.7.1 Flow A-7
A.1.7.2 Anemometers A-8
A.1.7.3 Gas Sensors A-9
A.1.8 System Fabrication A-9

A.2 GROUND OXYGEN DEPLETION MONITORING SYSTEM A-10
A.2.1 GODM Electronics A-10
A.2.2 GODM Operation A-10
A.2.3 GODM Fabrication A-11

A.3 VIDEO CAMERA CONTROLLER A-12

APPENDIX B COMPUTER PROGRAMS FOR CONTROLLING DATA GATHERING FOR THE HILL FIRE

B.1 Introduction B-1
B.2 Control Program For Fire Atmosphere Sampling Systems (FASS) B-2
B.3 Control Program For The Ground Oxygen Depletion Monitors (GODM) B-14
B.4 Control Program For Hill Fire Video Camera B-20
B.5 Control Program For Lightning Field Mill Experiment On The Hill Fire B-22

A.1. FIRE ATMOSPHERE SAMPLING SYSTEM

A.1.0 Introduction

The design and fabrication of an Fire Atmosphere Sampling System (FASS) was undertaken to meet joint U.S. Forest Service-U.S. Defense Nuclear Agency 1989 Canadian Mass Fire Experiment program objectives. The primary goals, pertaining to the development of the FASS, were to (1) measure, in real time, concentrations of CO, CO_2, and O_2, (2) collect particles less than 5.0 um in size for several phases of the fire, (3) collect samples of gases generated in the fire for later analysis, and (4) make fire dynamics measurements (wind velocities and temperatures) during the fire. Team members decided that six systems would be required to accurately characterize the fire atmosphere. Experience gained during the 1988 Canadian Mass Fire Experiments suggested that each system should be self-contained and capable of independent operation.

Aside from meeting the objectives stated above, primary concerns in the design were portability, low power consumption, and the capability to withstand the harsh fire environment. Due to the fact that the systems were likely to be set up a considerable distance from a road, the system had to be compact and light enough to be back-packed over rugged terrain. Again because of the remoteness of the sites, and the possibility of deploying the packages in the field several days before the burn, low power consumption was critical. Since the system was to be suspended only 12 m above the ground, it had to be capable of withstanding the high heat pulse generated by the fire. No known commercially manufactured systems, capable of meeting project requirements, were available at the time the development effort was undertaken.

The FASS can conveniently be broken down into a number of sub-systems. These include the computer/support electronics, particulate matter collection, phase integrated gas collection, real time gas analysis, canister sampling, and fire dynamics sub-systems. The design approach was modular, that is, any single sub-system with the exception of the computer/support electronics could be upgraded or removed, without significant detrimental effects to the rest of the system. Power to all sub-systems is supplied by a single 12 volt, 8 amp-hour battery. A block diagram of the FASS is given in Figure A.1.0-1.

A.1.1 Computer/Support Electronics

The nucleus of the FASS is its on-board microcomputer and supporting electronics. Control of all other sub-systems, as well as the acquisition of data and the communication with external devices are accomplished using the computer. A low power, 1M byte solid state data storage device holds collected information. The microcomputer and data storage device are purchased units, while most of the support electronics were designed and built in-house to meet the specific needs of the FASS. Five circuit boards, as described below, hold the computer, data storage device, and support electronics.

A.1.1.1 System Board

The system board (Figure A.1.1.1-1) holds the particulate matter filter sub-system flow control circuits, computer, trigger detection circuits, digital buffer and power interface circuits, high-channel analog multiplexer, and miscellaneous voltage supply and reference circuits.

There are two identical particulate matter flow control circuits (Figure A.1.1.1-2) located on the system board; one for the glass fiber filter sub-system and another for the teflon filter sub-system (also refer to the Particulate Matter Collection Sub-Systems section below). The function of these circuits is to control the speed of each sub-system's pump such that a flow of 1.7 liters/min. is maintained for the duration of the particulate matter collection process. This is accomplished by supplying the pump's

motor with a pull down driving pulse (U3,Q18/Q19) whose width is dependent on flow rate (U11/U12), as measured by a McMillian, model 100-7 electronic flow meter. If the flow begins to drop, the pulse width is lengthened, speeding up the pump and thus increasing the flow. Similarly, flow rate is reduced by narrowing the pulse used to drive the pump's motor. Diodes D2 and D3 clamp potentially damaging noise spikes generated by the pump motors to 12 volts.

The ONSET Corp. Model 5 microcomputer (Figure A.1.1.1-3) is a small, but powerful unit, and was designed specifically for remote-site data acquisition and control. All of the computer's integrated circuits (ICs) are of CMOS construction, resulting in low power consumption. Important features of the computer (TT5-A1) include a data acquisition section having 10 bit (0.1%) resolution and 11 channels of analog input, 17 programmable digital I/O lines, two RS-232 type serial channels, and 32K bytes of memory for program and data storage. To simplify programming, the computer has a TTBASIC (a unique version of standard BASIC) interpreter.

The FASS can be triggered by either sensing an approaching fire or by receiving a signal pulse from another FASS which has already detected the fire. An approaching fire is sensed by an AD590 temperature sensor which has been placed some distance away from the tower (up to 50 m) in the direction the fire is likely to approach. The FASS is triggered (U9A,U8C,U8D,U7A) and enters the flaming phase of data collection whenever the temperature on the detection sensor exceeds 67 degrees centigrade. The FASS that first detects the fire sends out a +5V digital signal (U8A-Q17) on the LINK+/- wires to trigger the other FASSs (LINK+/- wires serially connect all FASSs). In a manner similar to that of the temperature trigger, comparator U9 forces the FASS into the flaming phase data collection mode upon detection of a digital signal on the LINK+/- lines. Any time the system is not armed (i.e., during installation or at night), the reset line of the D-type flip-flop U7A is asserted high, inhibiting both temperature and digital triggers. This circuit was incorporated to minimize the possibility of receiving a false trigger, which would result in all FASSs collecting invalid data. Additional protection against false triggering is implemented in software.

All of the computer's digital input/output (I/O) lines are buffered (RPACK1,RPACK2,U5,U6) to help protect the computer from damage due to spurious transients (e.g., lightning noise). Some of the buffered output signals are used to turn on devices or circuits requiring substantial amounts of power (e.g., pumps, valves, etc.) Due to the low current output capabilities of CMOS ICs, the buffers cannot control these devices directly; they must be driven indirectly through transistors.

Eight additional lines of digital output control (besides the computer's 17 programmable digital I/O channels) are gained by using serial-to-parallel converter U4 (Figure A.1.1.1-4). All of the outputs of this serial-to-parallel converter use transistors to drive their loads.

Multiplexers, located on both the system board (Figure A.1.1.1-5) and the analog board (Figure A.1.1.3-1), are used to double the number of analog signals that can be digitized by the ONSET system. On the system board, multiplexer U1 steers six analog inputs into ONSET data acquisition channels 8, 9, and 10.

Several power supplies and reference voltages are generated on the system board (Figure A.1.1.1-6). Band-gap diode D1 produces the basic 2.5 volt reference used by the other supply circuits in this section. As a system performance check, this reference voltage is recorded each time the FASS logs data. A stable 4.092 volts, generated by U2B, is used to reference the computer's analog to digital converter. Since the setting of the 4.092 volts affects all other analog readings, adjustment of potentiometer R2 to produce exactly 4.092 volts at the V REF test point must be done before any other adjustments are made. Power for the Particulate Matter Collection Sub-Systems' pressure sensors is provided by unity gain amplifier U2D. Voltages to power the gas bag pump (1.8V) and the real time gas pump (2.5V) are supplied by U2C,Q11 and U13A,Q13 respectively.

A.1.1.2 Digital Board

The digital circuit board (Figure A.1.1.2-1) contains the electronics necessary to collect, and transfer to the computer, the pulse (digital) information generated by both triaxial and cup type anemometers (also refer to the Fire Dynamics Sub-System). Collection of the data consists primarily of counting the number of pulses generated by the anemometers during the sampling interval. In the case of the triaxial anemometers, direction of rotation is also determined. Both triaxial and cup anemometer data collected are transferred to the computer via a common serial link. This is accomplished by first shifting all of the triaxial data and then all of the cup anemometer data over the link. Which type of data being sent over the link is determined by digital multiplexer U1.

A triaxial wind velocity sensor consists of three separate turbine type anemometers assembled in a standard x-y-z configuration. Movement of an anemometer's blades is sensed by a pair of reflective infrared switches mounted on the housing of each anemometer. As a blade moves across the sensing portion of each switch, a digital pulse is generated. Since the two switches are slightly separated, one pulse will be generated a little ahead of the other. Direction of rotation of each anemometer is resolved by determining the order in which the two pulses are generated. Power to the infrared sensors is supplied by U10 (Figure A.1.1.2-2). A Hex Schmitt buffer (U11A-F) detects the output pulse of each infrared detector and converts it to the correct digital voltage level. Direction sensing is achieved by OR gates (Figure A.1.1.2-3) U15A, B, and C, while the "Q" outputs of D flip-flops U16A, U16B, and U17A, temporarily store direction information. Wind speed data is collected by binary counters U12, U19, and U20, which totalize the pulse output of each anemometer. At each sample period (0.5 seconds for the Hill experiment), the computer generates a pulse to latch (capture) direction and speed information into parallel-to-serial shift registers U13, U14, U18, and U21. Once the data is latched into the shift registers, U17B produces a pulse to reset the counters to zero. Next the computer generates a series of pulses to shift the latched data, via digital multiplexer U1 and the serial link into the computer.

For the simpler cup anemometers, only the number of pulses generated are counted. The circuitry is similar to that of the triaxial anemometers; the exception being that there is no direction sensing circuitry. Schmitt buffers U9C, U9D, and U9E detect the pulses generated by the cup anemometers. Counters U6, U7, and U8 (Figure A.1.1.2-4) totalize the pulses from the 9, 6, and 3 m anemometers, while U2, U3, and U4 are the companion parallel to serial shift registers. Type D flip-flop U5A produces a counter reset pulse after the counter data has been latched into the shift registers. The process of shifting the data into the computer (is the same as) for the triaxial anemometers.

In addition to the collection of anemometer information, canister valve control circuits (Figure A.1.1.2-5) are located on this board. Each of the three canister control valves (refer to the canister sub-system) is driven by a transistor located on the digital board. The transistors are required since the digital output lines of the computer cannot provide the power necessary to drive the valves directly.

A.1.1.3 Analog Board

The analog board (Figure A.1.1.3-1) holds the circuitry required to interface the thermocouple probes, gas sensors, pressure sensors, and analog output of the anemometers to the data acquisition section of the computer. Multiplexers (U1-U2) located on this board increase the number of analog channels of the FASS. All of the circuits on the board are designed using components having low current requirements. To further extend battery life, power to the circuits and sensors on this board is removed when not making measurements.

Thermocouple conditioning is accomplished by cold junction compensation and amplification circuitry (Figures A.1.1.3-2 and A.1.1.3-3). Cold junction reference ICs (U3, U6,U7,U8,U9) output a compen-

sating voltage (40.6 uV/C) tailored to the type K thermocouples used by the FASS. The outputs of the inlet, and the 3, 6, and 9 m tower mounted thermocouples are amplified (U10A,B,C,D) by a factor of 49, yielding a scaling of 2 degrees centigrade per count. The output of the gas stream monitoring thermocouple is amplified (U4A) by 98, for a 1 degree per count scaling factor.

Voltage outputs of the CO, CO_2, and O_2 sensors all require conditioning (Figures A.1.1.3-4 and A.1.1.3-5) to be compatible with the A/D converter. Amplifier U11C boosts the output of the CO_2 sensor by a factor of 4, resulting in a full scale range of 20,000 ppm. Output of the O_2 sensor is amplified by U11D to give a nominal scaling factor of 0.05% O_2 per count. The output of the CO sensor is amplified by U15 to provide a full scale range of 2000 ppm. Note that a low noise, stable bias voltage, required by the CO sensor, is supplied by a mercury cell. Voltage follower U11A supplies the reference voltage to the 3, 6, and 9 m vane (direction) potentiometer. The voltage output of each vane potentiometer (0-2.5V) is approximately linear with vane position (0-360 Deg.).

A pair of differential amplifiers (Figure A.1.1.3-6), one for each of the two particulate matter filter sub-systems, increase the voltage output of their respective pressure sensors to levels required by the data acquisition section. A stable 4.092 volts, generated on the system board, supplies both 0-1 PSI sensors. The output of the glass fiber flow pressure sensor is amplified by U12C and U12D, while U5A and U5B amplify the output of the Teflon flow pressure sensor. The output of the differential amps is inversely related to the pressure on the sensors. In the case of the Glass Fiber pressure amplifier, potentiometer R31 sets the offset voltage (3.600 volts with no differential pressure applied to the sensor), while R31 sets the amplifier gain. Potentiometers R33 and R37 perform these respective adjustments for the teflon pressure amplifiers.

In addition to the digital output, an AC voltage, proportional to wind speed, is generated by each of the triaxial array anemometers. This AC voltage must be converted to a DC voltage to be read by the ONSET computer's A/D converter (Figure A.1.1.3-7). There is one true-RMS-to-DC converter (U17,U18,U19) for each of the triaxial anemometers. Scaling resistors on each converter provide an DC output level directly compatible with the ONSET computer. A -5V, required by the RMS converters, is supplied by U16.

Each analog channel is buffered (Figure A.1.1.3-8), using a voltage follower, before being input to the computer's data acquisition section. Buffers (U13,U14) provide a low input impedance to the computer's A/D converter.

A.1.1.4 Data Storage Boards

Two circuit boards, manufactured by QSI and collectively termed the QSTORE system, make up the high capacity solid state data storage device. The control board contains circuits to receive and format the data, while the receptacle board holds the actual memory device. Each time FASS data is to be stored, the ONSET computer (located on the system board) sends data over a serial link at 4800 Baud to the QSI control board. A microcomputer on the control board formats the data and sends it, a byte at a time, to the receptacle board. The receptacle board holds a removable 1M byte storage module, which contains non-volatile CMOS memory ICs (data is not lost from this type of memory when power is removed). At the end of the experiment, data is up-loaded into a higher level computer (e.g., a personal computer) for data analysis by a special module reading device.

A.1.2 Particulate Matter Collection Sub-Systems

The collection of particulate matter is accomplished using two nearly identical sub-systems; one sub-system containing 37 mm glass fiber filters (Figure A.1.2-1), the other containing 37 mm Teflon filters. The function of both of these sub-systems is to collect particulate matter matter less than 5.0 um in size produced by the combustion process. For each of the flaming, intermediate, and smolder-

ing phases, particulate matter is collected on both glass fiber and teflon media (for a total of six filters per instrument).

To provide easier access to the filters, the Particulate Matter Collection Sub-System is located in a separate container attached to the lower side of the larger main FASS container.

Each sub-system consists of 5 principal components; (1) three cyclone 5.0 um cut-point (high pass) filters, (2) three 37 mm diameter filters, (3) a phase switching manifold, (4) a pump, and (5) a flow measuring and control circuit. All switching of the phase valves and the supplying of power to the pumps and flow control circuits is handled by the FASS's computer.

When a fire is sensed by the FASS, the process of collecting particulate matter begins. First, power is applied to the pumps and flow control circuits. Almost immediately, the two flaming phase valves (one each located on the glass fiber sub-system and on the Teflon sub-system manifolds) are opened, allowing air to be drawn into the cyclones and on through to the respective flaming phase glass fiber and Teflon filters. The cyclones are mechanical filters which permit only particles less that 5.0 um in size to pass. For the cyclones to function properly, the flow rate must be kept at 1.7 liters/min. To maintain this rate, the speed of each pump is controlled by a feedback circuit which is fed by an electronic flow meter (refer to System Board). The output of the flow meter is recorded at each sample period. A 50 ml volume (consisting of a plastic filter cassette and final glass fiber filter) is located between the pump and flow meter to dampen pulses and improve flow meter accuracy. To aid in determining system performance and to try to assess filter loading rates, a pressure sensor is used to monitor the pressure drop across the cyclone, filter, and switching valve.

At the end of the flaming phase time period, the flaming switching valves are turned off. The intermediate switching valves are now turned on, and particulate matter begins to collect on the two intermediate phase filters. A similar sequence is repeated at the transition between the intermediate and smoldering phases.

Note that the manifold holding the three valves controlling the Teflon filter switching has an additional valve mounted on it. Unlike the other three valves on this manifold, which all have a cyclone and a filter cassette attached to their inputs, this valve's input tube goes directly to the outside of the FASS. The function of this valve is to provide a supply of air to the real time gas sensors in the pre-fire and post-fire time periods.

The gas flows exiting each sub-system's flow meter are joined and then routed to the sample distribution manifold located in the main FASS container. This manifold simply provides a means of supplying gases to the real time gas sensor sub-system and the phase integrated gas sample collection sub-system. Excess gas is vented to the outside of the FASS.

A.1.3 Phase Integrated Gas Collection Sub-System

The phase integrated gas collection sub-system (Figure A.1.3-1) continuously collects a sample of gases produced during each of the flaming, intermediate, and smoldering phases of the fire. Approximately 1 liter of gas is collected in special 5 layer mylar sample bags for each of the three phases. Gas collected is suitable for a variety of post-fire analyses. For the Hill experiment, CO and CO_2 concentrations were evaluated.

Upon entering the flaming phase of data collection, the FASS computer provides power to the gas bag pump, which then begins drawing gas from the sample distribution manifold. This gas is pumped into the flaming phase collection bag via the bag distribution manifold and the flaming phase valve, which has been opened by the computer. The gas bags for the intermediate and smoldering phases are filled by computer selection of their respective valves at the appropriate times. Correct flow rate

to each bag is set by a simple needle type restriction located between the valve and the sample collection bag.

A.1.4 Real Time Gas Analysis Sub-System

The real time gas analysis sub-system provides a nearly continuous record of CO, CO_2, and O_2 concentration levels during the fire. In addition, this data is logged at less frequent intervals during the pre-fire and post-fire periods. An important feature of this sub-system is the pre-fire and during-fire CO and CO_2 sensor calibration checks with an on-board source of calibration gases. The CO and O_2 sensors are of the electrolytic type, while the CO_2 sensor is an infrared device. Signal conditioning is required to interface the output of sensors with the FASS computer (refer to the Analog Board section).

Figure A.1.4-1 is a block diagram showing the primary components of the real time gas analysis sub-system and the direction of flow through the system. During normal operation (i.e., not checking sensor calibration) the 3-way-valve is de-energized, and the sensors are supplied with gases pumped from the gas sampling manifold. The pump forces the flow through the sub-system at a rate of approximately 250 ml/min. A 1.5 m, 3.18 mm (0.125 inch) stainless steel tube serves to cool the gases, thus reducing the effects of temperature on the sensors. To aid in determining system performance, an in-line thermocouple was placed immediately after the cooling coil to monitor temperature of the gases supplied to the sensors. Figure A.1.4-2 is a graph showing typical inlet gas temperature and post-cooling gas temperatures for the duration of the fire.

Calibration gas, held in a gas sample bag, is pumped to the sensing devices when the 3-way-valve is energized. To insure that the sensors have equilibrated, the valve stays energized for 30 seconds. For the Hill experiments, the sensors were checked twice; once at the arming of the FASS, and once at the transition between the intermediate and smoldering phases.

A.1.5 Canister Sampling Sub-System

The canister sampling sub-system provides a means of collecting a high purity, short duration sample of the combustion gases. These 0.8 liter stainless steel canisters undergo a cleaning process prior to being evacuated and loaded into the FASS. To prevent contamination, the canisters are sealed at the conclusion of the field experiment.

Each FASS contains 3 canisters; one used for collecting a sample during each of the 3 phases of the fire. To maintain a high purity pathway, the canisters are ported to the outside environment via stainless steel tubing and valves, and a Teflon switching manifold. A canister is filled when a signal from the FASS computer opens its respective control valve for 30 seconds. The first canister (flaming phase) will be filled if either the temperature at the 3 m height exceeds 500 degrees centigrade or if 6 minutes have elapsed. Canisters are filled during the intermediate and smoldering phases when 3 minutes of their respective phases has elapsed.

A.1.6 Fire Dynamics Sub-System

The fire dynamics sub-system consists of a triaxial wind velocity measuring array, three cup and vane anemometers, and three radiation shielded temperature probes. The triaxial array is located at the top of the tower, at a height of 14 m. A cup and vane anemometer and a temperature probe are located on the tower at heights of 3, 6, and 9 m above the ground.

The triaxial array consists of three separate turbine type anemometers. The anemometers are of high quality design and construction, and have excellent wind response characteristics. To provide a cosine response, each anemometer is housed in a 304.8 mm long, 10.2 mm diameter tube. The 3

tubes are attached to a supporting frame in a standard x-y-z configuration. Mounted on the tower, the x axis ran north-south, the y axis east-west, and the z axis up-down (vertical). Using this configuration, and knowing both the speed and rotation direction of each anemometer, velocity (a vector quantity) can be determined.

Each triaxial array anemometer outputs both analog and digital signals proportional to wind speed. The digital signal is generated by a pair of reflective type infrared switches which sense the rotation of the anemometer's blades. The infrared switches are configured in such a manner that rotation direction as well as speed can be determined by the FASS circuitry (refer to the Digital Board). The analog (an AC voltage) output of each anemometer yields only wind speed.

The simpler cup and vane anemometers, located along the tower, provide only horizontal speed and direction at each of the 3 locations. Because of their proximity to the ground and the harsh conditions during a fire, relatively inexpensive anemometers are used. Accordingly, the function of these expendable anemometers is to collect pre-fire and approaching fire wind data. The digital output of the cup anemometers (one pulse per revolution) is totaled by the FASS circuitry. The vane portion of the anemometers output a DC voltage proportional to the direction (0-360 degrees).

To achieve a more accurate air temperature reading the thermocouple probes are placed in radiation shields. These inexpensive shields were fabricated by stacking 6 aluminum pie plates together (the pie plates were separated from one another by approximately 25 mm). Each stack of pie plates was attached to a 0.5 m length of conduit, which in turn was attached to the tower. A small hole was drilled through the first three plates to provide for thermocouple placement. The thermocouples themselves were constructed of 24 gage shielded type "K" wire.

A.1.7 System Tests

The FASS was designed to collect particulate matter and gas samples, measure temperature, wind speed and wind direction. To ensure that this equipment performs these functions adequately in harsh environments, various tests have been and still are being performed on different components and sub-systems of the box in the laboratory setting. In the brief outline below, tests that have been performed up to the present date are described and evaluated.

A.1.7.1 Flow

The flow system of the FASS was tested in order to establish the fact that the tower packages maintain flow at a constant pre-set rate while the system is operational.

The flow system of interest has six cyclones positioned on the exterior of the box exposed to the test environment. From these ports, test gases are pulled through six lines and eventually across six filter surfaces where particulate matter is collected. Three of these surfaces are glass fiber, the remainder Teflon. One glass fiber and one Teflon are exposed for each phase of the fire (flaming, intermediate, smoldering). Test measurements on this system were done in several ways: (1) with the six filters open to the environment (as in normal operation) while flow was monitored by the portable Zenith computer, and (2) with a flow testing apparatus attached to the cyclones. A Gillian soap film flow meter was used as the primary standard and its readings were compared to the converted bit readings logged by the portable Zenith computer, (3 and 4) with the gas canister subsystem toggled in combination with each of the above situations.

In these preliminary tests, it was apparent that the canister sampling subsystem switch had no effect on the flow of FASS. This ensures the integrity of the particualte matter measurements that depend on a constant flow for the entire time a sample is collected.

As expected, flow readings taken with the flow meter attached did vary slightly from the measurements taken without it. It can be noted though that within a given box, the six flow measurements all responded in a consistent manner, e.g. flow readings taken while the six lines are open to the environment were slightly higher than with the flow meter apparatus attached and by roughly the same amount. The results suggest normal deviations in the indicated rates of flow as measured by the FASS packages with that measured using a primary standard. The error is no more than 10% and generally less than 2%. Both limits of error are well within the acceptable error for measurements in fire environments.

A.1.7.2 Anemometers

A single triaxial anemometer was calibrated in the IFSL wind tunnel facility to check the accuracy of wind speed and direction calibrations. For this test, the anemometer was securely mounted to a heavy plate positioned in the middle of the wind tunnel (cross section measures 3.05 x 3.05 m). Readings were logged by the portable Zenith computer as the anemometer was rotated to sixteen specific positions of a 360° circle. These sixteen positions included north 0°, south 180°, east 90°, west 270°, and the 30, 45 and 60 degree angles lying in each quadrant between these major headings. Wind speed during this test remained a constant 2.7 m/s.

In addition, a calibration was performed on the anemometer while it faced 180°(south) to the wind. Data was recorded as wind speed varied in order to determine a calibration curve.

Ideally, for wind in any direction, the anemometer should measure the vector components of the wind speed in the N-S, E-W and vertical directions. The test data show that this cosine response is followed but not with the same degree of precision in each quadrant. Measurements taken at the angles which lie in the southwest or southeast quadrant matched a predicted cosine response at 10% or less error. One measurement in the northwest quadrant showed an error of 25%. Due to the time constraints for the experiment, the wind tunnel tests were not run prior to taking the measurements. The error has not significantly compromised the interpretation of the data.

It is suspected that the asymmetric design of the triaxial configuration may have resulted in the small error that can be corrected by separating the turbine anemometer housings both horizontally and vertically. Future testing will determine the optimal configuration.

A second data set was recorded while the anemometer faced 180° (to the south) and wind speed varied at 0.9, 1.8, and 2.7 m/s. From these data, wind speed was linearly related to the voltage output from the anemometer. Below 1.8 m/s, an alternate linear relationship was calculated with the intercept forced to zero. These linear relationships were used to convert all experimental data to wind speed.

Another triaxial anemometer was disassembled and a "single axis" anemometer (tube) was positioned "head on" in the middle of the same wind tunnel. Wind speeds varied at 0.22, 0.45, 0.9, 1.8, and 2.7 m/s while voltage was recorded on a Hewlett Packard 3456A voltmeter. Two linear relationships were derived, one for voltages above 0.58854 volts and another for values between this same voltage and zero. This second relationship forces a zero intercept and assigns voltages to wind speeds below the threshold level. These early tests showed a threshold at 0.45 m/s below which the anemometers do not respond in a linearly. Further tests are being run with the new configuration of the triaxial anemometer system to minimize other influences. We have a minimal effort underway at Montana State University, Department of Electrical Engineering to test and perfect a low-cost anemometer using present generation technology for use in high temperature environments.

A.1.7.3 Gas Sensors

For the purpose of confirming the accuracy of the CO and CO_2 gas sensors of the FASS, a test was conducted to compare FASS sensor readings with instruments in the IFSL Combustion Lab. A laboratory test fire was staged while both the tower package and Horiba PIR 2000 CO and CO_2 gas analyzers sampled gases from the same sample line that originates in the stack above the fire bed.

Both CO and CO_2 data from the Horiba instruments were recorded in real time by a Hewlett Packard data acquisition system. Since the Horiba instruments have a linear voltage output with gas concentrations, the composition can be calculated easily. Data generated by FASS sensors were also recorded in real time as voltage readings and stored in the FASS EPROM (Erasable Programmable Read Only Memory). A BASIC program was developed to convert FASS reading to CO_2 concentration, using the non-linear relationship supplied by the sensor manufacturer.

The data generated with the Horiba instruments were calibrated against known gas standards that were introduced into the sample line before the fire. The data generated with the FASS sensors were calculated in the conversion program with two known calibration points.

Because the data generated by the FASS were recorded four times as often as the data generated by the Horiba, each successive set of four data points was averaged for comparison to the Horiba data set. The two data sets for CO_2 are graphed in Figure A.1.7.3-1.

Most important in the graph is that the two instruments track almost identically with the exception of the initial spike at the beginning of the FASS data due to sensor warm up. Other than the spike at 130 seconds, the FASS values are always at or slightly above the Horiba values. This suggests that a slight calibration correction is needed. The fact that the Horiba curve is more jagged is due to a lower filter time constant in the Horiba.

In order to test the CO_2 detector for possible interferences from water vapor in the smoke sample, a CO_2 standard was bubbled through a gas scrubber containing distilled water at 25 C. The CO_2 standard became saturated with water as it bubbled through the impinger. The saturated CO_2 standard was supplied to FASS and measured by the CO_2 detector. The results of the saturated CO_2 measurements were then compared to the results of dry CO_2 measurement. No perceptible differences were noted. A similar experiment with saturated zero air also showed negligible response to the water vapor.

Because of time limitations the CO data has not been compared and graphed for this paper. Examination of this data as well as additional sensor tests are planned in the near future.

A.1.8 System Fabrication

To reduce weight, two standard electrical type aluminum equipment boxes are used to house the FASS. These are made of heavy gage aluminum and both have large hinged doors permitting easy access to FASS components. All the sub-systems, with the exception of the particulate matter collection sub-systems, are located in a 60.9 X 50.8 X 40.6 cm container. The particulate matter collection sub-systems are located in a smaller 25.4 X 30.5 X 20.3 cm container which is bolted to the bottom of the larger box. Both boxes are lined with a ceramic fiber insulating material to protect them from the high temperatures of the fire environment.

All electrical connections on the FASS circuit boards were made using standard wire-wrap techniques. Figures A.1.8-1, A.1.8-2, and A.1.8-3 give the electronic component layout of the respective system, digital, and analog signal conditioning circuit boards.

A.2.0 GROUND OXYGEN DEPLETION MONITORING SYSTEM

A Ground Oxygen Depletion Monitoring (GODM) system was developed to meet joint U.S. Forest Service-U.S. Defense Nuclear Agency 1989 Canadian Mass Fire Experiment program objectives. One objective of the 1989 program was to measure oxygen and temperature levels close to the ground surface (in the flaming zone) during the most active phase of the fire. To meet this objective, a micro-processor based instrument was designed and fabricated by U.S. Forest Service-Fire Chemistry (RWU-4404) personnel. The systems were to be deployed in close proximity to the Fire Atmosphere Sampling Systems (FASS), which were designed to monitor the atmosphere just above the flaming zone. A total of six GODM systems were deployed for the 1989 Canada experiments.

Design considerations for the GODM were similar to those of the FASS. Portability, low power consumption, and the ability to withstand the heat pulse from the fire were primary concerns. Accordingly, only lightweight components requiring low power were selected for use in the system. The extremely harsh environment near the ground surface during a fire dictated that the system be buried at least 25 cm below the surface. This constraint in turn mandated that the system be housed in a watertight container to prevent damage from ground water.

A.2.1 GODM Electronics

Principle GODM elements are the computer, support electronics, and sensing devices (Figure A.2.1-1). An ONSET Corp. Model 5 computer, identical to the one used in the FASS, controls the acquisition of the data. Data collected by the system are stored in an ONSET 128K byte memory expansion module made specifically for the Model 5 computer. Support electronics consist primarily of analog signal conditioning, and generation of control and reference voltages. The computer and all support electronics are mounted on a single circuit board (Figure A.2.1-2).

The computer and control electronics are shown in Figure A.2.1-3. Low output drive capability of the CMOS computer make it necessary to drive higher power loads through transistors. Transistor pair Q1 and Q2 control the +5 volt power supplied to the signal conditioning circuits, while transistor pair Q3 and Q4 control the +12 volt supply.

Four thermocouples, one each to measure temperatures at the 0.5 and 1.5 m heights, and two to measure the gas sensor temperature are used in the system. A reference voltage is generated for each thermocouple by U2-U5 (Figure A.2.1-4). Thermocouple signal amplification is provided by quad amp U6. To provide for high resolution (1 degree C per A/D step) amplifiers U6C and U6D have a nominal gain of 98 (adjusted by R8 and R9 respectively). A greater range is achieved by U6A and U6B, which amplify the signal by 47.5 (adjusted by R3 and R4 respectively), providing a scaling factor of 2 degrees per step. Buffering of the amplified signals is provided by unity gain amplifiers U1A-U1D.

Electrolytic type sensors, whose outputs are nominally 45 mV in air (21% O_2), are used to monitor oxygen depletion. The sensor signals are amplified (Figure A.2.1-5) by U8A (0.5 m O_2 level) and by U8B (1.5 m O_2 level) to give a scaling factor of 0.1% O_2 per A/D step. Potentiometer R18 sets the gain of U8A, while R19 performs the same for U8B. As a check of system performance, the 12 volt battery supply and a 2.5 volt reference are also recorded. Buffering of these signals is the function of voltage followers U7A-D. A stable 4.092 volts, generated by D1 and U8C, is used to reference the computer's A/D converter. This reference level yields a resolution of 4 mV per A/D step. Voltage for the air sampling pumps is generated by U8D and transistor driver Q5.

A.2.2 GODM Operation

The GODM's computer was programmed to acquire data in three phases. First the computer sampled pre-fire conditions once every 2 minutes, saving a maximum of 2 hours (60 readings) prior to the fire.

High frequency sampling (1 sample every 0.2 sec) commences whenever the temperature on either of the inlet thermocouples exceeds 65 degrees centigrade. This rapid sampling phases lasts for 10 minutes, and, upon completion of this phase, the system returns to the lower sampling rate of 1 sample every 2 minutes. This post-fire phase of data collection continues until the memory is full. For a more complete description of the data collection process, refer to the sampling protocol discussion in the main text.

Combustion gases enter the buried system via two 3.2 mm stainless steel collection tubes. The orifice of one tube is located 0.5 m above the ground surface, the other at 1.5 m. Before taking readings, pumps are activated to draw samples through these tubes into the oxygen sensors' chambers. In addition to the collection tube, the gases also travel through a buried, 1.5 m length of coiled stainless steel tubing. These coils, which are placed in-line between the instrument box and the collection tubes, function to cool the combustion gases. The pumps produce a flow rate of about 250 cc/min. and run for at least 30 seconds before an O_2 reading is taken (the pumps are on continuously during the high frequency sampling phase). Thermocouples attached to the tubes in the vicinity of the orifices measure the temperature of the sampled gases. Another pair of thermocouples measure the temperature of the cooled gases at the O_2 sensors. Both sample gas streams are vented to the above-n-line between the instrument box and the collection

A.2.3 GODM Fabrication

Figure A.2.3-1 shows the physical layout of the principle electronic and mechanical components of the GODM instrument. These components consist of two electrolytic oxygen sensors (G.C. Industries, Model # 33-270), two small sampling pumps (Gilian Instrument Corp., Model # B-800408), two 37 mm filter holders (each containing a 37 mm diameter glass fiber filter and packed with glass wool), an in-house fabricated circuit board containing the GODM electronics, and a 12 volt battery (Power-Sonic Model PS-1250).

Housings for the oxygen sensors were machined from 3.5 cm aluminum round stock (Figure A.2.3-2). The electronic components, as described in the above section, were mounted on a 14x11.4 cm circuit board (Figure A.2.3-3). All circuit connections were made using wire-wrap techniques. The system was housed in 24.1x17.8x15.2 cm watertight polycarbonate box (Hoffman # A-1076PC1). Collection (sampling probes) tubes and cooling coils were fabricated from 3.2 mm o.d. x 1.78 mm i.d. stainless steel tubing. To maintain the watertight integrity, all connections to the outside of the box were made using sealed fittings. Since the GODM was buried in the ground at the sampling site, it was not necessary to insulate the instrument.

A.3.0 VIDEO CAMERA CONTROLLER

A high resolution Panasonic Model AG-450 S_VHS video camera was purchased to record the fire as it passed through the FASS array. Since this camera has only a two hour record capability, a Video Camera Controller (VCC) was developed to delay the recording action until fire was in the vicinity of the towers. Figure A.3.0-1 is a block diagram of the VCC.

Just prior to leaving the site the day of the burn, the VCC (figure A.3.0-2) and camera were turned on. At this time, the computer begins to toggle the camera between a 240 second pause and a 4 second record mode by pulsing Q1 (the output of Q1 is wired to the camera's remote pause/record switch). This alternating sequence continues until a fire is detected by the computer. The fire detection sensor is a pair of insulated wires extending approximately 300 m away from the camera tower in the direction of probable ignition (the center of the experimental unit for the 1989 Canada Mass Fires). When the fire reaches the wire, the insulation burns off, causing the two wires to short together. This short results in a positive voltage being applied to analog channel 0. If the camera is in the pause mode (as detected by channel 1), the camera's pause controller is toggled once more to place the camera in the record mode. If the camera happens to be in the 4 second record mode when the fire is detected, the VCC program merely ends. In either case, the camera stays in the full record on mode until the tape expires.

Figure A.1.0-1 Functional block diagram of the FASS.

Figure A.1.1.1-1 Schematic diagram of the interconnections of the primary circuits located on the system board.

Figure A.1.1.1-2 Schematic diagram of the particulate flow control circuits located on the system board.

Figure A.1.1.1-3 Schematic diagram of the computer and support circuits located on the system board.

Figure A.1.1.1-4 Schematic diagram of the power drivers located on the system board.

Figure A.1.1.1-5 Schematic diagram of the high channel analog multiplexer located on the system board.

Figure A.1.1.1-6 Schematic diagram of the power supplies located on the system board.

Figure A.1.1.2-1 Schematic diagram of the interconnections of the primary circuits located on the digital board.

Figure A.1.1.2-2 Schematic diagram of the interface circuits located on the digital board.

Figure A.1.1.2-3 Schematic diagram of the 3D wind circuits located on the digital board.

Figure A.1.1.2-4 Schematic diagram of the 2D wind circuits located on the digital board.

Figure A.1.1.2-5 Schematic diagram of the canister control circuits located on the digital board.

Figure A.1.1.3-1 Schematic diagram of the interconnections of the primary circuits located on the analog board.

Figure A.1.1.3-2 Schematic diagram of the gas stream thermocouple signal conditioning circuit located on the analog board.

Figure A.1.1.3-3 Schematic diagram of the external thermocouple signal conditioning circuits located on the analog board.

Figure A.1.1.3-4 Schematic diagram of the CO signal conditioning circuit located on the analog board.

Figure A.1.1.3-5 Schematic diagram of the O_2 and CO_2 signal conditioning circuits located on the analog board.

Figure A.1.1.3-6 Schematic diagram of the pressure sensor signal conditioning circuits located on the analog board.

Figure A.1.1.3-7 Schematic diagram of the 3D wind RMS-DC converter circuits located on the analog board.

Figure A.1.1.3-8 Schematic diagram of the A/D interface buffer circuits located on the analog board.

Figure A.1.2-1 Block diagram of the glass fiber particulate collection sub-system located within the FASS.

Figure A.1.3-1 Block diagram of the phase integrated gas collection sub-system located within the FASS.

Figure A.1.4-1 Block diagram of the real time gas analysis sub-system located within the FASS.

Figure A.1.4-2 Typical inlet and internal temperatures as measured during the Hill experiments.

Figure A.1.7.3-1 Comparison of CO_2 as measured by the FASS and the Horiba during an experimental burn in the IFSL combustion facility

Figure A.1.8-1 Electronic component layout of the FASS system circuit board.

Figure A.1.8-2 Electronic component layout of the FASS digital circuit board.

Figure A.1.8-3 Electronic component layout of the FASS analog signal conditioning circuit board.

Figure A.2.1-1 Functional block diagram of the GODM.

Figure A.2.1-2 Block diagram of the primary circuits of the GODM.

Figure A.2.1-3 Schematic diagram of the computer and support circuits of the GODM.

Figure A.2.1-4 Schematic diagram of the thermocouple signal conditioning circuits of the GODM.

Figure A.2.1-5 Schematic diagram of the 0_2 signal conditioning circuits of the GODM.

Figure A.2.3-1 Diagram of the physical layout of the GODM.

Figure A.2.3-2 Diagram of the 0_2 sensor housing used in the GODM.

Figure A.2.3-3 Diagram of the layout of the circuit board used in the GODM.

Figure A.3.0-1 Block diagram of the video camera and the VCC.

Figure A.3.0-2 Schematic diagram of the computer and support circuits of the VCC.

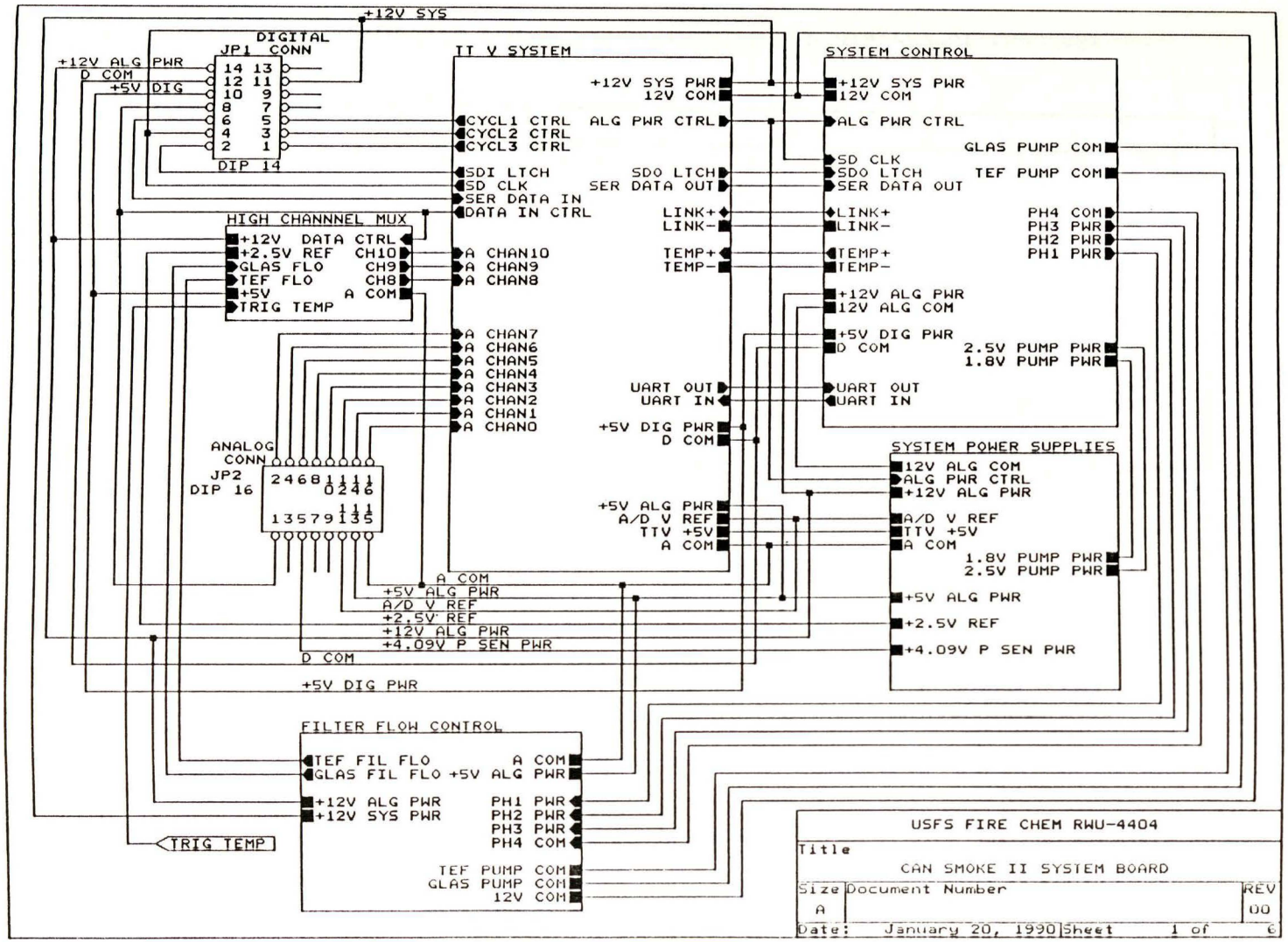

Figure A.1.1.1-1 Schematic diagram of the interconnections of the primary circuits located on the system board.

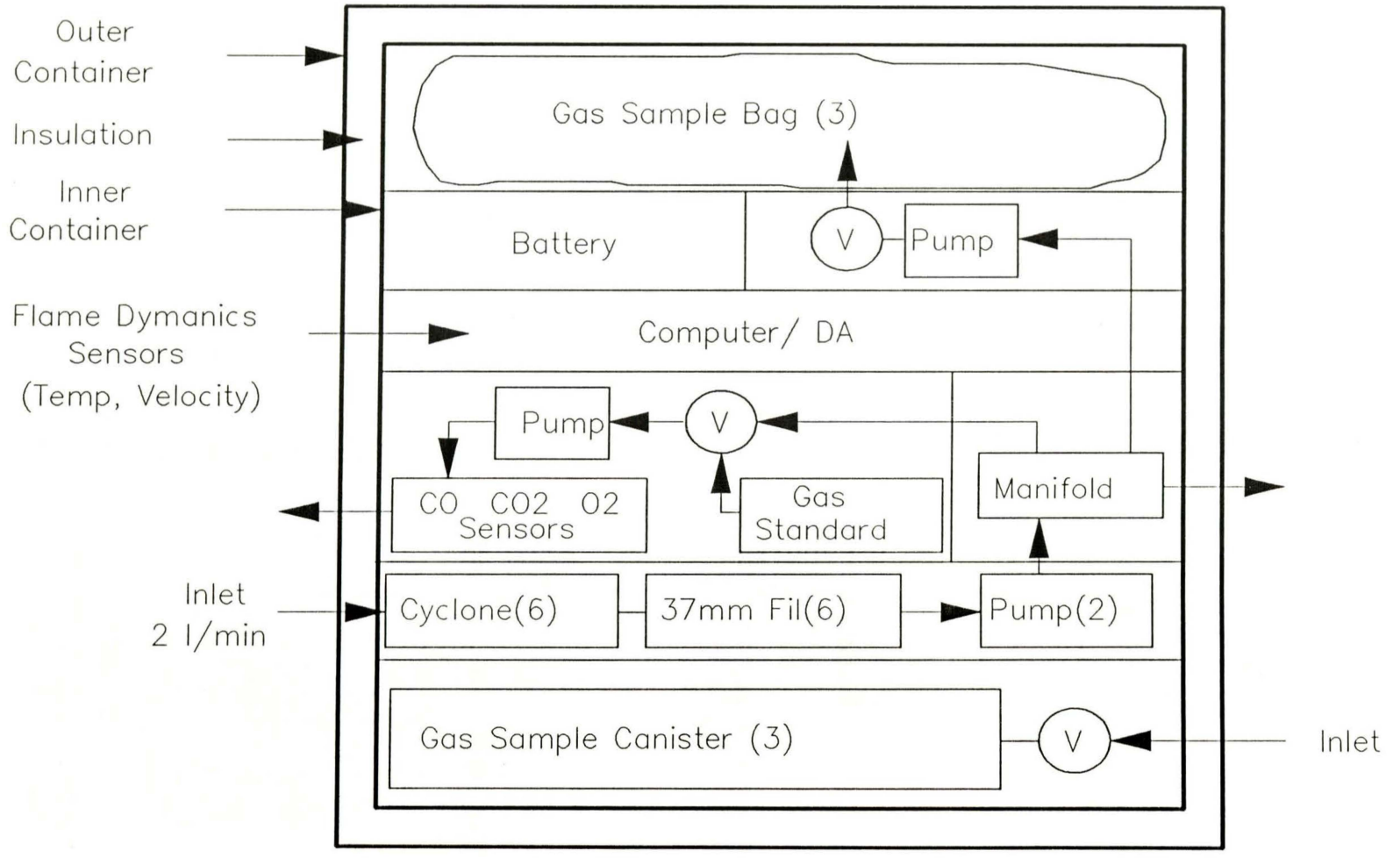

Figure A.1.0-1 **Functional block diagram of the FASS.**

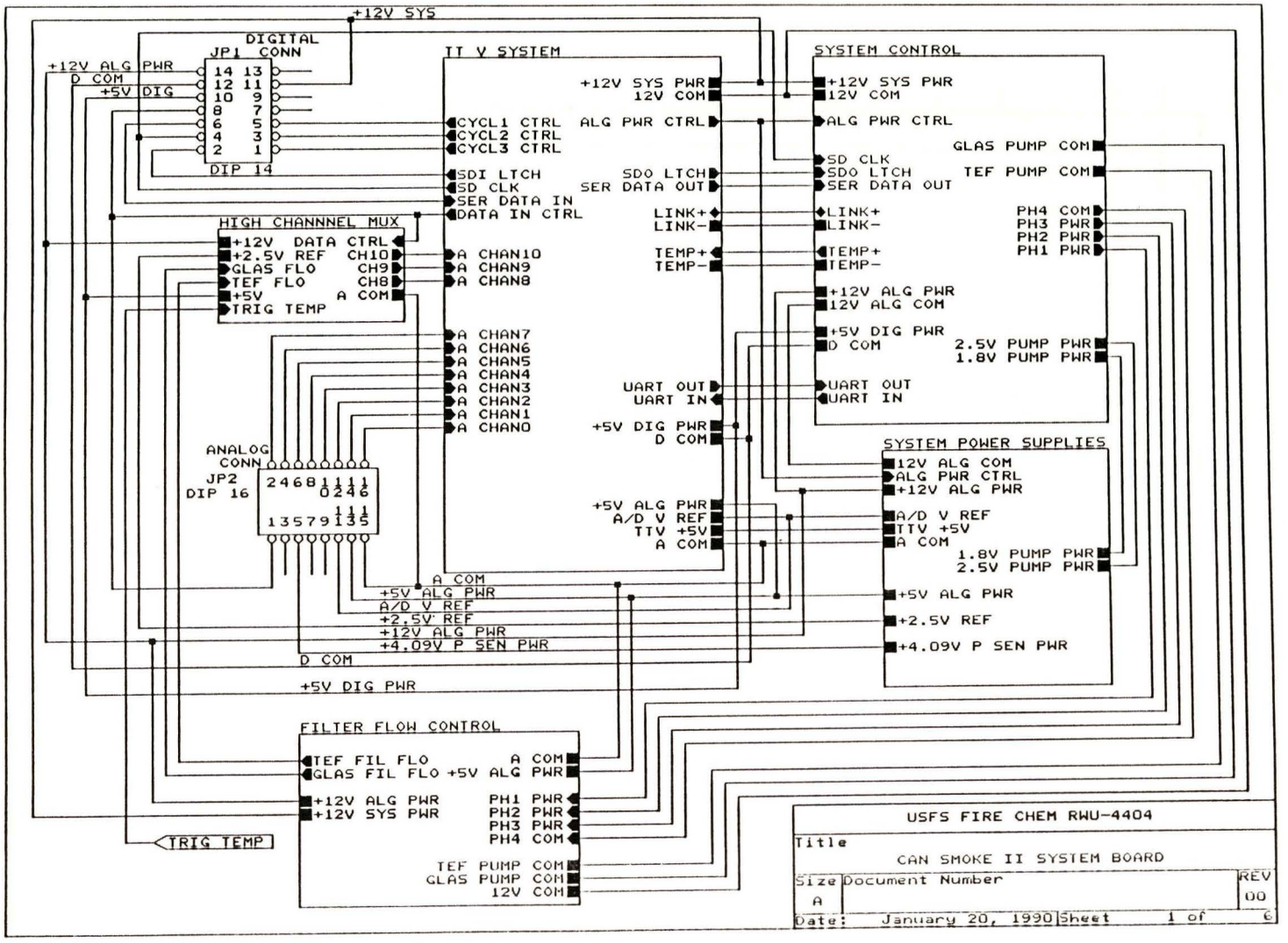

Figure A.1.1.1-1 Schematic diagram of the interconnections of the primary circuits located on the system board.

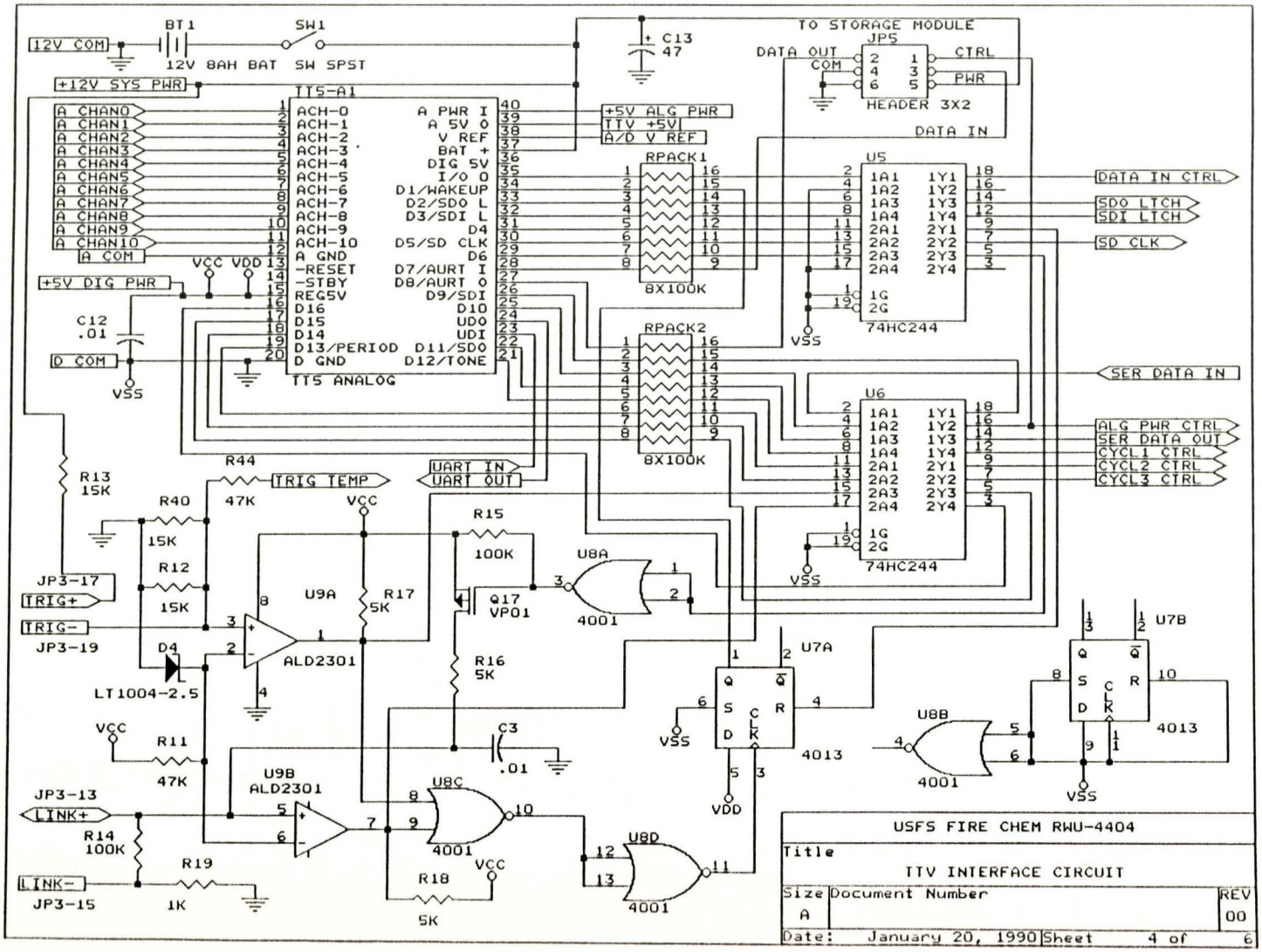

Figure A.1.1.1-3 Schematic diagram of the computer and support circuits located on the system board.

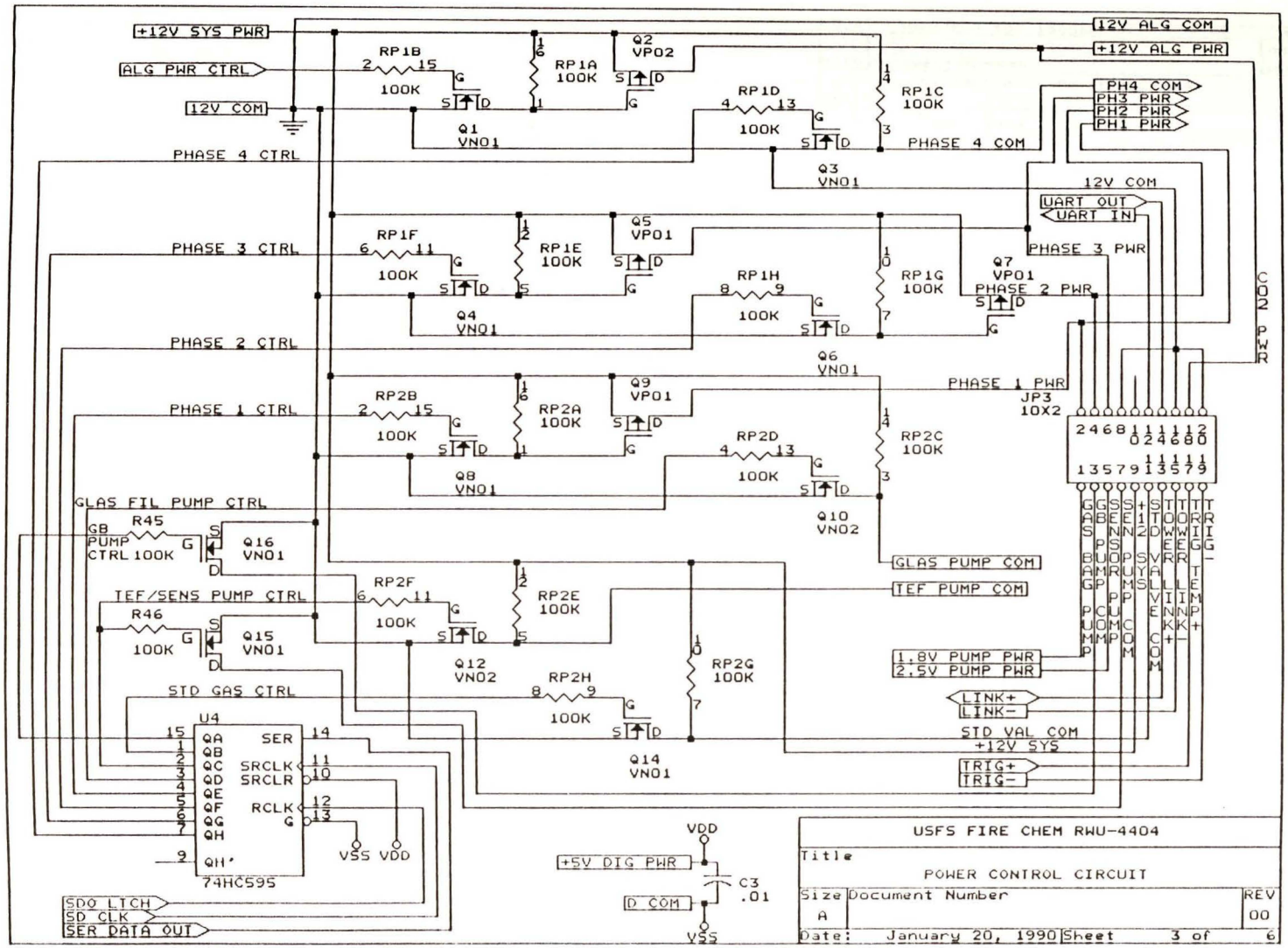

Figure A.1.1.1-4 Schematic diagram of the power drivers located on the system board.

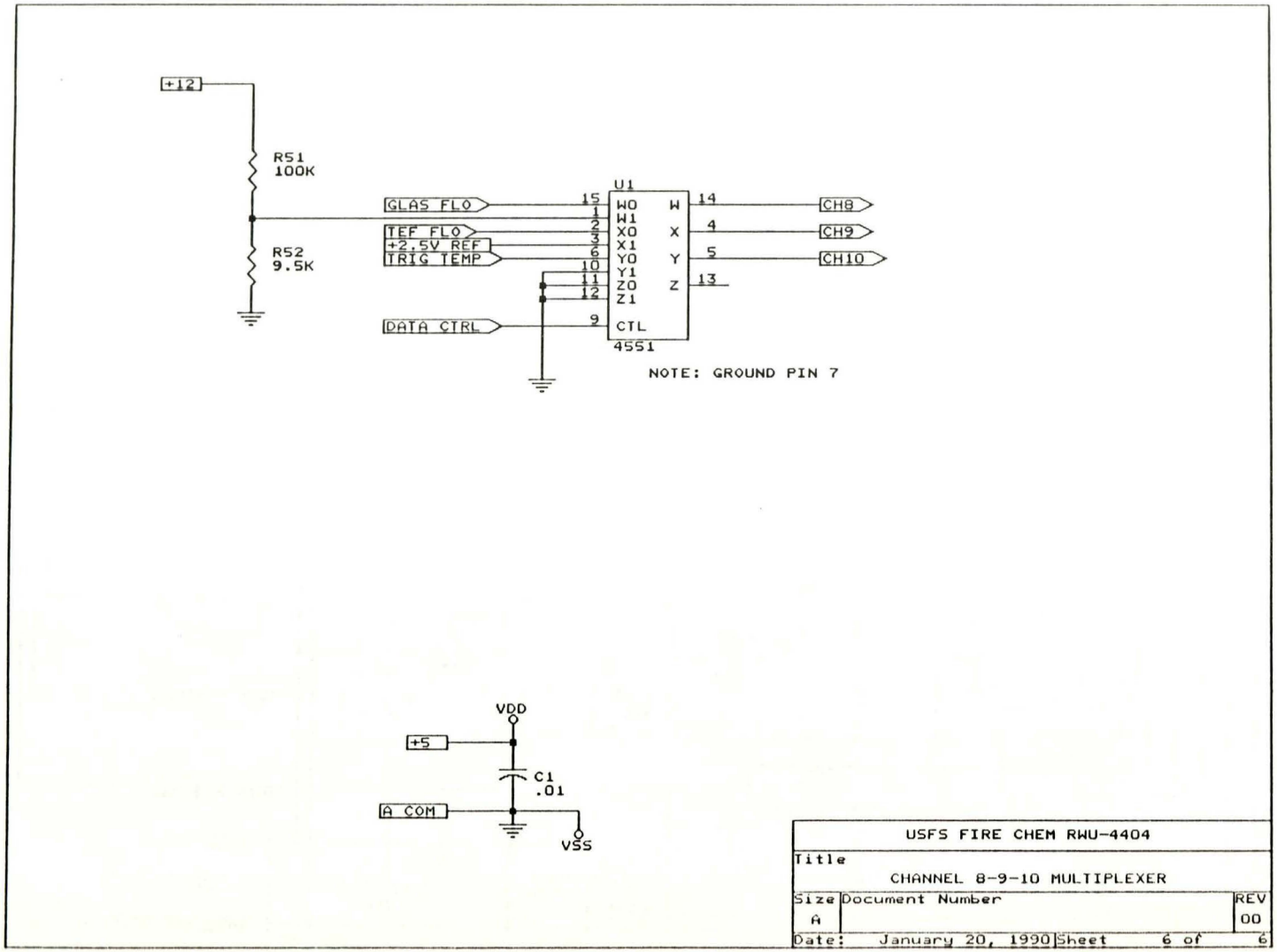

Figure A.1.1.1-5 Schematic diagram of the high channel analog multiplexer located on the system board.

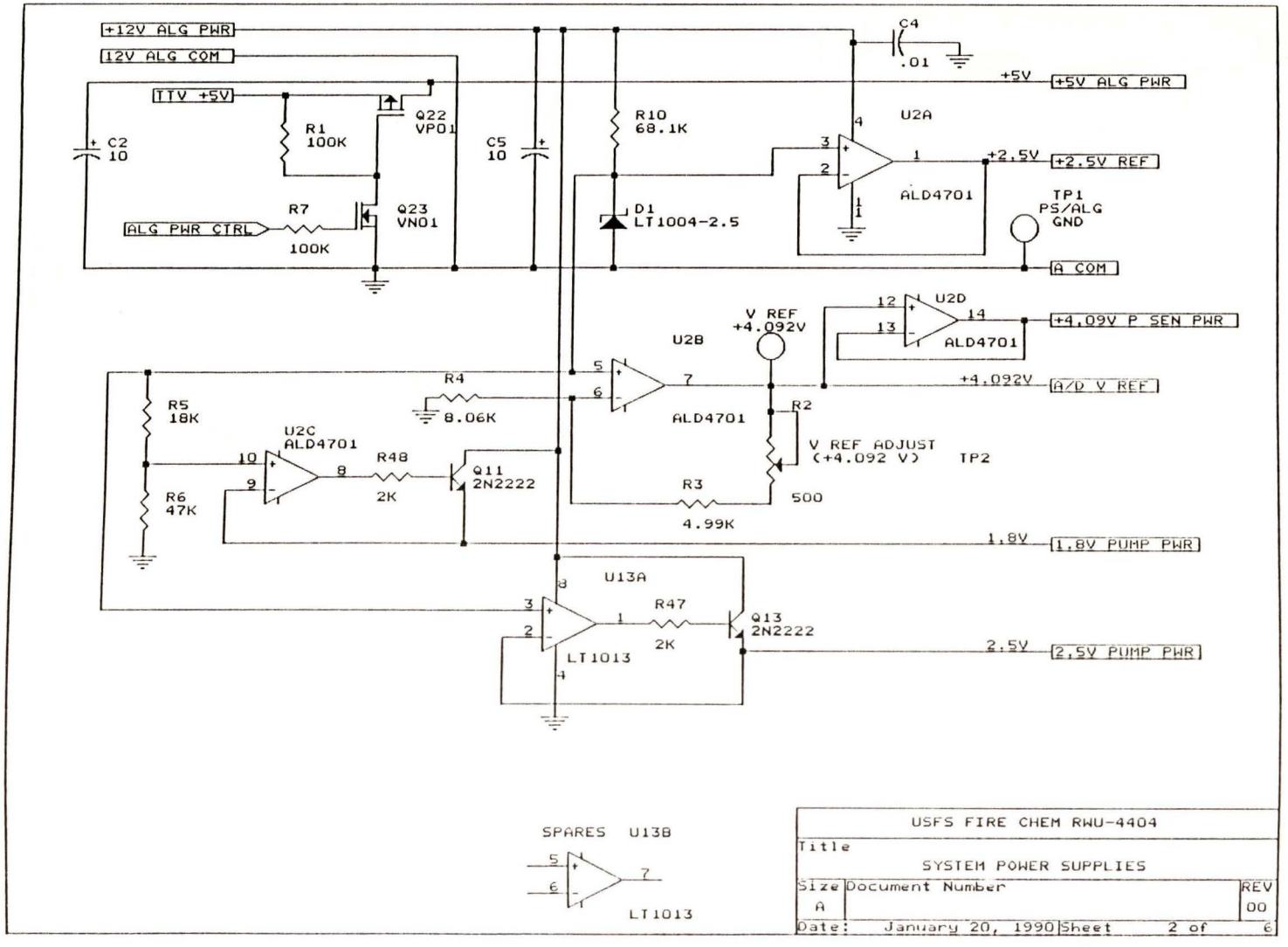

Figure A.1.1.1-6 Schematic diagram of the power supplies located on the system board.

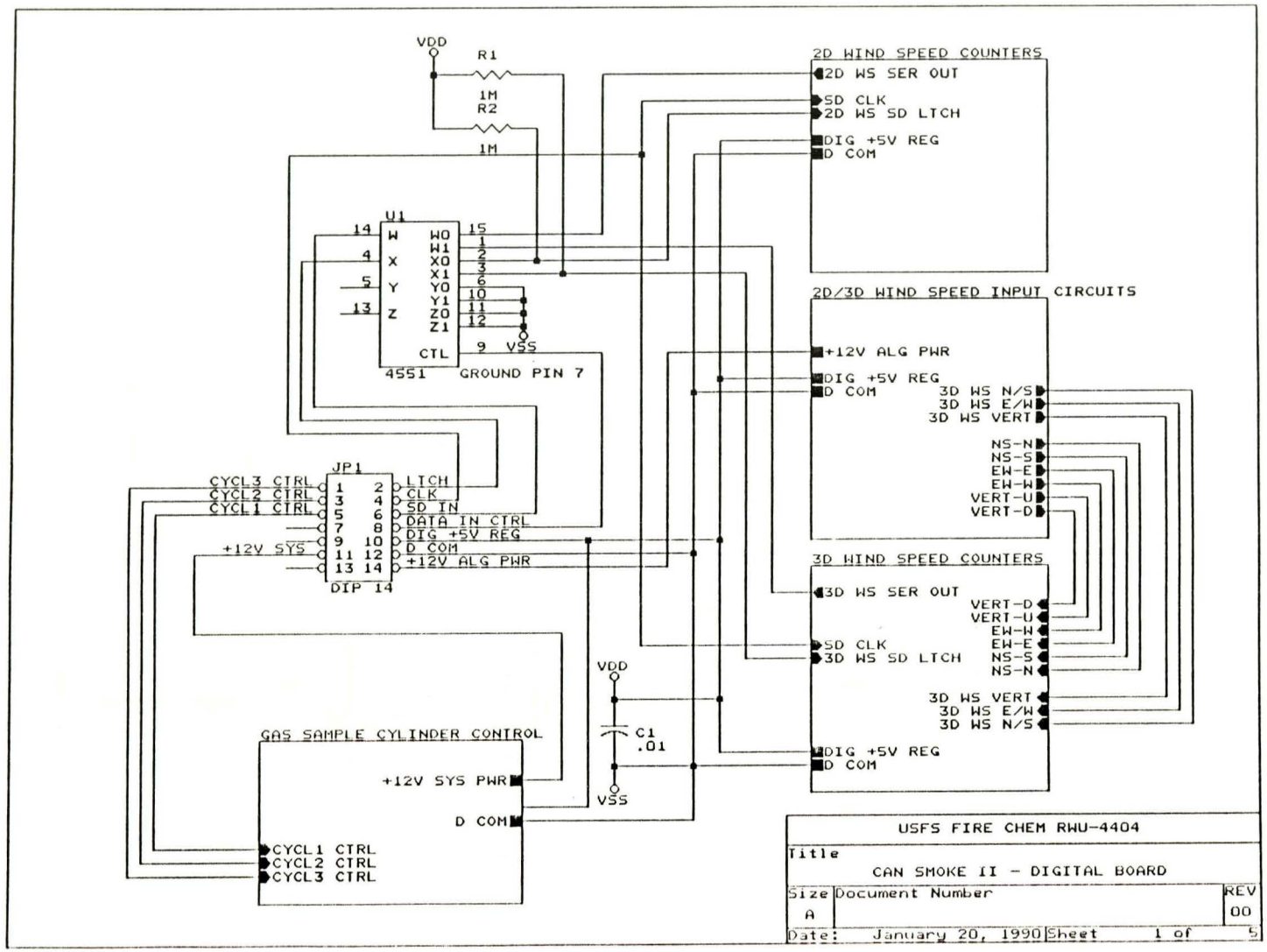

Figure A.1.1.2-1 Schematic diagram of the interconnections of the primary circuits located on the digital board.

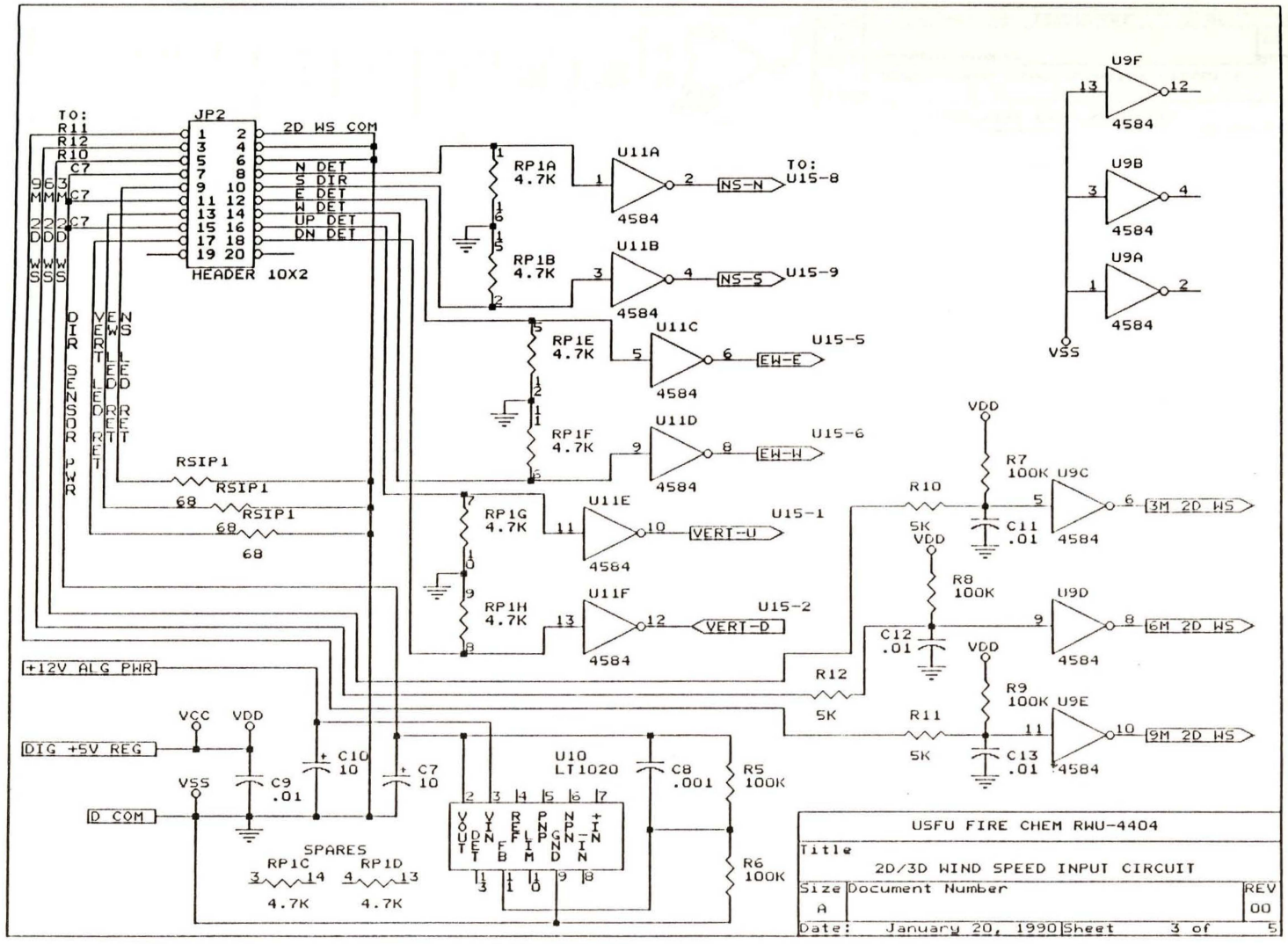

Figure A.1.1.2-2 Schematic diagram of the interface circuits located on the digital board.

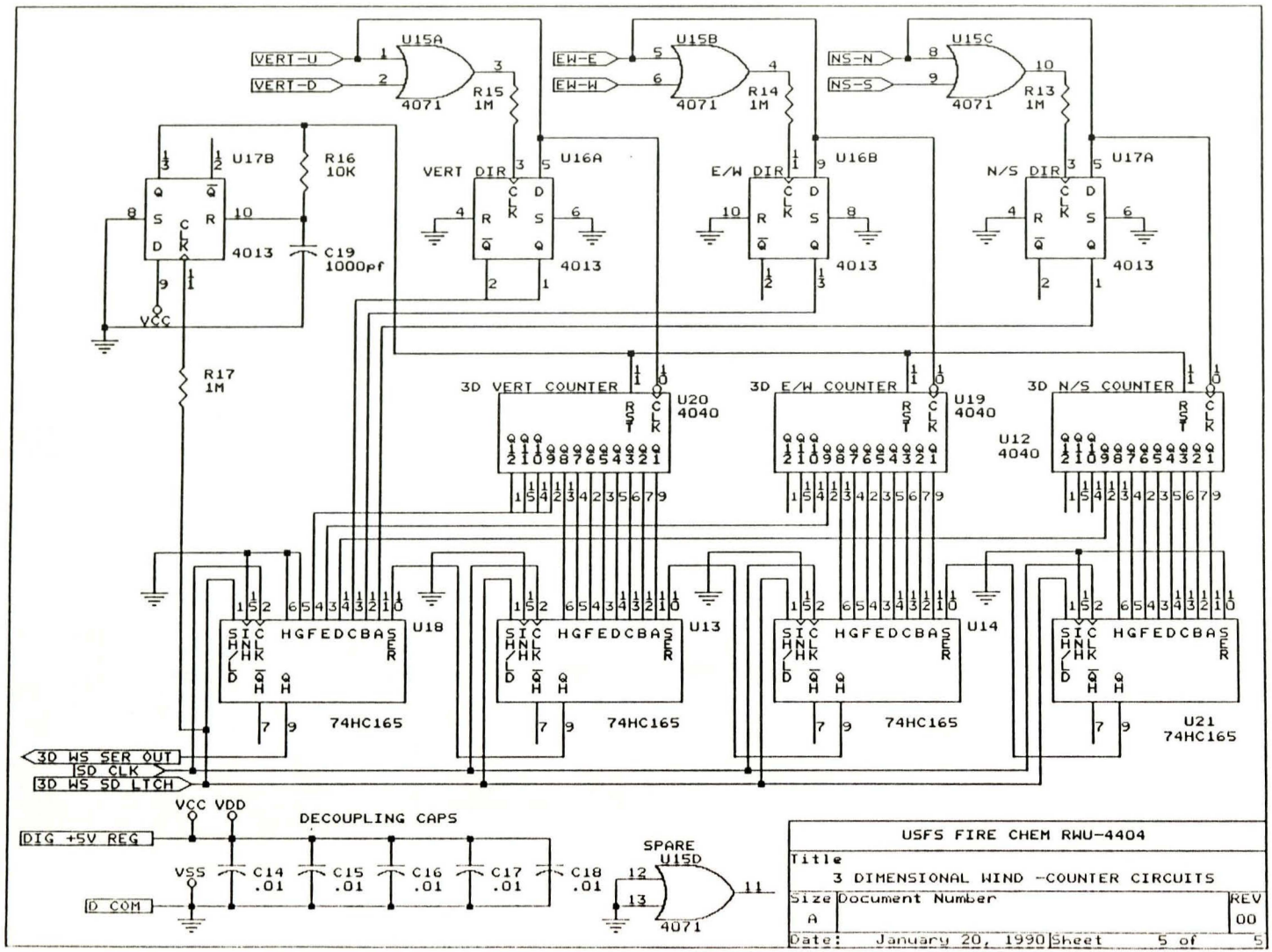

Figure A.1.1.2-3 Schematic diagram of the 3D wind circuits located on the digital board.

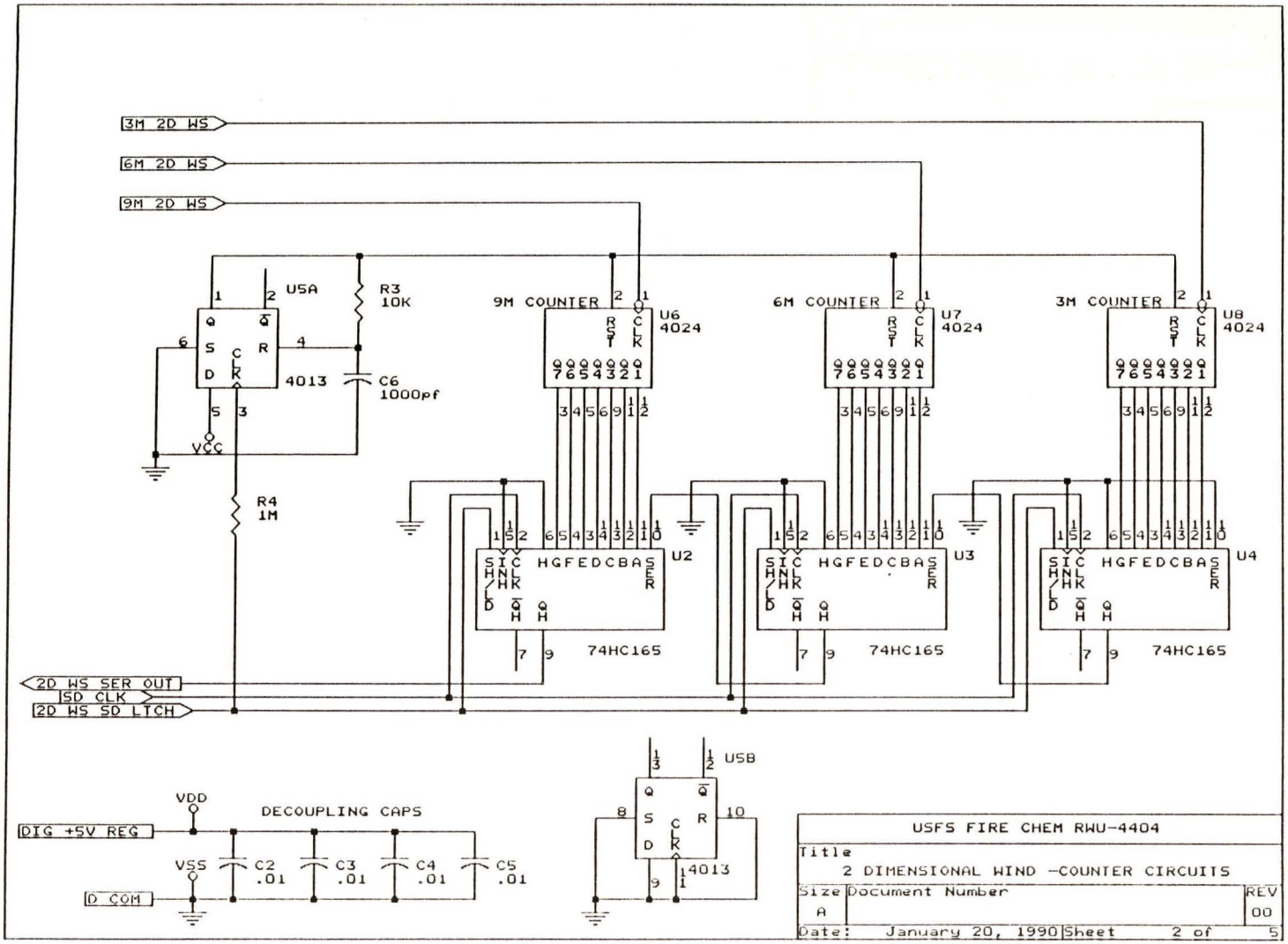

Figure A.1.1.2-4 Schematic diagram of the 2D wind circuits located on the digital board.

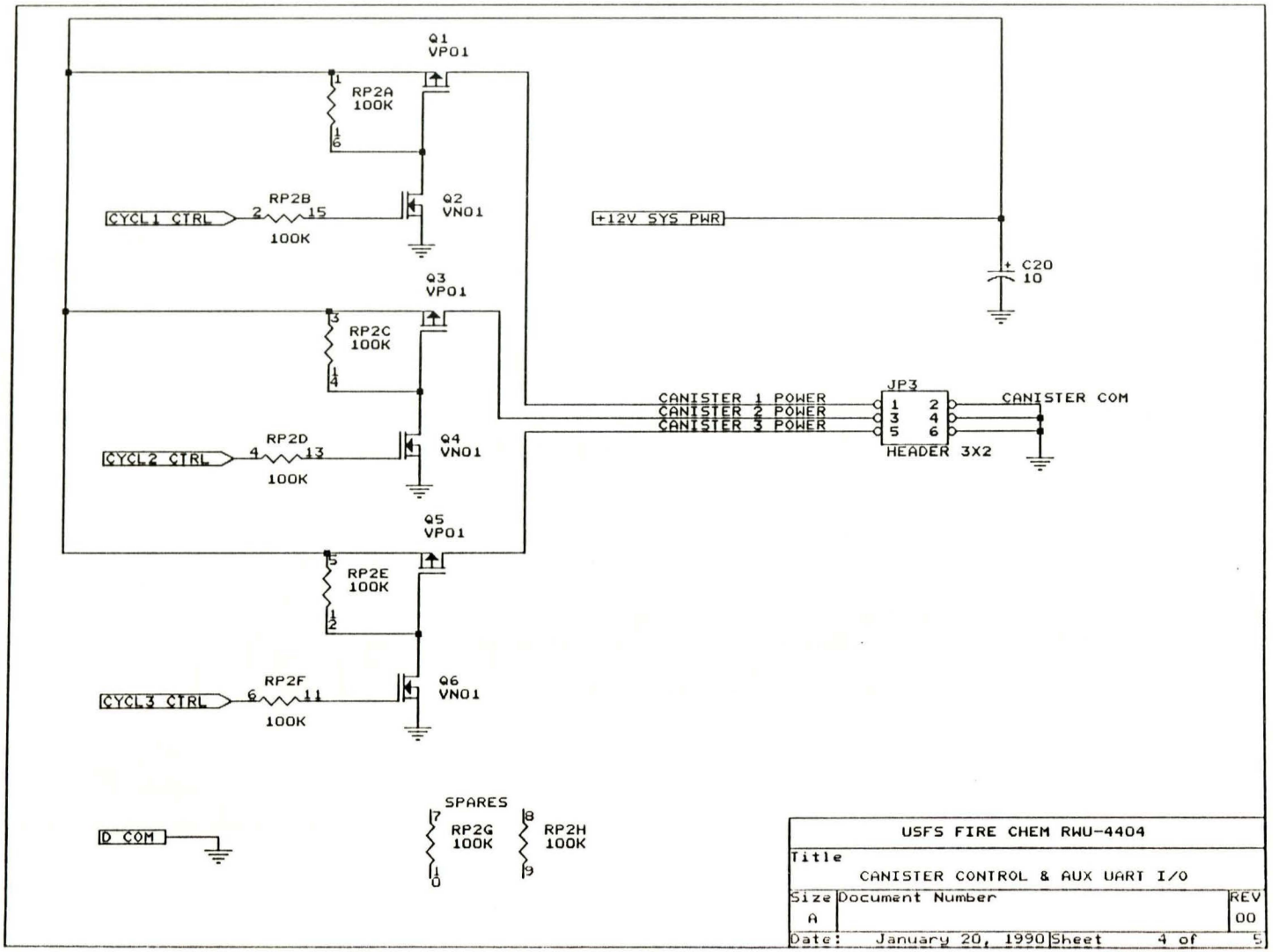

Figure A.1.1.2-5 Schematic diagram of the canister control circuits located on the digital board.

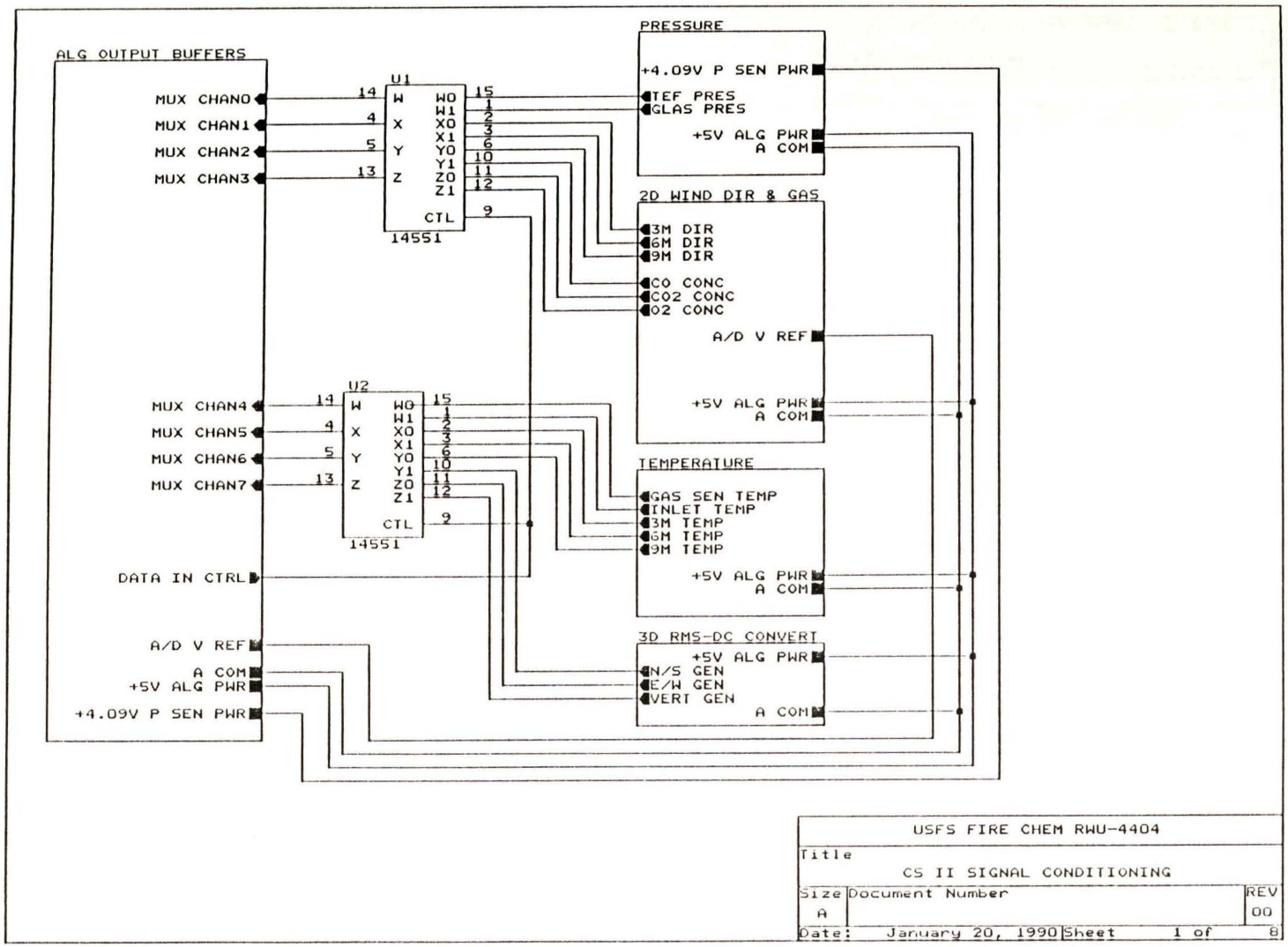

Figure A.1.1.3-1 Schematic diagram of the interconnections of the primary circuits located on the analog board.

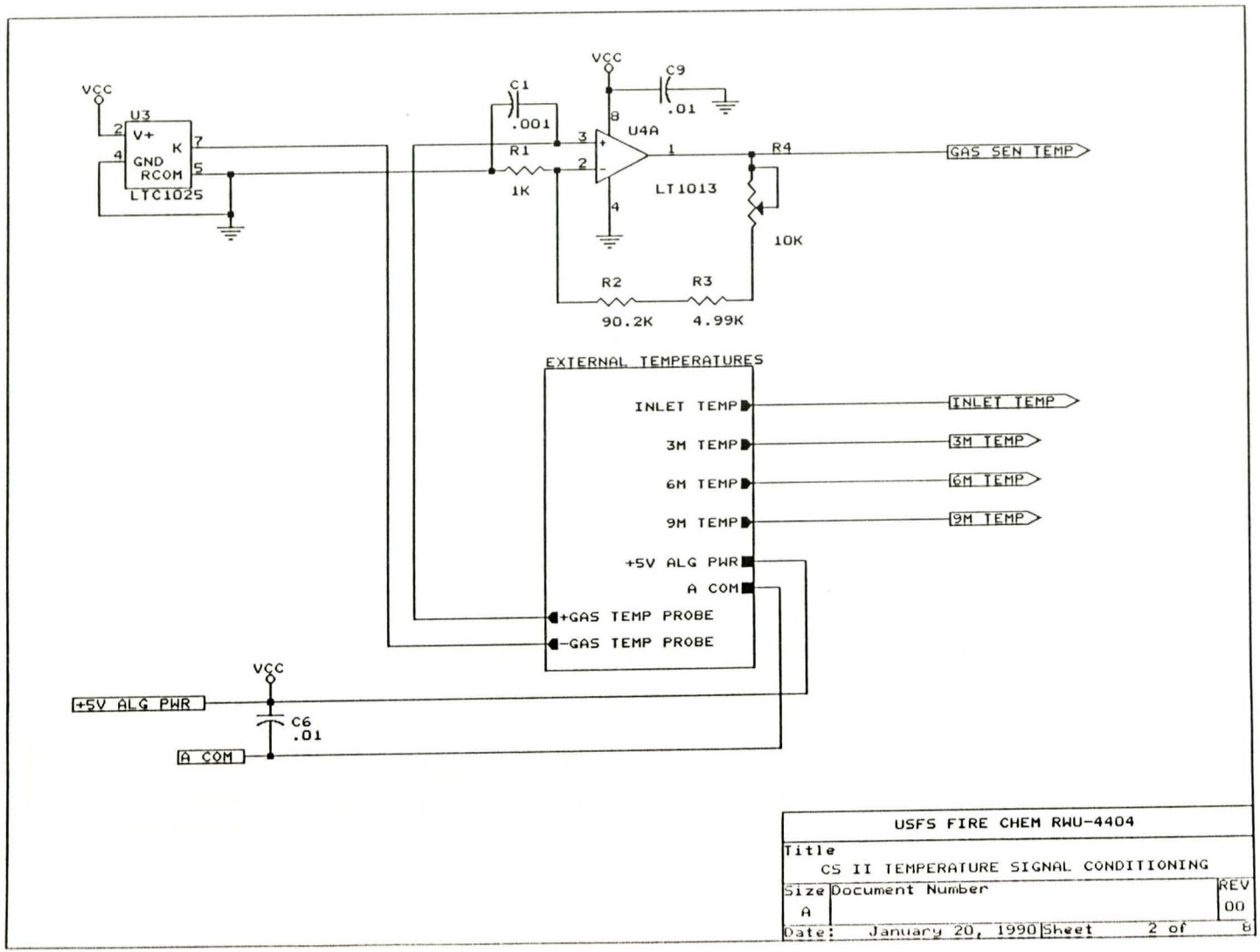

Figure A.1.1.3-2 Schematic diagram of the gas stream thermocouple signal conditioning circuit located on the analog board.

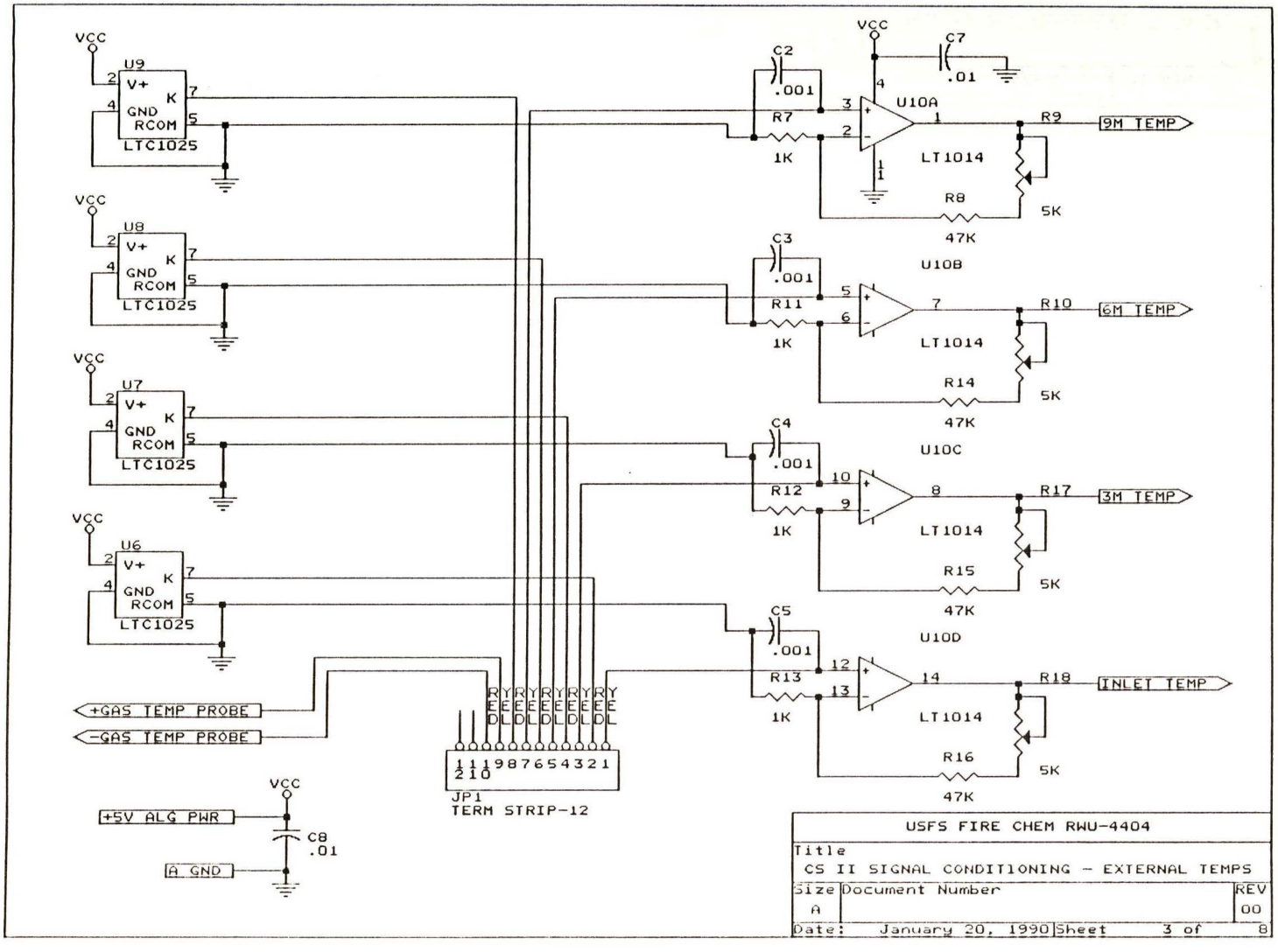

Figure A.1.1.3-3 Schematic diagram of the external thermocouple signal conditioning circuits located on the analog board.

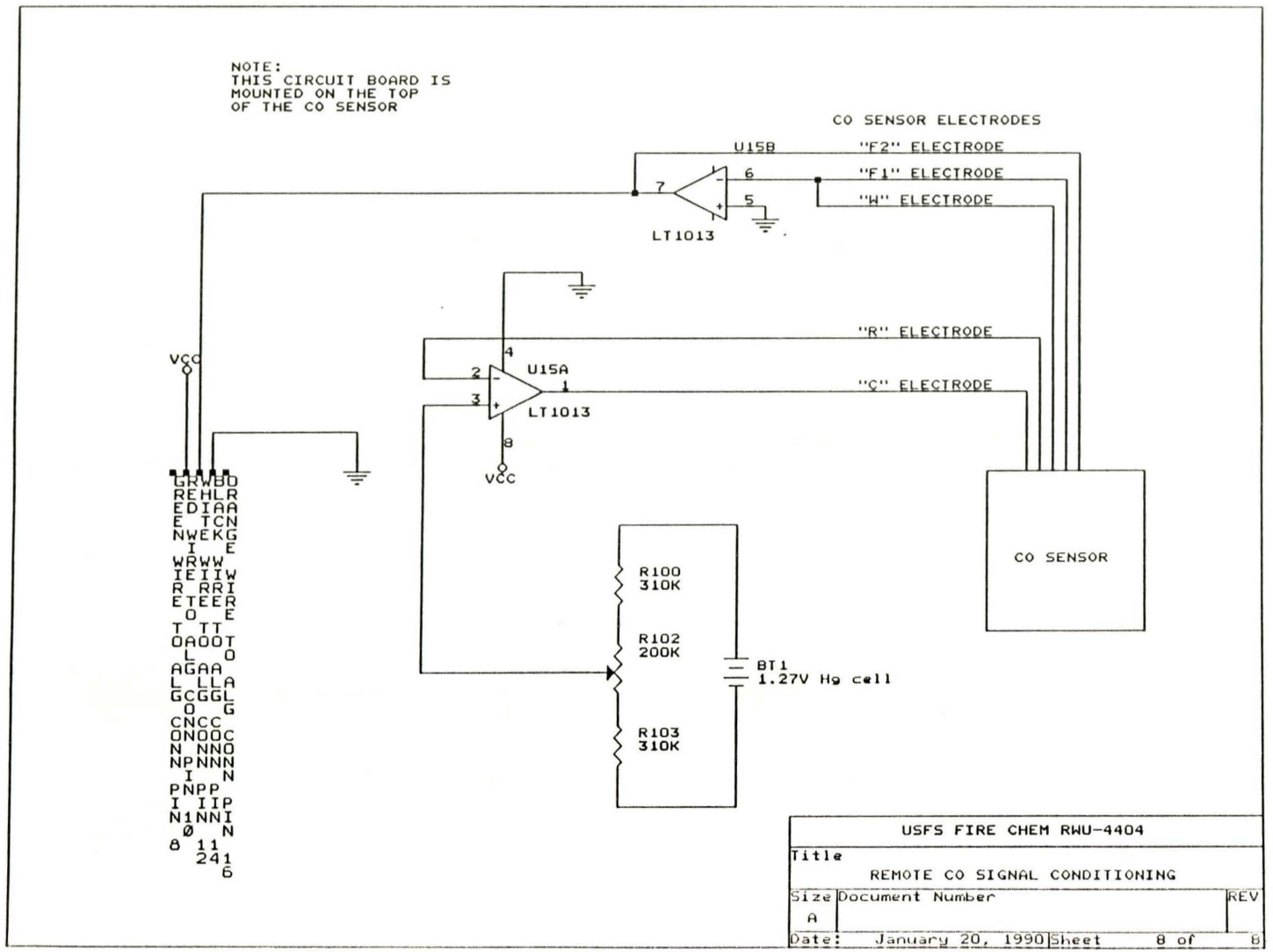

Figure A.1.1.3-4 Schematic diagram of the CO signal conditioning circuit located on the analog board.

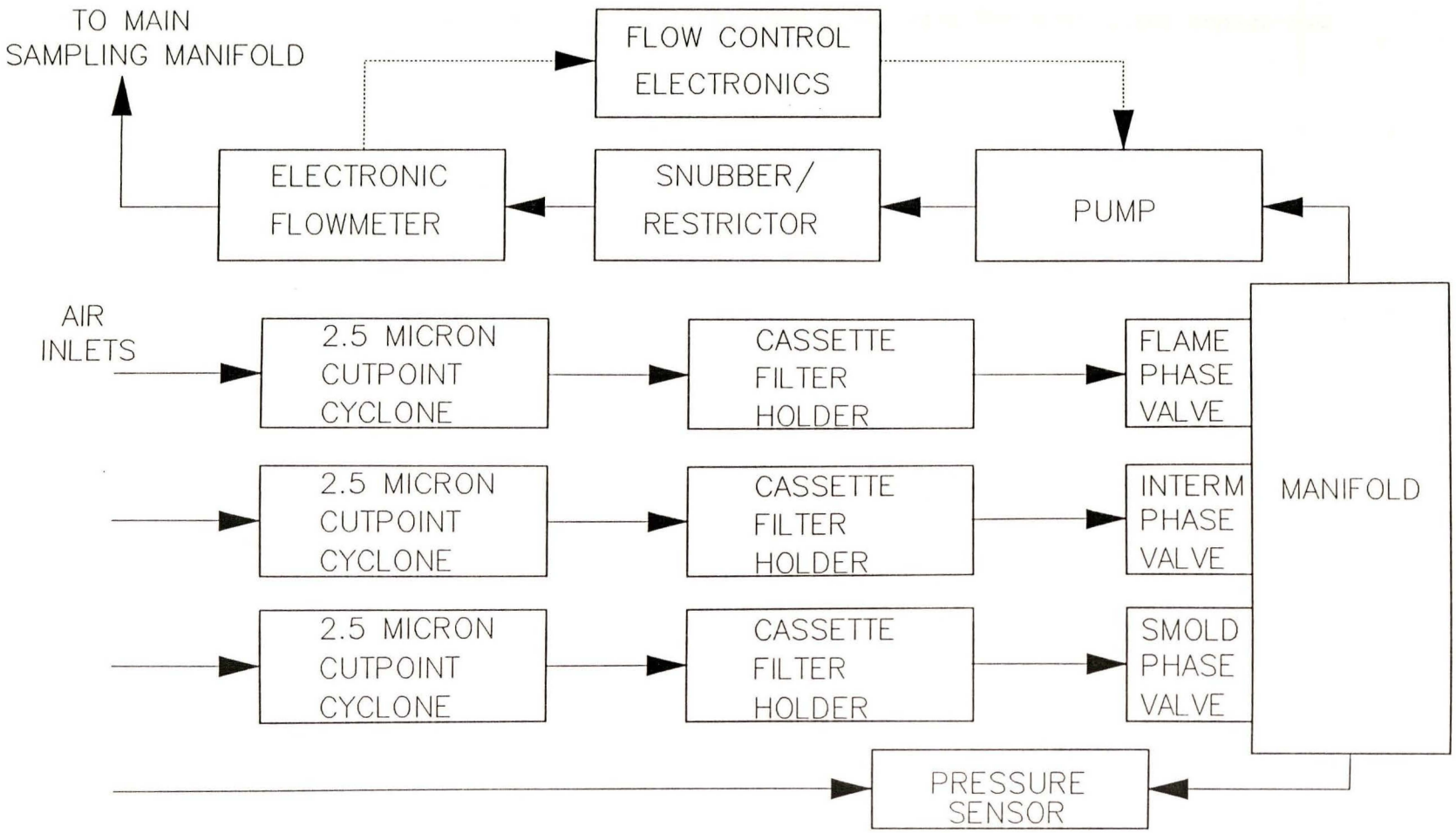

Figure A.1.2-1 Block diagram of the glass fiber particulate collection sub-system located within the FASS.

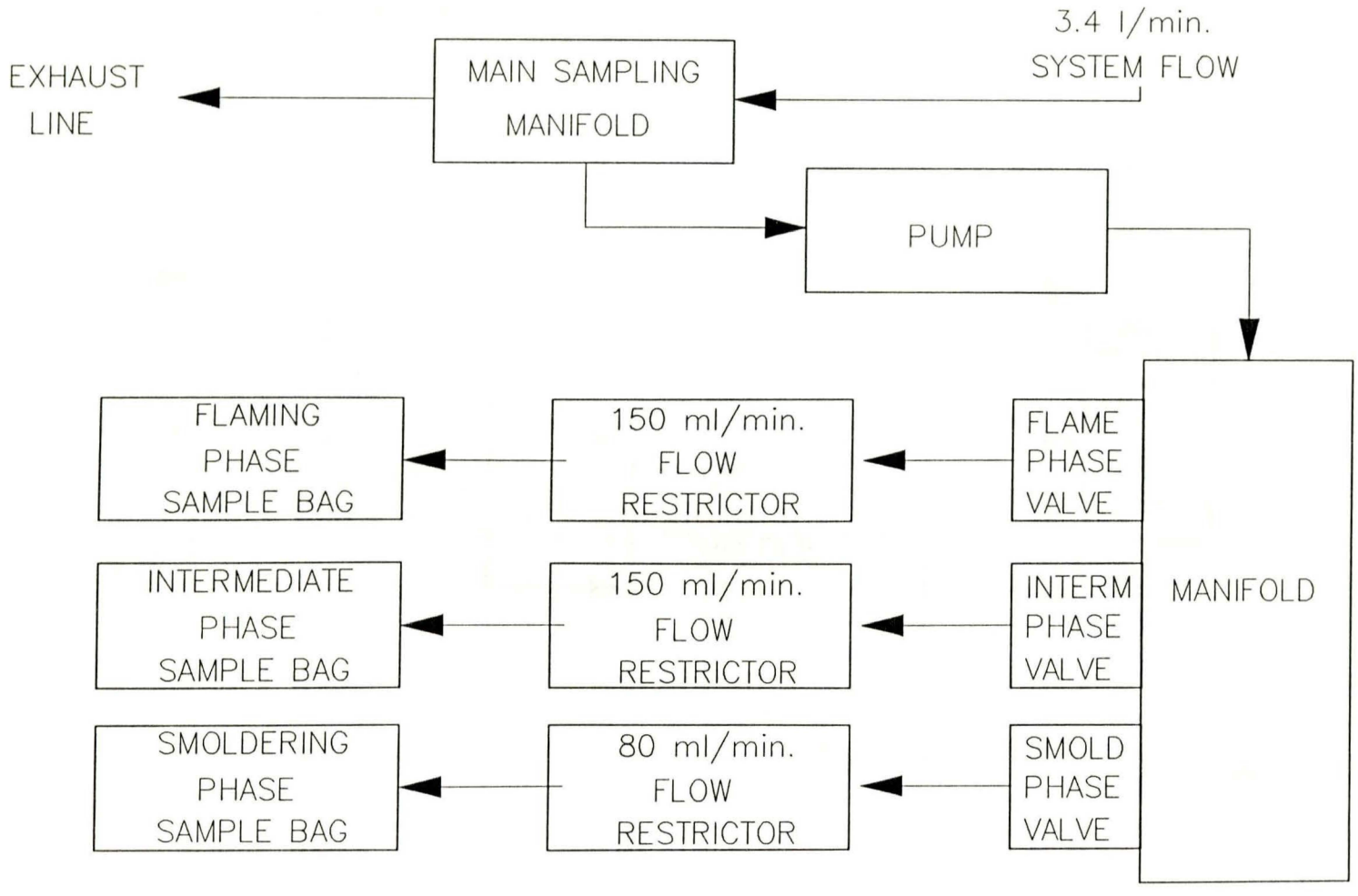

Figure A.1.3-1 Block diagram of the phase integrated gas collection sub-system located within the FASS.

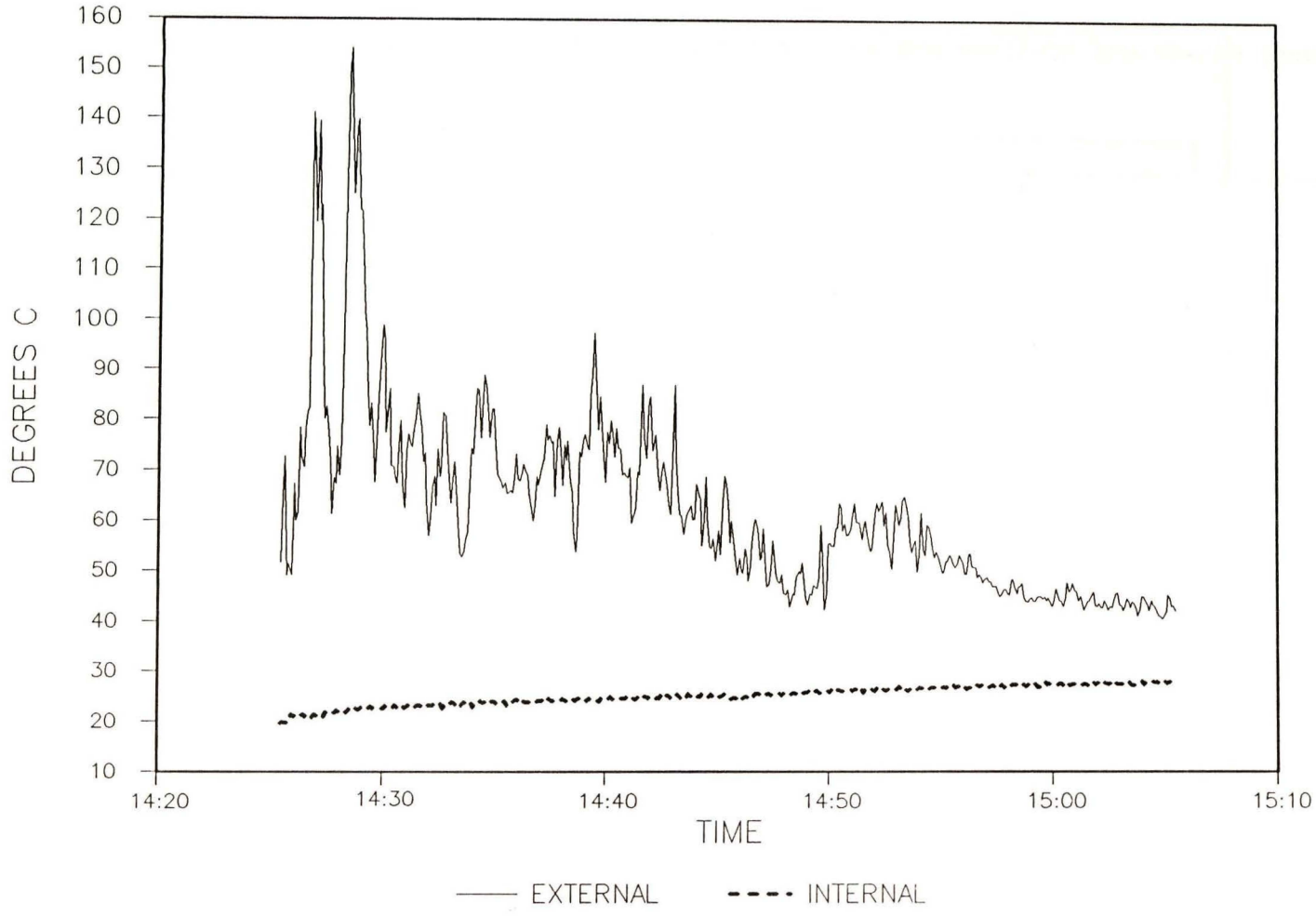

Figure A.1.4-2 Typical inlet and internal temperatures as measured during the Hill experiments.

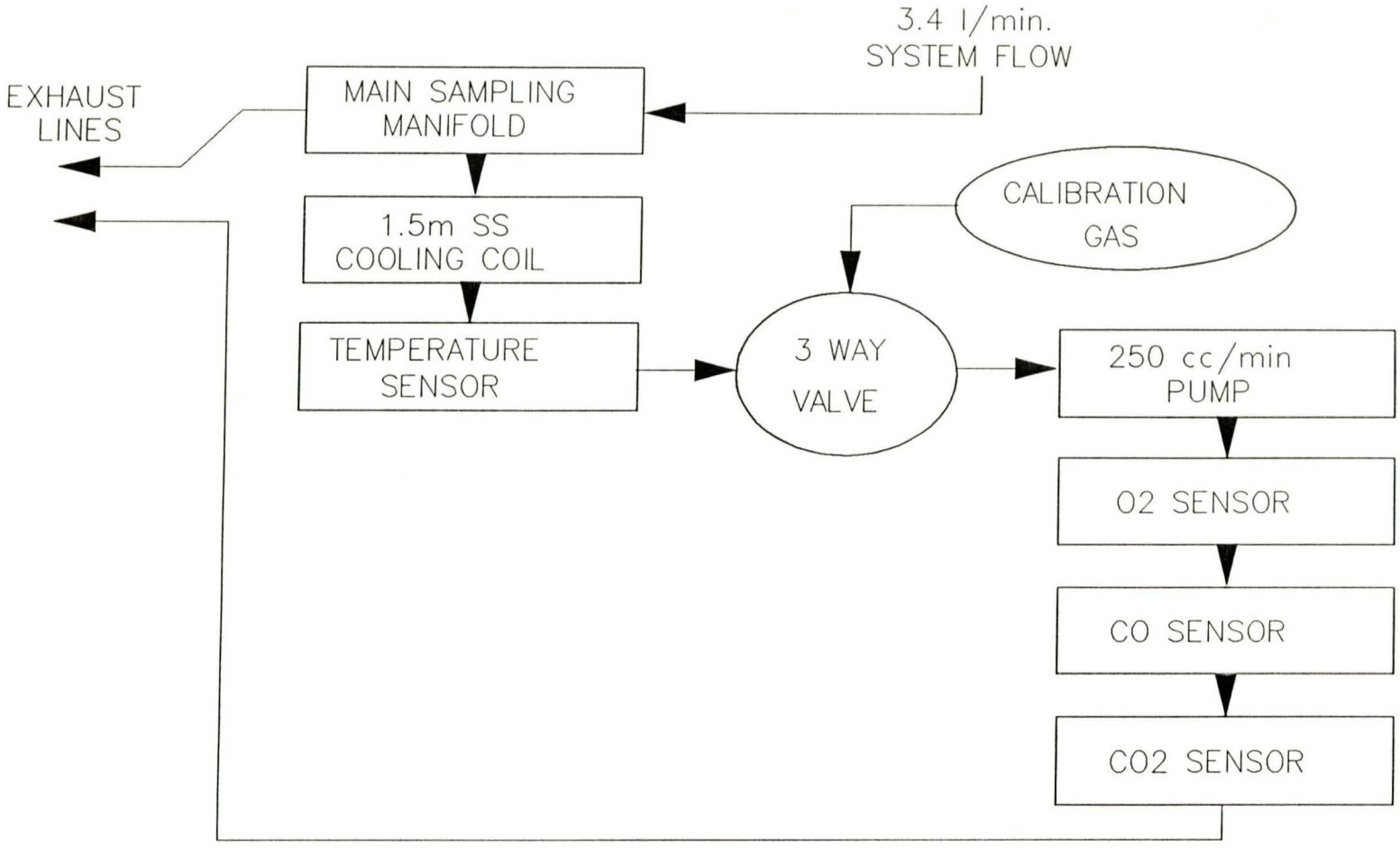

Figure A.1.4-1 Block diagram of the real time gas analysis sub-system located within the FASS.

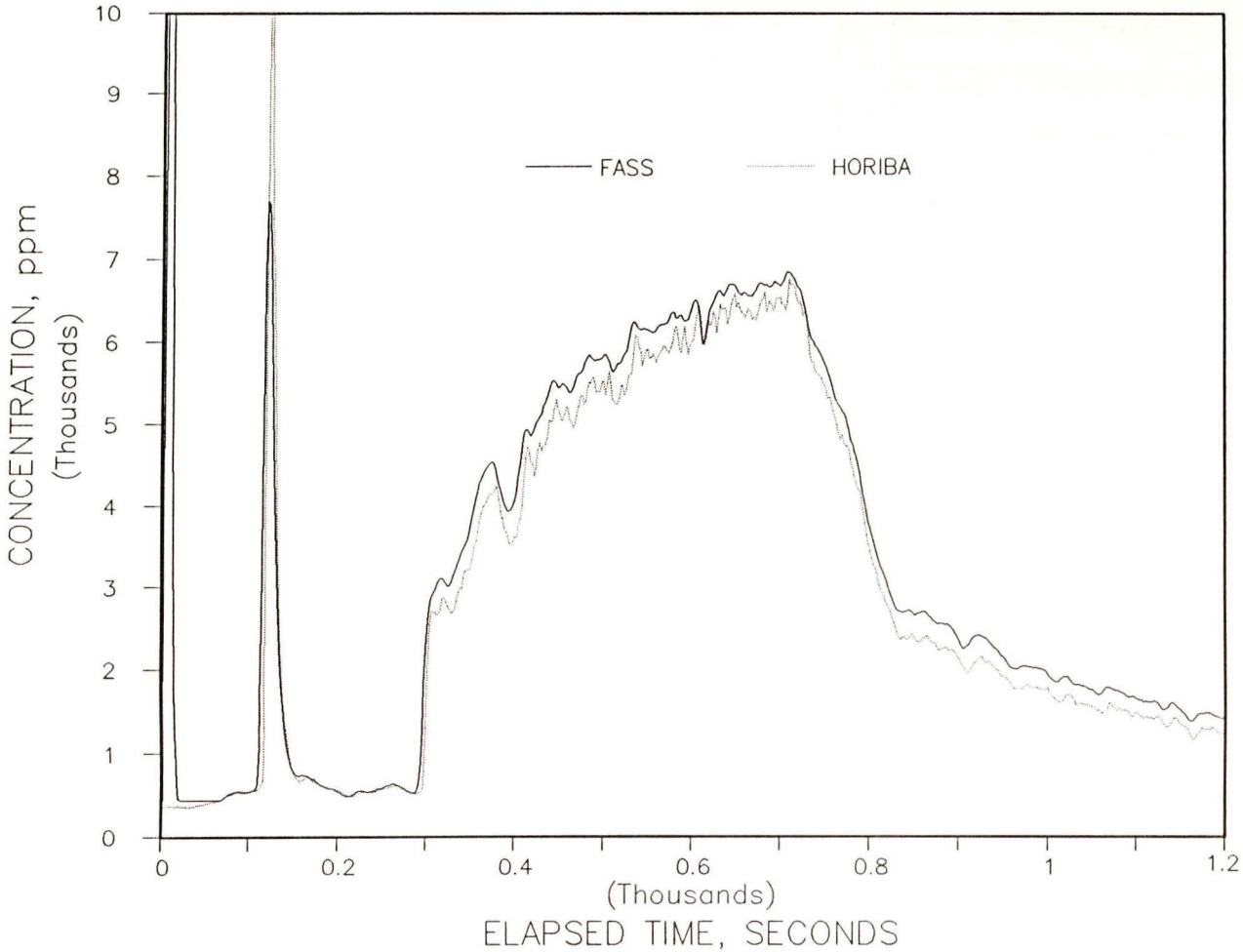

Figure A.1.7.3-1 Comparison of CO_2 as measured by the FASS and the Horiba during an experimental burn in the IFSL combustion facility

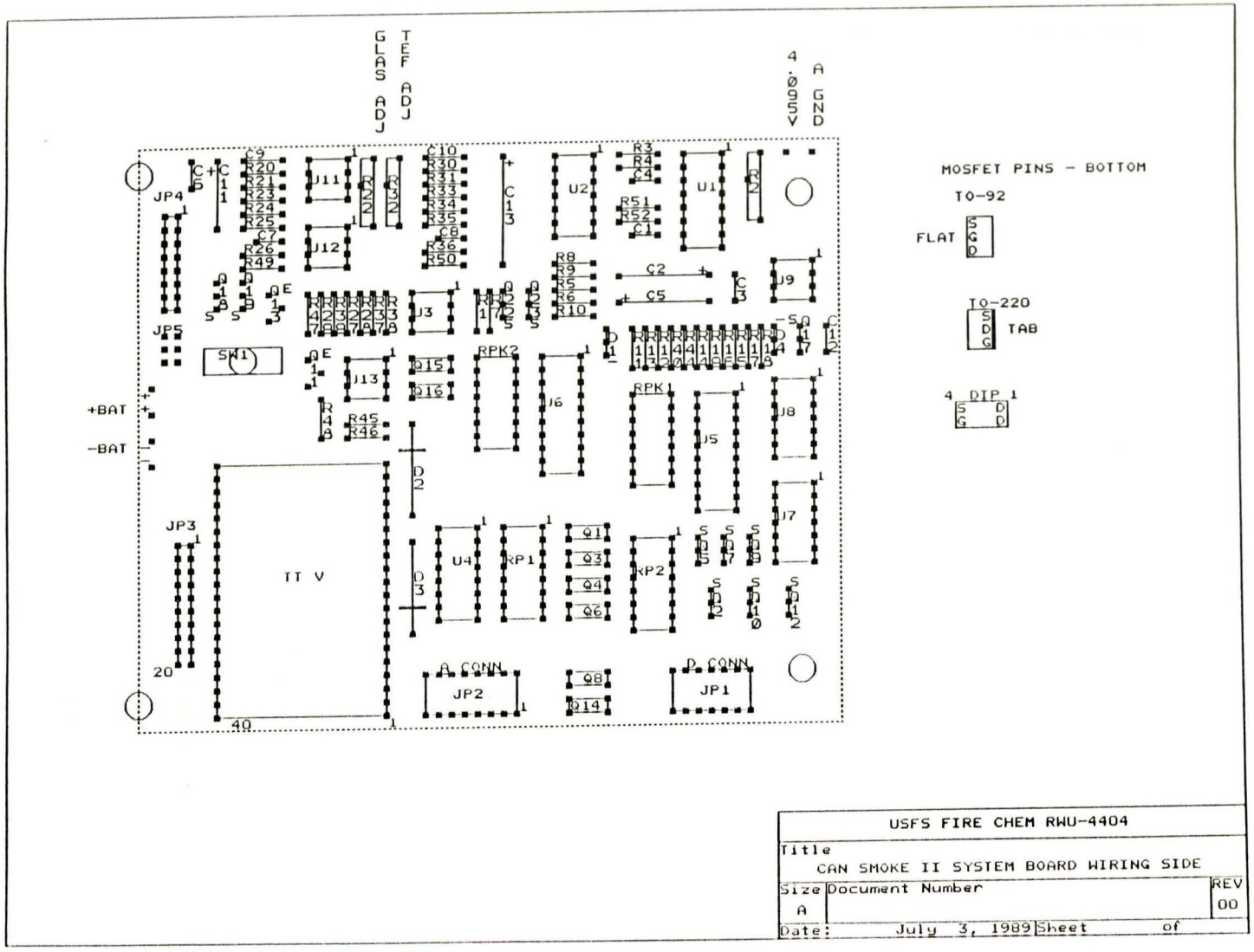

Figure A.1.8-1 Electronic component layout of the FASS system circuit board.

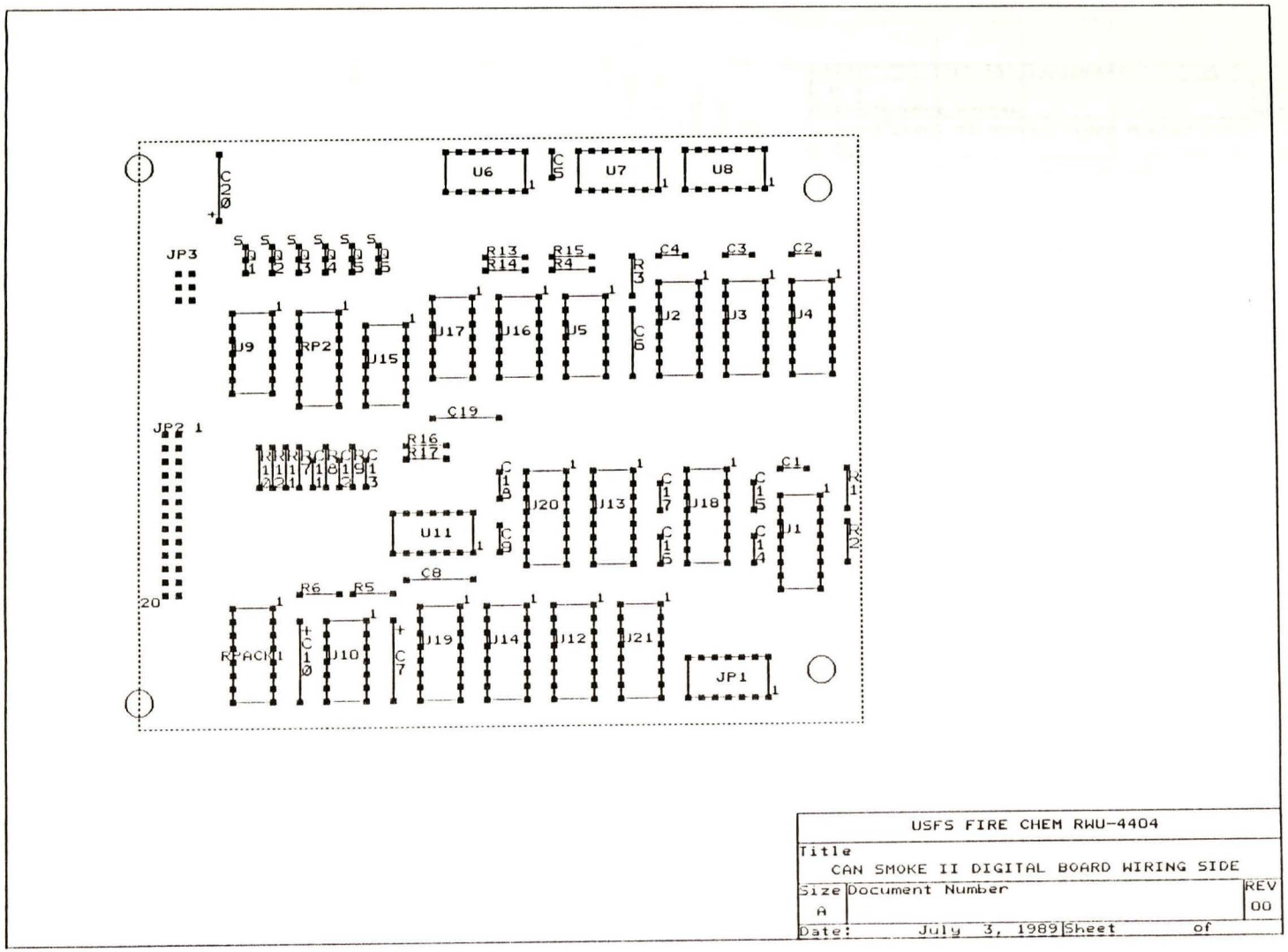

USFS FIRE CHEM RWU-4404		
Title: CAN SMOKE II DIGITAL BOARD WIRING SIDE		
Size: A	Document Number	REV: 00
Date: July 3, 1989	Sheet of	

Figure A.1.8-2 Electronic component layout of the FASS digital circuit board.

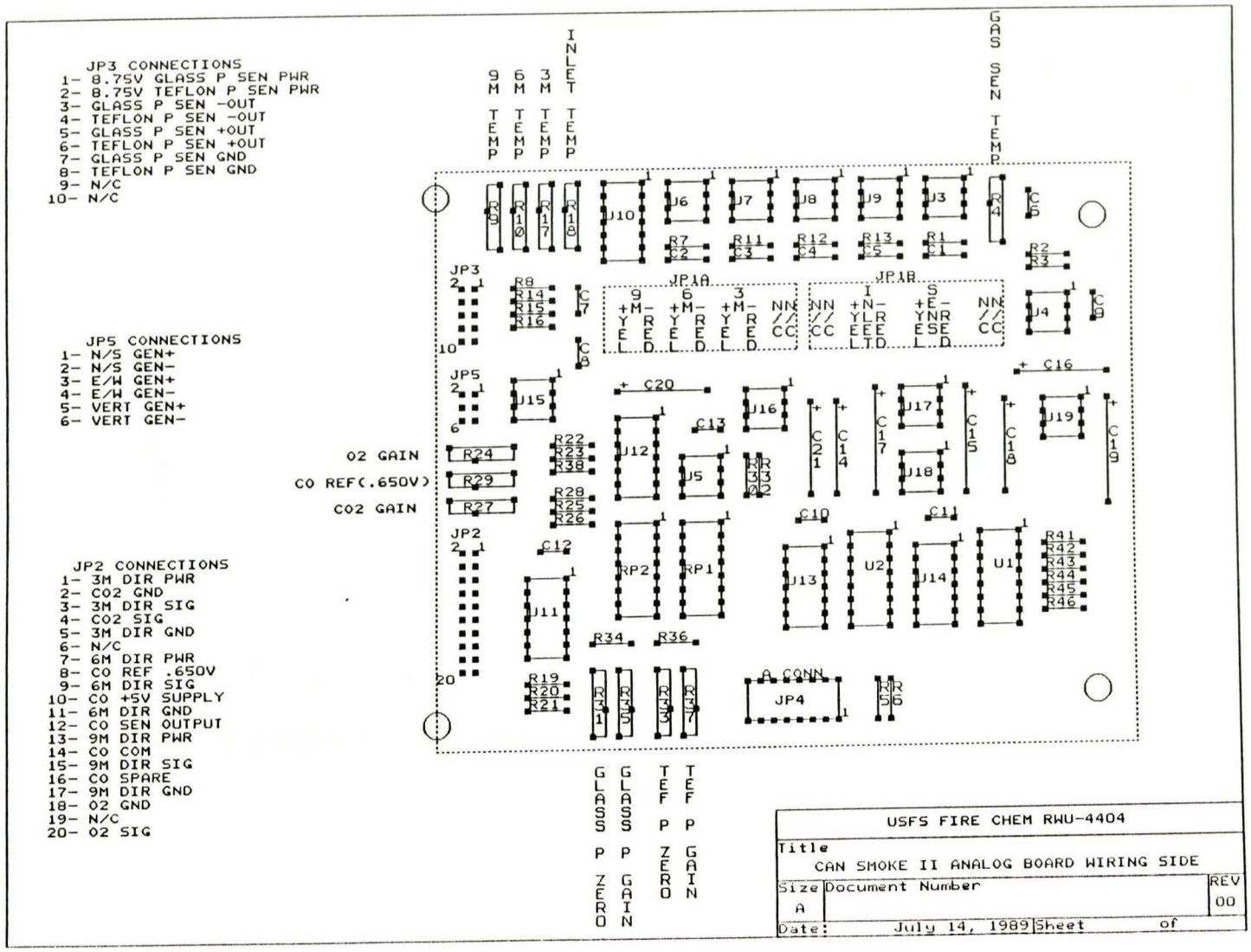

Figure A.1.8-3 Electronic component layout of the FASS analog signal conditioning circuit board.

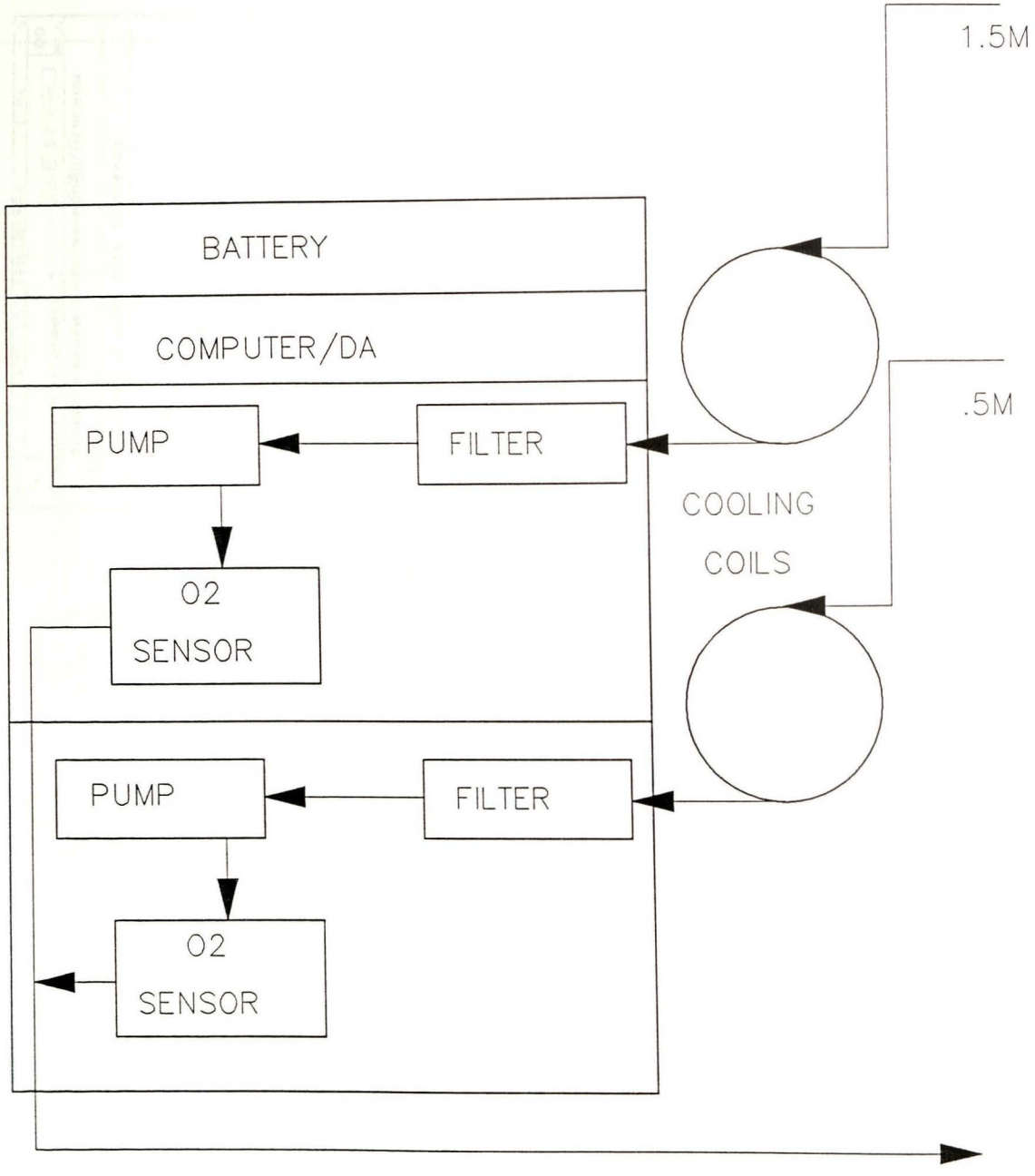

Figure A.2.1-1 Functional block diagram of the GODM.

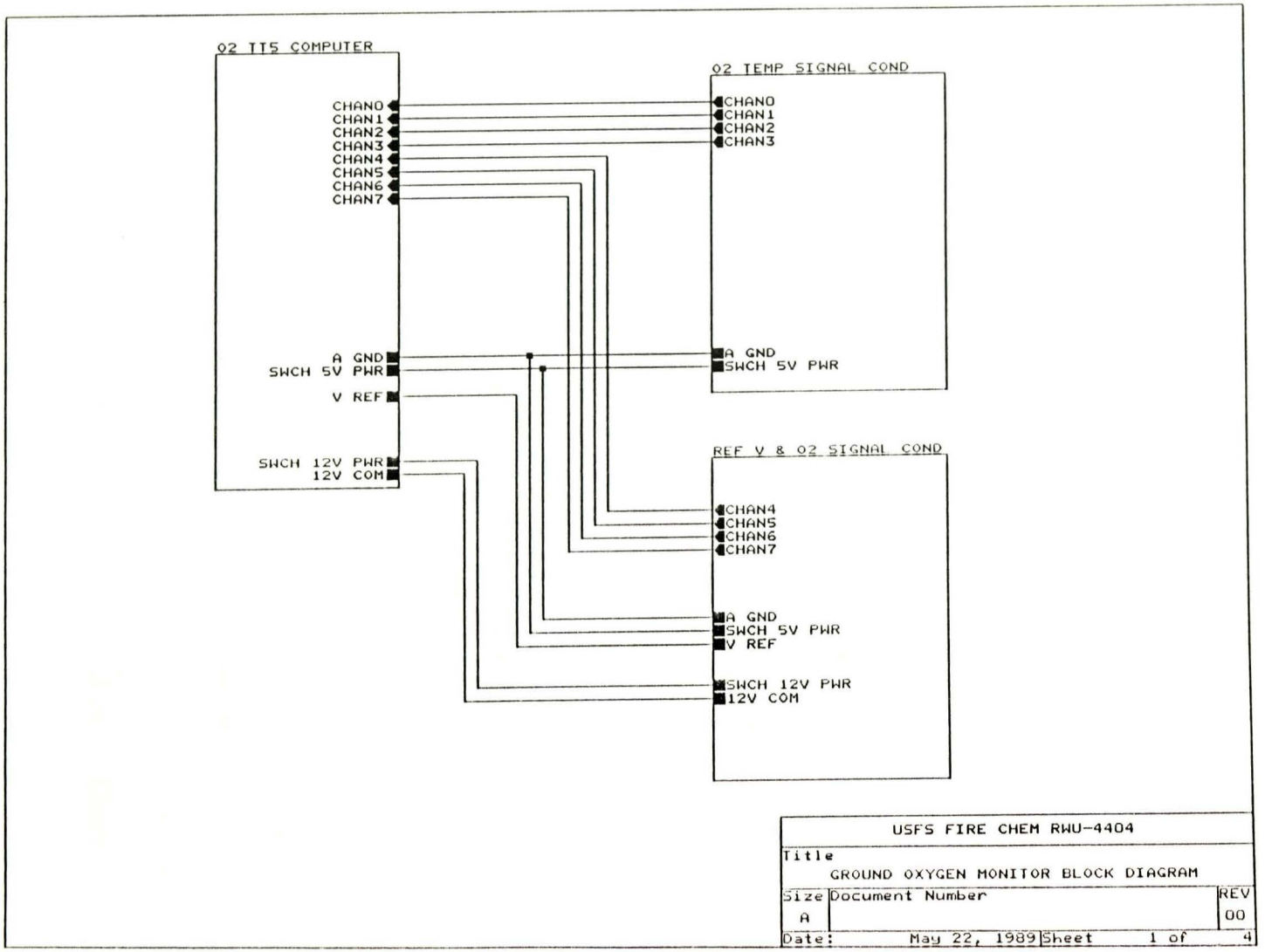

Figure A.2.1-2 Block diagram of the primary circuits of the GODM.

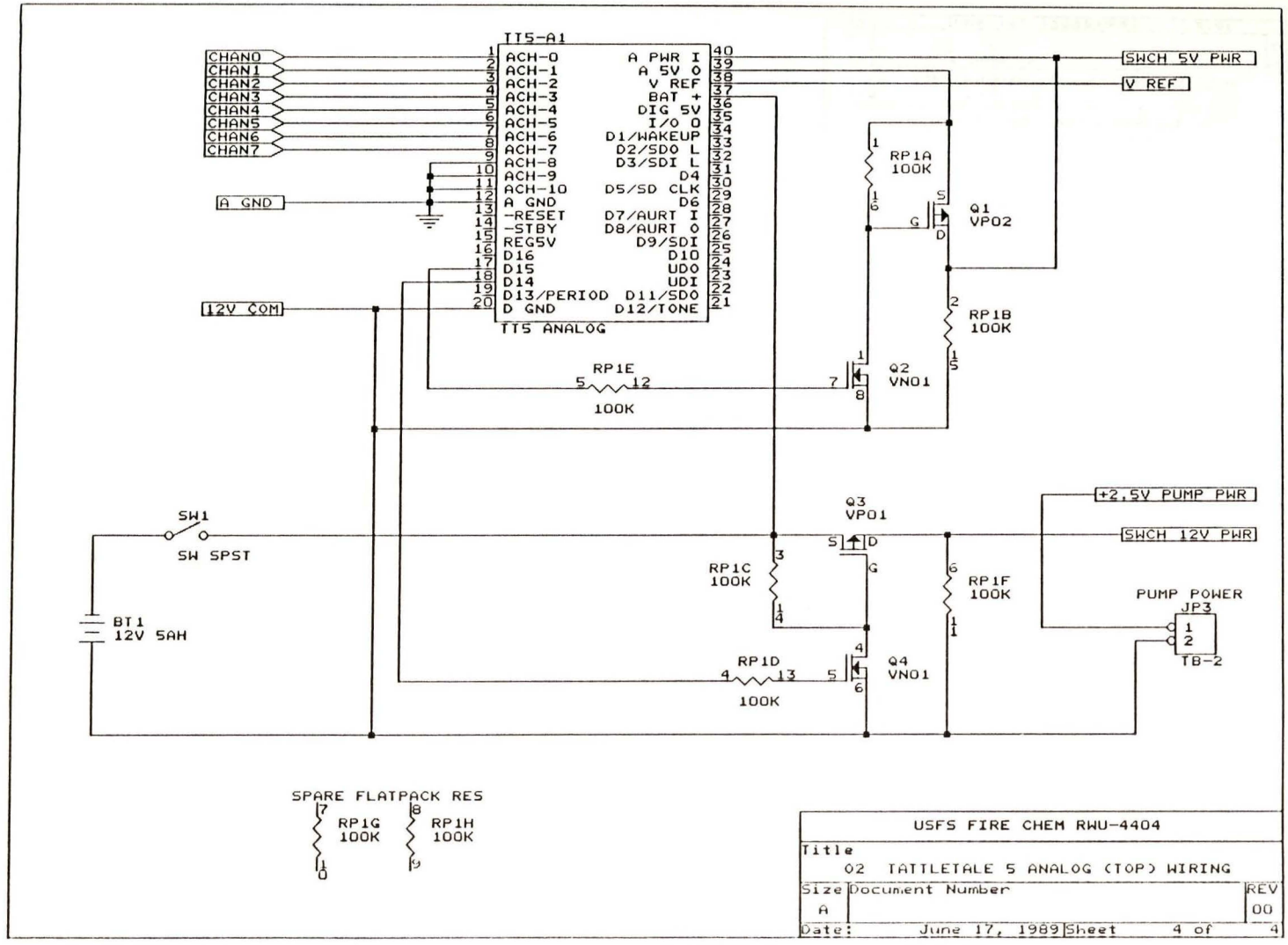

Figure A.2.1-3 Schematic diagram of the computer and support circuits of the GODM.

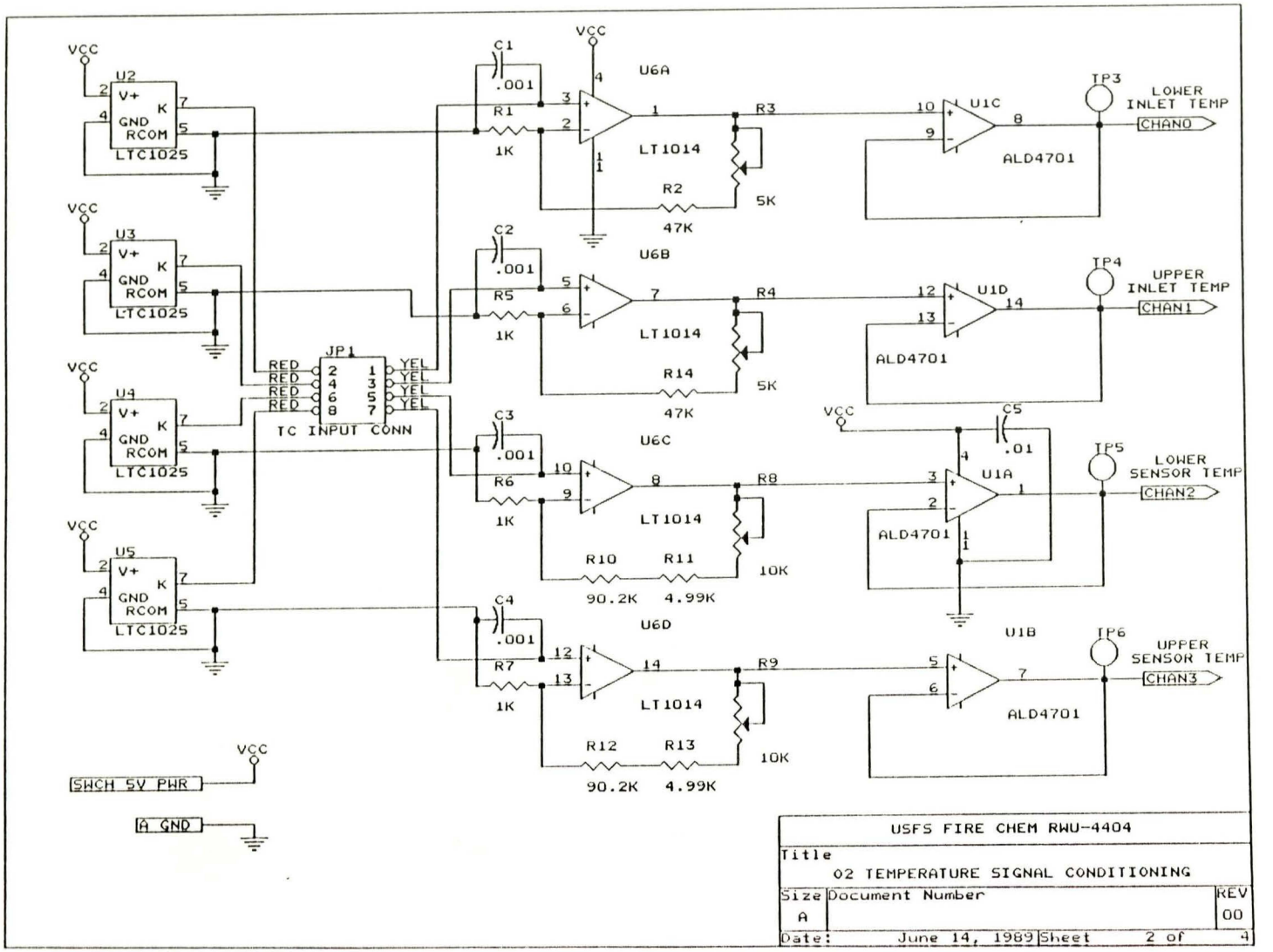

Figure A.2.1-4 Schematic diagram of the thermocouple signal conditioning circuits of the GODM.

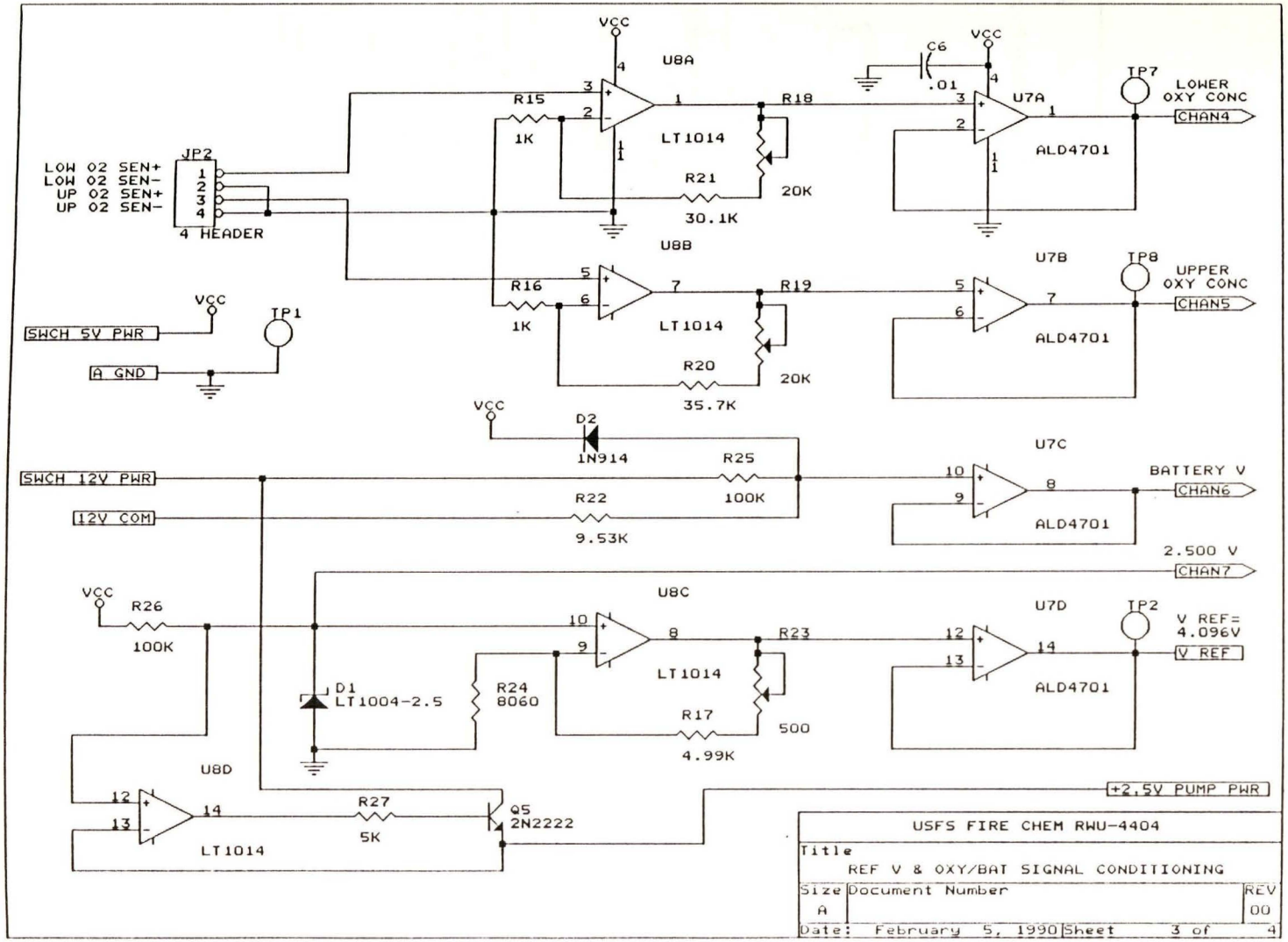

Figure A.2.1-5 Schematic diagram of the 0_2 signal conditioning circuits of the GODM.

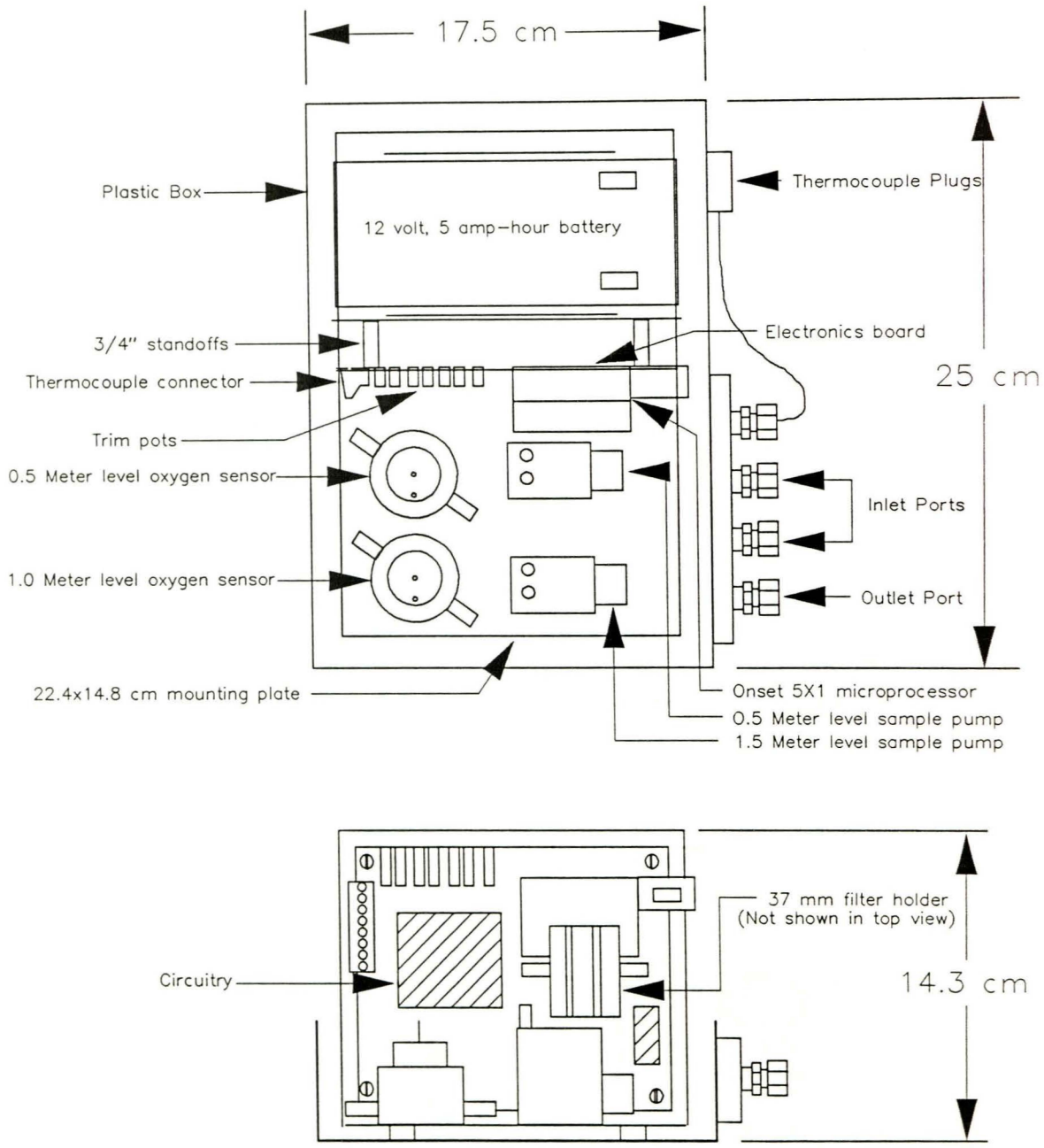

Figure A.2.3-1 Diagram of the physical layout of the GODM.

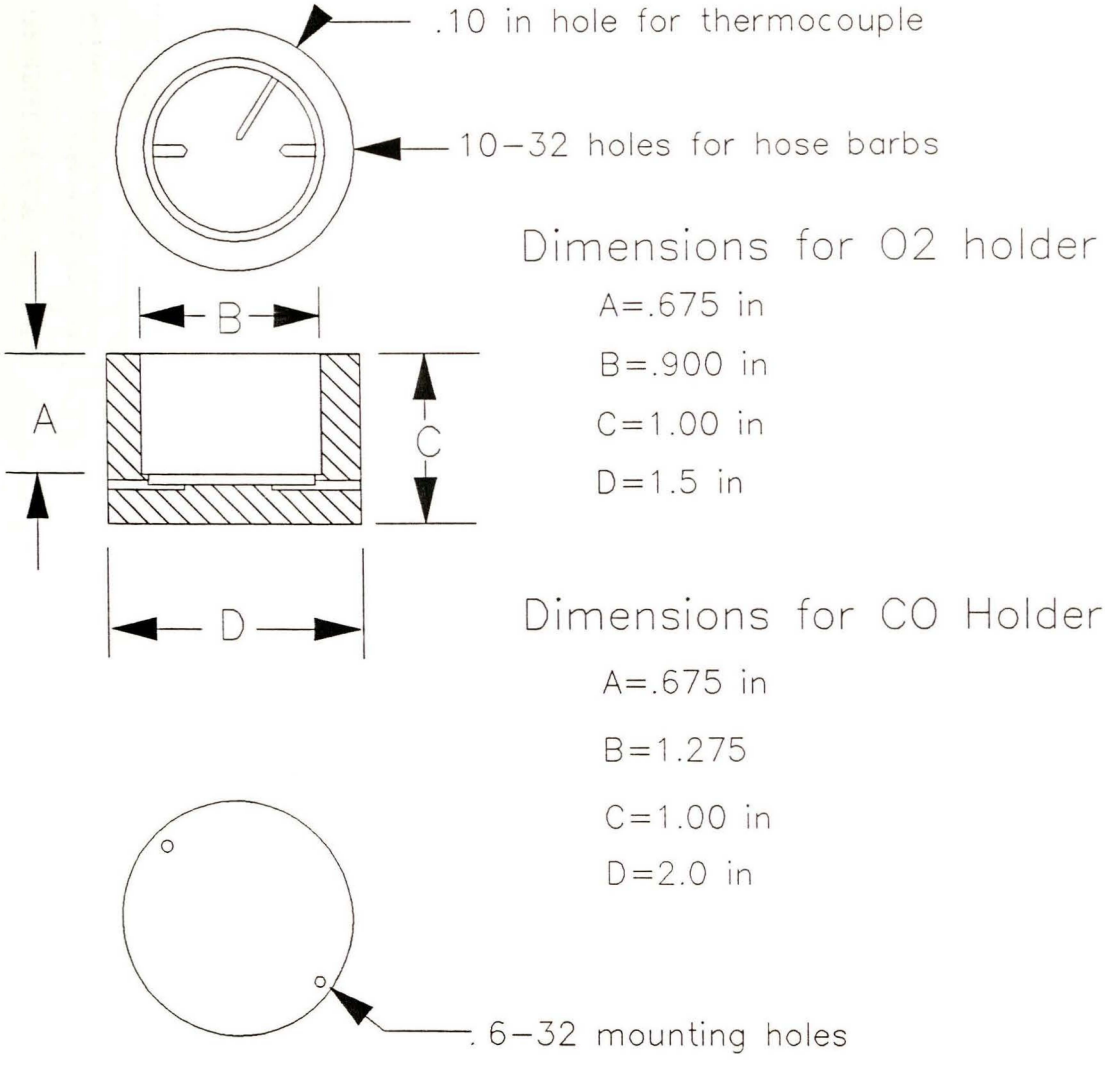

Figure A.2.3-2 Diagram of the 0_2 sensor housing used in the GODM.

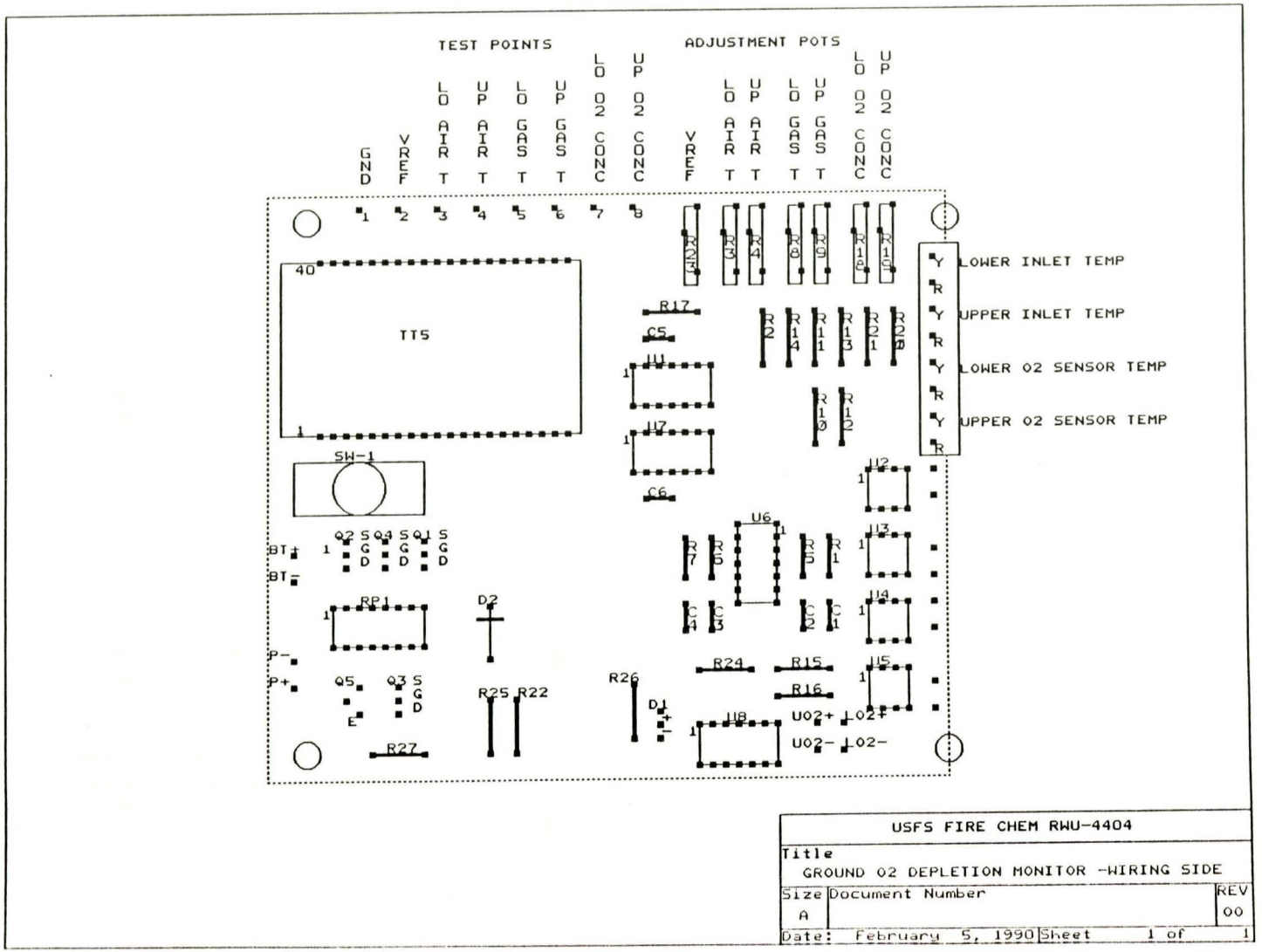

Figure A.2.3-3 Diagram of the layout of the circuit board used in the GODM.

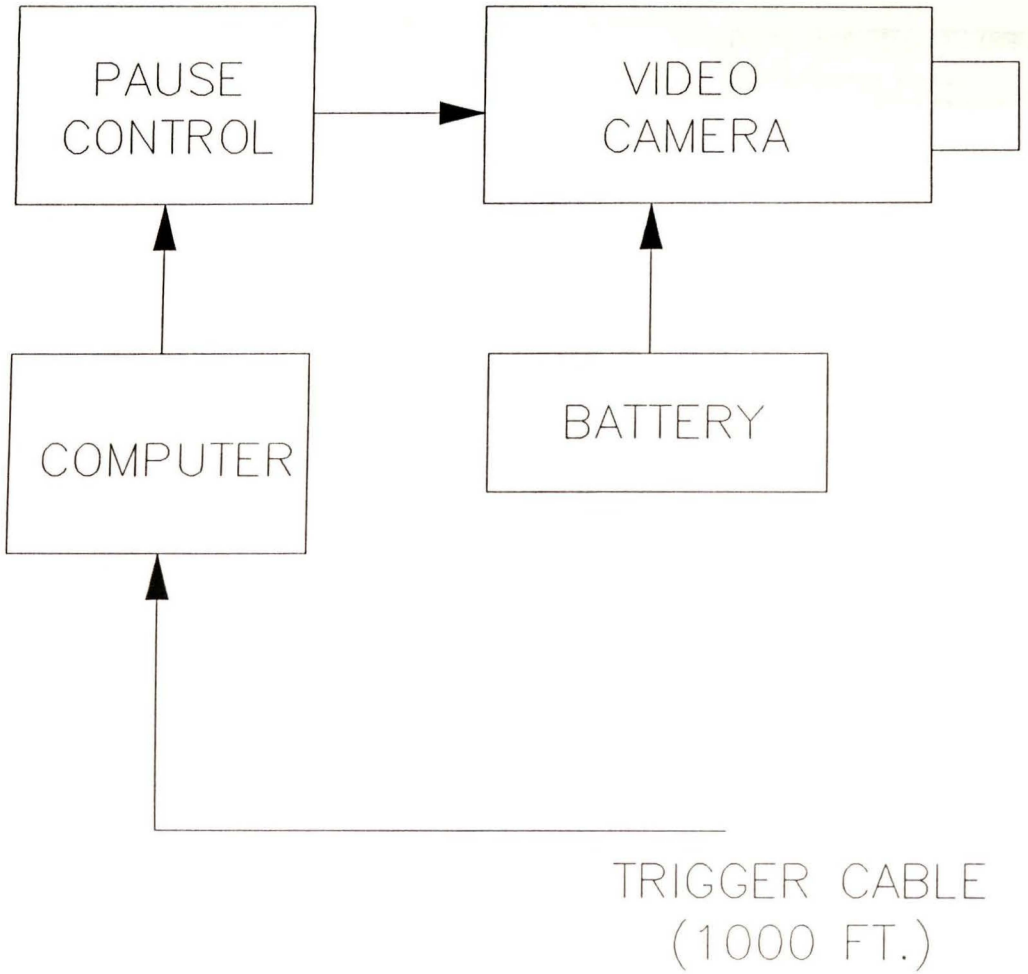

Figure A.3.0-1 Block diagram of the video camera and the VCC.

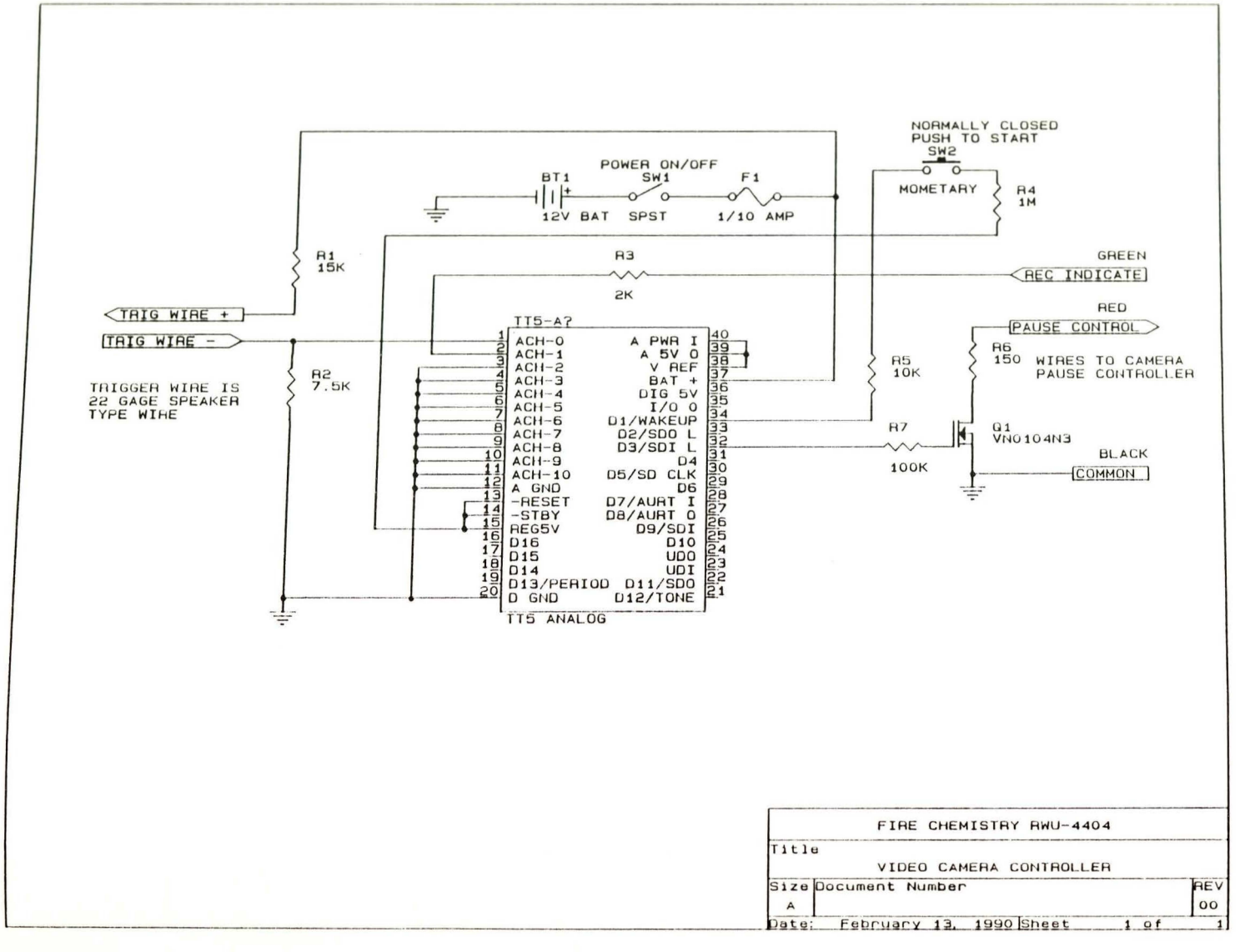

Figure A.3.0-2 Schematic diagram of the computer and support circuits of the VCC.

--- APPENDIX B ---

Computer Programs for Controlling Data Gathering for the Hill Fire

B.1 Introduction

All data acquisition systems deployed in the Hill PB contained battery powered microcomputers made by Onset Computer Corporation (the Tattletale model 5). These computers were programmed to sense the fire, read and store all parameters, and activate power supplies, pumps, valves, etc. This appendix contains listings of the programs developed for the tower mounted fire atmosphere sampling systems (FASS), the buried ground oxygen depletion monitors (GODM), the video camera aimed at the tower array during the fire, and the field mill atmospheric charge and lightning experiment.

The microcomputers interpret a special BASIC language, called TTBASIC. This language is specially designed for the data logger and is incompatible with other systems. The language is simple to program and is faster than more complete versions of BASIC. There are some language features that should be kept in mind when reading these programs. In particular, the language only supports four-byte integers, and variable names are the letters A to Z. One integer array, represented by @(n), is provided for up to 1024 elements. Some of the more important variable definitions are included at the start of the FASS and GODM programs. Special variables designated by '?' and '?(n)' are provided for dealing with time. A large data file is available to store other data, much like a ram disc. The FASS computer had a 1 Megabyte EPROM storage system while the other experiments had an added 128K of RAM. Many other features of the language are specific to the data logging function, and the Onset manual should be consulted for further information. Of particular interest is a SLEEP command that allows low power operation, and accurate timing during the experiment. Many examples of the SLEEP command are given in the programs.

The Tattletale system communicates with a more powerful host computer through an RS-232 link. We used a standard IBM PC with Microsoft QuickBASIC 4.0 to develop programs in TTBASIC. These control programs were transferred to the Tattletale before the experiment. A special feature of the transfer program allowed more descriptive line labels, and added line numbers at transfer time. These line labels were retained in the TTBASIC listing as remarks to note most program branch points (e.g. REM [TOWER PACKAGE START]). Other QuickBASIC programs were written to test the system functions, transfer data after the experiment, and perform preliminary data reduction. It is beyond the scope of this report to include these other special programs.

B.2 Control Program for Fire Atmosphere Sampling Systems (FASS)

'TWR00 - start of the tower package program
'@(0) - run counter set by quick basic
'@(1) - number of pre-flaming readings
'@(2) - number of flaming + intermediate readings
'@(3) - number of smoldering A readings
'@(4) - number of smoldering B readings

'@(5) - arm sec (all armed by basic)
'@(6) - arm min
'@(7) - arm hour
'@(8) - arm day
'@(9) - arm month
'@(10) - arm year
'@(11) - arm time in absolute ? format
'@(12) - fire approach time in ? format
'@(13) - fire trigger cause, 15 or 16

'@(19) - Analog reading time in ?-t0 format
'@(20) - Flame detection time, sec
'@(21) - Flame detection time, min
'@(22) - Flame detection time, hour
'@(23) - Flame detection time, day
'@(24) - Flame detection time, month
'@(25) - Flame detection time, year
'@(26) - External false triggers
'@(27) - Internal false triggers
'@(28) - Total false triggers detected

'@(30) - Init masks, set bit 0 '@(38) - Init masks, clear bit 0
'@(31) - Init masks, set bit 1 '@(39) - Init masks, clear bit 1
'@(32) - Init masks, set bit 2 '@(40) - Init masks, clear bit 2
'@(33) - Init masks, set bit 3 '@(41) - Init masks, clear bit 3
'@(34) - Init masks, set bit 4 '@(42) - Init masks, clear bit 4
'@(35) - Init masks, set bit 5 '@(43) - Init masks, clear bit 5
'@(36) - Init masks, set bit 6 '@(44) - Init masks, clear bit 6
'@(37) - Init masks, set bit 7 '@(45) - Init masks, clear bit 7

'@(47) - Value of S for current reading (to separate phases later)
'@(48) - Data reading time 2msbs
'@(49) - Data reading time 2lsbs
'@(50) - 3D wind E
'@(51) - 3D wind F
'@(52) - 3D wind G
'@(53) - 3D wind H
'@(54) - 2D wind E
'@(55) - 2D wind F
'@(56) - 2D wind G
'@(57) - PCLR 0, CHAN 0
'@(58) - PCLR 0, CHAN 1
'@(59) - PCLR 0, CHAN 2
'@(60) - PCLR 0, CHAN 3

```
'@(61) - PCLR 0, CHAN 4
'@(62) - PCLR 0, CHAN 5
'@(63) - PCLR 0, CHAN 6
'@(64) - PCLR 0, CHAN 7
'@(65) - PCLR 0, CHAN 8
'@(66) - PCLR 0, CHAN 9
'@(67) - PCLR 0, CHAN 10
'@(68) - PSET 0, CHAN 0
'@(69) - PSET 0, CHAN 1
'@(70) - PSET 0, CHAN 2
'@(71) - PSET 0, CHAN 3
'@(72) - PSET 0, CHAN 4
'@(73) - PSET 0, CHAN 5
'@(74) - PSET 0, CHAN 6
'@(75) - PSET 0, CHAN 7
'@(76) - PSET 0, CHAN 8, Bat test
'@(77) - PSET 0, CHAN 9, 2.5 V Ref
'@(78) - PSET 0, CHAN 10, Ground 0 V
'@(79) - END OF DATA FOR QSTOR =9999
'A - Debug flag
'B - Serial data out byte
'C - Canister valve flag: 0/not open; 1/filling; 2/full
'D - Data input from serial data input (temporary)
'E - 3D/2D wind speed, S/N = 0/1 ;3M
'F - 3D/2D wind speed, W/E = 0/1 ;6M
'G - 3D/2D wind speed, D/U = 0/1 ;9M
'H - set by basic (arm time in ? format ) find other var 3D wind direction
      bits
'I - for/next counter
'J - flaming length time in ? format (set by basic driver)
'K - code to indicate asm routines have been placed in memory (set only
      once)
'L - start of flaming + J (used during flaming only)
'M -
'N - Bit to be set or cleared in SDO byte
'O -
'P - Package number (set by basic driver)
'Q - Data transfer loop counter, return count for qstore sector
'R -
'S - Status of logger
' 0 -system not initialized
' 1 - Initialized, arm time defined but not armed
' 2 - System armed, ready to fire
' 3 - Flaming phase +intermediate phase (.5s readings)
' 4 - Smoldering phase .5s for 20 min, 2min for balance of memory
' 5 - Post fire, data is ready to download
'T - Time at start of program
'U -
'V -
'W -
'X - Data file pointer
'Y - Temporary time for internal delay
'Z - Length of data record in bytes
```

```
'Digital line assignments
' D0 (out) Data input control, A/B analog and SDI bank switch
' D1 (in ) Wake up! There's a fire.
' D2 (out) SDO latch
' D3 (in ) SDI latch
' D4 (out) Arm D1 to allow wake up or toggle on/off to reset
' D5 (out) SDO clock
' D6 (out) Everybody else wake up! I sensed a temperature trigger.
' D7 (in ) Aux UART in (from 1M memory EPROM)
' D8 (out) Aux UART out (to 1M memory EPROM)
' D9 (in ) SDI data line
' D10 (out) Analog power on, before any readings, pumps, etc
' D11 (out) SDO data line
' D12 (out) Canister 1 valve open
' D13 (out) Canister 2 valve open
' D14 (out) Canister 3 valve open
' D15 (in ) Temperature sensor detects a fire at your location!
' D16 (???) Unused

' Serial data out - each bit has a separate function ; uses var B
' lsb 0 undefined
' 1 Standard cal gas to air monitors
' 2 Teflon filter pump, gas sensors pump, CO2 sensor,(on in phase 4
      too)
' 3 Glass filter pump, gas bag pump
' 4 Phase 1 control, flaming valves
' 5 Phase 2 control, intermediate valves
' 6 Phase 3 control,smoldering valves
' msb 7 Phase 4 control, 4th valve on teflon filter manifold

'Time (?) array
'?(0) - seconds
'?(1) - minutes
'?(2) - hours
'?(3) - day
'?(4) - month
'?(5) - year


1600 REM [TOWER PACKAGE START]
1620 PRINT "Tower program started on package #",#3,P
1640 U=0:V=0:X=0
1660 @(79)=9999
1680 GOSUB 31800 : REM 31800=LOAD ASM
1690 GOSUB 31800 : REM 31800=LOAD ASM
1700 PCLR 0,2,5,6,10,12,13,14
1720 PSET 10 : B=0 :SDO B,8 : PCLR 10
1730 PSET 4 : PSET 8
1760 SLEEP 0 : SLEEP 200
1770 PRINT "Requesting module type from qstore"
1780 X=0: USEND 4800,"",\27,"d"; : UGET 4800,1,X,200
1790 M=0: IF X>0 X=0 : M=GET (X,#1)
1800 PRINT "Module type = ",#3,M
```

```
1810 IF M=0 PRINT "Qstore module not responding!! All data may be lost!",\7
1820 IF M=8 | M=1 PRINT "Qstore is responding normally."
1840 IF M=1 PRINT "Waiting for module to clear"
1850 IF M=1 X=0 : USEND 4800,"",\27,"mm"; : UGET 4800,1,X,2000
1860 X=0 : USEND 4800,"",\27,"{";
1870 Y=?
1880 REM [WAIT ERASE CHECK]
1890 PRINT "Erased module check time = ",(?-Y)/100
1900 UGET 4800,1,X,2000
1910 IF X=0 GOTO 1880 : REM 1880=WAIT ERASE CHECK
1920 X=0 : M=GET(X,#1)
1930 IF M=0 PRINT "Module is erased"
1940 IF M<>0 PRINT "Module is not erased!! Install a new one and reload ."
     :STOP
1950 GOSUB 6570 : REM 6570=SAVE ZERO SECTOR
1970 @(11)=H
1980 T = ?
2000 Z = 2*32
2010 X=0 : FOR I=0 TO 60*Z+200 STEP 4 : STORE X,#4,0 : NEXT I
2030 GOSUB 2180 : REM 2180=INIT MASKS
2050 A = 0
2080 REM [NORMAL RUN]
2090 IF S = 0 PRINT 'SYSTEM NOT INITIALIZED - - RETURN TO MAIN MENU' : STOP
2100 IF S = 1 GOSUB 2260 : REM LOOP UNTIL ARM TIME IS REACHED
     : REM 2260=WAIT ARM TIME
2110 IF S = 2 GOSUB 3000 : REM SYSTEM IS WAITING FOR A FIRE
     : REM 3000=WAIT FOR FIRE
2120 IF S = 3 GOSUB 7000 : REM FLAMING BURN IN PROGRESS
     : REM 7000=START FLAMING
2130 IF S = 4 GOSUB 9000 : REM SMOLDERING BURN IN PROGRESS
     : REM 9000=START SMOLDERING
2140 IF A=1 & S = 5 PRINT 'SYSTEM HAS FIRE DATA- OFF LOAD OR QUIT'
2150 IF S = 5 GOTO 10000 : REM 10000=STOP TAKING DATA
2160 GOTO 2080 : REM LOOP FOREVER,<CNTRL-C> STOPS IT : REM 2080=NORMAL RUN
2180 REM [INIT MASKS]
2200 @(30)=1 :@(31)=2 :@(32)=4:@(33)=8: @(34)= 16:@(35)=32:@(36)=64
     :@(37)=128
2210 FOR I=0 TO 7
2220 @(38+I)=255-@(30+I)
2230 NEXT I
2240 RETURN
2260 REM [WAIT ARM TIME]
2270 PCLR 4 : REM ALLOW TRIGGER AND COUNT FALSE TRIGGERS
2290 SLEEP 0
2300 REM [WAIT ARM LOOP]
2310 IF A = 1 | A=0 PRINT "SEC FROM START = ",(?-T)/100,
     " SEC TO ARM TIME = ",(H-?)/100
2320 GOSUB 2400 : REM 2400=CHECK TRIGGER
2330 IF ? < H SLEEP 200 : GOTO 2300 : REM 2300=WAIT ARM LOOP
2350 S = 2 : REM SYSTEM IS ARMED
2360 PRINT 'SYSTEM ARMED'
2370 PRINT "FALSE TRIGGERS: Temp, External, Total = ",#5,@(27),@(26),@(28)
2380 RETURN
```

```
2400 REM [CHECK TRIGGER]
2420 IF PIN(1)=0 GOTO 2530 : REM 2530=END TRIGGER CHECK
2430 @(28)=@(28)+1
2450 IF PIN(16)=1 @(26)=@(26)+1
2460 IF PIN(15)=1 @(27)=@(27)+1
2480 PRINT "Total false trg = ",@(28)
2490 PRINT "False external trg = ",@(26)
2500 PRINT "False temp trg = ",@(27)
2510 PRINT "*** FIX THE SOURCE OF THE TRIGGERS!! ***",\7
2520 PSET 4 : PCLR 4 : REM ENABLE TRIGGER AGAIN
2530 REM [END TRIGGER CHECK]
2540 RETURN
3000 REM [WAIT FOR FIRE]
3010 PSET 4 : REM DISABLE TRIGGER
3020 X = 60*Z +200 : REM FIRST CAL POINT AT END OF PRE-BURN DATA
3030 @(12) = ? : REM ACTUAL 0 TIME AT START OF FIRST CAL (JUST ARMED)
3040 S=20 : GOSUB 4000 :S=2 : REM 4000=SENSOR CALIBRATION
3080 REM [TIME SYNC]
3090 RTIME
3100 IF ?(0) <> I I = ?(0) : IF A = 1 PRINT "Sync time ", ?(0)
3110 IF ?(0) <> 0 GOTO 3080 : REM 3080=TIME SYNC
3140 PRINT 'SYSTEM WAITING FOR A FIRE'
3150 PCLR 4
3160 SLEEP 0
3170 REM [WAIT FOR FIRE LOOP]
3180 SLEEP 200
3190 RTIME
3200 F=0
3210 IF A=0 & (?(2)<12 | ?(2)>=19) GOSUB 2400 : GOTO 3170
       : REM 2400=CHECK TRIGGER : REM 3170=WAIT FOR FIRE LOOP
3220 IF A=0 & PIN(1)=1 GOSUB 3430 :PSET 4 : PCLR 4 : REM 3430=VERIFY TRIGGER
3230 IF A=1 & @(1) > 5 GOTO 3310 : REM 3310=FIRE DETECTED
3240 IF F<>0 @(13)=F :PSET 4: GOTO 3310 : REM 3310=FIRE DETECTED
3250 IF A=1 PRINT "Pre-fire reading time ",#6,(?-@(12))/100,".",#2,
       (?-@(12))%100
3270 IF A = 0 & ?(1)%2 = 0 GOSUB 4280 : GOTO 3170 : REM 4280=GET BASELINE
       : REM 3170=WAIT FOR FIRE LOOP
3280 IF A = 1 & ?(1)%1 = 0 GOSUB 4280 : GOTO 3170 : REM 4280=GET BASELINE
       : REM 3170=WAIT FOR FIRE LOOP
3290 GOTO 3170 : REM 3170=WAIT FOR FIRE LOOP
3310 REM [FIRE DETECTED]
3340 IF @(13)<>16 PSET 6
3360 B=0 : SDO B,8
3370 S = 3 : @(12) = ? : RTIME : REM FIRE APPROACHING, SET TIME (@(12))
3380 FOR I= 0 TO 5 : @(20+I)=?(I) : NEXT I : REM SAVE FLAMING TIME
3390 IF A = 1 PRINT "Fire approaching at ";
3400 IF A = 1 PRINT ?(2),":",?(1),":",?(0)," on ",?(4),"/",?(3),"/",?(5)
3410 RETURN
3430 REM [VERIFY TRIGGER]
3440 Y=?
3450 IF PIN(16)=1 F=16 : GOSUB 3560 : RETURN : REM 3560=CHECK L TRIGGER
3460 GOSUB 3490 : REM 3490=CHECK T TRIGGER
3470 RETURN
```

```
3490 REM [CHECK T TRIGGER]
3500 PSET 10 : PCLR 0
3510 IF (?-Y)<10 GOTO 3490 : REM 3490=CHECK T TRIGGER
3520 F=CHAN(10)
3530 IF F<610 F=0 :REM MUST HAVE BEEN A SPIKE
3540 RETURN
3560 REM [CHECK L TRIGGER]
3570 IF PIN(16)=0 F=0 : RETURN
3580 IF (?-Y)<100 GOTO 3560 : REM 3560=CHECK L TRIGGER
3590 RETURN
4000 REM [SENSOR CALIBRATION]
4010 PRINT 'Calibrating sensors'
4020 PSET 10 : GOSUB 4210 : REM POWER ON : REM 4210=DELAY 1
4030 N=1 : GOSUB 5220 : REM CAL GAS SOURCE VALVE : REM 5220=SETBIT
4040 N=7 : GOSUB 5220 : REM OPEN 4TH VALVE ON TEFLON MANIFOLD : REM 5220=SETBIT
4050 N=2 : GOSUB 5220 : REM TURN ON THE TEFLON FILTER PUMP + SENSOR PUMP + CO2
     : REM 5220=SETBIT
4060 SDO B,8
4070 Y=?
4080 IF A=1 PRINT "starting wait loop"
4090 REM [WAIT TILL STABLE]
4110 IF ? < Y+6000 GOTO 4090 : REM 4090=WAIT TILL STABLE
4120 @(1)=0 : GOSUB 5150 :SLEEP 0 : REM 5150=ZERO WIND COUNT
4130 REM [CAL LOOP]
4140 SLEEP 50
4150 @(1)=@(1)+1 :GOSUB 6000 : GOSUB 6200 : REM 6000=GET DATA
     : REM 6200=STORE DATA
4160 IF @(1)<10 GOTO 4130 : REM 4130=CAL LOOP
4170 @(1)=0
4180 B=0 : SDO B,8
4190 RETURN
4210 REM [DELAY 1]
4230 Y=?
4240 REM [DELAY LOOP]
4250 IF ?-Y < 1 GOTO 4240 : REM 4240=DELAY LOOP
4260 RETURN
4280 REM [GET BASELINE]
4290 IF ?(0)=2 GOSUB 4330 : REM 4330=BASELINE ON
4300 IF ?(0)=32 GOSUB 5000 : REM 5000=SAVE BASELINE
4310 RETURN
4330 REM [BASELINE ON]
4340 PRINT "Analog Power is on"
4350 PSET 10 : GOSUB 4210 : REM 4210=DELAY 1
4360 N=7 : GOSUB 5220 : REM OPEN 4TH VALVE ON TEFLON MANIFOLD : REM 5220=SETBIT
4370 N=2 : GOSUB 5220 : REM TURN ON TEFLON FILTER PUMP + SENSOR PUMP + CO2
     : REM 5220=SETBIT
4380 SDO B,8 : REM TURN ON HERE
4390 RETURN
5000 REM [SAVE BASELINE]
5010 X = (@(1)%60)*Z+200 : REM WRAP AROUND LAST 60 READINGS (2 HR)
5020 PRINT " Baseline stored at x =",#6,X
5040 GOSUB 5150 : REM 5150=ZERO WIND COUNT
5050 Y=?
```

```
5060 REM [WIND0 DELAY]
5070 IF ?<Y+50 GOTO 5060 : REM 5060=WIND0 DELAY
5090 GOSUB 6000 : REM 6000=GET DATA
5100 GOSUB 6500 : @(1)=@(1)+1 : REM 6500=STORE BASELINE DATA
5110 B=0 : SDO B,8 : PCLR 10
5120 PRINT "Analog power off"
5130 RETURN
5150 REM [ZERO WIND COUNT]
5170 PCLR 0 : D=SDI (24)
5180 PSET 0 : D=SDI (32) : PCLR 0
5190 RETURN
5220 REM [SETBIT]
5240 B = B | @(N+30)
5250 RETURN
5270 REM [CLRBIT]
5290 B = B & @(N+38)
5300 RETURN
5320 REM [CALC 3D WIND]
5340 D = 0 : E = 0 : F = 0 : G = 0 : H = 0
5350 PSET 0 : REM TURN ON 3D (2D IS OFF)
5360 D = SDI(32) : REM BRING IN 3D DATA
5370 CALL &H7320, 0 : REM CONVERT 3D DATA
5380 RETURN
5400 REM [CALC 2D WIND]
5420 D = 0 : E = 0 : F = 0 : G = 0 : H = 0
5430 PCLR 0 : REM TURN ON 2D (3D IS OFF)
5440 D=SDI(24) : REM BRING IN 2D DATA
5450 CALL &H112,0 : REM CONVERT 2D DATA
5460 RETURN
6000 REM [GET DATA]
6010 @(47)=S
6020 @(19) = ?-@(12)
6030 @(49) = @(19) : @(48)=@(49)/256/256
6050 GOSUB 5320 : REM 5320=CALC 3D WIND
6060 @(50)=E : @(51)=F : @(52)=G : @(53)=H : REM DIRECTION BITS ARE PACKED
6070 GOSUB 5400 : REM 5400=CALC 2D WIND
6080 @(54)=E : @(55)=F : @(56)=G
6090 PCLR 0
6100 FOR I=0 TO 10
6110 @(57+I)=CHAN(I)
6120 NEXT I
6130 PSET 0
6140 FOR I=0 TO 10
6150 @(68+I)=CHAN(I)
6160 NEXT I
6180 RETURN
6200 REM [STORE DATA]
6210 Q=0 : CALL &H72C2,0 : REM QSTOR MOVES FROM @() TO DATA FILE X=0
6240 X=0 : USEND 4800,Q,X
6250 IF A=1 PRINT "STO t = ", #12, ?-@(12)
6260 RETURN
6500 REM [STORE BASELINE DATA] ' Sub to store data for 1 scan to data file
6510 IF A=1 | A=0 PRINT "Storing time = ",#12,?-@(12)," at X = ",X
```

```
6520 FOR I=47 TO 78
6530 STORE X,#2,@(I)
6540 NEXT I
6550 RETURN
6570 REM [SAVE ZERO SECTOR]
6590 @(47)=0 :REM NO STATUS
6600 @(48)=@(0):@(56)=@(0) :REM RUN COUNTER DOUBLE STORAGE
6610 @(49)=P : @(57)=P :REM PACKAGE NUMBER
6620 FOR I= 5 TO 10
6630 @(45+I)=@(I)
6640 NEXT I
6650 GOSUB 6200 : REM 6200=STORE DATA
6660 RETURN
6680 REM [SAVE FIRE PARAMETERS]
6700 @(47)=31 : REM CODE FOR FIRE PARAMETERS
6710 @(48)=(@(12)-@(11))/256/256 :@(49)=@(12)-@(11) :REM TIME FROM ARM TO
     FLAMES
6720 FOR I=20 TO 27
6730 @(30+I)=@(I)
6740 NEXT I
6750 @(58)=@(1) :@(59)=@(2) :@(60)=@(3)
6760 @(61)=@(13)
6770 FOR I=62 TO 78 : @(I)=0 : NEXT I
6780 SLEEP 50 :REM DONT OVERRUN QSTOR
6790 GOSUB 6200 : REM 6200=STORE DATA
6800 RETURN
6830 REM [SAVE BASELINE DATA]
6840 V=0
6850 IF @(1) > 60 V=@(1)-60
6860 FOR W= V TO @(1)-1
6870 SLEEP 50
6880 X=(W%60)*Z+200
6890 FOR I=1 TO 32
6900 @(I+46)=GET (X,#2)
6910 NEXT I
6920 GOSUB 6200 : REM 6200=STORE DATA
6930 NEXT W
6940 RETURN
7000 REM [START FLAMING]
7030 IF A=1 | A=0 PRINT 'Starting flaming phase'
7040 PSET 10 : REM TURN A.2D AND PUMPS
7050 L = J + 60000 + ? : REM SET L = END TIME OF FLAMING PHASE
7060 X = (60+1)*Z : REM SAVE SPACE FOR 60 BASELINE READINGS
7070 GOSUB 5150 : REM 5150=ZERO WIND COUNT
7080 PSET 4 : REM INHIBIT TRIGGER WAKEUP
7090 N=0 : GOSUB 5220 : REM GAS BAG PUMP : REM 5220=SETBIT
7100 N=2 : GOSUB 5220 : REM TEFLON FILTER PUMP ON + SENSOR PUMP + CO2
     : REM 5220=SETBIT
7110 N=3 : GOSUB 5220 : REM GLASS FIBER FILTER PUMP ON : REM 5220=SETBIT
7120 N=4 : GOSUB 5220 : REM FLAMING PHASE VALVES ON : REM 5220=SETBIT
7130 SDO B,8
7160 Y=?+36000 : C=0
7180 REM [FLAMING LOOP]
```

```
7190 IF A=0 SLEEP 50
7200 IF A=1 SLEEP 600
7220 IF S=3 & C=0 & @(62)>250 PSET 12 : C=1 : S=32 : Y=?+3000
     :IF A=0 PRINT "FILL CAN 12 T"
7230 IF S=3 & C=0 & ?>Y PSET 12 : C=1 : S=32 : Y=Y+3000
     :IF A=0 PRINT "FILL CAN 12 Y"
7240 IF S=32 & C=1 & ?>Y PCLR 12 : C=2 : S=3 : IF A=0 PRINT "FILL 12 OFF"
7260 IF S=30 & C=0 & ?>Y PSET 13 : C=1 : S=33 : Y=Y+3000
     : IF A=0 PRINT "FILL CAN 13"
7270 IF S=33 & C=1 & ?>Y PCLR 13 : C=2 : S=30 : IF A=0 PRINT "CAN 13 OFF"
7280 GOSUB 6000 : REM 6000=GET DATA
7290 IF A=1 & @(2)%10=0 PRINT "STORING ",@(2)," AND ",(L-?)/100," SECONDS TO
     GO"
7300 GOSUB 6200 : @(2)=@(2)+1 : REM 6200=STORE DATA
7310 IF A=1 & @(2) = 20 GOSUB 8000 : REM 8000=START INTERMEDIATE
7320 IF S=3 & ?>(L-60000) GOSUB 8000 : REM 8000=START INTERMEDIATE
7330 IF A=1 & @(2) = 40 S=4 : RETURN
7340 IF ? < L GOTO 7180 : REM 7180=FLAMING LOOP
7350 S = 4 : REM END OF FLAMING TIME REACHED
7360 RETURN
8000 REM [START INTERMEDIATE]
8020 S=30
8030 N=4 : GOSUB 5270 : REM FLAMING PHASE VALVE OFF : REM 5270=CLRBIT
8040 N=5 : GOSUB 5220 : REM INTERMEDIATE PHASE VALVE ON : REM 5220=SETBIT
8050 SDO B,8
8060 PRINT "INTERMEDIATE PHASE STARTED"
8080 Y=?+18000 : C=0
8090 RETURN
9000 REM [START SMOLDERING]
9030 N=5 : GOSUB 5270 : REM FLAMING VALVES OFF : REM 5270=CLRBIT
9040 N=6 : GOSUB 5220 : REM SMOLDERING VALVES ON : REM 5220=SETBIT
9050 N=1 : GOSUB 5220 : REM START WITH SENSOR CAL CHECK (WHILE BAGS FILL)
     : REM 5220=SETBIT
9060 SDO B,8
9080 Y = ? + 6000: C=0 : S=40
9090 L = L + 120000 : REM 20 MIN SMOLDERING PHASE SAMPLE
9100 PRINT 'STARTING SMOLDERING PHASE A: CAL ON'
9120 REM [SMOLDERING LOOP A]
9130 IF A=0 SLEEP 50
9140 IF A=1 SLEEP 600
9160 IF S=4 & C=0 & ?>Y PSET14 : C=1 : S=42 : Y=Y+3000
     : IF A=0 PRINT "FILL CAN 14"
9170 IF S=42 & C=1 & ?>Y PCLR14 : C=2 : S=4 : IF A=0 PRINT "CAN 14 OFF"
9180 GOSUB 6000 : REM 6000=GET DATA
9200 IF S=40 & ?>Y N=1 : GOSUB 5270 : SDO B,8 : S=4 : Y=Y+12000
     :IF A=0 PRINT "CAL OFF" : REM 5270=CLRBIT
9210 IF A=1 & @(3)%10=0 PRINT "STORING ",@(3)," AND ",(L-?)/100," SECONDS TO GO"
9220 GOSUB 6200 : @(3)=@(3)+1 : REM 6200=STORE DATA
9230 IF A=1 & @(3) = 20 GOTO 9250 : REM 9250=END OF SMOLDER A
9240 IF ? < L GOTO 9120 : REM 9120=SMOLDERING LOOP A
9250 REM [END OF SMOLDER A]
9260 B=0 : SDO B,8 : PCLR 10 : REM ALL OFF
9270 GOSUB 6680 : REM 6680=SAVE FIRE PARAMETERS
```

```
9280 GOSUB 6830 : REM 6830=SAVE BASELINE DATA
9300 S=41
9340 REM [SMOLDERING LOOP B]
9350 PRINT "Start smolder B"
9370 FOR I=1 TO 10
9380 IF A=0 SLEEP 900 : REM LOOP 1.5 MINUTES WHEN IN FIRE
9390 IF A=1 SLEEP 90 : REM LOOP 9.0 SECONDS WHEN DEBUGGING
9400 NEXT I
9410 PSET 10 : REM TURN ON A.2D
9420 N=2 : GOSUB 5220 : REM TEFLON PUMP ON + OTHER SENSORS : REM 5220=SETBIT
9430 N=7 : GOSUB 5220 : REM PHASE 4 VALVE OPEN : REM 5220=SETBIT
9440 SDO B,8 : REM DO IT
9450 IF A=0 SLEEP 3000 : REM WAIT 30 SEC WHEN IN FIRE
9460 IF A=1 SLEEP 600 : REM WAIT 6 SECONDS WHEN DEBUGGING
9470 GOSUB 6000 : REM 6000=GET DATA
9480 IF A=1 PRINT "STORING ",@(4)," AT END + ",(?-L)/100," SECONDS"
9490 GOSUB 6200 : @(4)=@(4)+1 : REM 6200=STORE DATA
9500 B=0 : SDO B,8 : PCLR 10 : REM ALL OFF
9510 IF A=1 & @(4) <= 10 GOTO 9340 : REM DEBUGGING : REM 9340=SMOLDERING LOOP B
9520 IF A=0 & @(76) >= 190 & @(4) <= 300 GOTO 9340 : REM IN FIRE
     : REM 9340=SMOLDERING LOOP B
9530 S = 5
9540 RETURN

10000 REM [STOP TAKING DATA]
10010 IF A=1 PRINT 'DONE TAKING DATA'
10030 PSET 4 : B=0 : SDO B,8 : PCLR 10
10040 IF A=1 PRINT 'GOING INTO DEEP SLEEP'
10050 W = X
10060 REM [SLEEP]
10080 SLEEP 500 : ITEXT X, 0 : IF W = X GOTO 10060 : REM 10060=SLEEP
10090 IF A=1 & S=5 PRINT 'SYSTEM HAS FIRE DATA -- OFF LOAD OR QUIT'
10100 STOP

30000 REM [SEND DATA]
30020 @(79)=9999 : GOSUB 30340 : REM 30340=INIT PRINT DATA
30030 GOSUB 30430 : REM 30430=GET NEXT SECTOR
30040 PRINT "TOWER PACKAGE DATA"
30050 PRINT "PACKAGE NUMBER ",@(49)
30060 PRINT "FLAMING SAMPLE TIME (.01 SEC) ",60000
30070 PRINT "FLAMES DETECTED ?? SECONDS AFTER ARM TIME."
30080 PRINT "TRANSFERRING THE RUN NUMBER"
30090 PRINT #4,@(48)
30100 @(48)=0 :REM SO FIRST TIME CALC WILL BE THE ARM TIME SEC
30130 REM [PRINT SECTOR LOOP]
30140 IF @(47)>255 GOTO 30180 : REM 30180=SEND DATA END
30150 GOSUB 30220 : REM 30220=PRINT SECTOR
30160 GOSUB 30430 : REM 30430=GET NEXT SECTOR
30170 GOTO 30130 : REM STATUS SHOULD BE <255 : REM 30130=PRINT SECTOR LOOP
30180 REM [SEND DATA END]
30190 PRINT "**END OF DATA**"
30200 GOTO 10000 : REM 10000=STOP TAKING DATA
30220 REM [PRINT SECTOR]
```

```
30240 PRINT #4,@(47);
30250 IF @(48)>&H7FFF PRINT #10,0;:GOTO 30270 : REM 30270=SKIP TIME
30260 PRINT #10,@(48)*256*256+@(49);
30270 REM [SKIP TIME]
30280 FOR I=50 TO 79
30290 PRINT #5,@(I);
30300 NEXT I
30310 PRINT ""
30320 RETURN
30340 REM [INIT PRINT DATA]
30350 PSET 8 : PSET 10
30370 SLEEP 0 : SLEEP 200
30380 X=0: USEND 4800,"",\27,"s",\0,\0; : UGET 4800,1,X,200
30390 M=0
30400 IF X>0 X=0:M= GET (X,#1)
30410 RETURN
30430 REM [GET NEXT SECTOR]
30440 X=0: USEND 4800,"",\27,"I";
30450 UGET 4800,133,X,200
30460 X=0
30470 S=GET(X,#1)*256+GET(X,#1) :REM SECTOR NUMBER
30480 M=GET(X,#1)
30490 P=GET(X,#1)
30500 C=GET(X,#1)
30520 FOR I=1 TO 32
30530 @(46+I)=GET(X,#2)
30540 NEXT I
30550 RETURN

31800 REM [LOAD ASM]
31810 Y=&H72C2
31840 ASM Y, LDX #&H4000 ;STX &H72BC
31860 ASM Y, LDX #&H7002-47*4 ;STX &H72BE
31880 ASM Y, LDAA #33; STAA &H72C0; CLR &H72C1
31890 X=Y
31900 ASM Y, LDX &H72BE; LDD 0,X; DEX; DEX; DEX; DEX; STX &H72BE
31920 ASM Y, LDX &H72BC; STAA 0,X;INX
31940 ASM Y, CMPA #27; BNE U
31960 ASM Y, STAA 0,X ; INX
31980 U=Y
31990 ASM Y, STAB 0,X;INX
32000 ASM Y, CMPB #27 ; BNE V
32010 ASM Y, STAB 0,X;INX
32020 V=Y
32040 ASM Y, STX &H72BC
32060 ASM Y, DEC &H72C0; BNE X
32070 ASM Y, LDX &H72BC; LDAA #27; STAA 0,X; INX
32080 ASM Y, LDAA #&H6A; STAA 0,X; INX
32090 ASM Y, STX &H72BC; LDD &H72BC; SUBD #&H4000
32110 ASM Y, STD &H7006+4*16
32120 ASM Y, RTS
32160 Y=&H7320
32180 ASM Y, LDAA &H7013
```

```
32190 ASM Y, STAA &H7017
32210 ASM Y, LDAA &H7012
32220 ASM Y, STAA &H701B
32240 ASM Y, LDAA &H7011
32250 ASM Y, STAA &H701F
32270 ASM Y, LDAA &H7010; TAB
32290 ASM Y, ANDA #&H7; STAA &H7023
32310 ASM Y, TBA; ANDA #&H8
32320 ASM Y, LSRA; LSRA; LSRA; STAA &H7016
32340 ASM Y, TBA; ANDA #&H10
32350 ASM Y, LSRA; LSRA; LSRA; LSRA; STAA &H701A
32370 ASM Y, TBA; ANDA #&H20
32380 ASM Y, LSRA; LSRA; LSRA; LSRA; LSRA; STAA &H701E
32390 ASM Y, RTS
32440 Y = &H112
32460 ASM Y, LDAA &H7013
32470 ASM Y, STAA &H7017
32490 ASM Y, LDAA &H7012
32500 ASM Y, STAA &H701B
32520 ASM Y, LDAA &H7011
32530 ASM Y, STAA &H701F
32540 ASM Y, RTS
32550 RETURN
```

B.3 Control Program for the Ground Oxygen Depletion Monitors (GODM)

```
'@ variable definitions

'@(0) -run counter set by quick basic
'@(1) -number of pre-flaming readings
'@(2) -number of flaming readings
'@(3) -number of smoldering readings

'@(5) -arm sec
'@(6) -arm min
'@(7) -arm hour
'@(8) -arm day
'@(9) -arm month
'@(10) -arm year

'@(11) -raw lower inlet temp
'@(12) -raw upper inlet temp
'@(13) -raw lower O2 sensor temp
'@(14) -raw upper O2 sensor temp
'@(15) -raw lower O2 conc
'@(16) -raw upper O2 conc
'@(17) -raw pump voltage
'@(18) -raw reference voltage

'@(19) -time of reading in ? format

'@(20) -start of flaming sec
'@(21) -start of flaming min
'@(22) -start of flaming hours
'@(23) -start of flaming day
'@(24) -start of flmaing month
'@(25) -start of flaming year

'A -analog channel for next counter
'B -
'C -
'D -DEBUGGING flag
'E -
'F -fire approaching time in ? format
'G -
'H -arm time in ? format
'I -for/next counter
'J -flaming length time in ? format, set by BASIC
'K -
'L -start of flaming + J
'M -
'N -for/next counter, smoldering times
'O -
'P -package number, set by BASIC
'Q -data transfer loop counter
'R -
```

```
'S -status of logger
' 0 -system not initialized
' 1 -initialized, arm time defined but not armed
' 2 -system armed, ready to fire
' 3 - flaming phase with active data collection
' 4 -smoldering phase data every 1/10 min
' 5 -post fire, is ready to be downloaded
'T -time at start of program
'U -
'V -prefire sample start pointer
'W -data file index pointer (to test for text input from host after fire)
'X -data file pointer
'Y -temporary time for internal delay
'Z -length of data record in bytes

'Digital line assignments
'D14 pset 14 = pump on
' pclr 14 = pump off
'D15 pset 15 = A.2D stuff on
' pclr 15 = A.2D stuff off

'Time (?) array
'?(0) -seconds
'?(1) -minutes
'?(2) -hours
'?(3) -day
'?(4) -month
'?(5) -year


1000 ASM &H9A, DW 2,0 : REM MAXIMIZES THE DATAFILE SIZE
1010 T = ? : Z = 4+2*8 : REM TIME + 8 CHAN
1020 X=0 : FOR I=0 TO 60*Z STEP 2 : STORE X,#2,0 : NEXT I : REM INIT MEMORY
1030 D = 0 : REM DEBUG FLAG IS ON
1050 REM [NORMAL RUN]
1060 IF S = 0 PRINT 'SYSTEM NOT INITIALIZED - - RETURN TO MAIN MENU' : STOP
1070 IF S = 1 GOSUB 2000 : REM LOOP UNTIL ARM TIME IS REACHED
          : REM 2000=WAIT ARM TIME
1080 IF S = 2 GOSUB 3000 : REM SYSTEM IS WAITING FOR A FIRE
          : REM 3000=WAIT FOR FIRE
1090 IF S = 3 GOSUB 7000 : REM FLAMING BURN IN PROGRESS
          : REM 7000=START FLAMING
1100 IF S = 4 GOSUB 8000 : REM SMOLDERING BURN IN PROGRESS
          : REM 8000=START SMOLDERING
1110 IF D=1 & S = 5 PRINT 'SYSTEM HAS FIRE DATA- OFF LOAD OR QUIT'
1120 IF S = 5 PCLR 14, 15 : GOTO 9000 : REM 9000=STOP TAKING DATA
1130 GOTO 1050 : REM 1050=NORMAL RUN
2000 REM [WAIT ARM TIME]
2010 REM S=1 >> LOOP UNTIL ARM TIME IS REACHED
2020 IF D = 1 PRINT "SECONDS FROM START = ",(?-T)/100
2030 IF D = 1 PRINT "SECONDS TO ARM TIME = ",(H-?)/100
2040 IF ? < H SLEEP 200 : GOTO 2000 : REM 2000=WAIT ARM TIME
2050 S = 2 : REM SYSTEM IS ARMED
```

```
2060 IF D = 1 PRINT 'SYSTEM ARMED'
2070 REM GET PROGRAM IN SYNC TO SAMPLE ON THE SECOND
2080 REM WAITING FOR ARM TIME WILL ONLY GET TO NEAREST 2 SEC
2090 REM [TIME SYNC]
2100 RTIME
2110 IF ?(0) <> I I = ?(0) : IF D = 1 PRINT "Sync time ", ?(0)
2120 IF ?(0) <> 0 GOTO 2090 : REM 2090=TIME SYNC
2130 RETURN
3000 REM [WAIT FOR FIRE]
3010 REM S=2 >> WAITING FOR A FIRE
3020 REM NOW LOOP UNTIL ONE OF AIR PROBES > 65 DEG. C
3030 IF D = 1 PRINT 'SYSTEM WAITING FOR A FIRE'
3040 SLEEP 0 : F = ?
3050 REM [WAIT FOR FIRE LOOP]
3060 SLEEP 200 : RTIME
3070 REM OFF BETWEEN 10 PM AND 10 AM
3080 IF D = 0 & (?(2) < 10 | ?(2) >= 22) GOTO 3050
        : REM 3050=WAIT FOR FIRE LOOP
3090 REM DURING DAY TIME HOURS GO ON TO COLLECT PRE-FIRE DATA
3100 PSET 15 : GOSUB 6070 : REM TURN ON A.2D - WAIT 10MS : REM 6070=DELAY 1
3110 GOSUB 5000 : REM 5000=GET DATA
3120 IF D = 1 & ?(0)=0 PRINT "Pre-fire time ",#6,(?-F)/100,".",#2,(?-F)%100
3130 REM START PUMP EVERY 2 MIN DURING FLAMING (1 MIN DURING DEBUGGING)
3140 IF D = 0 & ?(1)%2 = 0 GOSUB 4000 : GOTO 3170 : REM 4000=GET BASELINE
        : REM 3170=END WAIT CHECK
3150 IF D = 1 & ?(1)%1 = 0 GOSUB 4000 : GOTO 3170 : REM 4000=GET BASELINE
        : REM 3170=END WAIT CHECK
3160 PCLR 15 : REM ELSE JUST CHECK FIRE SENSORS
3170 REM [END WAIT CHECK]
3180 IF D=0 & @(11)<=33 & @(12)<=33 GOTO 3050 : REM 3050=WAIT FOR FIRE LOOP
3190 IF D=1 & @(11)<=33 & @(12)<=33 & @(1)<10 GOTO 3050
        : REM 3050=WAIT FOR FIRE LOOP
3200 PCLR 14, 15 : REM TURN ALL OFF TO INIT FLAMING SAMPLE
3210 S = 3
3220 RETURN
4000 REM [GET BASELINE]
4010 IF ?(0)=2 PSET 14 : IF D=1 PRINT" Pump is on"
4020 IF ?(0)=32 GOSUB 4050 : REM 4050=SAVE BASELINE
4030 RETURN
4050 REM [SAVE BASELINE]
4060 X=(@(1)%60)*Z : REM WRAP AROUND LAST 60 READINGS (2 HR)
4070 IF D=0 PRINT " Baseline stored at x =",#6,X
4080 REM USE BYTES 0 TO 60*Z-1
4090 GOSUB 6000 : @(1)=@(1)+1 : REM 6000=STORE DATA
4100 PCLR 14,15 : IF D=1 PRINT " Pump is off"
4110 RETURN
5000 REM [GET DATA]
5010 @(19) = ?
5020 FOR A = 0 TO 7
5030 @(11+A) = CHAN(A)
5040 NEXT A
5050 RETURN
6000 REM [STORE DATA] REM SUB TO STORE DATA FOR 1 SCAN
```

```
6010 STORE X, #4, @(19) - F : REM TIME FROM START OF FLAMING
6020 FOR A = 0 TO 7
6030 STORE X, #2, @(11+A) : REM CHANNEL READINGS
6040 NEXT A
6050 RETURN
6070 REM [DELAY 1]
6080 REM HOLD FOR 1 TIC (10MS) FOR POWER UP
6090 Y=?
6100 REM [DELAY LOOP]
6110 IF ?-Y<1 GOTO 6100 : REM 6100=DELAY LOOP
6120 RETURN
7000 REM [START FLAMING]
7010 REM S=3 >> START TAKING DATA, ONE SAMPLE EVERY SECOND
7020 F = ? : RTIME : REM FIRE APPROACHING, SET TIME (F)
7030 FOR I = 0 TO 5 : @(20+I)=?(I) : NEXT I : REM SAVE FLAMING TIME
7040 IF D = 1 PRINT "FIRE APPROACHING AT ";
7050 IF D = 1 PRINT ?(2),":",?(1),":",?(0)," ON ",?(4),"/",?(3),"/",?(5)
7060 IF D = 0 PRINT 'STARTING FLAMING PHASE'
7070 PSET 15, 14 : REM TURN ON A.2D AND PUMPS
7080 L = J + ? : REM SET L = END TIME OF FLAMING PHASE
7090 X = 60*Z : REM SAVE SPACE FOR 60 BASELINE READINGS
7100 SLEEP 0
7110 REM [FLAMING LOOP]
7120 IF D=1 SLEEP 200
7140 IF D=0 SLEEP 20
7160 GOSUB 5000 : REM 5000=GET DATA
7170 IF D=1 & @(2)%100=0 PRINT "STORING ",@(2)," AND ",(L-?)/100," SECONDS
        TO GO"
7180 GOSUB 6000 : @(2)=@(2)+1 : REM 6000=STORE DATA
7190 IF ? < L GOTO 7110 : REM 7110=FLAMING LOOP
7200 S = 4 : REM END OF FLAMING TIME REACHED
7210 RETURN
8000 REM [START SMOLDERING]
8010 REM S=4 >> FLAMING PHASE DONE, START SMOLDERING PHASE
8020 REM ONE SAMPLE EVERY 2 MIN
8030 IF D=0 PRINT 'STARTING SMOLDERING PHASE'
8040 REM [SMOLDERING LOOP]
8050 PCLR 14, 15 : REM SHUT OFF A.2D AND PUMPS
8060 FOR N=1 TO 30
8070 IF D=0 SLEEP 300 : REM LOOP 1.5 MINUTES WHEN IN FIRE
8080 IF D=1 SLEEP 30 : REM LOOP 9.0 SECONDS WHEN DEBUGGING
8090 NEXT N
8100 PSET 15,14 : REM TURN ON A.2D AND PUMPS
8110 IF D=0 SLEEP 3000 : REM WAIT 30 SEC WHEN IN FIRE
8120 IF D=1 SLEEP 600 : REM WAIT 6 SECONDS WHEN DEBUGGING
8130 GOSUB 5000 : REM 5000=GET DATA
8140 IF D=1 & @(3)%10=0 PRINT "STORING ",@(3)," AT ",(?-L)/100," SECONDS
        PAST FLAMING"
8150 GOSUB 6000 : @(3)=@(3)+1 : REM 6000=STORE DATA
8160 IF D=0 & @(17) >= 217 & 60+@(2)+@(3) <= 6963 GOTO 8040 : REM IN FIRE
        : REM 8040=SMOLDERING LOOP
8170 IF D=1 & @(17) >= 217 & @(3) <= 20 GOTO 8040 : REM DEBUGGING
        : REM 8040=SMOLDERING LOOP
```

```
8180 S = 5
8190 REM BATTERY IS LOW (10 VOLTS) IF @(17) = 217 OR LESS
8200 RETURN
9000 REM [STOP TAKING DATA]
9010 IF D=1 PRINT 'DONE TAKING DATA'
9020 PCLR 14, 15 : REM PUMP OFF, A/D OFF
9030 IF D=1 PRINT 'GOING INTO DEEP SLEEP'
9040 W = X
9050 REM [SLEEP]
9060 SLEEP 500 : ITEXT X, 0 : IF W = X GOTO 9050 : REM 9050=SLEEP
9070 IF D=1 & S=5 PRINT 'SYSTEM HAS FIRE DATA -- OFF LOAD OR QUIT'
9080 STOP

30000 REM [SEND DATA]
30010 PRINT "GROUND PACKAGE DATA"
30020 PRINT "PACKAGE NUMBER ",P
30030 PRINT "FLAMING SAMPLE TIME (.01 SEC) ",J
30040 PRINT "FLAMES DETECTED ",(F-H)/100,".",(F-H)%100," SECONDS AFTER ARM
      TIME."
30050 PRINT "TRANSFERRING @() ARRAY "
30060 REM THERE SHOULD BE 5 LINES BEFORE THE RUN NUMBER IN @(0)
30070 FOR Q = 0 TO 25
30080 PRINT #6, @(Q)
30090 NEXT Q
30110 PRINT "TRANSFERRING PRE-FIRE BASELINE DATA "
30120 V=0
30130 IF @(1) > 60 V=@(1)-60
30140 FOR Q= V TO @(1)-1
30150 X=(Q%60)*Z
30160 PRINT #6,Q,#12,GET (X,#4); : REM TIME FROM START
30170 FOR I=0 TO 7
30180 PRINT #5,GET (X,#2);
30190 NEXT I
30200 PRINT ""
30210 NEXT Q
30230 PRINT "TRANSFERRING FLAMING DATA"
30240 X= 60*Z
30250 FOR Q = 0 TO @(2)-1
30260 PRINT #6,Q,#12,GET (X,#4); : REM TIME FROM START
30270 FOR I=0 TO 7
30280 PRINT #5,GET (X,#2);
30290 NEXT I
30300 PRINT ""
30310 NEXT Q
30330 PRINT "TRANSFERRING SMOLDERING DATA"
30340 FOR Q = 0 TO @(3)-1
30350 PRINT #6,Q,#12,GET (X,#4); : REM TIME FROM START
30360 FOR I=0 TO 7
30370 PRINT #5,GET (X,#2);
30380 NEXT I
```

```
30390 PRINT ""
30400 NEXT Q
30420 PRINT "**END OF DATA**"
```

B.4 Control Program for Hill Fire Video Camera

```
210 PCLR 3 : REM CLEAR CAMERA CONTROL LINE
220 A=0
221 REM CAMERA MUST BE IN THE ACTIVE RECORD MODE WHEN
        THE JUMPER PIN IS PULLED TO START THE PROGRAM
270 REM [ARM LOOP]
280 PRINT "pull jumper on tattletale to start"
290 FOR K = 1 TO 20000000
300 SLEEP 0
310 SLEEP 500 : IF PIN(1) = 1 GOTO 340 : REM 340=START
320 NEXT K
340 REM [START]
350 PRINT "start control sequence"
370 GOSUB 630 : REM 630=TOGGLE
400 REM [CONTROL LOOP]
420 PRINT "camera should be paused"
430 A = 1
440 FOR I = 1 TO 400
450 SLEEP 0
460 IF CHAN(0) > 512 GOSUB 700 : REM 700=ROLL EM
470 SLEEP 50
480 NEXT I
490 PRINT CHAN(1)
510 GOSUB 630 : REM 630=TOGGLE
520 PRINT "camera should be recording"
530 A = 2
540 FOR I = 1 TO 8
550 SLEEP 0
560 IF CHAN(0) > 512 GOSUB 700 : REM 700=ROLL EM
570 SLEEP 50
580 NEXT I
590 PRINT CHAN(1)
600 GOSUB 630 : REM 630=TOGGLE
610 GOTO 400 : REM 400=CONTROL LOOP
630 REM [TOGGLE]
640 PSET 3
650 SLEEP 0
660 SLEEP 50
670 PCLR 3
680 RETURN
700 REM [ROLL EM]
720 SLEEP 0
730 PRINT "fire detected"
740 SLEEP 50
750 IF CHAN(0) > 512 GOTO 780 : REM 780=FIRE HERE
760 RETURN
780 REM [FIRE HERE]
790 PRINT "trigger accepted"
810 IF A = 2 GOTO 840 : REM 840=DEEP SLEEP
820 GOSUB 630 : REM 630=TOGGLE
840 REM [DEEP SLEEP]
860 PRINT "roll em!"
```

```
870 FOR J = 1 TO 200000000
880 SLEEP 0
890 SLEEP 500
900 NEXT J
920 STOP
```